ZooKeys 977: 1–23 (2020)
doi: 10.3897/zookeys.977.55040
https://zookeys.pensoft.net

RESEARCH ARTICLE

A peer-reviewed open-access journal
ZooKeys
Launched to accelerate biodiversity research

First record of the genus *Boholina* (Copepoda, Calanoida, Pseudocyclopidae) in Vietnam, with description of a new species from an anchialine cave in Tra Ban Island

Duc Luong Tran[1,2], Cheon Young Chang[3]

1 *Department of Aquatic Ecology, Institute of Ecology and Biological Resources, Academy of Science and Technology, 18, Hoang Quoc Viet Rd, Caugiay District, Hanoi, Vietnam* **2** *Graduate University of Science and Technology, Vietnam Academy of Science and Technology, 18 Hoang Quoc Viet Rd, Cau Giay District, Hanoi, Vietnam* **3** *Department of Biological Science, Daegu University, Gyeongsan 712-714, South Korea*

Corresponding author: Cheon Young Chang (cychang@daegu.ac.kr)

Academic editor: D. Defaye | Received 3 June 2020 | Accepted 11 September 2020 | Published 22 October 2020

http://zoobank.org/87B72CD0-160B-47A9-B8F6-5D831F0CB938

Citation: Tran DL, Chang CY (2020) First record of the genus *Boholina* (Copepoda, Calanoida, Pseudocyclopidae) in Vietnam, with description of a new species from an anchialine cave in Tra Ban Island. ZooKeys 977: 1–23. https://doi.org/10.3897/zookeys.977.55040

Abstract

A new species, *Boholina reducta* **sp. nov.**, was found in a brackish pool within an anchialine cave in Tra Ban Island in Bai Tu Long Bay, north Vietnam. The new species is clearly distinguished from all the six species currently known in the genus *Boholina* by the following unique characteristics: reduction of the septum between gonopores; narrow and pointed rostrum; basal segment of mandibular palp armed with three setae; maxillule without seta on the basal exite, and exopod with 11 setae; second and third endopodal segments of the maxilliped bearing three setae each; exopod of male right leg 5 2-segmented, with two strong and one vestigial spines on the outer margin of the distal segment; and last exopodal segment of female leg 5 bearing only one spine on the outer margin. We provide a description of the new species, along with detailed illustrations and scanning electron microscopy photographs. The identification key to *Boholina* species is updated as well. This is the first record of the genus *Boholina* from Vietnam.

Keywords
Bai Tu Long Bay, Biodiversity, new species, SEM, taxonomy

Introduction

The family Boholinidae was established for a single genus *Boholina* by Fosshagen and Iliffe (1989) on the basis of a combination of morphological characteristics: well-developed mouthparts; 3-segmented rami on P1–P4; female P5 with 3-segmented exopod and slightly reduced 2-segmented endopod; right antennule of male geniculated; and male P5 with a highly complex grasping organ. Fosshagen and Iliffe (1989) argued that it differed from the families Pseudocyclopidae Giesbrecht, 1893 and Ridgewayiidae Wilson, 1958 by the modified terminal spine on the distal exopodal segment of P4 and the inner seta on the coxal segment of female P5 (Fosshagen and Iliffe 1989).

However, Bradford-Grieve et al. (2014) considered Boholinidae and Ridgewayiidae as junior synonyms of Pseudocyclopidae, based on a morphology-based cladistic analysis, and placed the genus *Boholina* in the Pseudocyclopidae. To date, 14 genera have been recognized in Pseudocyclopidae as follows: *Badijella* Kršinic, 2005; *Boholina* Fosshagen, 1989; *Brattstromia* Fosshagen, 1991; *Exumella* Fosshagen, 1970; *Exumellina* Fosshagen, 1998; *Hondurella* Suárez-Morales & Iliffe, 2007; *Normancavia* Fosshagen & Iliffe, 2003; *Pinkertonius* Bradford-Grieve, Boxshall & Blanco-Bercial, 2014; *Placocalanus* Fosshagen, 1970; *Pseudocyclops* Brady, 1872; *Ridgewayia* Thompson & Scott, 1903; *Robpalmeria* Fosshagen & Iliffe, 2003; *Stargatia* Fosshagen & Iliffe, 2003 and *Stygoridgewayia* Tang, Barron & Goater, 2008 (Walter and Boxshall 2020). Among these genera, *Pseudocyclops* and *Ridgewayia* have a worldwide distribution from temperate, subtropical to tropical shallow waters (Ohtsuka et al. 1999; Boxshall and Halsey 2004; Figueroa 2011a, b). Other genera are known from the North Atlantic and Mediterranean (*Exumella*, *Badijella*), Belize (*Brattstromia*), Bahamas (*Exumellina*, *Normancavia*, *Robpalmeria*, *Stargatia*), Western Caribbean (*Hondurella*), Australia and New Zealand (*Stygoridgewayia*, *Pinkertonius*). Most species of the Pseudocyclopidae were reported from shallow benthopelagic or anchialine cave habitats, while *Stygoridgewayia* was found in fresh groundwater in Australia (Bradford-Grieve et al. 2014).

The genus *Boholina* currently comprises six valid species: *B. crassicephala* Fosshagen & Iliffe, 1989 and *B. purgata* Fosshagen & Iliffe, 1989 from an anchialine cave on San Vicente, Bohol Island (Philippines); *B. parapurgata* Boxshall & Jaume, 2012 and *B. munaensis* Boxshall & Jaume, 2012 from anchialine and brackish waters of low salinity in Muna Island (Indonesia); *B. ganghwaensis* Moon & Soh, 2014 from burrows of the manicure crab in muddy habitats on Ganghwa Island, Korea; and the recently introduced *B. laorsriae* Boonyanusith, Wongkamhaeng & Athibai, 2020 from a freshwater pool within a cave located about 6.5 km from the Andaman Sea,

Thailand (Fosshagen and Iliffe 1989; Boxshall and Jaume 2012; Moon and Soh 2014; Boonyanusith et al. 2020).

In this paper, we describe a new species of *Boholina*, based on specimens from an anchialine habitat of a karstic cave in Tra Ban Island, north Vietnam, along with detailed illustrations drawn under a differential interference microscope and by scanning electron microscopy. We also discuss its morphological relationships with congeners.

Materials and methods

Nha Tro Cave (or Hang Cam Cave) is located in Vietnam, on Tra Ban Island in Bai Tu Long Bay. The island is 20 km from Cam Pha City in Quang Ninh Province, and about 12 km from the mainland; it has an area of about 76.37 km² (Fig. 1A). The main geological composition of the island is stratified limestone, silicate and claystone (Uong et al. 2013).

The cave has a large entrance at 17 m above sea level (20°57'31.0"N, 107°29'12.1"E); a few meters from the entrance there is a larger downward-sloping hall (Fig. 1B). On the left of the cave is a steeply climbing branch, terminating after a few meters. On the right is the main gallery along the length of the cave with enormous boulders due to rockfalls and large concretions.

The floor is composed of pools and clay deposits; concretions are abundant with several discs, the largest one reaching three meters in diameter. The dimension of the cave is about 350 m in length, 10 m high and 15 m in depth (Donatis et al. 2010).

Copepods were collected from a pool inside the Nha Tro Cave (Fig. 1B). The pool is in a permanently dark section about 200 m from the cave exit. Physico-chemical characteristics of the pool on 9 May 2018 are as follows: water temperature 19.8 °C; pH 7.82; dissolved oxygen 0.76 mg/L; water hardness ($CaCO_3$) 154 mg/L; electrical conductivity 1.12 mS/cm; salinity 0.18‰. Copepods were taken from the pool in knee-deep water, with a hand net with mesh size of 80 μm. They were fixed in about 80% ethanol in the field, and later stored in about 70% ethanol. Specimens were dissected and mounted in glycerol or lactophenol. The mounted specimens were observed under a differential interference contrast microscope with Nomarski optics (Nikon Eclipse Ni-U). All drawings were made with the aid of a camera lucida.

Material used for scanning electron microscopy (SEM) was fixed in 2.5% glutaraldehyde in 0.1M phosphate buffer (pH 7.2–7.4) for 2 hours, followed by fixation in 1% cold osmium tetroxide (at about 5°C) in the same buffer for 12 hours. After dehydration through a graded series of ethanol (70, 80, 90, 95 and 100%) for 30 minutes each, the material was critical point dried, coated with gold/palladium, and then examined with a scanning electron microscope Hitachi TM3000 TableTop operated at 15 KV. The following abbreviations are used, where required, throughout the text and figures: Endp = endopod; Exp = exopod; P1–P5 = swimming legs 1–5. General

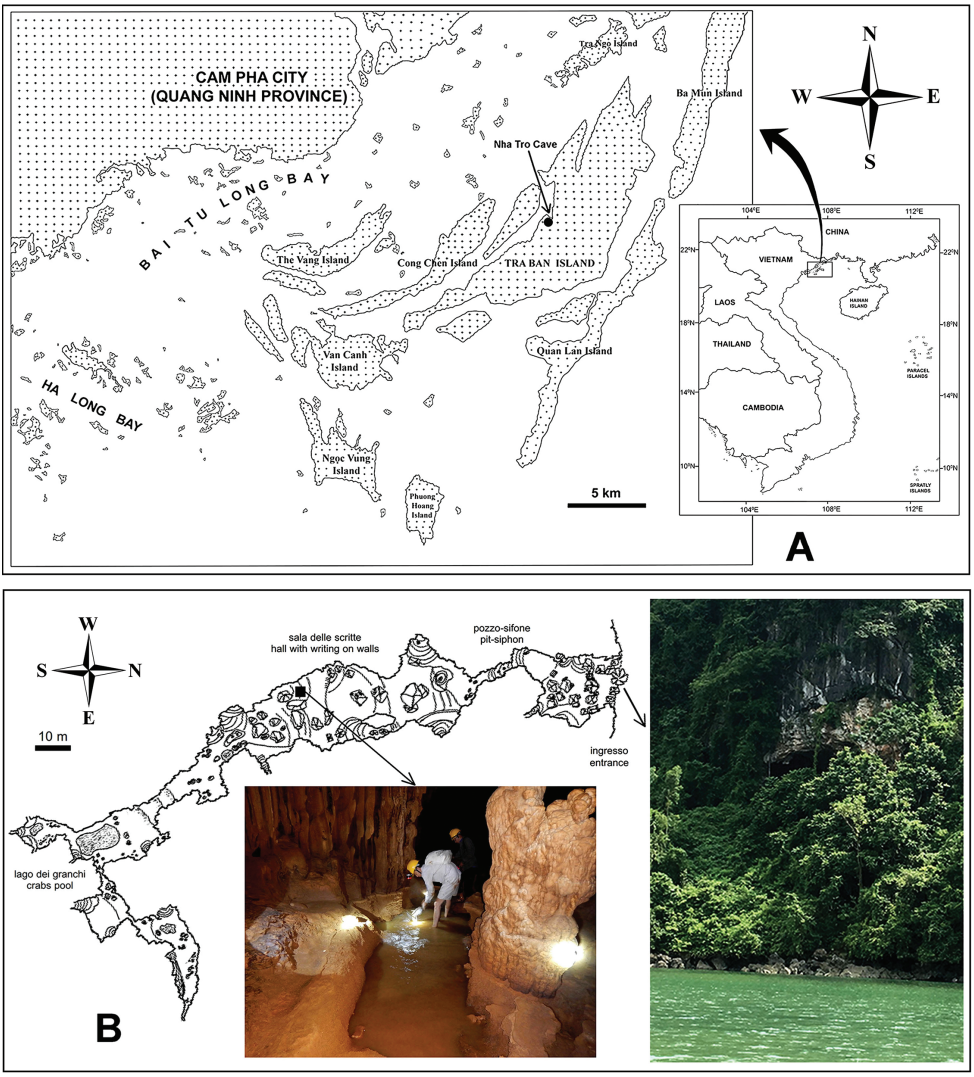

Figure 1. Sampling locations of *Boholina reducta* sp. nov. **A** map of the Bai Tu Long Bay showing the location of Nha Tro Cave (arrow) **B** map of the Nha Tro Cave (cited from Donatis et al. 2010), designating the entrance from the sea and the type locality of the new species.

terminology for the description follows Huys and Boxshall (1991), including analysis of caudal setae (I–VII) and antennule segmentation (evident segments labeled with Arabic numerals, and ancestral segments with Roman numerals), and the terminology and homology for maxillary and maxilliped structures by Ferrari and Ivanenko (2001, 2008) is adopted herein.

Type specimens are deposited in the Institute of Ecology and Biological Resources (IEBR), Hanoi, Vietnam.

Taxonomy

Order Calanoida G.O. Sars, 1903
Family Pseudocyclopidae Giesbrecht, 1893
Genus *Boholina* Fosshagen & Iliffe, 1989

***Boholina reducta* sp. nov.**
http://zoobank.org/909D70A1-A05C-4E8B-B222-077DE414F090
Figs 2–9

Type material. *Holotype*: ♀ (IEBR-COP3480–3481), 933 μm long; Quang Ninh Province, Tra Ban Island, Nha Tro Cave; 20°57'31.0"N, 107°29'12.1"E; 9 May 2018; D.L. Tran leg.; a pool inside the cave; dissected and mounted on two slides in glycerol. ***Allotype*:** ♂ (IEBR-COP3482–3483), 812 μm long; same data as for holotype; dissected and mounted on two slides in glycerol. ***Paratypes*:** 2 ♂♂ (IEBR-COP3484, 3485) and 5 ♀♀ (IEBR-COP3486–3490); same data as for holotype; dissected and mounted in glycerol.

Additional material. 60 ♂♂ and more than 100 ♀♀, same data as for holotype, preserved in 70% ethanol, IEBR-COP-AED05.2018.13; 5 ♂♂ and 5 ♀♀, same data as for holotype, prepared for SEM examination, retained in the collection of the first author (DLT).

Type locality. A pool inside the Nha Tro Cave (geographic coordinates of the cave entrance: 20°57'31.0"N, 107°29'12.1"E) in Tra Ban Island, Bai Tu Long Bay, Quang Ninh Province, north Vietnam.

Etymology. The proposed name refers to reduction of the terminal spine on the distal exopod segment of P5 in the male as well as the proximal outer spine on the distal exopodal segment of P5 in the female, which are the most remarkable characteristics differentiating this new species from all the congeneric species of *Boholina*.

Diagnosis. Boholinid form in both sexes. Postero-lateral corners of second and third pedigerous somites rounded, fourth and fifth pedigerous somites completely fused. Rostrum represented by a narrow chitinized projection with pointed tip. Medial lobe of distal segment A2 endopod with nine setae. Mandibular palp basis with three setae; distal segment of endopod with 11 setae; seta on first segment of exopod present. Maxillule exopod with 11 setae and seta on basal exite absent. Second and third segments of maxilliped endopod with three setae each. Terminal spine on exopod of leg 4 modified with row of large spinules on mid-inner margin. ***Female:*** Gonopores on double-somite located close together on mid-ventral surface, septum between gonopores reduced to vestige deep inside genital opening. P5 Exp-3 with only one spine on outer margin and four setae on inner margin; distal segment of P5 endopod with one seta on outer margin. ***Male:*** Process at antepenultimate segment of right antennule absent. Right P5 exopod 2-segmented; distal segment with three spines, including a vestigial one on outer margin, while terminal and inner spine absent.

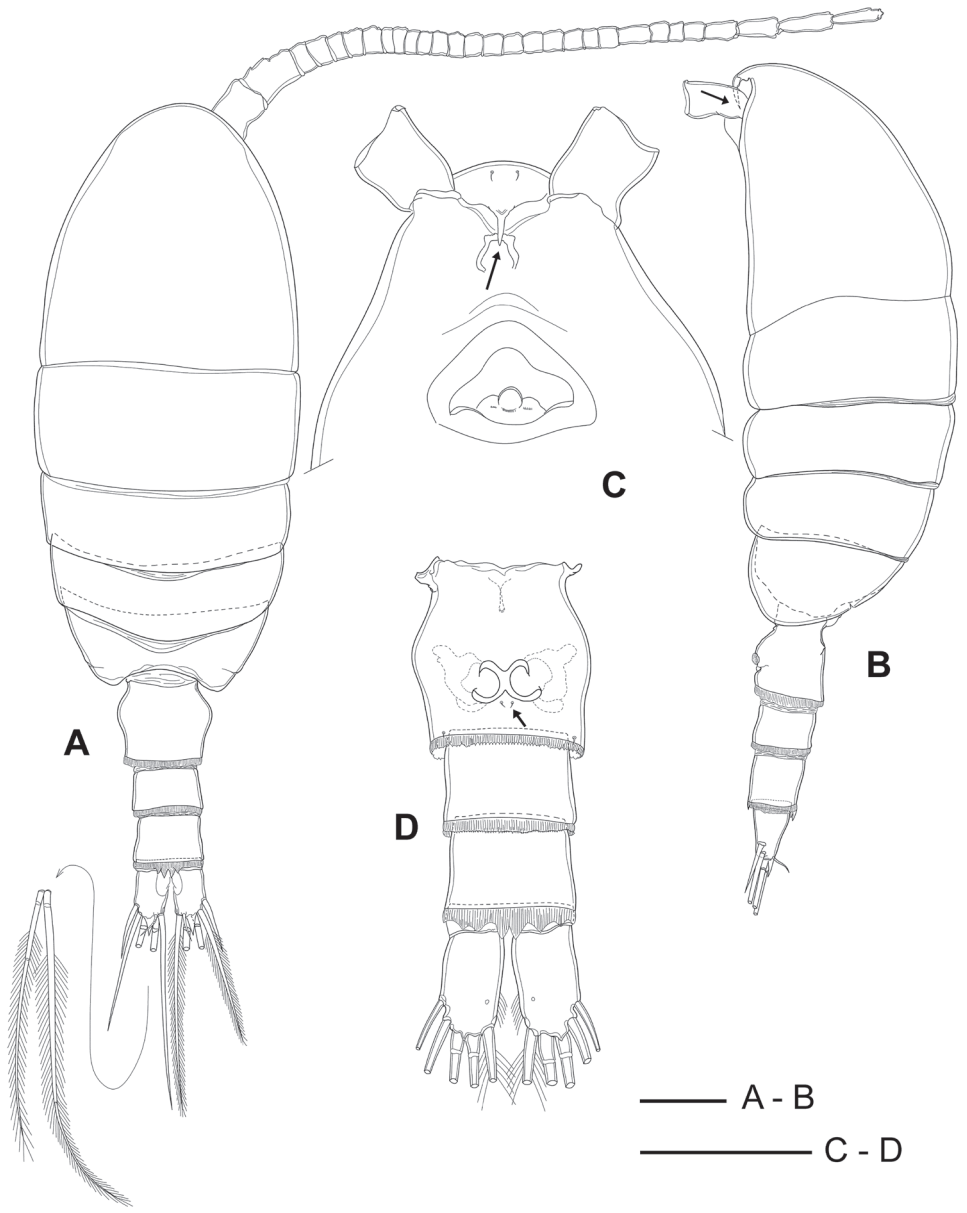

Figure 2. *Boholina reducta* sp. nov., holotype female. **A** habitus, dorsal view **B** habitus, lateral view (arrow indicating tip of rostrum) **C** rostrum, ventral view (arrow indicating tip of rostrum) **D** urosome, ventral view (arrow indicating sensilla near gonopores). Scale bars: 100 μm.

Description of adult female. Total length (without furcal setae) 858–944 μm (mean 892 μm, *N* = 20). Ratio of prosome to urosome length about 3.1:1 (Fig. 2A, B). Prosome ovoid in dorsal view, 5-segmented, comprising cephalosome; first pedigerous somite separated from cephalosome; second and third free pedi-

gerous somites with postero-lateral corners rounded; fourth and fifth pedigerous somites completely fused.

Urosome 4-segmented, comprising genital double-somite, two free abdominal somites and anal somite. Genital double-somite slightly asymmetrical, widest about at mid-length; posterior margin ornamented with smooth hyaline membrane dorsally and small dentate hyaline frill ventrally, about as long as wide; paired gonopores equal in size, located close together on mid-ventral surface, the septum between gonopores reduced to vestige, deep inside genital opening; gonoporal plates small, and gonoporal slits large; two pairs of sensilla present (Figs 2D, 9C, D, arrows), one pair positioned adjacent to posterior margin of gonopores and second pair located ventrolaterally near posterior margin of double-somite. Third and fourth abdominal somites cylindrical, subequal in length (Fig. 2D); third with finely serrated hyaline membrane all around posterior margin, fourth with posterior margin hyaline membrane expanded mid-dorsally to four large spines functioning as pseudoperculum concealing anal opening and mid-ventrally with finely serrated hyaline membrane on posterior margin. Anal somite extremely short, posterior margin smooth, concealed within posterior rim and hyaline membrane of second free abdominal somite.

Caudal rami (Fig. 2A, D) short, about 1.5 times longer than wide, with pointed dorsal process in middle of distal margin; distal inner margin with a row of setules; ventral surface with a small pore near inner distal edge; ornamented six caudal setae; seta I lacking, seta II spiniform, about 1.2 time as long as caudal ramus; setae III–VI plumose, ratio of setae V:IV:VI:III:II as 5.8:4.3:4.1:2.4:1.0; dorsal seta VII short, naked, about 0.5 times as long as seta II.

Rostral filaments absent, rostrum represented by a narrow chitinized projection with pointed tip (Figs 2B, C, 9B, arrows); pair of long sensilla present in proximal part of rostrum.

Antennules (Figs 2A, 3A) symmetrical, extending to middle area of pedigerous somite 5, 24-segmented with ancestral segments II–IV and XXVII–XXVIII fused, X–XI party fused, other articulations expressed, ventral surface of segment 1 with a row of small oblique spines. Armature formula as follows (s - setae, ae - aesthetasc): segment 1 (ancestral segment I) 1s + 1ae, segment 2 (II–IV) 6s + 1ae, segment 3 (V) 2s + 1ae, segment 4 (VI) 2s, segment 5 (VII) 2s + 1ae, segment 6 (VIII) 2s, segment 7 (IX) 2s + 1ae, segment 8 (X–XI) 3s + 2ae, segment 9 (XII) 1s, segment 10 (XIII) 1s + 1ae, segment 11 (XIV) 1s + 1ae, segment 12 (XV) 1s + 1ae, segment 13 (XVI) 1s + 1ae, segment 14 (XVII) 1s, segment 15 (XVIII) 1s + 1ae, segment 16 (XIX) 1s, segment 17 (XX) 1s, segment 18 (XXI) 1s + 1ae, segment 19 (XXII) 1s, segment 20 (XXIII) 1s, segment 21 (XXIV) 2s, segment 22 (XXV) 2s + 1ae, segment 23 (XXVI) 2s, segment 24 (XXVII–XXVIII) 5s + 1ae.

Antenna (Figs 3B, 8A) biramous. Coxa and basis separate, coxa small, with a seta. Basis robust with two setae on inner distal corner. Endopod 2-segmented; proximal segment elongated, 2.2 times as long as wide, with two naked setae at 1/3 distal length of inner margin; distal segment with two lobes, medial lobe bearing six setae distally and three setae on inner distal margin, outer lobe with six long setae terminally and a short sub-terminal seta, outer margin ornamented with small serrated process (Fig. 3B, arrow)

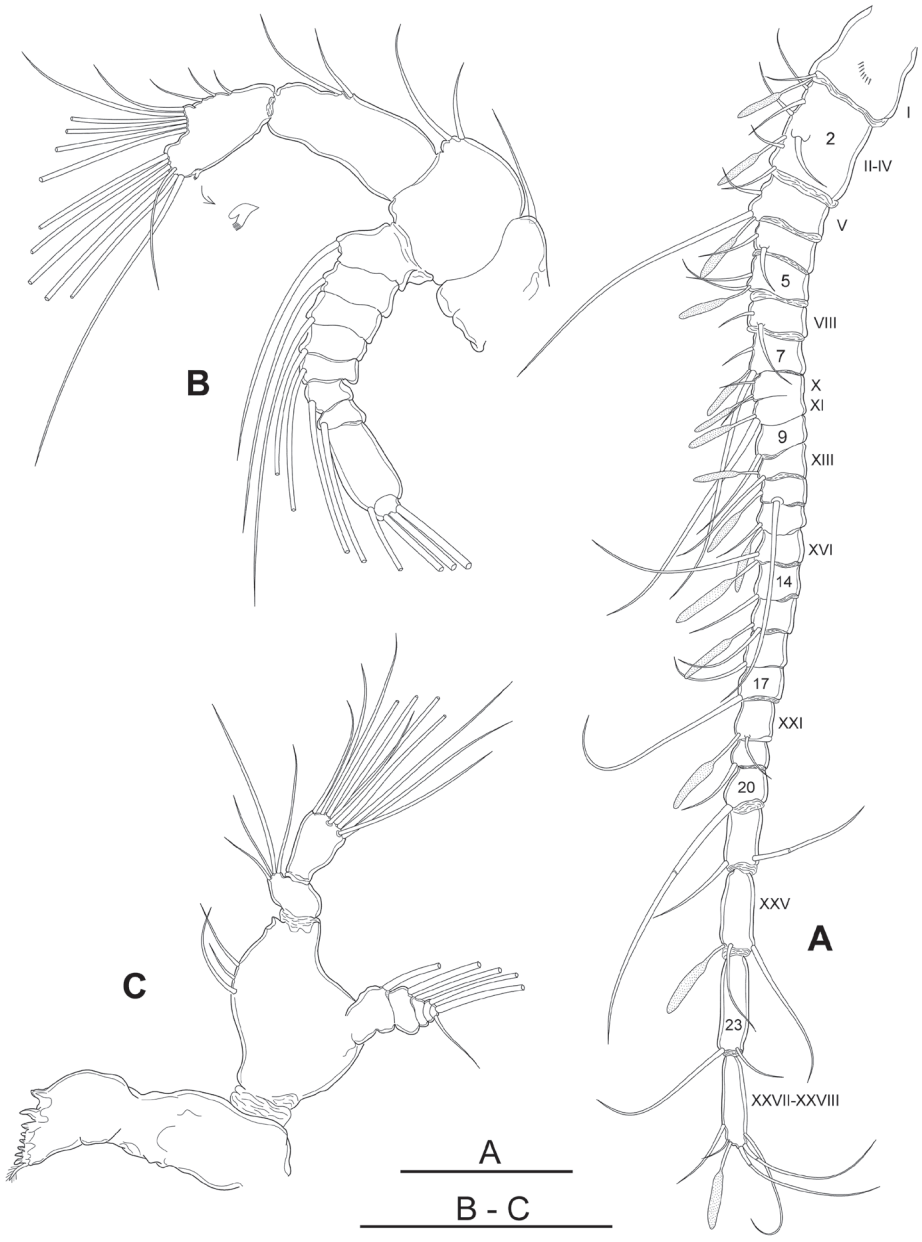

Figure 3. *Boholina reducta* sp. nov., holotype female. **A** antennule **B** antenna (arrow indicating small serrated process) **C** mandible. Scale bars: 100 μm.

subdistally on medial margin and adjacent tiny spinules. Exopod 9-segmented, with setal formula of 1, 1, 1, 1, 1, 1, 1, 1, 3.

Mandible (Figs 3C, 8B) with about eight small teeth on gnathobase plus small distal spinulose seta; ventral-most teeth largest. Mandibular palp biramous; basis robust

with three unequal smooth setae on inner margin. Exopod 5-segmented, setal formula 1, 1, 1, 1, 2. Endopod 2-segmented, proximal with four smooth setae at distomedial angle, distal segment with 11 naked setae on distal margin.

Maxillule (Figs 4A, 8C) with 10 marginal spinulose spines, one naked seta on anterior surface and four stiff setae on posterior surface of praecoxal arthrite. Coxal epipodite with seven plumose setae and two naked setae; coxal endite with four plumose setae. Basis fused to exopod, proximal basal endite with four plumose setae, distal basal endite sub-separated with endopod carrying five plumose setae; basal exite bared. Exopod completely fused to basis bearing 11 plumose setae, posterior surface with a slender oblique row of setules. Endopod with segments 1 and 2 fused, segments 2 and 3 separate, with three plumose, four bare and seven (2 plumose + 5 bare) setae, respectively.

Maxilla (Figs 4B, 8D) 7-segmented, comprising syncoxa, basis and 5-segmented endopod. Syncoxa with five setae on praecoxal endite and three setae on coxal endite. Basis with two endites, each armed with three apical setae. Endopod 5-segmented; proximal endopodal segment developed, enditic-like; second and third segments partly fused; other segments divided; setal formula 4, 2, 2, 2, 2.

Maxilliped (Figs 4C, 8E) well developed, 8-segmented with syncoxa, basis and free 6-segmented endopod. Syncoxa comprising praecoxa and coxa, completely fused; praecoxa with three endites; proximal and middle praecoxal endites each bearing one plumose seta, distal praecoxal endite with two plumose setae; coxa with one endite armed with one long plumose seta and two short, naked setae; oblique rows of spinules situated on posterior proximal of middle praecoxal endite and coxal endite. Basis elongated, armed with three plumose setae, inserted at distal 1/3 of medial margin and carrying rows of setules along medial margin and posterior face of segment. Endopod 6-segmented, with setal formula 2, 3, 3, 3, 3 + 1, 4.

P1–P4 (Fig. 5A–D) biramous, with 3-segmented rami. Intercoxal sclerites of P1–P4 naked on both frontal and caudal surfaces. First to second endopodal segments of P1–P4 with pointed process on distolateral corners. Articulations between endopodal and exopodal segments ornamented with rows of tiny spinules. Armature of P1–P5 as in Table 1.

Basis of P1 with distally pointed digitiform process on anterior; inner basal seta crooked, bilaterally spinulate, reaching to distal end of second endopodal segment; second exopodal segment with conspicuous spinulate process distally in outer distal corner of segment. Outer proximal spine on third exopodal segment of P1 flagellate, other outer spines on P2–P4 with serrate marginal membrane(s) as figured. Terminal spine on exopod of P1 with naked outer margin and plumose internally; on P2 and P3 with serrate membrane externally and plumose internally; that on P4 modified with row of large spinules on mid-inner margin and armed slender spinules on outer margin and distal part of inner margin (Figs 5D, 9A).

P5 (Figs 5E, F, 8F) biramous, with 3-segmented exopod and 2-segmented endopod, intercoxal sclerite smooth and unornamented. Basis small, 1.4 times as wide as long, with acute process on posterior surface near base of exopod. Exopod longer than

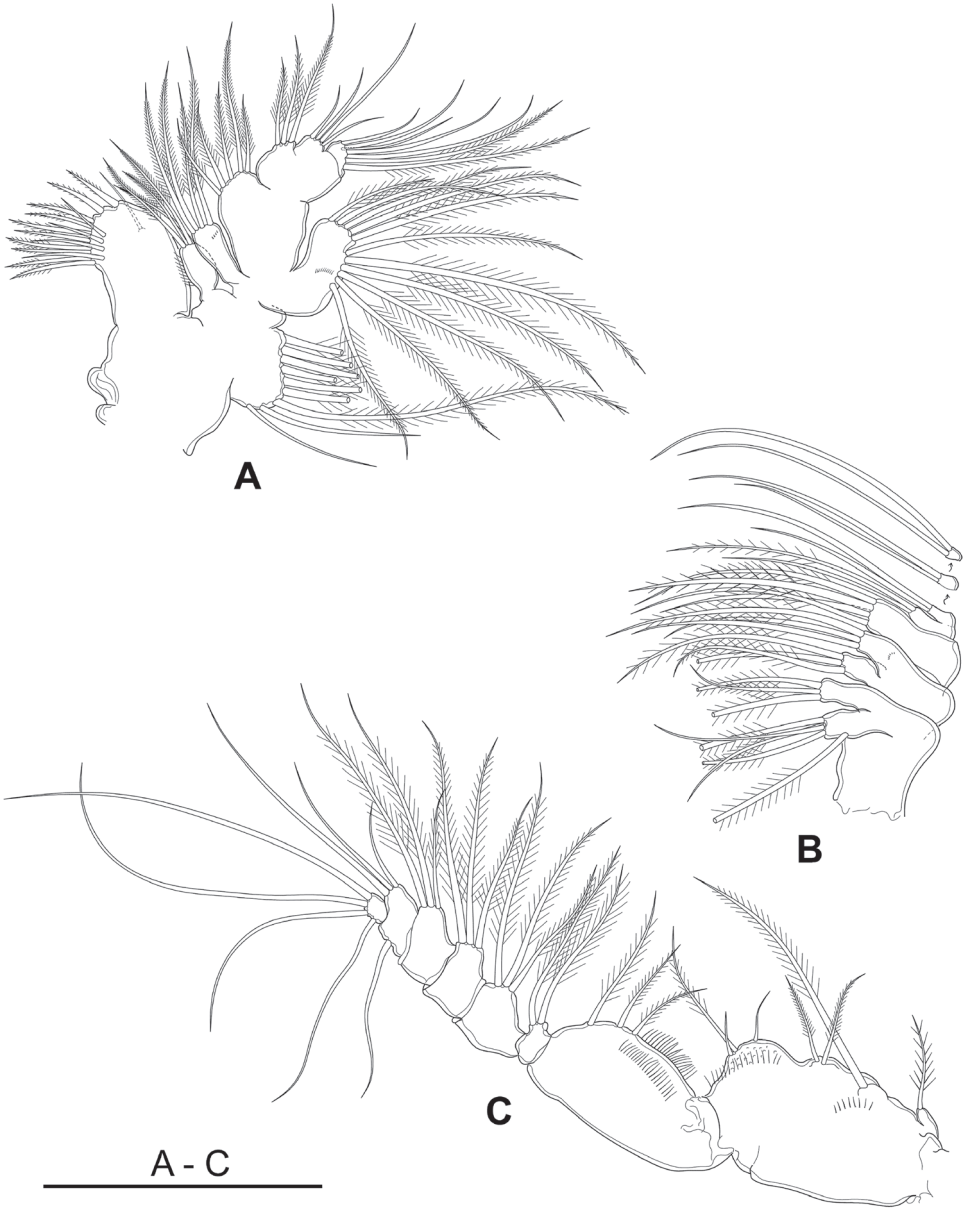

Figure 4. *Boholina reducta* sp. nov., holotype female. **A** maxillula **B** maxilla **C** maxilliped. Scale bar: 100 μm.

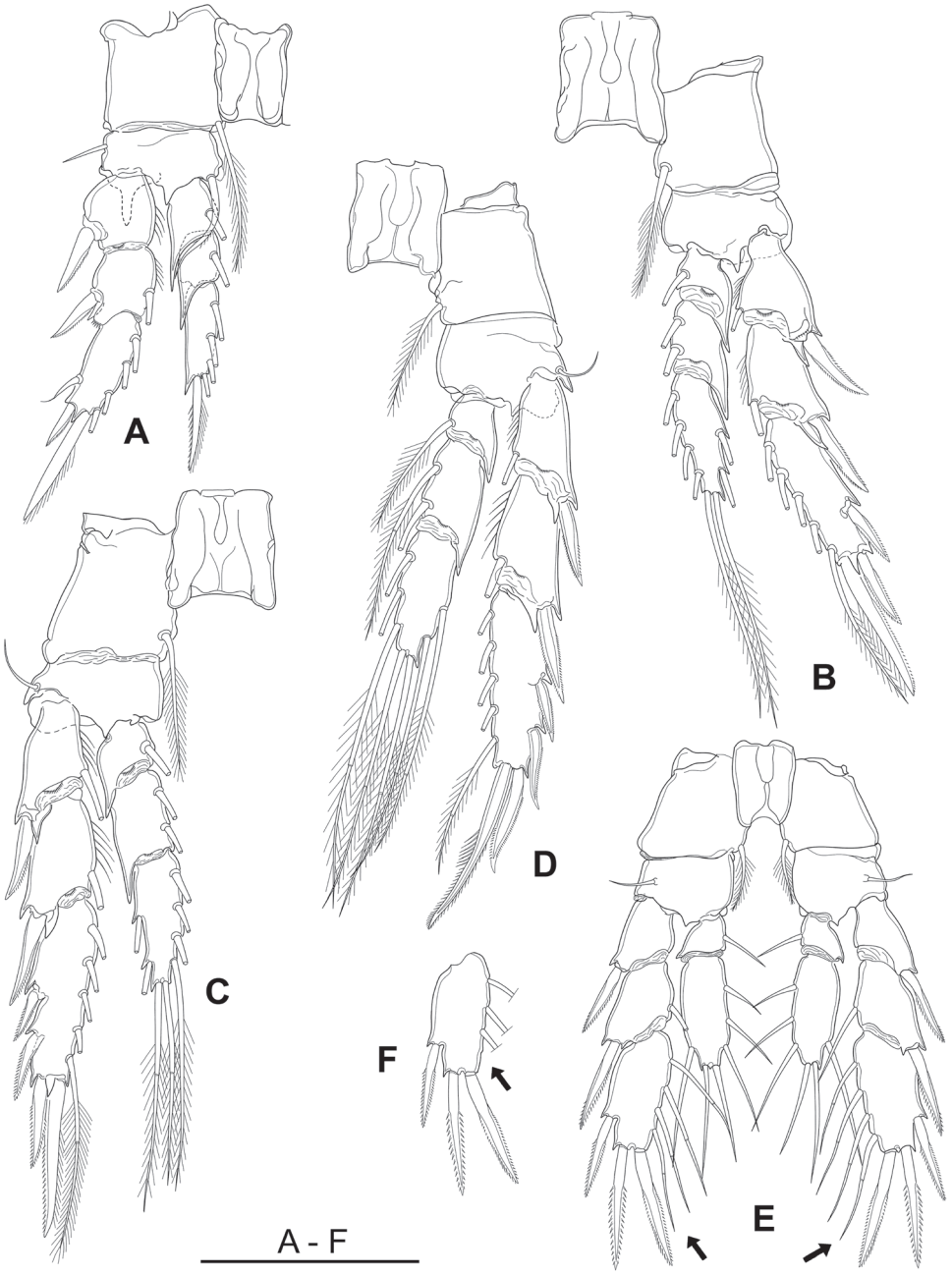

Figure 5. *Boholina reducta* sp. nov. **A**–**E** holotype female, **F** paratype female. **A** P1, posterior **B** P2, posterior **C** P3, posterior **D** P4, posterior **E** P5, posterior (arrows indicating the presence of distal inner setae) **F** distal segment exopod of left P5 (arrow indicating a trace of the distal inner seta). Scale bar: 100 μm.

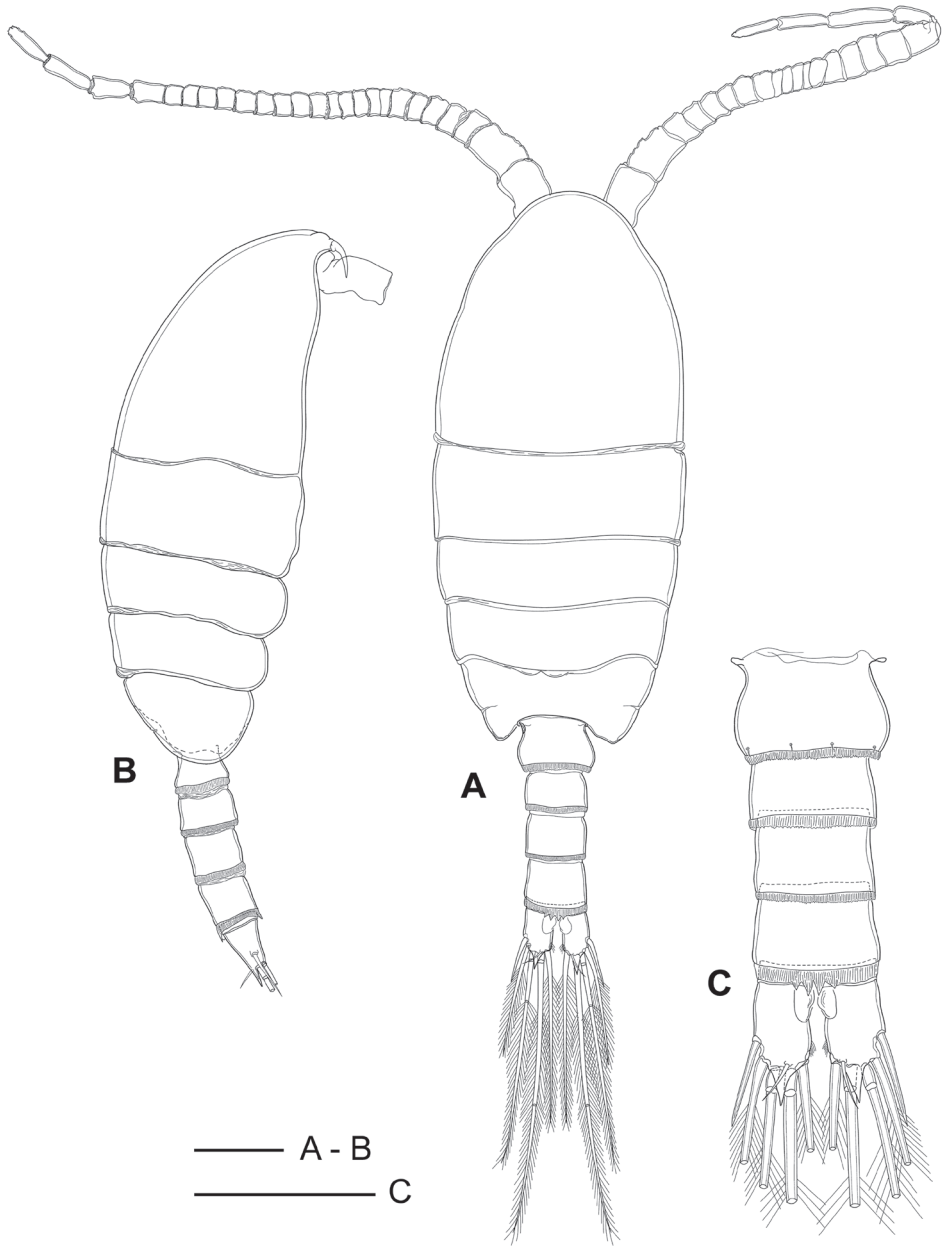

Figure 6. *Boholina reducta* sp. nov., allotype male. **A** habitus, dorsal view **B** habitus, lateral view **C** urosome, dorsal view. Scale bars: 100 μm.

endopod: tip of endopod only reaching to proximal inner seta on third exopodal segment. Distal endopodal segment 2.4 times as long as wide, armed with three inner, two apical and one outer naked setae. First and second exopodal segments each ornamented

Table 1. Armature of female P1–P5 in *B. reducta* sp. nov. (spines denoted by Roman, and setae by Arabic numerals). Armature on the lateral margin of any segment is given first, followed by the elements on the apical and medial margins.

	Coxa	Basis	Exopodite	Endopodite
P1	0-1	1-1	I-0; I-1; II,I,4	0-1; 0-1; 0,I+1,3
P2	0-1	0-0	I-1; I-1; II,I,5	0-1; 0-2; 2,2,4
P3	0-1	1-0	I-1; I-1; III,I,5	0-1; 0-2; 2,2,4
P4	0-1	1-0	I-1; I-1; III,I,5	0-1; 0-2; 2,2,3
P5	0-1	1-0	I-0; I-1; I,II,4	0-1; 1,2,3

with a small pore on anterior surface at origin of outer spine. Distal exopodal segment 2.1 times as long as wide, bearing lateral spine (about 38–41 μm), subapical and apical spines of same length (about 51–54 μm); inner margin with four naked setae.

Description of adult male. Body smaller than female, 756–825 μm long (mean 799 μm, N = 20). Ratio of prosome to urosome length about 2.7:1 (Fig. 6A, B). Prosome 5-segmented as in female: cephalosome completely separated from first pedigerous somite; second and third pedigerous somites with rounded ventroposterior corners; fourth and fifth pedigerous somites fused, with only marked articulation dorsolaterally; posterior corners of fifth pedigerous somites rounded in lateral view.

Urosome 5-segmented (Fig. 6A–C), comprising genital somite, three free abdominal somites and anal somite. Genital somite slightly asymmetrical, distal part of right margin protuberant, slightly more expanded than left margin (Fig. 6C); both lateral margins smooth; four sensilla along dorsoposterior margin; posterior margin with finely serrated hyaline membrane. Second to fourth free abdominal somites cylindrical, subequal in size; second and third somites with finely serrated hyaline membrane on posterior margin; fourth with posterior margin hyaline membrane expanded middorsally to four large spines functioning as pseudoperculum concealing anal opening and mid-ventrally with finely serrated hyaline membrane on posterior margin. Anal somite short, ring-like, with posterior margin smooth.

Caudal rami symmetrical, 1.5–1.6 times as long as wide (mean 1.57, N = 10), bearing distal spinous process dorsally and row of small setules on distal inner margin; ventral surface with a small pore near inner distal edge; ornamented six caudal setae, included to caudal setae II–VII and absent seta I.

Antennules shorter than in female, asymmetrical. Left antennule non-geniculate, 24-segmented and extending to middle area of pedigerous somite 5, armature segments as in female. Right antennule (Fig. 7A) geniculate, 22-segmented, extending to middle of last pedigerous somite; segments 13–18 broadened; segments 17–18 with knife-like projection on inner margins; armature formula as follows (s - setae, ae - aesthetasc): segment 1 (ancestral segment I) 1s + 1ae, segment 2 (II–IV) 6s + 1ae; segment 3 (V) 2s + 1ae; segment 4 (VI) 2s; segment 5 (VII) 2s + 1ae; segment 6 (VIII) 2s; segment 7 (IX) 2s + 1ae; segment 8 (X) 1s + 1ae; segment 9 (XI) 1s + 1ae; segment 10 (XII) 1s; segment 11 (XIII) 1s + 1ae; segment 12 (XIV) 1s + 1ae; segment 13 (XV) 1s + 1ae; segment 14 (XVI) 1s + 1ae; segment 15 (XVII) 1s + 1ae; segment 16 (XVIII) 1s; seg-

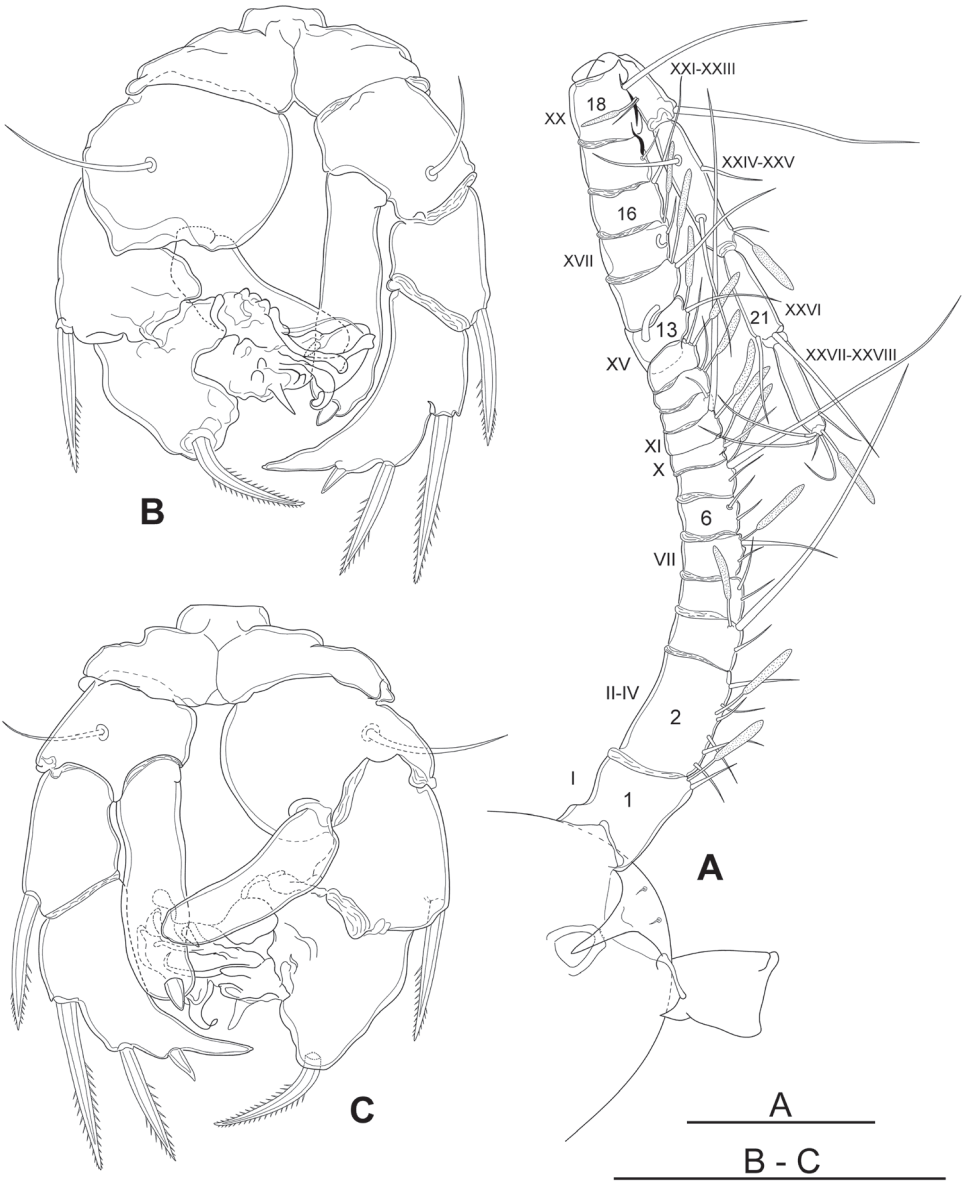

Figure 7. *Boholina reducta* sp. nov., allotype male. **A** rostrum and antennule, ventral view **B** P5, posterior **C** P5, anterior. Scale bars: 100 μm.

ment 17 (XIX) 1s; segment 18 (XX) 1s; segment 19 (XXI–XXIII) 2s + 1ae; segment 20 (XXIV–XXV) 4s + 1ae; segment 21 (XXVI) 2s; segment 22 (XXVII–XXVIII) 5s + 1ae.

Antennae, mouthparts and P1–P4 as in female.

P5 (Figs 7B, C, 9E, F) strongly asymmetrical, biramous; coxae and intercoxal sclerite fused to form common base, without armed elements on anterior and posterior

surface. Right P5: basis about as long as wide, with slender outer basal seta located on posterior surfaces; exopod 2-segmented, first segment with long bilaterally serrate outer spine (39–42 μm), distal segment large in base and tapering on the tip, slightly curved inward, inner margin smooth; outer margin armed with three spines, proximal serrated spine (48–51 μm), middle serrated spine (33–38 μm) and distal short spine vestige (9–11 μm), terminal spine absent; endopod forming an elongate lobe, about 3.8 times as long as wide, armed with two slightly sigmoid spines, apical spine 11–13 μm long and inner spine 8–9 μm, subdistally. Left P5: basis robust, about 1.08 times as wide as long, with slender outer basal seta located on posterior surface; exopod 3-segmented, first segment with a long serrate outer spine (40–42 μm), second segment modified, bearing strongly reflexed spine (35–38 μm) on outer margin; third segment highly transformed bearing multiple short processes and one long, naked modified seta; endopod unarmed, forming an elongate rounded lobe, about 3.2 times as long as wide.

Variability. One female paratype (IEBR-COP3488) and three females among ten additional specimens examined showed asymmetrical P5 Exp-3, with a distal inner seta on right leg (Fig. 5E, arrows) while lacking on left one (Fig. 5F, arrow).

Remarks. The new species agrees well with the generic diagnosis of *Boholina* given by Fosshagen and Iliffe (1989), Boxshall and Jaume (2012), Moon and Soh (2014), and Boonyanusith et al. (2020): fourth and fifth pedigerous somites completely fused; urosome 4-segmented in the female and 5-segmented in the male with very short anal somite, telescoped within the preceding free abdominal somites in both sexes; genital openings paired, located ventromedially or ventrolaterally of genital double-somite; caudal rami produced into a pointed dorsal process in the middle of the distal margin; female antennule 24-segmented, with segments 8 and 9 partly fused or completely separated; P1 with 3-segmented endopod, each segment with a pointed outer distal corner, distal segment without any outer seta; P4 with slightly modified distomedial spine on the distal segment of the exopod; P5 with 2-segmented endopod in the female; and in the male P5 with a complex grasping organ and a highly modified exopod, reduced 1-segmented endopod on both sides.

Among six congeneric species currently recognized in *Boholina*, *B. reducta* sp. nov. shares the paired gonopores located either side of the ventral midline with *B. ganghwaensis*, *B. parapurgata* and *B. purgata*, and shares rounded postero-lateral corners of the second and third free pedigerous somites with *B. munaensis*, *B. crassicephala* and *B. laorsriae*. The new species is similar to *B. laorsriae* by the medial lobe of the distal segment of the antennary endopod having nine setae (while other congeners have eight setae). *Boholina reducta* sp. nov. resembles *B. munaensis* in bearing the single seta on the outer margin of the female P5 Endp-2 (against two in the other congeners). The new species is also similar to *B. ganghwaensis* in having the distal segment of the mandibular palp endopod with 11 setae (versus ten setae in the other congeners) (Table 2).

However, *B. reducta* sp. nov. is distinguished from all six congeners by the unique characteristics as follows (see Table 2): (1) a pair of gonopores are located close together on the mid-ventral surface of the genital double somites, and the septum between gonopores is only visible in the inner part of the genital opening. In *Boholina*, there are three species (*B. ganghwaensis*, *B. parapurgata* and *B. purgata*) with gonopores

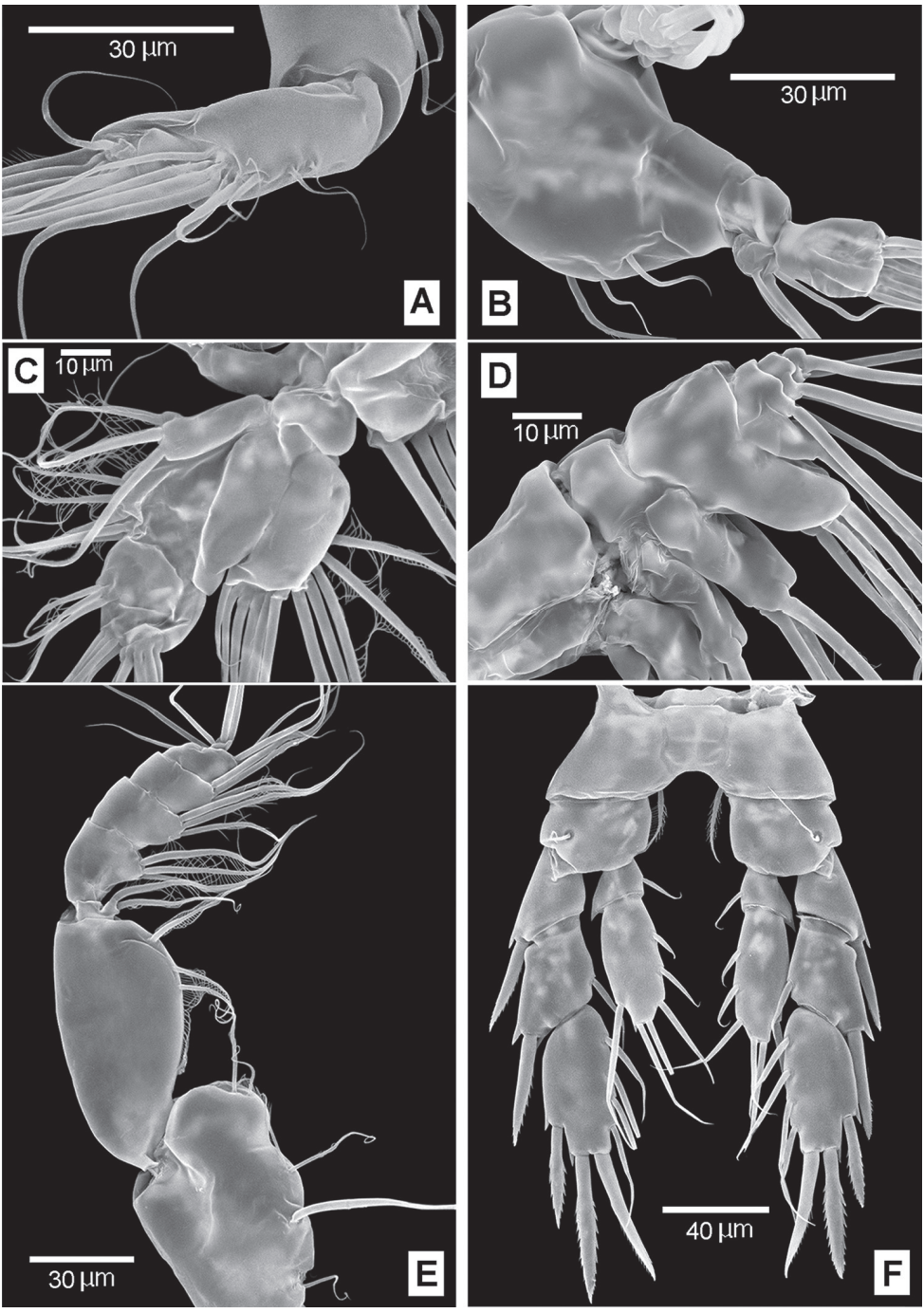

Figure 8. *Boholina reducta* sp. nov., SEM micrographs, female. **A** distal segment of antennary endopod **B** mandibular palp **C** maxillula **D** maxilla **E** maxilliped **F** P5, posterior.

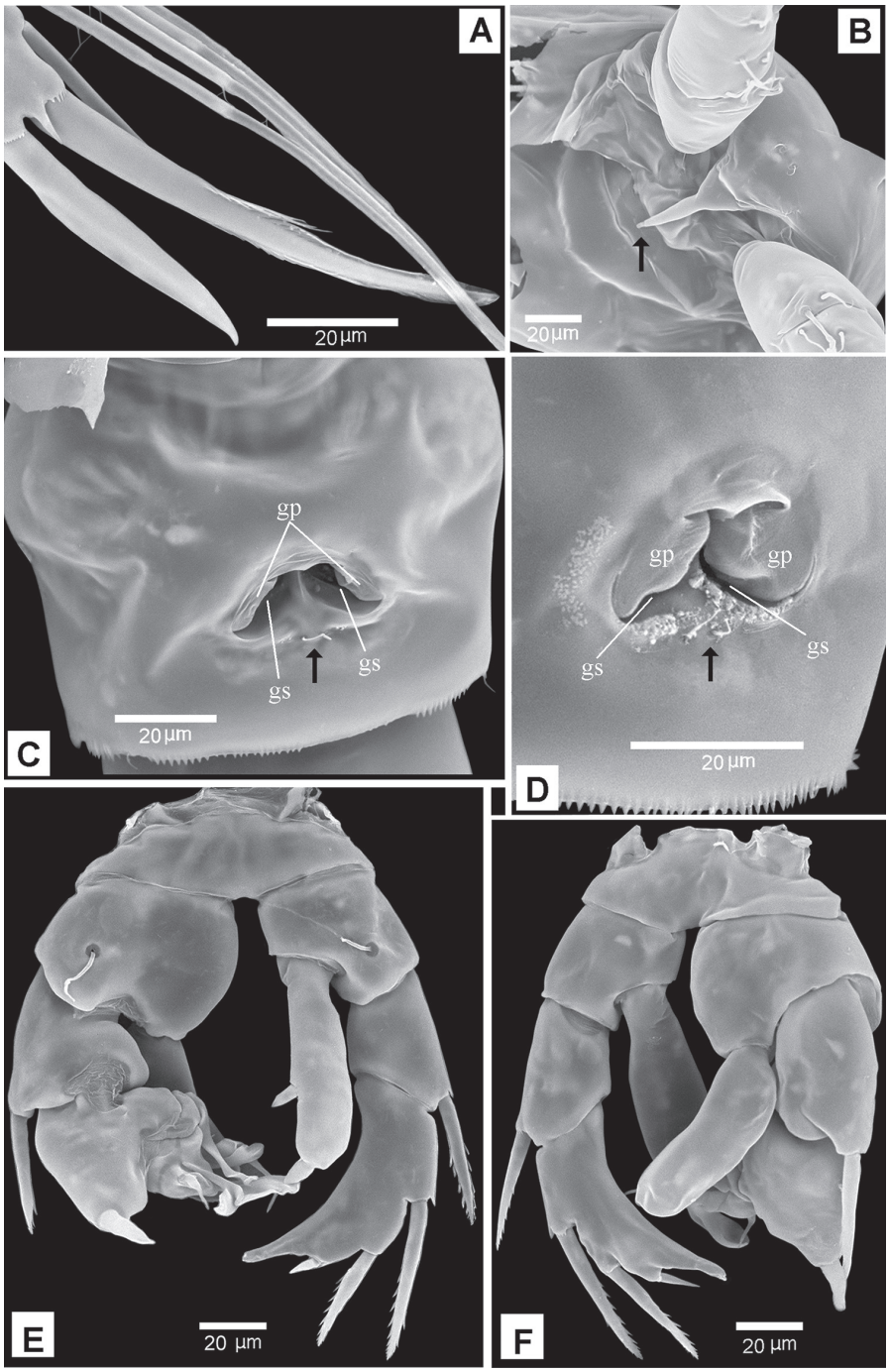

Figure 9. *Boholina reducta* sp. nov., SEM micrographs **A–D** female **E–F** male **A** distal spines of P4 Exp-3 **B** rostrum, ventral view (arrow indicating tip of rostrum) **C** genital double-somite, ventral view (arrow indicating sensilla near gonopores) **D** gonopores, latero-ventral view (arrow indicating sensilla near gonopores) **E** P5, posterior **F** P5, anterior. Abbreviations: gp, gonoporal plates; gs, gonoporal slits.

Table 2. Morphological comparison of seven species of the genus *Boholina*.

	B. ganghwaensis	*B. parapurgata*	*B. purgata*	*B. munaensis*	*B. crassicephala*	*B. laorsriae*	*B. reducta* **sp. nov.**
Female							
Body length (mm)	1.03–1.29	0.93–1.11	0.73–0.79	0.70–0.77	0.75–0.85	0.68–0.73	0.86–0.94
Posterior angle of tergites of pedigerous somites 2–3	Pointed	Pointed	Pointed	Rounded	Rounded	Rounded	Rounded
Shape of rostrum	Narrow rounded	Narrow rounded	Narrow rounded	Transverse crest	Transverse crest	Narrow rounded	Narrow pointed
Gonopores on double-somite	Either side of ventral midline	Either side of ventral midline	Either side of ventral midline	Ventrolaterally	Ventrolaterally	Ventrolaterally	Close together on ventral midline
Small hook-like inner process on gonoporal plate	Present	Absent	Absent	Absent	Absent	Absent	Absent
Septum between gonopores	Narrow	Narrow	Narrow	Large	Large	Large	Reduced
Length/width ratio of caudal ramus	1.6	1.5	?	1.5	?	1,8	1.5
Distal exopodal segments of antenna	Completely separated	Completely separated	Not separated?	Completely separated	Not separated?	Completely separated	Completely separated
No. of setae on medial lobe of antennary Enpd-2	8	8	8	8	8	9	9
No. of setae on basis of mandibular palp	4	4	4	4	4	4	3
No. of setae on distal endopodal segment of mandibular palp	11	10	10	10	10	10	11
Setal formula on exopod of mandibular palp	1:1:1:1:2	0:1:1:1:2	1:1:1:1:2	0:1:1:1:2	1:1:1:1:2	1:1:1:1:2	1:1:1:1:2
Basis and first endopodal segment of maxillule	Incompletely separated	Fused	Fused	Fused	Fused	Separated	Incompletely separated
First and second endopod segment of maxillule	Incompletely separated	Separated	Fused	Separated	Fused	Fused	Fused
No. of setae on exopod of maxillule	10	10	10	10	10	10	11
Seta on basal exite of maxillule	Present	Present	Present	Present	Present	Present	Absent
Setal formula on endopod of maxilliped	2:4:4:3:3+1:4	2:4:4:3:3+1:4	2:4:4:3:3+1:4	2:4:4:3:3+1:4	2:4:4:3:3+1:4	2:4:4:3:3+1:4	2:3:3:3:3+1:4
Outer seta on P3 basis	Present	Absent	Present	Absent	Present	Present	Present
Location of spinule row of distomedial spine of P4 Exp-3	Distal end	Distal end	Distal end	Distal end	Distal end	Distal end	Middle
Length/width ratio of distal endopod segment of P5	2.5	2.6	?	2.6	?	2.0	2.4
Length ratio of inner distal spine and outer terminal spine of P5	1.03	0.78–0.82	?	1.40	?	1.8	1.0
No. of spines on outer margin of P5 Exp-3	2	2	2	2	2	2	1
No. of setae on inner margin of right P5 Exp-3	3	3	3	3	3	3	4
No. of setae on outer margin of P5 Endp-2	2	2	2	1	2	2	1

	B. ganghwaensis	*B. parapurgata*	*B. purgata*	*B. munaensis*	*B. crassicephala*	*B. laorsriae*	*B. reducta* **sp. nov.**
Male							
Body length (mm)	0.87–0.93	0.66–0.71	0.64–0.73	0.68	0.70–0.77	0.65–0.67	0.76–0.83
Process at the antepenultimate segment of right antennule	Present	Absent	Present	Absent	Present	Absent	Absent
Apical spine on P5 basis	Present on both legs	Present on right leg only	Present on right leg only	Absent	Absent	Absent	Absent
No. of segments of right P5 exopod	1	1	1	1	1	1	2
Armature on the distal segment of right P5 exopod	3 strong + 1 vestigial spines	3 strong + 1 vestigial spines	3 strong + 1 vestigial spines	4 strong spines	4 strong spines	4 strong spines + 1 short spiniform seta	2 strong + 1 vestigial spines
Length/width ratio of right P5 endopod	3.2	3.6	2.6	?	?	3.0	3.8
Large inner spiniform process on right P5 endopod	Absent	Absent	Absent	Present	Absent	Absent	Absent
Armature of right P5 endopod	2 slender spines	2 sigmoid spines	2 slender spines	Absent	2 slender spines	2 slender spines	2 sigmoid spines

located on either side of the ventral midline on genital double somites. However, the separation between gonopores is clearly visible in ventral view of the genital double somites (Fosshagen and Iliffe 1989; Boxshall and Jaume 2012; Moon and Soh 2014). In other species of *Boholina*, the gonopores are widely separated (Fosshagen and Iliffe 1989, Boonyanusith et al. 2020), (2) the rostrum has a narrow finger-like process with pointed tip. The shape of rostrum of new species is unique in the Pseudocyclopidae, (3) the basis of mandibular palp has three setae in the new species, while there are four setae in all the species of *Boholina*, (4) there is no outer seta on basal exite of maxillule and there are 11 setae on exopod of maxillule, while there are only ten setae in other species of *Boholina*, (5) the second and third endopodal segments of maxilliped have three setae each, (6) the distomedial spine of P4 Exp-3 is modified with a row of spinules inserted in the middle of inner margin of the spine, (7) the female P5 Exp-3 has only one spine on outer margin, and the proximal outer spine is missing. In *Boholina*, the outer margin of female P5 Exp-3 generally has two spines, (8) female P5 Exp-3 has four setae on the inner margin, while there are three setae both rami in the other species of *Boholina* (Fosshagen and Iliffe 1989; Boxshall and Jaume 2012; Moon and Soh 2014 and Boonyanusith et al. 2020), (9) right P5 exopod has two segments in the male, and (10) the distal segment of right P5 exopod in male has only two strong spines and one short vestigial spine on outer margin and the terminal spine of the segment, which are unique in the genus. This is the first record of *Boholina* and Pseudocyclopidae from Vietnam waters. An updated key to the seven valid species of *Boholina* is provided.

A key to species of the genus *Boholina* (modified from Boonyanusith et al. 2020)

1 Female P5 Exp-3 with four spines in total; male right P5 exopod 1-segmented and distal segment with terminal spine **2**

– Female P5 Exp-3 with three spines in total; male right P5 exopod 2-segmented and distal segment without terminal spine ..... ***Boholina reducta* sp. nov.**

2 Gonopores in female located ventrolaterally; male right P5 exopod with four well-developed spines..... **3**

– Gonopores in female located close together on mid-ventral surface; male right P5 exopod with three well-developed spines..... **5**

3 Female P5 Endp-2 with one seta on outer margin; male right P5 endopod with large spinous process on inner margin..... ..... ***B. munaensis* Boxshall & Jaume, 2012**

– Female P5 Endp-2 with two setae on outer margin; male right P5 endopod without large spinous process on inner margin..... **4**

4 Inner apical spine on female P5 Exp-3 about 1.8 times as long as outer one; male right P5 exopod with minute spiniform seta on inner margin; male left P5 endopod small, much shorter than right P5 endopod..... ..... ***B. laorsriae* Boonyanusith, Wongkamhaeng & Athibai, 202**0

– Apical spines on female P5 Exp-3 subequal in length; male right P5 exopod without spiniform seta on inner margin; male left P5 endopod large, as long as right P5 endopod..... ***B. crassicephala*** **Fosshagen & Iliffe, 1989**

5 Two apical spines on female P5 Exp-3 shorter than segment; the antepenultimate segment of male right antennule with rounded process; male right P5 endopod with two slender spines **6**

– Outer terminal spine on female P5 Exp-3 longer than segment, inner apical spine just shorter; the antepenultimate segment of male right antennule without process; male right P5 endopod with two sigmoid spines..... ..... ***B. parapurgata*** **Boxshall & Jaume, 2012**

6 Outer terminal spine on female P5 Exp-3 shorter than inner apical spine; female gonoporal plate with small hook-like process; male right P5 endopod about 3.2 times as long as wide..... ***B. ganghwaensis*** **Moon & Soh, 2014**

– Outer terminal spine on female P5 Exp-3 longer than inner apical spine; female gonoporal plate without small hook-like process; male right P5 endopod about 2.6 times as long as wide .... ***B. purgata*** **Fosshagen & Iliffe, 1989**

Acknowledgements

Authors appreciate the critical reviews of Dr Seong Yong Moon and Dr Viatcheslav Ivanenko that greatly improved the manuscript. This research is funded by Vietnam National Foundation for Science and Technology Development (NAFOSTED) under grant number 106.05–2017.321. This work was partly supported by a National Research Foundation of Korea (NRF) grant awarded to CY Chang by the Korean government (MSIT) (No. 2019R1F1A1058977).

References

Barthélémy R, Ohtsuka S, Cuoc C (1998) Description and female genital structures of a new species of the demersal calanoid copepod *Ridgewayia* from southern Japan. Journal of Natural History 32(9): 1303–1318. https://doi.org/10.1080/00222939800770651

Boonyanusith C, Wongkamhaeng K, Athibai S (2020) A new species of *Boholina* (Crustacea, Copepoda, Calanoida) and a first record for stygobiotic calanoid fauna from a cave in Thailand. ZooKeys 904: 1–22. https://doi.org/10.3897/zookeys.904.37609

Boxshall GA, Halsey SH (2004) An Introduction to Copepod Diversity. The Ray Society, London, 966 pp.

Boxshall GA, Jaume D (2012) Three new species of copepods (Copepoda: Calanoida and Cyclopoida) from anchialine habitats in Indonesia. Zootaxa 3150(1): 36–58. http://dx.doi.org/10.11646/zootaxa.3150.1.2

Bradford-Grieve JM, Boxshall GA, Blanco-Bercial L (2014) Revision of basal calanoid copepod families, with a description of a new species and genus of Pseudocyclopidae. Zoological Journal of the Linnean Society 171(3): 507–533. https://doi.org/10.1111/zoj.12141

Cuoc C, Defaye D, Brunet M, Notonier R, Mazza J (1997) Female genital structures of Metridinidae (Copepoda: Calanoida). Marine Biology 129: 651–665. https://doi.org/10.1007/s002270050208

Donatis P, Dorigo L, Mocchiutti A, Muscio G, Sello U, Tran TV (2010) Le grotte di Ha Long Bay, Vietnam 2005–2007. Circlo Speleologico e Idrologico Friulano, Udine, Italy, 79 pp.

Ferrari FD, Ivanenko VN (2001) Interpreting segment homologies of the maxilliped of cyclopoid copepods by comparing stage-specific changes during development. Organisms Diversity and Evolution 1: 113–131. https://doi.org/10.1078/1439-6092-00009

Ferrari FD, Ivanenko VN (2008) The identity of protopodal segments and the ramus of maxilla 2 of copepods (Copepoda). Crustaceana 81(7): 823–835. https://doi.org/10.1163/156854008784771702

Figueroa DF (2011a) Phylogenetic analysis of *Ridgewayia* (Copepoda: Calanoida) from the Galapagos and of a new species from the Florida Keys with a reevaluation of the phylogeny of Calanoida. Journal of Crustacean Biology 31(1): 153–165. https://doi.org/10.1651/10-3341.1

Figueroa DF (2011b) Two new calanoid copepods from the Galapagos Islands: *Pseudocyclops juanibali* sp. n. and *Pseudocyclops saenzi* sp. n. Journal of Crustacean Biology 31(4): 725–741. https://doi.org/10.1651/10-3374.1

Fosshagen A (1970) Marine biological investigations in the Bahamas. 15. *Ridgewayia* (Copepoda: Calanoida) and two new genera of calanoids from the Bahamas. Sarsia 44(1): 25–58. https://doi.org/10.1080/00364827.1970.10411178

Fosshagen A, Iliffe TM (1989) *Boholina*, a new genus (Copepoda: Calanoida) with two new species from an anchialine cave in the Philippines. Sarsia 74(3): 201–208. https://doi.org/10.1080/00364827.1989.10413429

Fosshagen A, Iliffe TM (1991) A new genus of calanoid copepod from an anchialine cave in Belize. In: Uye SI, Nishida S, Ho JS (Eds) Proceedings of the Fourth International Conference on Copepoda. Bulletin of Plankton Society of Japan. Special volume: 339–346.

Fosshagen A, Iliffe TM (1998) A new genus of the Ridgewayiidae (Copepoda, Calanoida) from an anchialine cave in the Bahamas. Journal of Marine Systems 15: 373–380. https://doi.org/10.1016/S0924-7963(97)00071-7

Fosshagen A, Iliffe TM (2003) Three new genera of Ridgewayiidae (Copepoda, Calanoida) from anchialine caves in the Bahamas. Sarsia 88(1): 16–35. https://doi.org/10.1080/00364820308465

Huys R, Boxshall GA (1991) Copepod evolution. The Ray Society, London, 468 pp.

Kršinic F (2005) *Badijella jalzici* – a new genus and species of calanoid copepod (Calanoida, Ridgewayiidae) from an anchialine cave on the Croatian Adriatic coast Published in collaboration with the University of Bergen and the Institute of Marine Research, Norway, and the Marine Biological Laboratory, University of Copenhagen, Denmark. Marine Biology Research 1(4): 281–289. https://doi.org/10.1080/17451000500262025

Moon SY, Soh HY (2014) A new species of *Boholina* (Copepoda, Calanoida, Boholinidae) from Ganghwa Island in western Korea. Journal of the Marine Biological Association of the United Kingdom 94(3): 537–545. https://doi.org/10.1017/S002531541300177X

Ohtsuka S, Fosshagen A, Putchakarn S (1999) Three new species of the demersal calanoid copepod *Pseudocyclops* from Phuket, Thailand. Plankton Biology and Ecology 46(2): 132–147.

Suárez-Morales E, Iliffe TM (2007) A new genus of Ridgewayiidae (Copepoda: Calanoida) from a karstic cave of the Western Caribbean. Journal of Crustacean Biology 27(2): 339–350. https://doi.org/10.1651/S-2720.1

Tang D, Barron H, Goater S (2008) A new genus and species of Ridgewayiidae (Copepoda: Calanoida) from subterranean waters of northwestern Australia. Journal of Crustacean Biology 28(3): 551–563. https://doi.org/10.1651/07-2869R.1

Uong DK, Le DA, Tong PT, Tran THN, Bui QD, Nguyen TH (2013) Khai quat ve dieu kien tu nhien, tai nguyen thien nhien 50 dao ven bo Bac Bo Vietnam (co dien tich tu 1 km^2 tro len) [Overview of geographical conditions and natural resources of fifty islands on the Bac Bo coastline of Vietnam]. Tap chi Cac khoa hoc ve trai dat 35(4): 318–326. [In Vietnamese with English summary]

Walter TC, Boxshall G (2020) World of Copepods database. Pseudocyclopidae Giesbrecht, 1893. http://www.marinespecies.org/aphia.php?p=taxdetails&id=104098 [accessed 06 April 2020]

ZooKeys 977: 25–40 (2020)
doi: 10.3897/zookeys.977.57088
https://zookeys.pensoft.net

RESEARCH ARTICLE

A peer-reviewed open-access journal
ZooKeys
Launched to accelerate biodiversity research

A troglobitic species of the centipede *Cryptops* (Chilopoda, Scolopendromorpha) from northwestern Botswana

Gregory D. Edgecombe[1], Nesrine Akkari[2], Edward C. Netherlands[3], Gerhard Du Preez[3]

1 *The Natural History Museum, Cromwell Road, London SW7 5BD, UK* **2** *Naturhistorisches Museum Wien, Burgring 7, 1010 Wien, Austria* **3** *Unit for Environmental Sciences and Management, North-West University, Private Bag X6001, Potchefstroom 2520, South Africa*

Corresponding author: Gregory D. Edgecombe (g.edgecombe@nhm.ac.uk)

Academic editor: Pavel Stoev | Received 30 July 2020 | Accepted 4 September 2020 | Published 22 October 2020

http://zoobank.org/B920BFAD-B398-4F2E-809F-6AF184EEB804

Citation: Edgecombe GD, Akkari N, Netherlands AC, Du Preez G (2020) A troglobitic species of the centipede *Cryptops* (Chilopoda, Scolopendromorpha) from northwestern Botswana. ZooKeys 977: 25–40. https://doi.org/10.3897/zookeys.977.57088

Abstract

A new species of *Cryptops*, *C.* (*Cryptops*) *legagus* **sp. nov.**, occurs in caves in the Koanaka and Gcwihaba Hills in northwestern Botswana. Bayesian molecular phylogenetics using 18S rRNA, 28S rRNA, 16S rRNA and cytochrome *c* oxidase subunit I corroborates a morphological assignment to the subgenus *Cryptops* and closest affinities to southern temperate species in South Africa, Australia and New Zealand. The new species is not conspicuously modified as a troglomorph.

Keywords

biospeleology, Cryptopidae, molecular phylogenetics

Introduction

Cryptops Leach, 1815 is one of the most speciose and geographically widespread centipede genera. Its 150+ species are mostly epigean, but also include troglomorphic species. Troglomorphs display typical modifications of cavernicolous centipedes in

general, such as elongation of the antennae, legs and body, and some degree of depigmentation. Compared to epigean species, troglomorphic *Cryptops* usually have an increased number of tibial and tarsal saw teeth (a diagnostic character of the genus) associated with the elongate articles of the ultimate leg pair.

Troglomorphic species of *Cryptops* have been documented from scattered parts of the world. They include endemic species of the subgenus *Cryptops* from France (Matic 1960), the Canary Islands (Zapparoli 1990), and Brazil (Ázara and Ferreira 2014), and of the subgenus *Trigonocryptops* Verhoeff, 1906, from Spain (Ribaut 1915), Cuba (Matic et al. 1977), Australia (Edgecombe 2005, 2006), and Brazil (Ázara and Ferreira 2013). Several additional species collected from caves are epigean in most occurrences (Negrea 1993; Stoev 2001). A few other species, including records from Greece, Kenya, India, and Morocco, have been collected only from caves but do not depict troglomorphic characters (reviewed by Edgecombe 2005; also Stavropoulos and Matic 1990).

Herein we add to geographic coverage of troglobitic *Cryptops* by documenting a new species from caves in the Koanaka and Gcwihaba Hills in Ngamiland, northwestern Botswana.

Habitat

Cryptops legagus sp. nov. was collected from Diviner's (20°8'32.20"S, 21°12'36.60"E) and Dimapo (20°1'12.34"S, 21°21'38.41"E) caves, which are associated with the Koanaka and Gcwihaba Hills, respectively, in Ngamiland, Botswana. These hills, located 20 km apart, are composed of Precambrian dolomites from the Damara Sequence (Williams et al. 2012). Diviner's and Dimapo caves were discovered by means of gravimetric surveys and exploration drilling followed by the sinking of vertical shafts (70–100 cm diameter). No known natural openings exist. As a result of being sealed, the environmental conditions in these caves are very different from those of other caves with natural openings found on the same hills (Du Preez et al. 2015). Using a Fluke 971 meter, the average temperature and relative humidity levels in Diviner's Cave were 28.5 ± 0.5 °C and 93 ± 5.4%, respectively, as measured on 12 January 2016. Du Preez et al. (2015) reported similar temperature (maximum of 28 °C), but higher relative humidity (maximum 99.9%) levels in Dimapo Cave. Basic measurements in caves with natural openings from the same region recorded average temperature and relative humidity levels of 18 °C and 93%, respectively, during the hot summer months.

The type locality is Paradise Road Balcony, a sampling site within Diviner's Cave at which a single specimen (the holotype) was found dwelling in the cave sediment substrate and fig roots associated with the cave floor. Other invertebrates were also collected from this site, including the pseudoscorpion *Botswanoncus ellisi* Harvey and Du Preez, 2014. Two paratypes were collected from Calcite Baboon Chamber in Diviner's Cave and were primarily associated with large fig tree roots that penetrate the cave roof

[see Harvey and Du Preez (2014) for an optical image of the root system]. Paratype NHMW 10152 was collected from Pirates Cove, a site associated with Dimapo Cave. This single specimen was found inhabiting old termite structures associated with the cave floor. All specimens were collected at an average depth of 50 metres below surface.

Materials and methods

Morphology

Specimens were collected by hand and preserved in 70% ethanol. Types were photographed using a Nikon DS-Ri2 camera mounted on a Nikon SMZ25 stereomicroscope using NIS-Elements Microscope Imaging Software with an Extended Depth of Focus (EDF) patch. Images were edited with Adobe Photoshop CS6 and assembled in InDesign CS6.

Morphological terminology in descriptions follows recommendations by Bonato et al. (2010).

Type material is housed in the Naturhistorisches Museum Wien (prefix NHMW).

Molecular phylogenetics

A specimen from Diviner's Cave fixed in 70% ethanol was used for DNA sequencing. Genomic DNA was extracted using the KAPA Express Extract Kit (Kapa Biosystems, Cape Town, South Africa) as per the manufacturer's instructions. Polymerase chain reaction (PCR) amplifications were performed in a total volume of 25 µL, with 12.5 µL Thermo Scientific DreamTaq PCR master mix (2×) (2× DreamTaq buffer, 0.4 mM of each dNTP, and 4 mM MgCl2), 1.25 µl of each primer (10mM concentration), and 1 µl DNA. The final reaction volume was made up with Milli-q water.

Molecular markers included two nuclear ribosomal genes (18S rRNA and 28S rRNA) and two mitochondrial markers, one ribosomal (16S rRNA) and one protein-encoding (cytochrome *c* oxidase subunit I) following Boyer et al. (2007). The nuclear ribosomal genes were amplified in three overlapping fragments, the 18S rRNA gene was amplified using primer pairs 1F (5'-TACCTGGTTGATCCTGCCAGTAG-3') and 5R (5'-CTTGGCAAATGCTITCGC-3'); 3F (5'-GTTCGATTCCGGAGAGGGA-3') and 18Sbi (5'-GAGTCTCGTTCGTTATCGGA-3'); and 18Sa2.0 (5'-ATGGTTGCAAAGCTGAAAC-3') and 9R (5'-GATCCTTCCGCAGGTTCACCTAC-3') (Giribet et al 1996; Whiting et al. 1997). The fragments of the 28S rRNA gene were amplified using the primer sets 28SD1F (5'-GGGACTACCCCCTGAATTTAAGCAT-3') and 28Sb (5'-TCGGAAGGAACCAGCTAC-3') (Park and Foighil 2000; Edgecombe and Giribet 2006); 28Sa (5'-GACCCGTCTTGAAACACGGA-3') and 28Srd5b (5'-CCACAGCGCCAGTTCTGCTTAC-3') (Whiting et al. 1997; Schwedinger and Giribet 2005); and 28S4.8a (5'-ACCTATTCTCAAACTTTAAATGG-3') and 28S7bi (5'-GACTTCCCTTACCTACAT-3') (Schwedinger and Giribet 2005). A fragment of the 16S rRNA gene was amplified using

the primer pair 16Sar (5'-CGCCTGTTTATCAAAAACAT-3') and 16Sb (5'-CTCCGGTTTGAACTCAGATCA-3') (Xiong and Kocher 1991; Edgecombe et al. 2002). For COI, a fragment of the gene was amplified using the primer set LCO1490 (5'-GGTCAACAAATCATAAAGATATTGG-3') and HCO2198 (5'-TAAACTTCAGGGTGACCAAAAAATCA-3') (Folmer et al. 1994).

For PCR amplification the following conditions were used: initial denaturation at 95 °C for 5 min, followed by 35 cycles, entailing 95 °C denaturation for 30 s, annealing between 45–50 °C for 30 s with an end extension at 72 °C for 1 min, and following the cycles a final extension of 72 °C for 10 min. The PCR reactions were carried out using a ProFlex™ PCR thermal cycler (applied biosystems by life technologies). PCR products were sent to a commercial sequencing company (Inqaba Biotechnical Industries (Pty) Ltd, Pretoria, South Africa) for purification and sequencing in both directions. Resultant sequences were assembled, and chromatogram-based contigs were generated and trimmed using Geneious R11 (http://www.geneious.com) (Kearse et al. 2012). Sequence and species identity were verified against previously published sequences using the Basic Local Alignment Search Tool (BLAST) (Altschul et al. 1990). Sequences obtained in the current study were deposited in the NCBI GenBank database under accession numbers MT925726 (18S rRNA), MT928357 (28S rRNA), MT925727 (16S), and MT920964 (COI).

For the partitioned phylogenetic analysis, representative sequences (18S rDNA, 28S rDNA, 16S rDNA, and COI) from the Cryptopidae, Plutoniumidae, Scolopocryptopidae and Scolopendridae (outgroup) were downloaded from GenBank and aligned to the sequences generated in the current study (Table 1). Concatenated gene sequences were aligned using the Clustal W 2.1 alignment tool (Larkin et al. 2007) under the default settings as implemented in Geneious R11. The final alignment consisted of 27 sequences with a total of 5091 bp positions (1786 bp 18S rDNA, and 2070 bp 28S rDNA, 518 bp 16S rDNA, and 715 bp COI). The partitioned Bayesian inference (BI) analysis was performed using MrBayes 3.2.2 (Huelsenbeck and Ronquist 2001) implemented from within Geneious R11. Prior to the analyses, a model test was performed to determine the most suitable nucleotide substitution model according to the Akaike information criteria (AIC) using jModelTest 2.1.7 (Darriba et al. 2012). The model with the best AIC score for the 18S rRNA and 16S rRNA markers was the General Time Reversible model (Tavaré and Miura 1986) with an estimated proportion of invariable sites and a discrete gamma distribution (GTR + I + G). The model with the best AIC score selected for the 28S rRNA and COI markers was GTR + G. For the BI analysis, the alignment was partitioned according to the 18S rRNA (1–1786 bp), 28S rRNA (1787–3856 bp), 16S rRNA (3857–4375 bp) and COI (4376–5091 bp) genes; the Markov Chain Monte Carlo (MCMC) algorithm was run for 10 million generations, sampling every 100 generations, and using the default parameters. The first 25% of the trees were discarded as 'burn-in' with no 'burn-in' samples being retained. Results were visualised in Tracer (Rambaut et al. 2018) (implemented from within Geneious R11), to assess convergence and the 'burn-in' period.

Table 1. List of species and GenBank accession numbers used in the current study.

Family	Species	Country	18S	28Sb	28Sc	16S	COI
Cryptopidae	*Cryptops anomalans*	UK	KF676406	KF676353	–	KF676457	KF676499
	Cryptops australis	Australia	AY288692	AY288708	–	AY288723	–
	Cryptops doriae	Thailand	KF676407	KF676354	–	KF676458	KF676500
	Cryptops galatheae	Argentina	KF676408	KF676355	–	KF676459	KF676501
	Cryptops hortensis	UK	JX422708	JX422582	JX422597	JX422684	JX422662
	Cryptops lamprethus	New Zealand	JX422709	JX422583	JX422598	JX422685	JX422663
	***Cryptops legagus* sp. nov.**	**Botswana**	**MT925726**	**MT928357**	**MT928357**	**MT925727**	**MT920964**
	Cryptops niuensis	Fiji	JX422710	JX422584	JX422599	JX422686	–
	Cryptops parisi	UK	KF676409	KF676356	–	KF676460	KF676502
	Cryptops punicus	Italy	KF676410	–	–	KF676461	KF676503
	Cryptops sarasini	New Caledonia	JX422711	JX422585	JX422600	JX422687	JX422664
	Cryptops spinipes	Australia	AY288693	AY288709	–	AY288724	AY288743
	Cryptops trisulcatus	Italy	AF000775	AF000783	AF000783	HQ402493	HQ402544
	Cryptops typhloporus	South Africa	KF676411	–	–	KF676462	KF676504
	Cryptops indicus	Vietnam	KF676412	KF676357	–	KF676463	KF676505
	Cryptops weberi	Indonesia	HQ402518	HQ402535	HQ402535	KF676464	HQ402551
Plutoniumidae	*Theatops erythrocephalus*	Portugal	AF000776	HM453279	HM453279	HM453222	–
Scolopocryptopidae	*Newportia quadrimeropus*	Mexico	HQ402511	KF676358	–	HQ402494	HQ402546
	Newportia divergens	Guatemala	JX422714	KF676359	–	JX422691	JX422668
	Newportia ernsti	Dominican Republic	JX422715	JX422587	–	JX422692	JX422669
	Newportia monticola	Costa Rica	HQ402514	KF676360	HQ402531	HQ402497	KF676507
	Newportia stolli	Guatemala	JX422719	JX422591	–	JX422696	JX422673
	Newportia collaris	Brazil	KF676415	KF676361	–	KF676467	KF676508
	Scolopocryptops macrodon	Guyana	JX422721	JX422607	JX422607	JX422699	JX422675
	Scolopocryptops melanostomus	Fiji	JX422723	KF676363	JX422609	JX422701	JX422677
	Scolopocryptops miersii	Brazil	JX422720	KF676364	JX422606	JX422697	JX422674
Scolopendridae	*Scolopendra morsitans*	Senegal	HQ402519	HQ402537	HQ402537	HQ402501	HQ402553

Results

Order Scolopendromorpha Pocock, 1895
Family Cryptopidae Kohlrausch, 1881
Genus *Cryptops* Leach, 1815
Subgenus *Cryptops* Leach, 1815

***Cryptops* (*Cryptops*) *legagus* sp. nov.**
http://zoobank.org/D0C3D8B8-9EAD-4083-B85A-EB004500D761
Figs 1–6

Material. ***Holotype*.** NHMW 10149 (Figs 1–2), Paradise Road Balcony, Diviner's Cave, Koanaka Hills, 20°8'32.20"S, 21°12'36.60"E, leg. 25.xi.2012, G. Du Preez (see "Habitat").

***Paratypes*.** All leg. G. Du Preez. NHMW 10150, Diviner's Cave, leg. 27.iv.2011; NHMW 10151, 'Calcite Baboon Chamber', Diviner's Cave, leg. 27.iv.2011; NHMW 10152, 'Pirates Cove', Dimapo Cave (Gcwihaba Hills), leg. 1.v.2013.

Diagnosis. Cephalic plate contacts T1 without consistent overlap by either. Cephalic plate with paramedian sutures on posterior half and short anterolateral su-

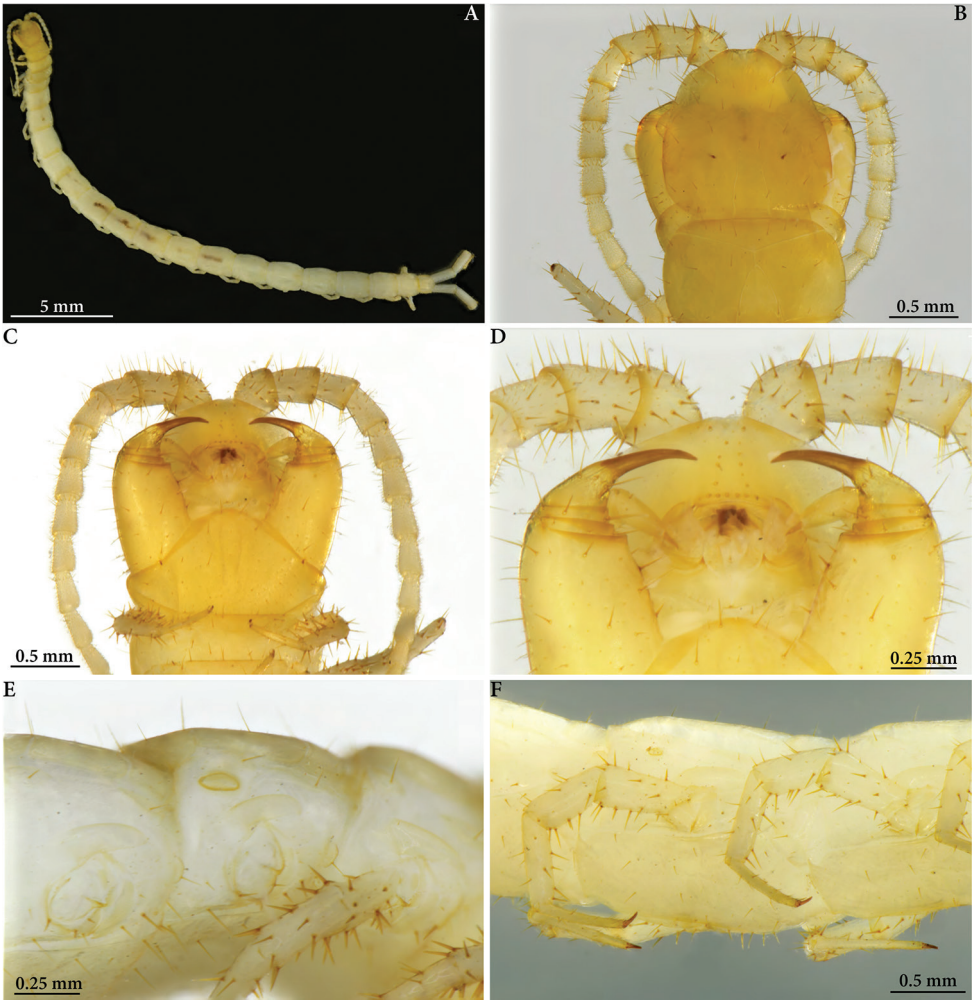

Figure 1. *Cryptops* (*Cryptops*) *legagus* sp. nov., holotype (NHMW 10149) **A** habitus, dorsal view **B** head and T1, dorsal view **C** head and segment 1, ventral view **D** detail of head, ventral view **E** segments 2–4, lateral view, showing spiracle on segment 3 **F** legs 9–10, lateral view.

tures. T1 with shallow V-shaped anterior transverse suture, short median suture and diverging curved, diagonal sutures. Paramedian sutures complete from T2. Pretarsal accessory spines elongate, more than half length of claw. Saw teeth on ultimate leg 1 + 6–8 + 3–4.

Description. The following is based on the holotype unless indicated otherwise, with variation in paratypes indicated in square parentheses.

Length (anterior margin of cephalic plate to posterior margin of telson) 28.5 mm [23.0–31.7 mm].

Cephalic plate orange; TT1–2, forcipular segment and basal part of antenna pale orange, other tergites, sternites and legs more yellow.

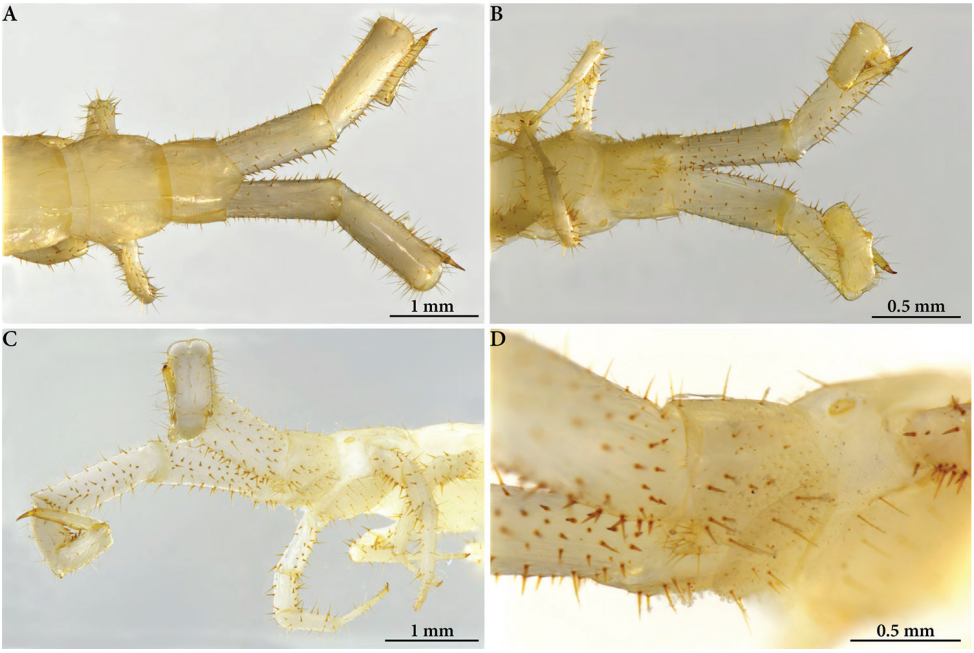

Figure 2. *Cryptops* (*Cryptops*) *legagus* sp. nov., holotype (NHMW 10149). **A–C** segments 19–21, dorsal, ventral and posterolateral views, respectively **D** ultimate leg-bearing segment, ventrolateral view.

Paramedian sutures on posterior half of cephalic plate gently sinuous and converging along most of their length, parallel on their anterior part. Anterolateral sutures short, straight. Fine, slender setae relatively sparse on cephalic plate and tergites, most arranged with bilateral symmetry.

Antenna of 17 articles, extending back to anterior part of T4 [posterior half of T3]. Basal 4–4.5 articles scattered with moderately long, pigmented setae; articles 5–10 with longer setae in a whorl around basal part of article, with short, dense setae prevalent; articles 11–17 densely covered with short setae.

Clypeal setae arranged as 2 (+2 small) + 2 + 2 + 2 + 1 + 2 and transverse band of 8 prelabral setae in holotype; paratypes include 2 (+2 small) + 1 + 2 + 2 + 2.

Coxosternal margin biconvex, bearing a short marginal seta and variably a longer submarginal seta on each side. Coxosternum with relatively sparse, symmetrically arranged short setae, more pervasively scattered with minute setae. Tibia but not femur complete on outer side of forcipule.

Both rami of anterior transverse suture on T1 nearly straight, converging to a point medially from which a short median suture extends posteriorly, then branches into divergent sutures with gentle outward convexity. Paramedian sutures complete from TT2–20; sutures on T2 with posterior half more strongly divergent posteriorly than anterior half, more or less bell-shaped, from T3 posteriorly progressively more parallel. Oblique sutures on TT2–3[4]. Lateral crescentic sulci on TT3–19.

Spiracles elongate oval in outline.

Figure 3. *Cryptops* (*Cryptops*) *legagus* sp. nov., paratype NHMW 10152 **A** head and segment 1, dorsal view **B** ultimate leg-bearing segment, posterolateral view, showing coxopleural pore field **C** distal articles of ultimate leg, showing femoral, tibial and tarsal saw teeth.

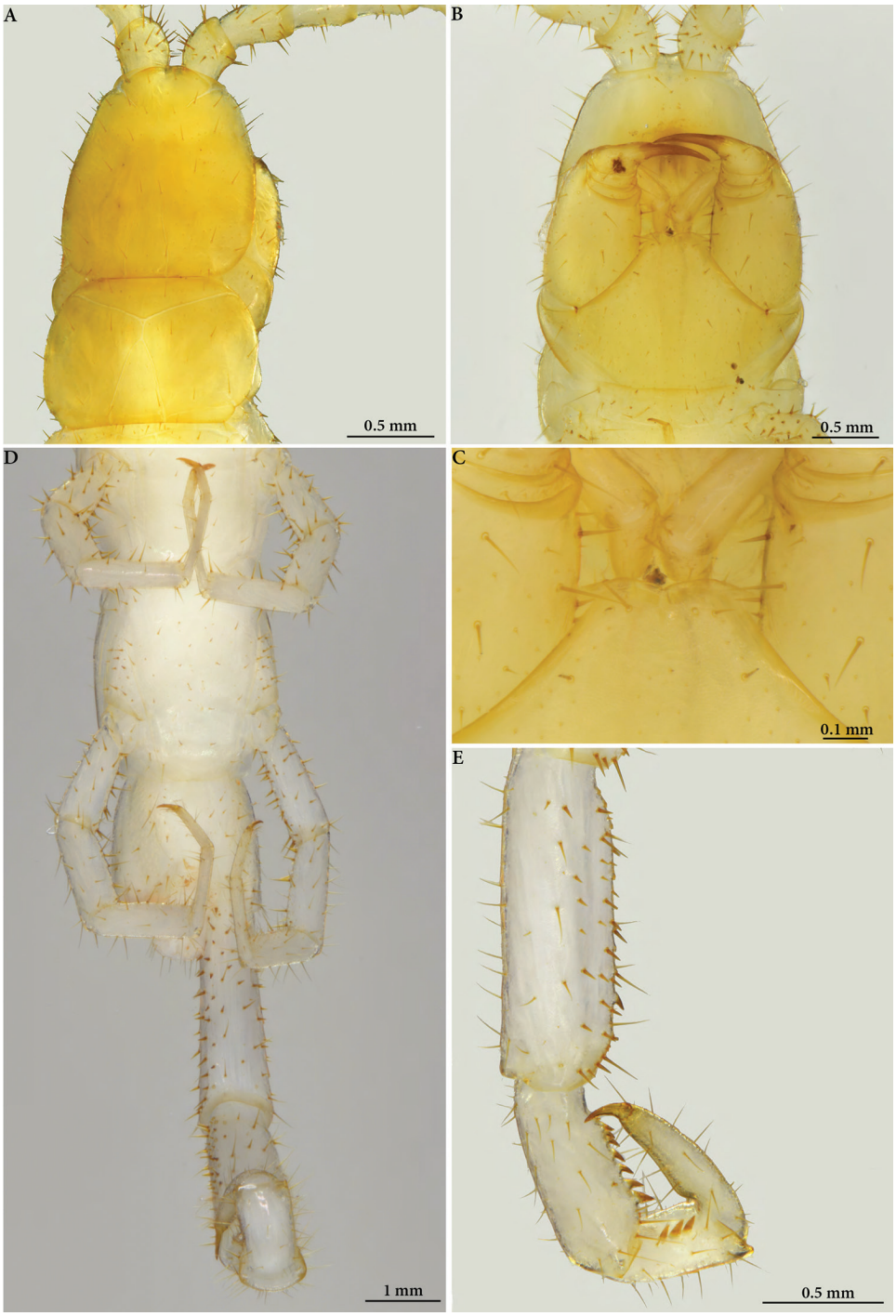

Figure 4. *Cryptops* (*Cryptops*) *legagus* sp. nov., paratype NHMW 10150 **A, B** head and segment 1, dorsal and ventral views **C** forcipular coxosternal margin, ventral view **D** segments 19–21, ventral view **E** distal articles of ultimate leg, showing femoral, tibial and tarsal saw teeth.

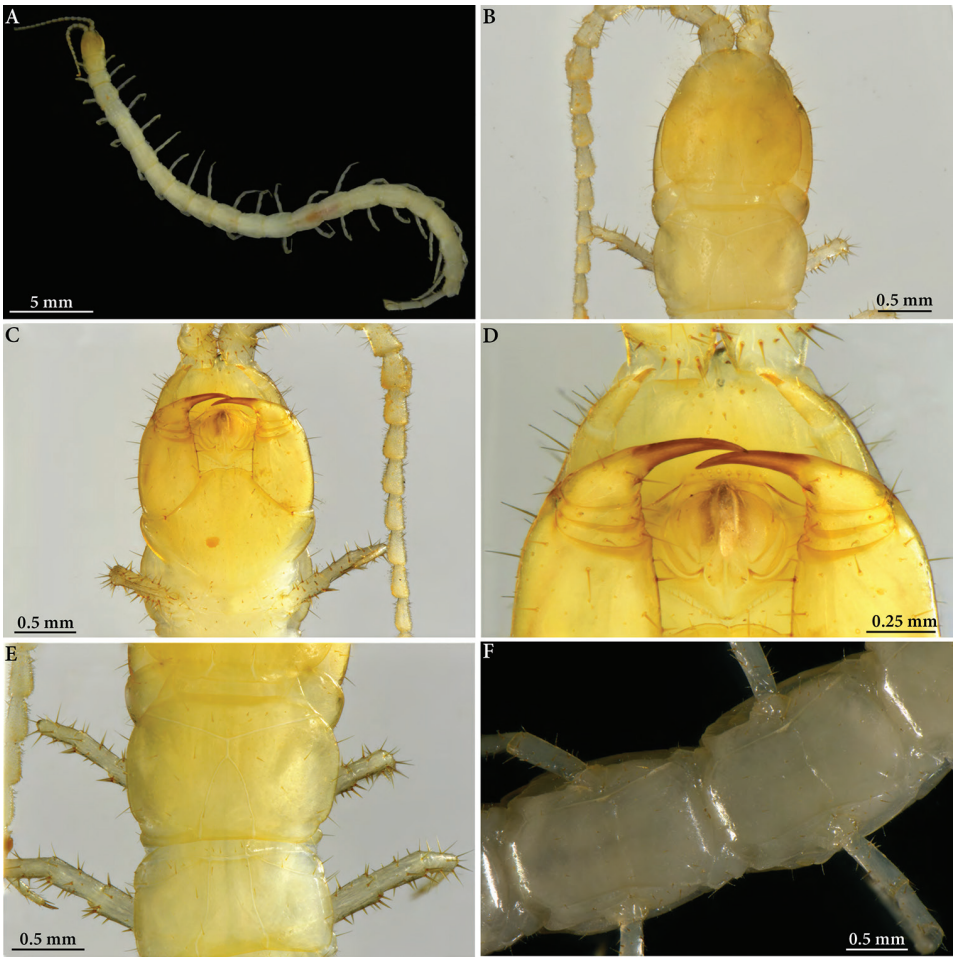

Figure 5. *Cryptops* (*Cryptops*) *legagus* sp. nov., paratype NHMW 10151 **A** habitus, dorsal view **B, C** head and segment 1, dorsal and ventral views **D** detail of head (clypeus, first maxilla and forcipule), ventral view **E** leg-bearing segments 1 and 2, dorsal view **F** cruciform sulci on sternites.

Sternites 2–19 with cruciform sulci. Endosternite on anterior segments without trigonal sutures.

Prefemur, femur and tibia on locomotory legs with strongly pigmented setae, many of those of tibia finer than on more proximal articles; tarsus with more slender, paler setae. Tarsal articulations distinct, mostly with negligible flexure on legs 1–18, flexed on legs 19–21 [all tarsi flexed in NHMW 10150]. Pretarsi of legs 1–20 with pair of long accessory spines, consistently more than half length of claw, up to 75% length of claw on some legs; accessory spines lacking on ultimate leg.

Tergite of ultimate leg-bearing segment with two straight sectors on posterior margin that converge medially to a blunt angle; shallow depression posteriorly. Sternite of ultimate leg-bearing segment with lateral margins gently convex outwards, posterior margin nearly straight or gently convex. Coxopleural pore field elongate oval, occupying anterior

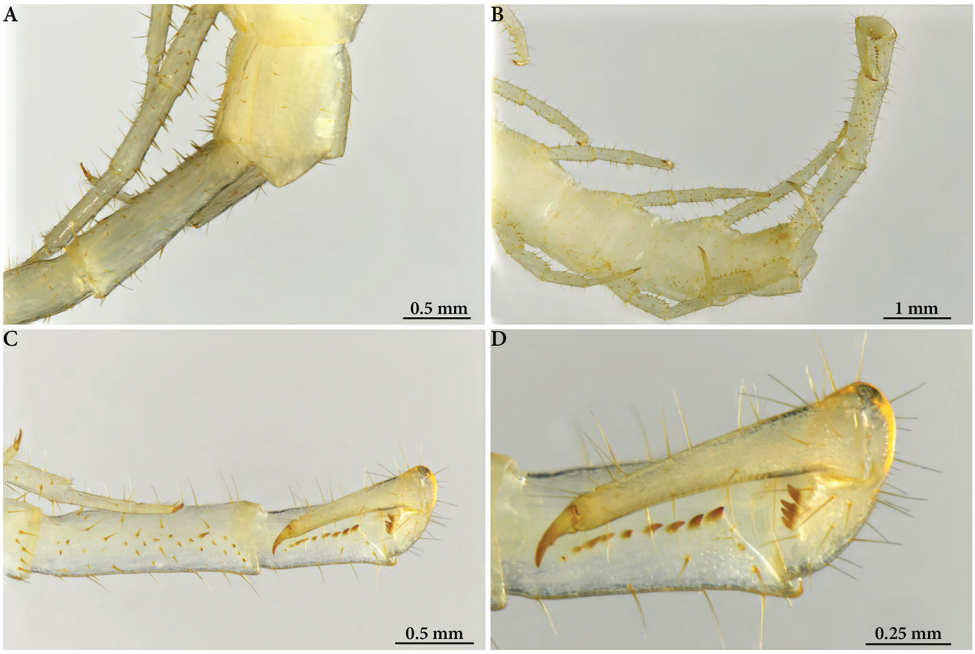

Figure 6. *Cryptops* (*Cryptops*) *legagus* sp. nov., paratype NHMW 10151 **A** segments 20–21, dorsal view **B** segments 18–21, ventrolateral view **C, D** distal articles of ultimate leg and detail of tibia, tarsus and pretarsus, ventral views, showing saw teeth.

75% of coxopleuron, pore-free margin with up to five fairly robust setae arranged as an anterior pair and a posterior row of three. All specimens with more than 30 coxal pores in area not concealed by sternite, ca 60 in highest count, a nearly complete pore field; pores variable in size; two or three short, robust setae and a few more tiny setae within pore field.

Ultimate leg of paratype (body length 25.8 mm) with prefemur 1.4 mm, femur 1.5 mm, tibia 0.9 mm, tarsus 1 0.5 mm, tarsus 2 0.65 mm, pretarsus 0.2 mm. Ultimate leg with distinctly densest and most robust, lanceolate setae on ventromedial parts of prefemur and femur, these articles sparsely setose dorsally. Saw teeth 1 + 6–7[8] + 3–4.

Etymology. *Legaga*, Tswana for "cave".

Discussion

As noted in the Introduction, troglobitic species of *Cryptops* are members of either of the subgenera *Cryptops* or *Trigonocryptops*. Most of the apomorphies for *Trigonocryptops* are not present in *C. legagus* sp. nov., and in these characters the species corresponds to the nominate subgenus. Notably, the endosternite is not delimited by trigonal sutures, the clypeus lacks an anterior setose area outlined by sutures, and the femur and tibia of the ultimate legs lack distal spinose projections.

No species of *Cryptops* shares the observed combination of suture configurations on the cephalic plate and T1. The inverted Y-shaped sutures on T1 are reminiscent of

C. trisulcatus Brölemann, 1902, and even more so to some specimens of *C. anomalans* Newport, 1844 (such as the synonymous *C. savignyi hirtitarsis* Brölemann; see Brölemann 1930, fig. 340) and a few other taxa of the *C. anomalans* group sensu Lewis (2011). The new species is readily distinguished from *C. trisulcatus* in having a substantially longer median suture on T1 and longer paramedian sutures on the posterior part of the cephalic plate. Our phylogenetic analysis (Fig. 7) does not recover an especially close relationship between *C. legagus* sp. nov. and either *C. trisulcatus* or *C. anomalans*, implying convergence in the shared suture patterns.

The molecular data indicate closest relationships to other Southern Hemisphere species of *Cryptops* (*Cryptops*). All four loci independently recover the New Zealand spe-

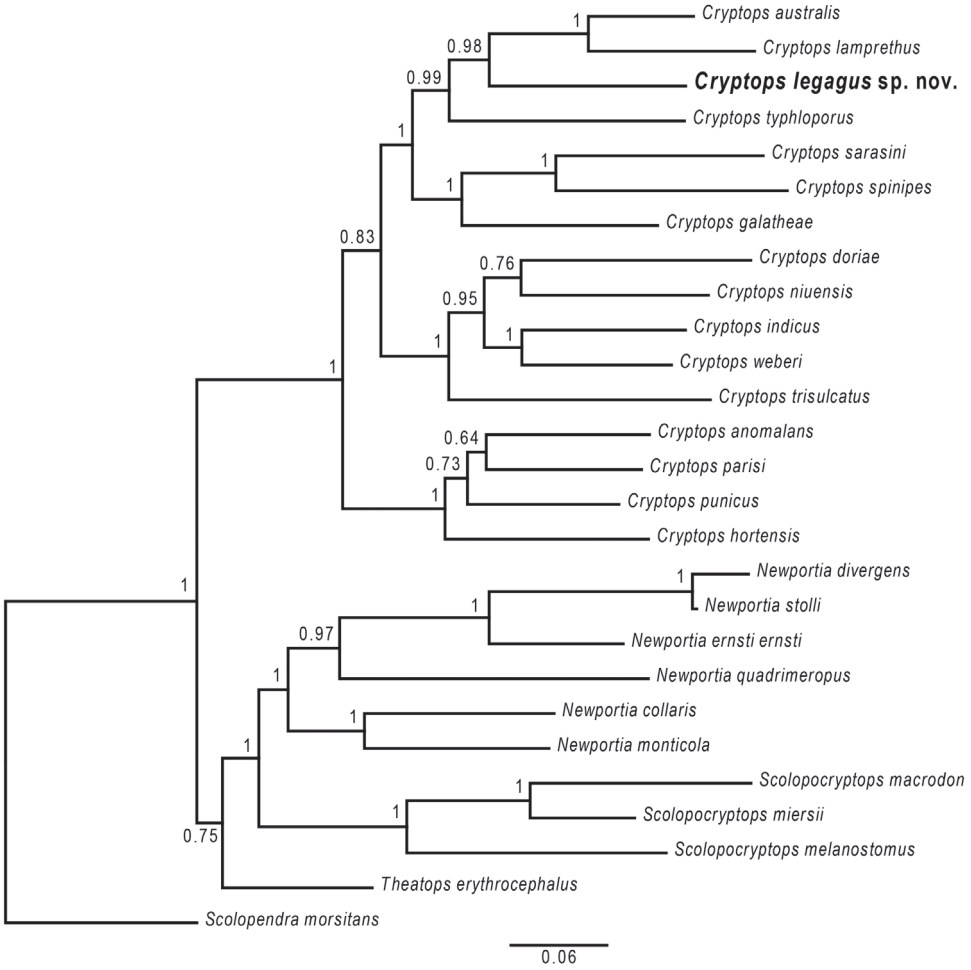

Figure 7. Bayesian tree for blind scolopendromorphs based on partitioned concatenated datasets of four molecular loci 18S rRNA, 28S rRNA, 16S rRNA and cytochrome *c* oxidase subunit I. Numbers at nodes are posterior probabilities. The scale bar represents 0.05 nucleotide substitutions per site.

cies *C. lamprethus* Chamberlin, 1920 as a close relative, and 16S and COI both find a clade including *C. lamprethus* and *C. typhloporus* Lawrence, 1955 from South Africa. The combined data for all four genes add the New Zealand/Australian *C. australis* Newport, 1845 to this clade, allying it most closely to *C. lamprethus*, with *C. legagus* sp. nov. and *C. typhloporus* as successive sister species. The three related species all lack sutures on the cephalic plate and T1 and are members of the *C. doriae* group within Old World *C.* (*Cryptops*) as defined by Lewis (2011). This consists of species having incomplete paramedian sutures on the cephalic plate, lacking an anterior transverse suture on T1, and bearing one or more femoral saw teeth on the ultimate leg. The first and third of these characters are shared by *C. legagus* sp. nov., although the sutures on the cephalic plate are longer in *C. legagus* sp. nov. than in all the others, and the T1 sutures differ strikingly. As relationships within this Southern temperate clade are strongly supported in the molecular tree (posterior probability 0.98–1 for all three nodes), as is a closer affinity between it and *C.* (*Trigonocryptops*) than to the nominate species of the *C. doriae* group, at least some of the characters delimiting groups morphologically are evidently homoplastic.

Despite its troglobitic occurrence, only the relatively pale pigmentation and elongate pretarsal accessory spines (shared with troglomorphic Australian *Cryptops*: Edgecombe 2005, 2006) suggest a degree of troglomorphy. Neither the antennae nor legs show much elongation, nor are the tergites/sternites conspicuously longer than in typical epigean species, nor are numbers of saw teeth on the ultimate legs particularly high. The slight troglomorphic modifications suggest that it is unlikely to be an epigean species.

Acknowledgements

The authors thank the Government of Botswana for facilitating access to the Gcwihaba Caves and the Potch Potholers for field assistance, and the journal's editor, Pavel Stoev, and referees Stylianos Simaiakis and Ivan Tuf, for advice. A special word of thanks is extended to Roger Ellis who coordinated the Gcwihaba Caves Project excursions.

References

Altschul SF, Gish W, Miller W, Myers EW, Lipman DJ (1990) Basic local alignment search tool. Journal of Molecular Biology 215: 403–410. https://doi.org/10.1016/S0022-2836(05)80360-2

Ázara LN de, Ferreira RL (2013) The first troglobitic *Cryptops* (*Trigonocryptops*) (Chilopoda: Scolopendromorpha) from South America and the description of a non-troglobitic species from Brazil. Zootaxa 3709(5): 432–444. https://doi.org/10.11646/zootaxa.3709.5.2

Ázara LN de, Ferreira RL (2014) *Cryptops* (*Cryptops*) *spelaeoraptor* n. sp. a remarkable troglobitic species (Chilopoda: Scolopendromorpha) from Brazil. Zootaxa 3826(1): 291–300. https://doi.org/10.11646/zootaxa.3709.5.2

Bonato L, Edgecombe GD, Lewis JGE, Minelli A, Pereira LA, Shelley RM, Zapparoli M (2010) a common terminology for the external anatomy of centipedes (Chilopoda). ZooKeys 69: 17–51. https://doi.org/10.3897/zookeys.69.737

Boyer SL, Clouse RM, Benavides LR, Sharma P, Schwendinger PJ, Karunarathna I, Giribet G (2007) Biogeography of the world: a case study from cyphophthalmid Opiliones, a globally distributed group of arachnids. Journal of Biogeography 34: 2070–2085. https://doi.org/10.1111/j.1365-2699.2007.01755.x

Brölemann HW (1902) Matériaux pour servir à une faune des myriapodes de France. Feuille des Jeunes Naturalistes 32(377): 98–104.

Brölemann HW (1930) Eléménts d'une Faune des Myriapodes de France. Chilopodes. Faune de France 25, Paris, Imprimerie Toulousaine, 405 pp.

Chamberlin RV (1920) The Myriopoda of the Australian Region. Bulletin of the Museum of Comparative Zoology at Harvard College 64: 1–269.

Darriba D, Taboada GL, Doallo R, Posada D (2012) jModelTest 2: more models, new heuristics and parallel computing. Nature Methods 9: 772. https://doi.org/10.1038/nmeth.2109

Du Preez GC, Forti P, Jacobs G, Jordaan A, Tiedt LR (2015) Hairy stalagmites, a new biogenic root speleothem from Botswana. International Journal of Speleology 44: 37–47. https://doi.org/10.5038/1827-806X.44.1.4

Edgecombe GD (2005) A troglomorphic species of the centipede *Cryptops* (*Trigonocryptops*) (Chilopoda: Scolopendromorpha) from Western Australia. Records of the Western Australian Museum 22: 315–323. https://doi.org/10.18195/issn.0312-3162.22(4).2005.315-323

Edgecombe GD (2006) A troglobitic cryptopid centipede (Chilopoda: Scolopendromorpha) from western Queensland. Records of the Western Australian Museum 23: 193–198. https://doi.org/10.18195/issn.0312-3162.23(2).2006.193-198

Edgecombe GD, Giribet G (2006) A century later – a total evidence re-evaluation of the phylogeny of scutigeromorph centipedes (Myriapoda: Chilopoda). Invertebrate Systematics 20: 503–525. https://doi.org/10.1071/IS05044

Edgecombe GD, Giribet G, Wheeler WC (2002) Phylogeny of Henicopidae (Chilopoda: Lithobiomorpha): a combined analysis of morphology and five molecular loci. Systematic Entomology 27: 31–64. https://doi.org/10.1046/j.0307-6970.2001.00163.x

Folmer O, Black M, Hoeh W, Lutz R, Vrijenhoek RC (1994) DNA primers for amplification of mitochondrial cytochrome *c* oxidase subunit I from diverse metazoan invertebrates. Molecular Marine Biology and Biotechnology 3: 294–299.

Giribet G, Carranza S, Baguna J, Riutort M, Ribera C (1996) First molecular evidence for the existence of a Tardigrada + Arthropoda clade. Molecular Biology and Evolution 13: 76–84. https://doi.org/10.1093/oxfordjournals.molbev.a025573

Harvey MS, Du Preez G (2014) A new troglobitic ideoroncid pseudoscorpion (Pseudoscorpiones: Ideoroncidae) from southern Africa. Journal of Arachnology 42: 105–110. https://doi.org/10.1636/K13-55.1

Huelsenbeck JP, Ronquist F (2001) MrBayes: Bayesian inference of phylogenetic trees. Bioinformatics 17: 754–755. https://doi.org/10.1093/bioinformatics/17.8.754

Kearse M, Moir R, Wilson A, Stones-Havas S, Cheung M, Sturrock S, Buxton S, Cooper A, Markowitz S, Duran C (2012) Geneious Basic: an integrated and extendable desktop

software platform for the organization and analysis of sequence data. Bioinformatics 28: 1647–1649. https://doi.org/10.1093/bioinformatics/bts199

Larkin MA, Blackshields G, Brown N, Chenna R, McGettigan PA, McWilliam H, Valentin F, Wallace IM, Wilm A, Lopez R (2007) Clustal W and Clustal X version 2.0. Bioinformatics 23: 2947–2948. https://doi.org/10.1093/bioinformatics/btm404

Lawrence RF (1955) A review of the centipedes (Chilopoda) of Natal and Zululand. Annals of the Natal Museum 13: 121–174.

Leach WE (1815) A tabular view of the external characters of the four classes of animals which Linné arranged under Insecta; with the distribution of the genera comprising three of these classes into orders, etc, and descriptions of several new genera and species. Transactions of the Linnean Society of London, Series 1, 11: 306–400. https://doi.org/10.1111/j.1096-3642.1813.tb00065.x

Lewis JGE (2013) A review of species in the genus *Cryptops* Leach, 1815 from the Old World and the Australasian region related to *Cryptops* (*Cryptops*) *doriae* Pocock, 1891 (Chilopoda: Scolopendromorpha: Cryptopidae). Zootaxa 2683: 1–34. https://doi.org/10.11646/zootaxa.3683.1.1

Matic Z (1960) Die Cryptopiden (Myriopoda, Chilopoda) der Sammlung des Speleologischen Institutes "E. Gh. Racovita" aus Cluj. Zoologischer Anzeiger 165: 442–447.

Matic Z, Negrea S, Fundora Martínez C (1977) Recherches sur les Chilopodes hypogés de Cuba (II). Résultats des expeditions biospélogiques cubanoroumaines à Cuba 2: 277–301.

Negrea Ş (1993) Sur une population troglobionte de *Cryptops anomalans* Newport, 1844 (Chilopoda, Scolopendromorpha) trouvée dans la grotte "Pestera de la Movile" (Dobrogea, Roumanie). Travaux de l'Institut de Spéologie "Émile Racovitza" 32: 87–94.

Newport G (1844) A list of the species of Myriapoda, Order Chilopoda, contained in the cabinets of the British Museum with synoptic descriptions of forty-seven new species. Annals & Magazine of Natural History 13: 94–101. https://doi.org/10.1080/03745484409442576

Newport G (1845) Monograph of the class Myriapoda, order Chilopoda; with observations on the general arrangement of the Articulata. Transactions of the Linnean Society of London 19: 265–302, 349–438. https://doi.org/10.1111/j.1096-3642.1842.tb00370.x

Park J-K, Foighil DÓ (2000) Sphaeriid and corbiculid clams represent separate heterodont bivalve radiations into freshwater environments. Molecular Phylogenetics and Evolution 14: 75–88. https://doi.org/10.1006/mpev.1999.0691

Rambaut A, Drummond AJ, Xie D, Baele G, Suchard MA (2018) Posterior summarisation in Bayesian phylogenetics using Tracer 1.7. Systematic Biology 67: 901–904. https://doi.org/10.1093/sysbio/syy032

Ribaut H (1915) Biospeleologica, XXXVI. Notostigmophora, Scolopendromorpha, Geophilomorpha (Myriapodes) (Première Série). Archives de Zoologie Expérimentale et Générale 55: 323–356.

Schwendinger PJ, Giribet G (2005) The systematics of the south-east Asian genus *Fangensis* Rambla (Opiliones: Cyphophthalmi: Stylocellidae). Invertebrate Systematics 19: 297–323. https://doi.org/10.1071/IS05023

Stavropoulos G, Matic Z (1990) Nouvelles contributions à l'étude de la faune de chilopodes (Chilopoda) de Grèce. Biologia Gallo-hellenica 17 (1): 37–48.

Stoev P (2001) A synopsis of the Bulgarian cave centipedes (Chilopoda). Arthropoda Selecta 10: 31–54.

Tavaré S, Miura RM (1986) Some probabilistic and statistical problems in the analysis of DNA sequences. Lectures on Mathematics in the Life Sciences (17): 57–86.

Whiting MF, Carpenter JC, Wheeler QD, Wheeler WC (1997) The Strepsiptera problem: phylogeny of the holometabologus insect orders inferred from 18S abd 28S ribosomal DNA sequences and morphology. Systematic Biology 46:1–68. https://doi.org/10.1093/sysbio/46.1.1

Williams BA, Ross CF, Frost SR, Waddle DM, Gabadirwe M, Brook GA (2012) Fossil *Papio* cranium from Ncumtsa (Koanaka) Hills, western Ngamiland, Botswana. American Journal of Physical Anthropology 149: 1–17. https://doi.org/10.1002/ajpa.22093

Xiong B, Kocher TD (1991) Comparison of mitochondrial DNA sequences of seven morphospecies of black flies (Diptera: Simuliidae). Genome 34: 306–311. https://doi.org/10.1139/g91-050

Zapparoli M (1990) *Cryptops vulcanicus* n. sp., a new species from a lava tube of the Canary Islands (Chilopoda, Scolopendromorpha). Vieraea 19: 153–160.

ZooKeys 977: 41–74 (2020)
doi: 10.3897/zookeys.977.56314
https://zookeys.pensoft.net

RESEARCH ARTICLE

A peer-reviewed open-access journal
ZooKeys
Launched to accelerate biodiversity research

First contribution to the doryctine fauna (Hymenoptera, Braconidae, Doryctinae) of Farasan Archipelago, Saudi Arabia, with new records and the description of a new species

Yusuf A. Edmardash[1], Usama M. Abu El-Ghiet[2,3], Ahmed M. Soliman[4,5], Zarrag I. A. Al-Fifi[2], Neveen S. Gadallah[1]

1 *Entomology Department, Faculty of Science, Cairo University, Giza, Egypt* **2** *Biology Department, Faculty of Science, Jazan University, Saudi Arabia* **3** *Plant Protection Department, Desert Research Center, Cairo, Egypt* **4** *Plant Protection Department, College of Food and Agriculture Sciences, King Saud University, Riyadh, Saudi Arabia* **5** *Zoology Department, Faculty of Science (Boys), Al-Azhar University, Nasr City, Cairo, Egypt*

Corresponding author: Neveen S. Gadallah (n_gadallah@hotmail.com)

Academic editor: K. van Achterberg | Received 8 July 2020 | Accepted 5 September 2020 | Published 22 October 2020

http://zoobank.org/D2CB068E-2792-4007-B8AF-D8B65B0B7A6C

Citation: Edmardash YA, Abu El-Ghiet UM, Soliman AM, Al-Fifi ZIA, Gadallah NS (2020) First contribution to the doryctine fauna (Hymenoptera, Braconidae, Doryctinae) of Farasan Archipelago, Saudi Arabia, with new records and the description of a new species. ZooKeys 977: 41–74. https://doi.org/10.3897/zookeys.977.56314

Abstract

The doryctine wasp species (Hymenoptera: Braconidae) of Farasan Archipelago (Saudi Arabia) are studied here for the first time. Six species are reported, of which *Mimodoryctes arabicus* Edmardash, Gadallah & Soliman is described and illustrated as a new species. *Neoheterospilus* sp. is most probably a new species but further collecting should be done to obtain the female. Four species are new records for Saudi Arabia as well as for the whole Arabian Peninsula: *Dendrosotinus ferrugineus* (Marshall, 1888), *Hecabalodes anthaxiae* Wilkinson, 1929, *Mimodoryctes proprius* Belokobylskij, 2001, and *Rhaconotus* (*Rhaconotus*) *carinatus* Polaszek, 1994. The newly recorded species are re-described and illustrated.

Keywords

Afrotropical region, Braconidae, Doryctinae, Doryctini, Hecabolini, Heterospilini, *Mimodoryctes*, Rhaconotini

Introduction

The Farasan Archipelago is situated in the southern part of the Red Sea ca. 40 km west of mainland of Jazan mainland coast (Saudi Arabia) [16°41'48"N, 42°7'20"E] (Muoftah 1990; Strumia and Dawah 2019), and has a width of approximately 120 km in SE-NW direction (Alfarhan et al. 2002). A total of 36 big and small islands make up the Farasan group of Islands (Alfarhan et al. 2002), the largest of which is Farasan Al-Kabir (= Greater Farasan, see Fig. 1) (369 km^2) (Strumia and Dawah 2019). In 1996 Farasan Al-Kabir was established as a protected area by the Saudi Wildlife Commission (SWC), for conserving and restoring animal wildlife, especially the only remaining wild population of Arabian gazelle (El-Demerdash 1996; Alfarhan et al. 2002). Although Farasan lies within the Afro-Asian phytogeographical zone, the floral elements recorded to have the affinity with the Afrotropical, South Palaearctic (Mediterranean) and Oriental regions (Strumia and Dawah 2019). There are no weather stations located in any part of the archipelago, the climate data is therefore is collected from Jazan meteorological station (Alfarhan et al. 2002). The Farasan Archipelago is characterized by the long hot season extending from April to October, and a short mild one (from November to March), with the mean annual temperature is 30 °C, and the mean relative humidity in winter 70–80% and in summer 65–78%.

Among the most important factors that makes Farasan Archipelago unique is the presence of two important Mangrove populations, *Avicennia marina* (Forssk.) (Acanthaceae), and *Rhizophora mucronata* Lam. (Rhizophoraceae), with their ecological and highly productive littoral biotopes which are important as a refuge for many small animals, birds and fish (Mandura et al. 1987). The flora of Farasan comprises 245 species in 152 genera and 52 families (http://ffa.myspecies.info/taxonomy/Term/12). Vegetation along the shoreline of Farasan and Al-Sajid islands is dominated by *Avicennia marina*, whereas Zifaf and Dumsuq islands are dominated by *Rhizophora mucronata* along with *Avicennia marina*. Vegetation in sandy beaches is dominated by halophytes, such as *Aeluropus lagopoides* (L.) (Poaceae), *Cressa cretica* L. (Convolvulaceae), *Halopeplis perfoliata* (Forssk.) (Amaranthaceae), *Limonium axillare* (Forssk.) (Plumbaginaceae), and *Zygophyllum* spp. (Zygophyllaceae) (Alfarhan et al. 2002). Communities of *Vachellia flava* (Forssk.) (Fabaceae), *Blepharis ciliaris* (L.) (Acanthaceae), *Commiphora gileadensis* (L.) (Burseraceae), *Euphorbia fractiflexa* Carter & Wood (Euphorbiaceae), and *Salvadora persica* L. (Salvadoraceae) are also present in almost all the major islands (Alwelaie et al. 1993).

The Doryctinae Foerster, 1863 is one of the richest, most diverse and most speciose subfamilies of the family Braconidae, second only to Microgastrinae in species richness (Shaw 1995; Marsh 1997; Yu et al. 2016). There are more than 2000 described species in ca. 198 genera and 15 tribes (Braet 2016; Yu et al. 2016; Chen and van Achterberg 2019), and the true number is estimated to be ca. 3000 species. The genus *Heterospilus* Haliday is the most diversified genus in terms of species number and host range (Belokobylskij et al. 2004; Yu et al. 2016). They are mostly distributed in tropical and subtropical regions and are especially diverse in the Neotropical region (Shenefelt

and Marsh 1976; Belokobylskij 1992; Marsh 1993, 1997; Marsh et al. 2013). The definition of the subfamily is problematic (Chen and van Achterberg 2019), as is not supported by the use of morphological characters alone, because of the presence of homoplasies (Belokobylskij et al. 2004). It should be revised on the basis of molecular studies (Zaldívar-Riverón et al. 2006, 2008).

Dorytines are cyclostome braconids, diagnosed by the following combination of characters: fore tibia with row or (rarely) cluster of stout pegs along the anterior edge that are distinct from regular setae; hind coxa often with basoventral tubercle; epicnemial and occipital carinae present, which are rarely absent; propleuron with a large, dorso-posterior flange just above the fore coxa, and extending slightly over the ventrolateral corner of the pronotum; ovipositor strongly sclerotized, distinctly darkened apically; dorsal valve of ovipositor double nodus subapically more or less developed (Quicke et al. 1993; van Achterberg 1993; Marsh 2002). One of the main characters that was traditionally used within doryctine genera is the relative length of basal sternal plate of T1 (= acrosternite *sensu* Belokobylskij 1995). This structure can be short and sessile, or long and petiolate (Belokobylskij 1995; Marsh 1997).

The first attempt to study the evolutionary relationships between the genera of Doryctinae was carried out by Belokobylskij et al. (2004) using morphological characters of 143 genera. However, most of the relationships could not be resolved with the characters used, resulting in an inability to propose a higher classification the subfamily Doryctinae. The monophyly of Doryctinae was also not recovered in some studies, whether based on morphological characters (e.g., Belokobylskij et al. 2004), or on molecular analysis (e.g., Dowton et al. 1998; Zaldivar-Riverón et al. 2007, 2008; Sharanowski et al. 2011), or on a combined morphological and molecular analysis of cyclostome braconids (Zaldivar-Riverón et al. 2006), and so it remains in doubt (Chen and van Achterberg 2019).

Species of the subfamily Doryctinae are not only diverse morphologically but also in their biology (Belokobylskij et al. 2004). From available host records, they are exclusively idiobiont ectoparasitoids of concealed or semi-concealed larvae of wood boring insects, including xylophagous beetles, Lepidoptera and sawflies (van Achterberg 1993; Belokobylskij et al. 2004), termites (Isoptera), and even (as exception) Embioptera (Shaw and Edgerly 1985). A few are known to be phytophagous in seeds (Marsh 1991; de Macêdo and Monteiro 1989; Marsh et al. 2000). Recently, several genera have been discovered to be gall inducers, while others are suspected of being predators of gallers (Zaldívar-Riverón et al. 2007, 2014). In Costa Rica, an unusual biology was discovered in species that are inquilines in figs, where they exhibit an extreme sexual dimorphism that resembles that of chalcid fig wasps (Ramírez and Marsh 1996; van Achterberg and Marsh 2002). A relatively few species are involved in different methods of biological control (Quicke 2015).

No taxonomic studies on this subfamily have been conducted in the Arabian Peninsula. Only three doryctine species have previously been reported there, *Rhaconotus arabicus* Belokobylskij, 2001, *Zombrus anisopus* Marshall, 1897 (Saudi Arabia) (Marshall 1900; Fahringer 1930; Fischer 1980; Belokobylskij 2001), and *Doryctophasmus ferrugineus* (Granger 1949) (United Arab Emirates, Yemen) (Belokobylskij 2015).

Materials and methods

The present study is based on specimens collected from Farasan Islands (Al-Sajid), using sweeping net and light trap. The specimens including the types of the new species are deposited in the King Saud University Museum of Arthropods, Plant Protection Department, College of Food and Agriculture Sciences, King Saud University, Riyadh, Saudi Arabia (**KSMA**). Genera were identified using Belokobylskij and Tobias (in Tobias et al. 1995), Belokobylskij (2001, 2006), Marsh (2002) and Belokobylskij et al. (2004). On the species level, several available keys, as well as original descriptions were used, like (arranged chronologically): Marshall (1900), Fischer (1968), Papp (1987), Belokobylskij (1983, 1994, 2001, 2006), Polaszek et al. (1994), Belokobylskij and Tobias (in Tobias et al. 1995), van Achterberg and Polaszek (1996), Shaw (1997), van Achterberg and Walker (1998), Shi et al. (2002), Belokobylskij and Maeto (2008), and Tang et al. (2013). The identification of *Rhaconotus carinatus* was confirmed by Andrew Polaszek who kindly examined the holotype (BMNH).

Morphological terminology follows Sharkey and Wharton (1997), Marsh (2002) and Marsh et al. (2013). Wing venation terminology is based on van Achterberg (1993). Body sculpture terminology follows Harris (1979). In the laboratory, the material was studied using a Leica M205 C stereomicroscope. The colour photographs were taken using a Canon EOS 70D camera attached to a Leica MZ 125 stereomicroscope. Individual source images were then stacked using HeliconFocus v.6.22 (HeliconSoft Ltd) extended of field software. Measurements of body parts were made with an ocular micrometer. Further image processing was done using the software Adobe Photoshop CS5.1 (v.12.1 X32) and Adobe Photoshop Lightroom v.5.2 Final (64 bit) [Ching Liu]. The Farasan map (Fig. 1) was plotted from satellite images of Google Earth (accessed 23 October 2019) using ArcGis 10.3, and colored with photoshop Cs6, the scale bar applied only to the magnified map.

Global distribution is based on Yu et al. (2016), in addition to some more recent literature. For tribal classification, we follow Chen and van Achterberg (2019).

List of abbreviations:

F = antennal flagellomeres; **mtn** = metanotum; **ODL** = diameter of ocellus; **OOL** = ocello-ocular line (distance between the outer edge of a lateral ocellus to the compound eye); **POL** = post-ocellar line (distance between the inner edges of the two lateral ocelli); **SOS** = sides of scutellum; **T** = metasomal terga. **Fore wing: 1-R1** = Radial vein; **1-SR+M** = first sector of sectio radii amalgamated with media; **2-SR** = second sector of sectio radii veins; **2-Cu** = second sector of cubital vein; **1-**, **2-** and **3-M** = first, second and third sectors of media, respectively; **3-SR** = third sector of sectio radii veins; **C+Sc+R** = costa, subcosta, and radius amalgamated into one vein; **Hind wing: R1**= radial vein; **SR** = **RS** = sectio radial vein; **SC+R** = subcosta and radius amalgamated into one vein; other veins have the same names as the fore wing.

Figure 1. Map of Farasan Archipelago.

Systematic accounts

Tribe Doryctini Foerster, 1863

Genus *Dendrosotinus* Telenga, 1941

Dendrosotinus Telenga, 1941: 80. Type species: *Dendrosoter ferrugineus* Marshall, 1888, by original designation.

Dendrosotinus ferrugineus (Marshall, 1888)

Figures 2A, B, 3A–D, 4A–C, 5A, B

Dendrosoter ferrugineus Marshall, 1888: 247, ♀.

Re-description of female. Body length: 4.8 mm; ovipositor length: 1.4 mm; fore wing length: 2.85 mm.

Head (Fig. 3B–D): Slightly wider than mesosoma (1.18×); coarsely rugose dorsally; temple with weak concentric striations, shiny; face coarsely rugose medially, weakly striated laterally behind eyes. Gena rugate above and smooth, with few punctures below. Head constricted behind eyes in dorsal view. Temple 0.58× as long as eye height. POL 1.6× OD, 0.95× OOL. Diameter of antennal socket 2.5× distance between socket to eye edge. Longitudinal eye diameter 1.1× its transverse diameter. Eyes slightly notched opposite to antennal base. Malar space 0.4× eye height, 1.1× as long as basal width of mandible. Face width 0.75× its height including clypeus. Anterior margin of clypeus bended forward,

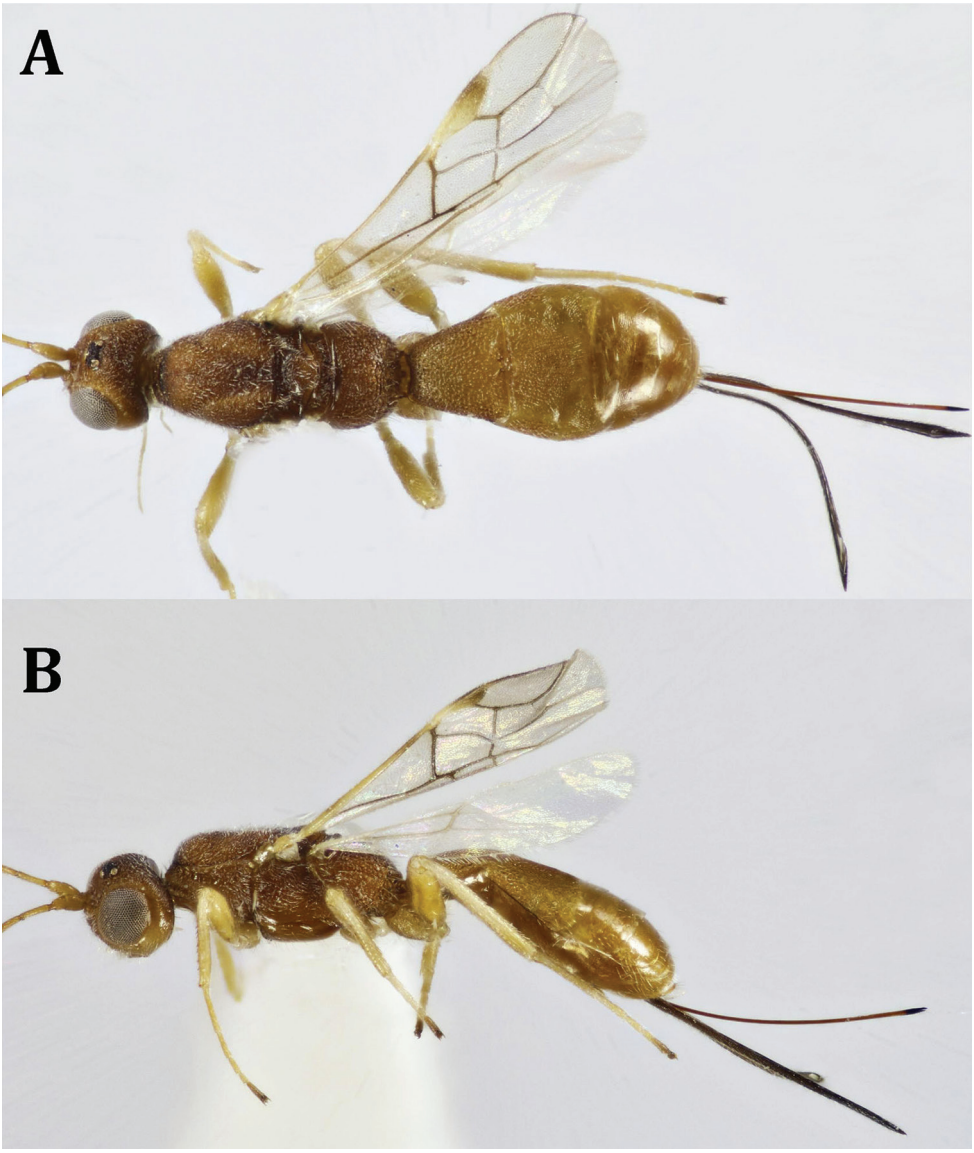

Figure 2. *Dendrosotinus ferrugineus* (Marshall), ♀: **A** dorsal habitus **B** lateral habitus.

slightly convex; hypoclypeal depression 0.9× distance between depression and eye. Tentorial pits small. Antenna broken (with 10 flagellomeres after being broken); scape short, 1.45× as long as its apical width; F1 5.0× as long as its apical width. Occipital carina thin and sharp, complete dorsally, but not meeting hypostomal carina ventrally.

Mesosoma (Fig. 4B, C): 1.9× as long as its maximum height. Pronotum with 6–7 transverse elements. Mesoscutum slightly and gently elevated above pronotum, coarsely rugose, moderately setose. Notauli deep, crenulate; lateral lobes of mesoscutum and

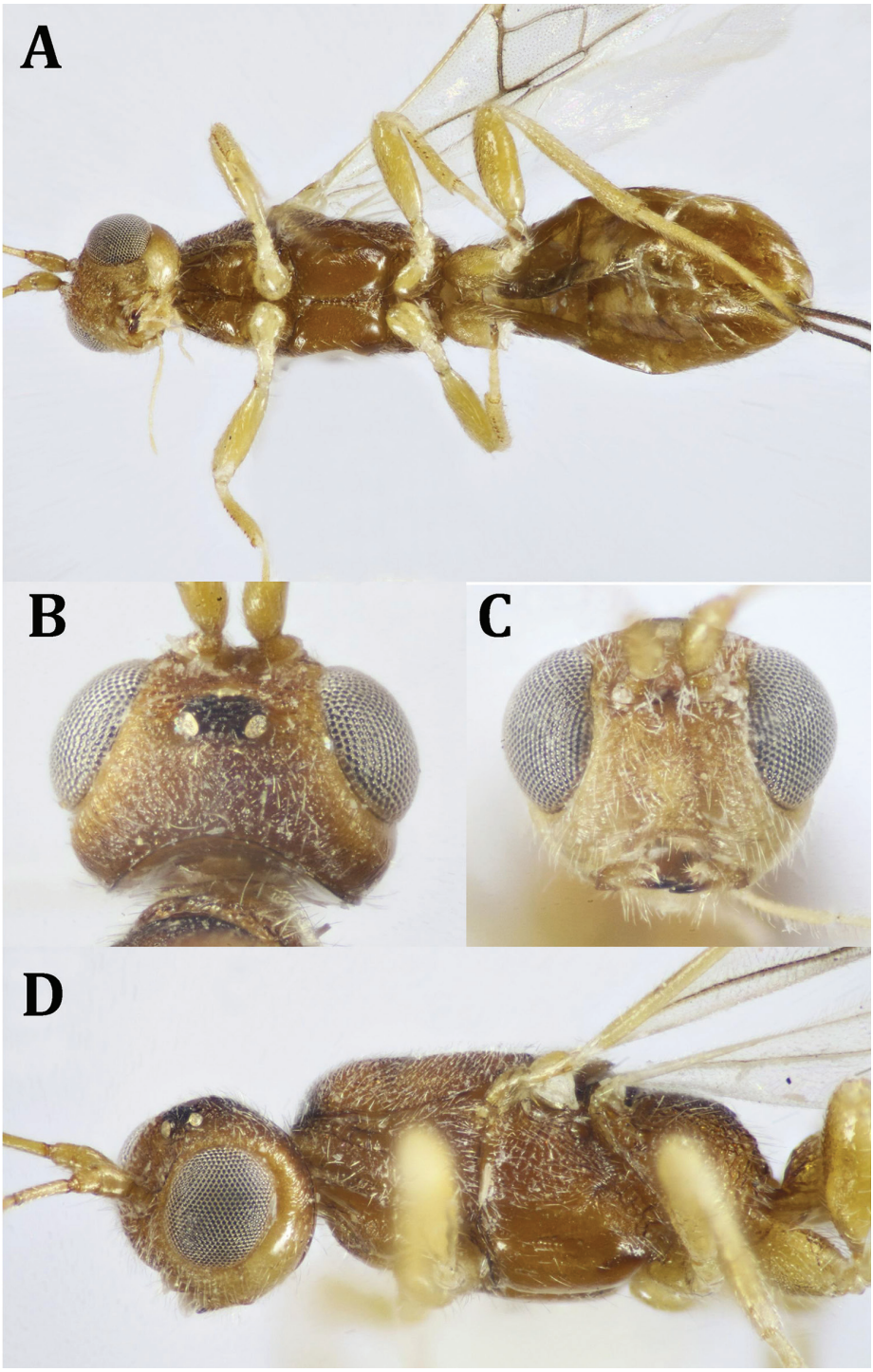

Figure 3. *Dendrosotinus ferrugineus* (Marshall), ♀: **A** ventral habitus **B** head, dorsal view **C** head, frontal view **D** head and mesosoma, lateral view.

anterior end slightly convex. Mesoscutellum about as long as its base, sparsely granulate, with sparse, short whitish setae. SOS smoothly rugate; mtn scrobiculate, with small rounded protrusion postero-medially overlapping base of propodeum, 0.4× as long as mesoscutellum. Propodeum coarsely rugose at basal two-thirds, transversely foveolate at posterior third, with postero-median projections, with long, fine whitish setae laterally and posteriorly. Mesopleuron weakly rugose above, smooth and shiny below; sternaulus short, weakly crenulate, not reaching lateral ends of mesopleuron. Metapleuron strongly areolate.

Wings (Fig. 4A): Fore wing with pterostigma 4.3× as long as its maximum width; metacarpe ca. as long as pterostigma. Vein r arising from middle area of pterostigma, 0.5× straight 3-SR, 0.55× 2-SR, 0.75× m-cu; r-m present; discoidal cell 1.9× as long as wide; 3-M entirely unsclerotized; 1-CU1 0.3× as long as 2-CU1, 1-M straight; 1-SR+M slightly curved; M+CU1 straight. Fore wing fringed with short fine setae along its costal and apical margins; hind wing entirely fringed with longer fine setae.

Legs (Fig. 5A): Fore femur 2.1× as long as its maximum width; fore and middle tibiae with row of short, thick dark spines along their inner margins; fore tibia with a comb of widely separated short spines distally. Hind tarsus 1.2× as long as hind tibia; hind basitarsus 0.9× as long as remaining hind tarsomeres combined; 2nd tarsomere 0.48× as long as basitarsus, 1.6× as long as telotarsus (excluding arolium).

Metasoma (Fig. 5B): Apical width of T1 2.3× as wide as its basal width, 1.3× its median length, densely roughly foveolate; length of T2 + T3 combined 0.7× its basal width, weakly longitudinally striated medially at basal two-thirds, smooth laterally and apically. Remaining tergites smooth and shiny. Ovipositor sheath, ca. as long as metasomal length, 2.88× as long as T1, 1.1× as long as mesosomal length, 0.6× fore wing length.

Color (Figs 2A, B, 4A): Head and mesosoma dark brown, metasoma reddish brown, with reddish antenna; palpi pale yellowish, legs yellowish, with dark brown telotarsi. Ovipositor red, with black apex; ovipositor sheath black. Wings hyaline, with pterostigma dark brown, yellow at basal half; parastigma yellowish; all wing veins dark brown. Hind wing with paler veins.

Material examined. Kingdom of Saudi Arabia. 1♀, Jazan, Farasan Islands, Al-Sajid; 16°51'25.46"N, 41°55'58.78"E; 10 Nov. 2017; Usama Abu El-Ghiet & El-Sheikh leg.; LT [KSMA].

General distribution. Armenia, Azerbaijan, Bosnia-Hercegovina, France, Greece, Israel, Italy, Russia, Spain, Turkey, former Yugoslavia (Yu et al. 2016), Saudi Arabia (Farasan Islands) (new record).

Tribe Hecabolini Foerster, 1863

Genus *Hecabalodes* Wilkinson, 1929

Hecabalodes Wilkinson, 1929: 105. Type species: *Hecabalodes anthaxiae* Wilkinson, 1929, by original designation.

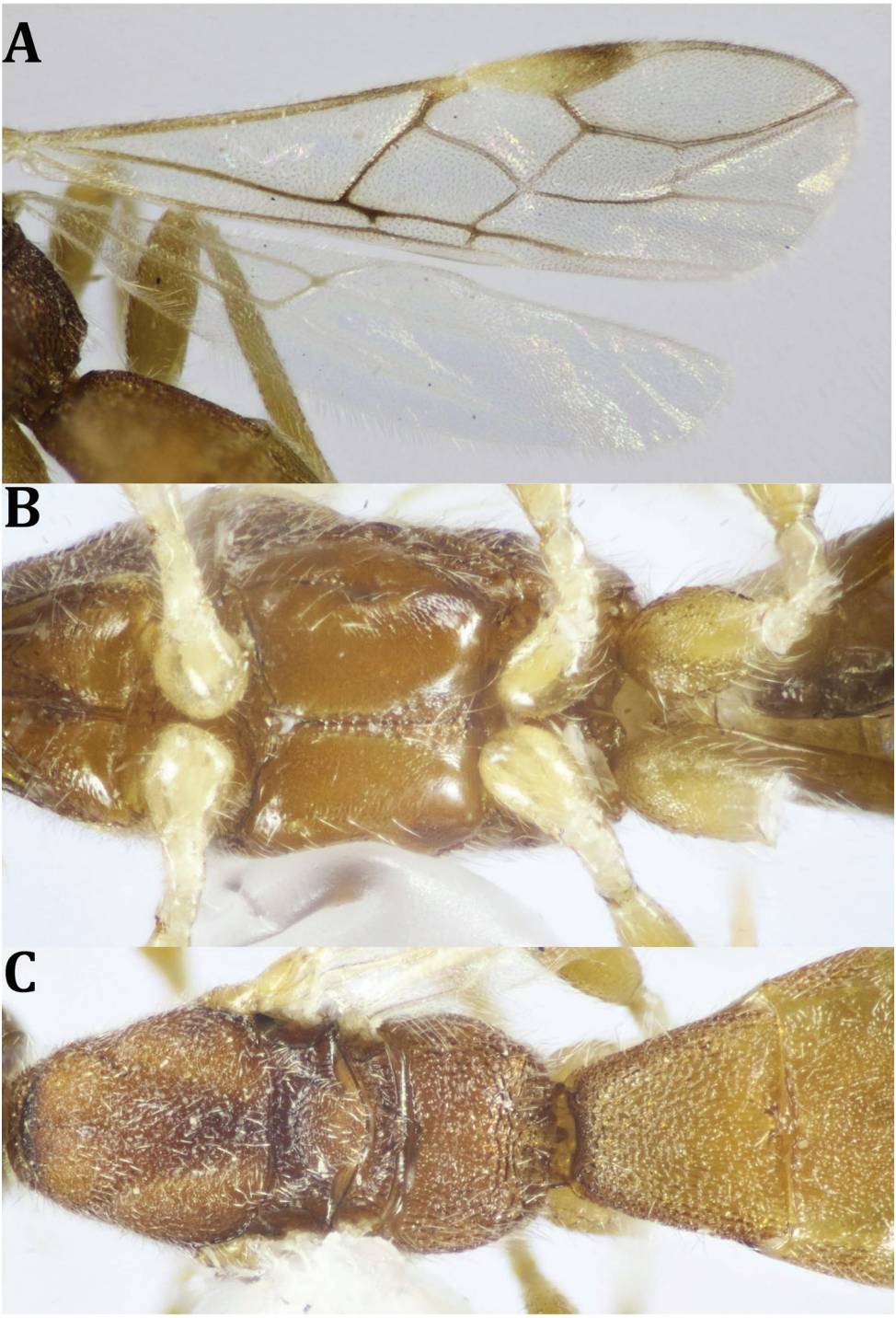

Figure 4. *Dendrosotinus ferrugineus* (Marshall), ♀: **A** fore and hind wings **B** mesosoma, ventral view **C** mesosoma, T1 and T2 (part).

Figure 5. *Dendrosotinus ferrugineus* (Marshall), ♀: **A** hind leg (tibial spines indicated) **B** propodeum and metasoma, dorsal view.

***Hecabalodes anthaxiae* Wilkinson, 1929**
Figures 6A–E, 7A–E

Hecabalodes anthaxiae Wilkinson, 1929: 106, ♀♂.

Re-description of female. Body length: 4.2 mm; ovipositor length: 2.35 mm; fore wing length: 2.5 mm. (we re-describe this species in full because of the short original description of Wilkinson (1929)): Dark brown, except for the yellowish hue on lateral sides of T1 and T2 as well as apex of T2 (Figs 6A, B, 7E); antenna orange, scape slightly darker (Fig. 6C); legs dark brown (except for the yellowish base of fore tibia, and all tarsi), telotarsi darker. Fore wing subhyaline, with distinct infuscation along marginal cell (Fig. 7D).

Head (Figs 6C–E, 7A): 1.3× as wide as its median length, slightly wider than mesoscutum; coarsely rugose; head behind eye broadly rounded; temple 0.6× as long as eye

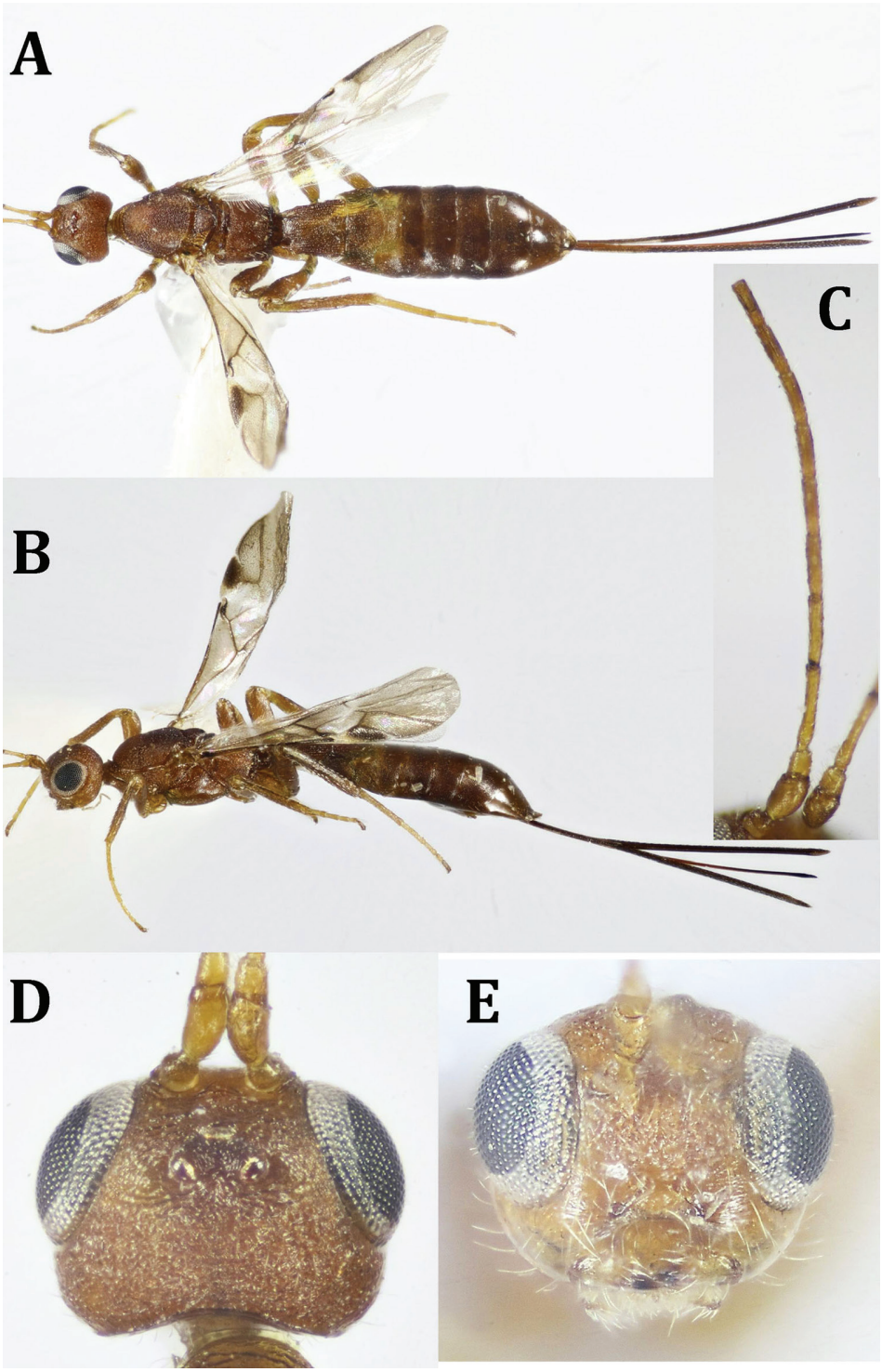

Figure 6. *Hecabalodes anthaxiae* Wilkinson, ♀: **A** dorsal habitus **B** lateral habitus **C** antenna (broken at tip) **D** head, dorsal view **E** head, frontal view.

height in dorsal view; POL 1.6× OD, 0.9× OOL; eye with few scattered short setae; malar space 0.4× as long as eye height, 1.2× as long as basal width of mandible, malar suture absent; face smooth laterally just behind eyes; face 1.5× as wide as eye width, 0.8× as long its length combined with clypeus; hypoclypeal depression more or less quadrate, ca. as wide as its distance from eye; occipital carina complete dorsally, not meeting hypostomal carina ventrally; antenna broken; scape twice as long as its maximum width; F1 6.5× as long as its apical width, 1.2× as long as F2; ocellar triangle with base longer than lateral sides. *Mesosoma* (Fig. 7A–C): 2.3× as long as its height; pronotum with two sharp transverse carinae dorsally; mesoscutum gently rounded above or at the same level of pronotum when seen from lateral view, flattened on disc, densely rugose, finely alutaceous laterally; notauli indistinct; mesoscutellum slightly convex, truncate at apex, finely sculptured, with a number of thick carinae laterally; mtn 0.4× as long as mesoscutum, with a short longitudinal median carina and 2–3 oblique submedian carinae on its depressed anterior part, convex postero-medially; propodeum finely and sparsely granulate, with two short postero-medial, parallel carinae, 0.3× as long as propodeal length, median longitudinal carina of propodeum absent; mesopleuron finely punctate, with irregular spaces in between, shiny; precoxal sulcus shallow, irregular, running ventrally along almost the entire length of mesopleuron. *Fore wing* (Fig. 7D): 3.6× as long as its maximum width; pterostigma 1.7× as long as maximum width; vein M + CU1 slightly curved; 1-SR+M nearly straight; vein r-m absent; vein r arising at basal third of pterostigma; 2-SR 1.75× as long as r, slightly longer than m-cu, 0.6× as long as 1-SR+M; 1CU1 0.2× as long as 2CU1. *Hind wing* (Fig. 7D): With fringe of long, fine setae along apical and anal margins; vein 1-M 1.7× as long as 1-rm. Legs. Hind coxa (Fig. 7C) 1.7× as long as wide, without distinct basoventral tubercle, finely punctate especially ventrally, with some fine whitish setae distally and laterally; hind femur 2.6× as long as wide; hind tarsus 1.1× as long as hind tibia; hind basitarsus slightly shorter than rest of tarsomeres combined; second tarsomere 0.55× as long as hind basitarsus, 2.2× as long as telotarsus (excluding arolium); outer edge of hind tibia with long, fine whitish setae. *Metasoma* (Figs 6A, B, 7E): 1.3× as long as head and mesosoma combined; T1 and basal half of T2 with distinct interrupted longitudinal striae, somewhat dotted in between; T1 1.5× as long as its apical width; T2 0.9× as long as its apical width, 2.7× as long as T3; posterior half of T2 finely reticulate, T3–5 (except posterior margin of T5 smooth and shiny), finely reticulate; T6 entirely smooth and shiny. Ovipositor sheath about as long as or slightly longer than metasoma (Fig. 6A, B), and the fore wing as well.

Material examined. Kingdom of Saudi Arabia, 1♀, Jazan, Farasan Islands, Al-Sajid; 16°51'25.46"N, 41°55'58.78"E; 10 Nov.2017; Abu El-Ghiet & El-Sheikh leg.; LT [KSMA].

General distribution. Sudan (Wilkinson, 1929), Saudi Arabia (Farasan Islands) (new record).

Remark. This species has not been collected during the 90 years or more since Wilkinson described the holotype from Sudan in 1929.

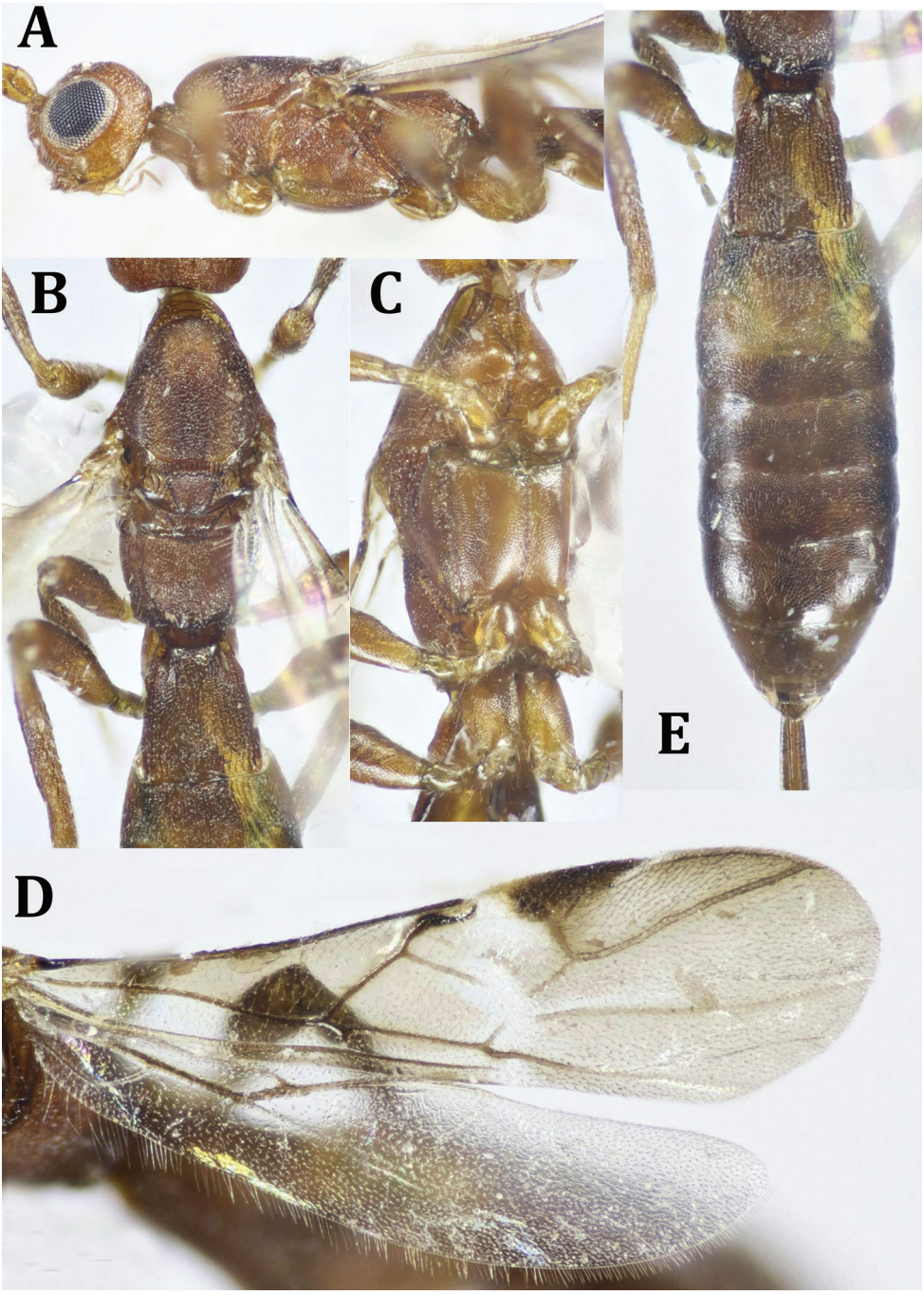

Figure 7. *Hecabalodes anthaxiae* Wilkinson, ♀: **A** head and mesosoma, lateral view **B** mesosoma and metasomal T1 **C** mesosoma, ventral view **D** fore and hind wings **E** metasoma, dorsal view.

Tribe Heterospilini Fischer, 1981

Genus *Neoheterospilus* Belokobylskij, 2006

Neoheterospilus Belokobylskij, 2006: 151. Type species: *Neoheterospilus koreanus* Belokobylskij, 2006, by original designation.

***Neoheterospilus* sp.**
Figures 8A–E, 9A–G

Description of male. Body length: 2.25 mm; fore wing length: 1.7 mm.

Head (Figs 8C–E, 9A): 0.7× as wide as its median length, distinctly wider than mesoscutum (1.3×). Head below eyes distinctly straight when seen from frontal view. Vertex distinctly smooth and shiny; frons superficially finely punctate, interspaces smooth. Head behind eyes gently rounded when seen from dorsal view; temple smooth, with few scattered setae, 0.6× eye length. Ocelli placed in an equilateral ocellar triangle. POL 1.6× OD, 1.0× OOL; diameter of antennal sockets 1.4× distance between socket and eye. Eye glabrous, slightly emarginate opposite to antennal sockets, 1.1× as high as broad. Malar space 1.1× as long as basal width of mandible, 0.4× as long as eye height; malar suture absent. Face slightly convex, very finely sculptured laterally, nearly smooth medially, with few scattered setae; its width 0.8× height of eye, and 1.2× as wide as its height. Clypeus very thin, transverse, moderately arched at free margin; hypoclypeal depression moderate, semi-oval, its width 0.6× face width. Occipital carina thin, complete dorsally, reaching hypostomal carina ventrally. Antenna slender, filiform, pointed at apex, without spine, 21-segmented, hardly longer than body length; scape nearly smooth, rather short, with few scattered setae, 1.2× as long as wide; flagellum densely setose, F1 slender, straight, 4.9× as long as its apical width, ca. as long as F2; penultimate segment 6.0× as long as F1, 0.7× as long as apical flagellomere.

Mesosoma (Fig. 9A–C): Almost smooth, lateral lobes of mesoscutum finely sculptured to alutaceous, not depressed, 1.9× as long as its height. Pronotum rather short, nearly straight, smooth, collar with longitudinal median and lateral carinae. Mesoscutum distinctly high, more or less perpendicularly elevated above pronotum; its maximum width 1.5× as wide as its middle length; median lobe of mesoscutum, slightly, but straightly protruding forwardly. Notauli wide and deep anteriorly, shallow and thinner posteriorly, broad anteriorly and meeting posteriorly before posterior margin of mesoscutum, distinctly foveolate. Prescutellar area in the form of two subquadrate plates, separated medially by a thin linear suture, mostly smooth, 0.4× as long as mesoscutellum. Mesoscutellum slightly convex at anterior half, with very fine lateral carina, its basal width 0.7× its median length. Subalar depression smooth, nearly rounded. Sternaulus moderately deep, straight, smooth, running along median area of lower part of mesopleuron. Metapleural lobe relatively large, nearly smooth, gently rounded posteriorly just above hind coxa. Propodeum smooth, nearly flattened, laterally carinate,

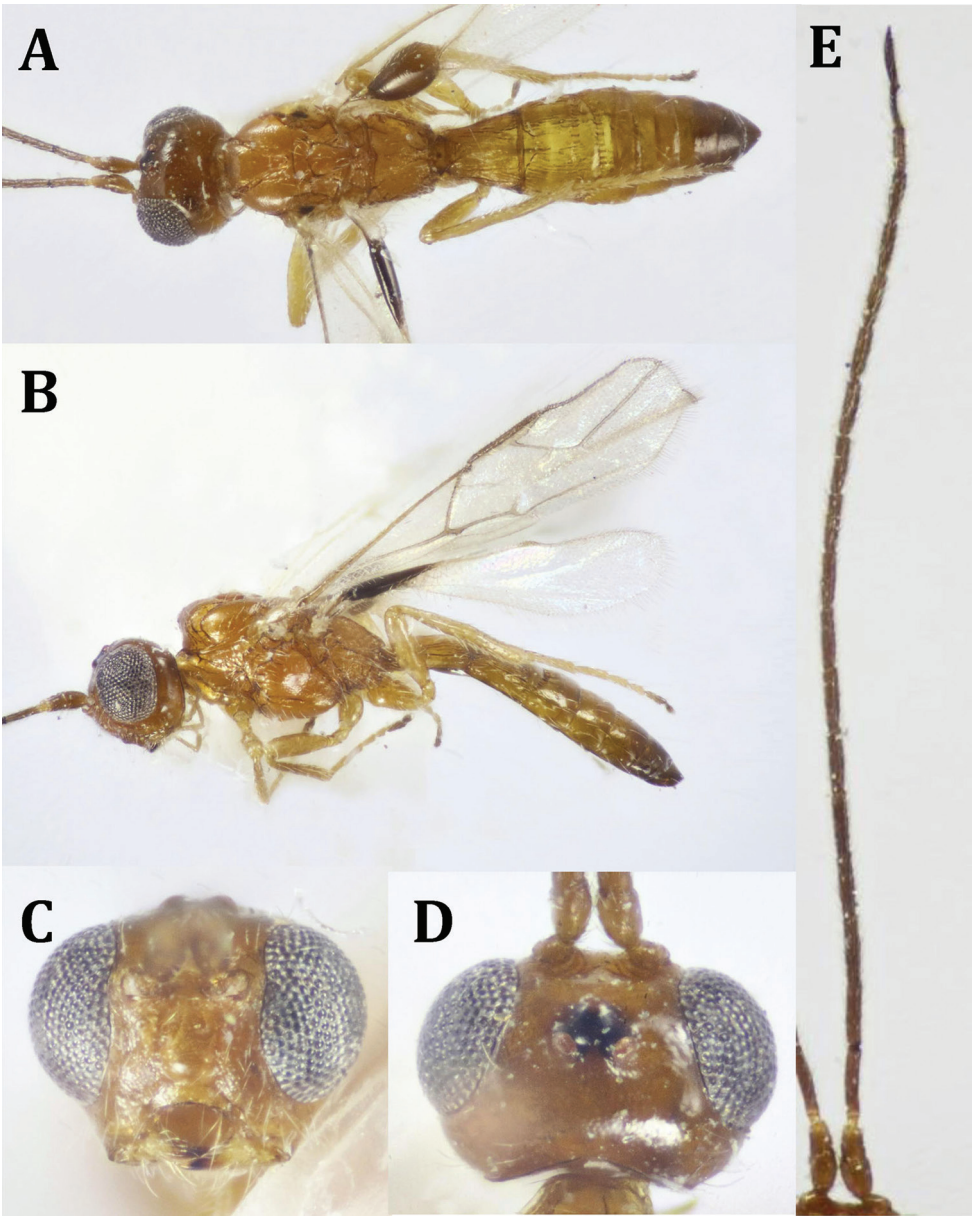

Figure 8. *Neoheterospilus* sp., ♂: **A** dorsal habitus **B** lateral habitus **C** head, frontal view **D** head, dorsal view **E** antenna.

with two short, posterior sublateral, oblique and slightly curved carinae at base as well as a median straight one, 0.1× as long as propodeal length; basal sublateral carina could also be seen, 0.4× as long as propodeum length; propodeal spiracle relatively small.

Wings (Fig. 9E, F): Fore wing 3.8× as long as its maximum width, 0.75× as long as body length; r arising near to the middle of pterostigma; Radial cell long (not

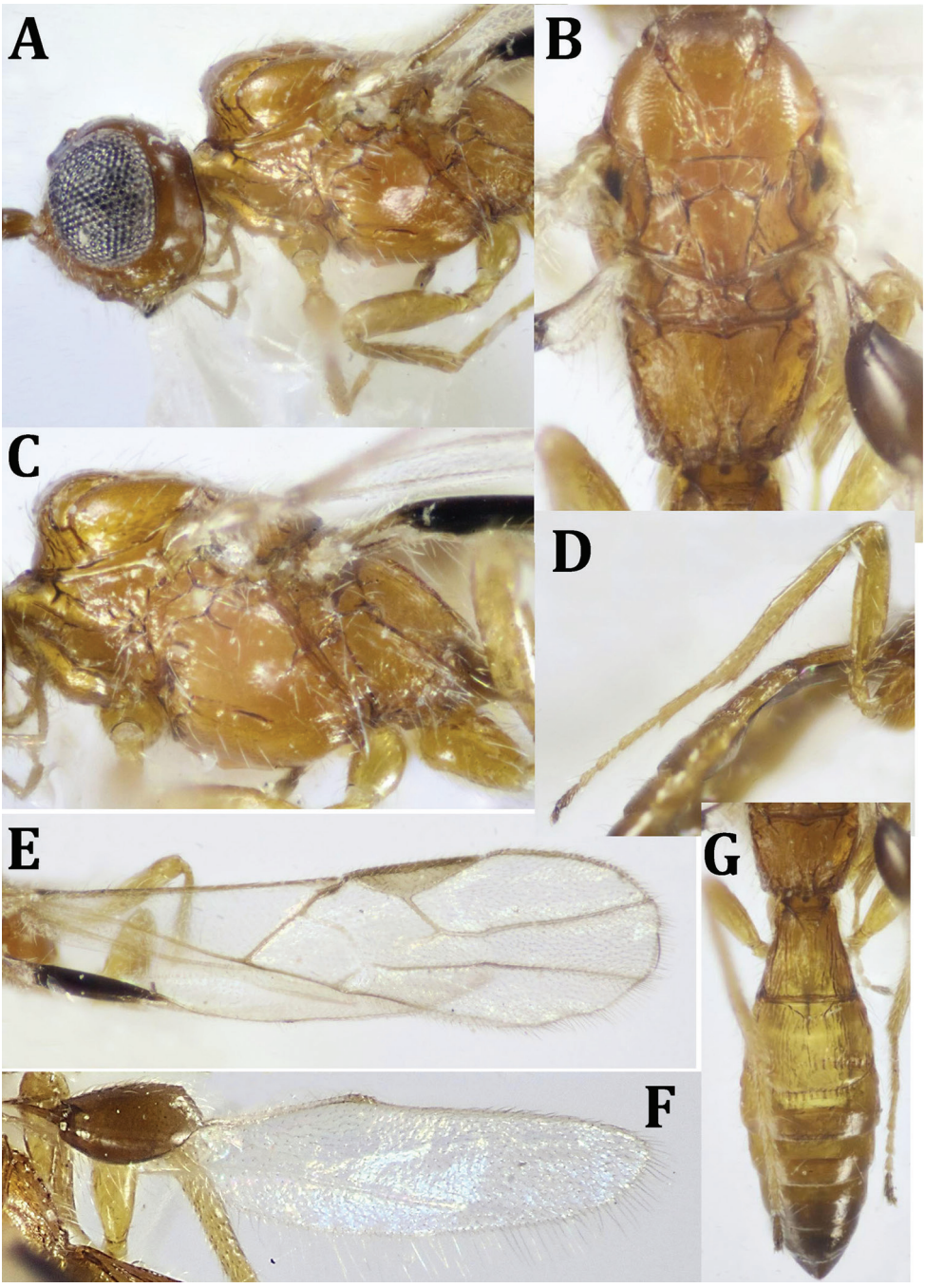

Figure 9. *Neoheterospilus* sp., ♂: **A** head and mesosoma, lateral view **B** mesosoma, dorsal view **C** mesosoma, lateral view **D** hind leg and metasoma (part), lateral view **E** fore wing **F** hind wing **G** propodeum and metasoma, dorsal view.

shortened); metacarpus longer than pterostigma; r 1.4× as long as maximum width of pterostigma; 3-SR 0.85× r, forming with it an obtuse angle; 3-SR 0.2× as long as SR1, straight; trace of 1-SR+M distinctly lower than 2-SR+M (very hardly seen to be measured); m-cu slightly curved; brachial cell broadly opened distally. Hind wing 4.6× as long as its maximum width, costal cell absent, Costal vein stigma-like subbasally. Whole edges of both wings surrounded with relatively long fringe of setae.

Legs (Fig. 9D): Hind coxa 1.2× as long as its maximum width, with small, but distinct baso-ventral tubercle; hind femur narrow, without blister dorsally, 4.2× as long as its maximum width; hind basitarsus 0.3× as long as hind tibia; hind tibia with weak blister near to the middle, second tarsomere of hind leg 0.64× as long as hind basitarsus.

Metasoma (Fig. 8A, B, 9G): Nearly glabrous, except for very few fine long setae laterally, 2.7× as long as its maximum width, 1.1× as long as head and mesosoma combined. T1 widened from base to apex, its apical width 2.1× its basal width, 1.0× its middle length, with small basal dorsope; with baso-median smooth area that narrowed posteriorly, not reaching middle of tergite, with very weak, irregular longitudinal striations that are obscured medially; T1 1.4× as long as propodeal length; T2 with a trace of short, semi-circular smooth area baso-medially; median length of T2 0.8× its basal width, 0.8× as long as T1 and 1.8× as long as T3, sculpturing as in T1, but very superficial and weaker. T3 ca. 2.0× as wide as long, with short, thick, widely separated longitudinal striations at base. Remaining tergites smooth and shiny.

Color (Figs 8A, B, 9E, F): Body generally reddish yellow, with head distinctly darker; antenna with scape and pedicel as body color, flagellum dark brown to black; maxillary and labial palpi pale brown; ocellar triangle black, last metasomal tergites dark brown to black. Wings hyaline, fore wing pterostigma and veins dark brown.

Material examined. Kingdom of Saudi Arabia. 1♂, Jazan, Farasan Islands, Al-Sajid; 16°51'25.46"N, 41°55'58.78"E; 25 Jan.2017; Usama Abu El-Ghiet & El-Sheikh leg.; LT [KSMA].

Remark. Although it cannot be matched with any of the species keyed out by Belokobylskij in his paper of *Neoheterospilus* (2006), it should not be described as new until females are collected (Belokobylskij, pers. comm.).

General distribution. Saudi Arabia (Farasan Islands) (new record).

Tribe Rhaconotini Fahringer, 1928

Genus *Rhaconotus* Ruthe, 1854

Rhaconotus Ruthe, 1845: 349. Type species: *Rhaconotus aciculatus* Ruthe, 1845 (by monotypy)

Hedysomus Foerster, 1863: 238. Type species: *Hedysomus elegans* Foerster, 1863 (by original designation)

Hormiopterus Giraud, 1869: 478. Type species: *Hormiopterus ollivieri* Giraud, 1869 (by monotypy)

Euryphrymnus Cameron, 1910: 100. Type species: *Euryphrymnus testaceiceps* Cameron, 1910 (by monotypy)

Rhaconotinus Hedqvist, 1965: 8. Type species: *Rhaconotinus caboverdensis* Hedqvist, 1965 (by original description)

Rhaconotus (*Rhaconotus*) *carinatus* Polaszek, 1994

Figures 10 (A–C), 11 (A–E)

Rhaconotus carinatus Polaszek in Polaszek et al., 1994: 79, ♀.

Diagnosis. Female: Body length: 4.5–4.8 mm; fore wing length: ca. 3.1 mm.

Generally dark reddish brown, with posterior margin of T4 and T5 yellowish in color (Fig. 10A, B) (in some specimens, head reddish, with black ocellar triangle); antenna with scape dark reddish brown, pedicel and basal half of flagellum reddish, rest of flagellum dark brown. Legs and palpi are pale yellowish (except dark brown telotarsus). Wings (Fig. 11D) hyaline, with slight, hardly seen fumigation behind pterostigma; pterostigma brownish, with pale basal and apical ends; veins brownish, with basal three-fourths of C+SC+R, basal two-thirds of 1-R1, and basal half of M+CU1 are pale brownish in color; ovipositor reddish, slightly dark at apex, ovipositor sheath black (Fig. 10A, B).

Head (Figs 10C, 11A, B) finely sculptured, with few scattered fine whitish, semi-erect setae when seen from dorsal view; face finely punctate, with distances between punctures, smooth medially just beneath antennal bases, and above hypoclypeal area, with denser appressed setae. Temple 0.6× eye height. Antenna 35-segmented. Mesoscutum (Figs 10C, 11C) with fine reticulation except nearly smooth posteromedially; propodeum finely reticulate, longitudinal median carina hardly seen just at base, as well as two shorter ones baso-laterally. Metasoma (Fig. 11E) with T2 and T3 fused, separated by a strong curved suture or groove, after which the longitudinal striations became weakly visible; T5 simple, broadly rounded posteriorly. Ovipositor sheath ca. as long as metasoma (Fig. 10A, B).

Material examined. Kingdom of Saudi Arabia. 1♀ & 1♂, Jazan, Farasan Islands, Al-Sajid; 16°51'25.46"N, 41°55'58.78"E; 7 Jan.2017; Abu El-Ghiet & El-Sheikh leg.; sweeping net [KSMA]; 1♀, Kingdom of Saudi Arabia, Jazan, Farasan Islands, Al-Sajid; 16°51'25.46"N, 41°55'58.78"E; 10 Nov.2017; Abu El-Ghiet & El-Sheikh leg.; LT [KSMA].

General distribution. Cameroon, Ghana, Madagascar, Nigeria, Senegal, Sierra Leone, Tanzania, Togo (Polaszek et al. 1994), Saudi Arabia (Farasan Islands) (new record).

Remark. Based on Polaszek et al. (1994) and van Achterberg and Polaszek (1996), our species differs from the African specimens in having the pterostigma distinctly infuscate medially, with pale basal and apical ends (distinctly infuscate in the African specimens); antenna 35-segmented (26–33 in the African specimens); lateral lobes of mesoscutum moderately setose (largely glabrous in the African specimens); propodeum finely reticulate, with a hardly visible median longitudinal carinae as well as two

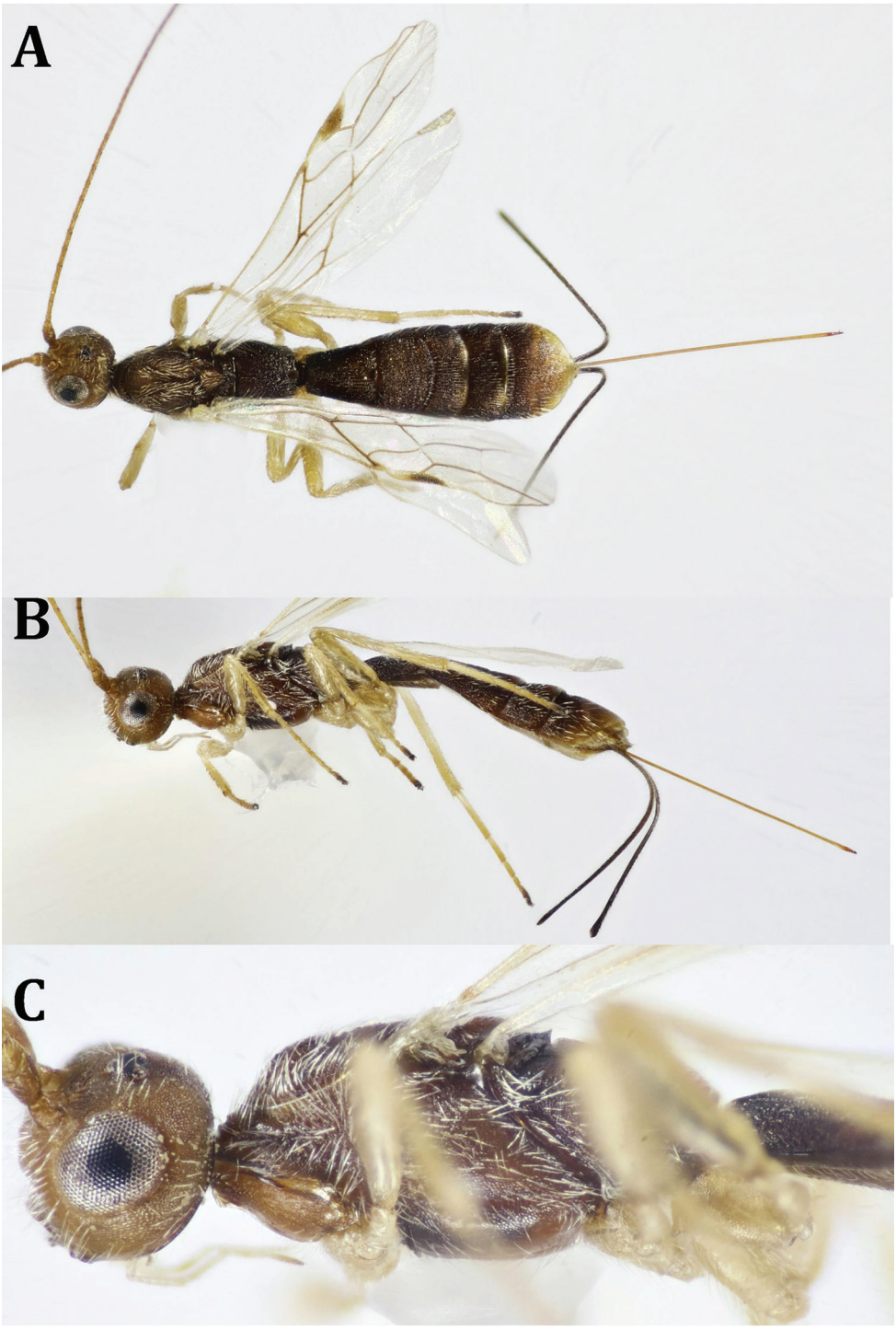

Figure 10. *Rhaconotus* (*Rhaconotus*) *carinatus* Polaszek in Polaszek et al. 1994, ♀: **A** dorsal habitus **B** lateral habitus **C** head and mesosoma, lateral view.

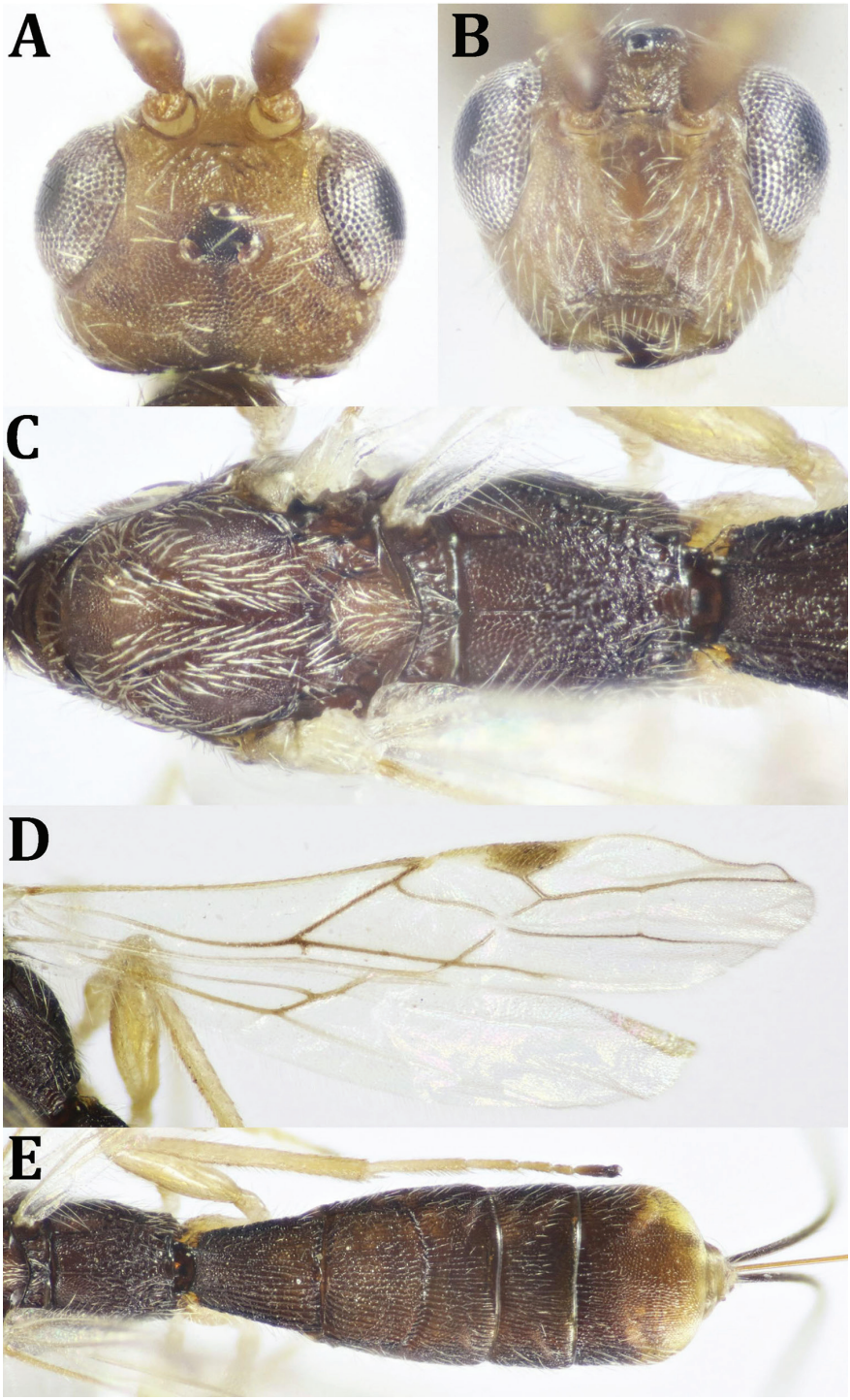

Figure 11. *Rhaconotus* (*Rhaconotus*) *carinatus* Polaszek in Polaszek et al. 1994, ♀: **A** head, dorsal view; **B** head, frontal view **C** mesosoma, dorsal view **D** fore and hind wings **E** propodeum and metasoma, dorsal view.

very short sublateral ones (almost smooth anteromedially in the African specimens, see fig. 30 in Polaszek et al. (1994) and fig. 366 in van Achterberg and Polaszek (1996)).

Genera with uncertain tribal relationships

Genus *Mimodoryctes* Belokobylskij, 2001

Mimodoryctes Belokobylskij, 2001: 749.

Type species. *Mimodoryctes proprius* Belokobylskij, 2001, by monotypy.

Mimodoryctes arabicus Edmardash, Gadallah & Soliman, sp. nov.

http://zoobank.org/D8226F4F-86DE-4987-A7CD-EABF927009DD
Figures 12A–E, 13A–D, 14A–E

Type material. Holotype: Kingdom of Saudi Arabia. ♀, Jazan, Farasan Islands, Al-Sajid; 16°51'25.46"N, 41°55'58.78"E; 10 Nov. 2017; Abu El-Ghiet & El-Sheikh leg.; LT [KSMA].

Description of holotype (female): Body length: 4.0 mm; ovipositor length: 1.0mm; fore wing length: 2.5 mm.

Head (Fig. 12C–E): 1.3× as wide as its median length, densely transversely striated in dorsal view; face coarsely rugose; frons not concave, without median carina, just a smooth slim area medially extending from between behind antennal bases, reaching clypeus; gena finely, obliquely striated; vertex and face sparsely setose. Temple roundly constricted behind eye, 0.5× as long as eye height. Clypeus coarsely rugose. Ocelli small; ocellar triangle with base 1.5× as long as its sides; POL 1.6× OD, 0.8× OOL. Eyes 2.1× as high as its width, with sparse short setae. Malar space 0.5× eye height, 0.6× basal width of mandible. Face width 0.9× eye height; hypostomal depression small, rounded, its width 0.9× distance of depression from eye edge. Head gently narrowly rounded behind eye when seen from frontal view. Antenna slender, broken (with 11 flagellomeres after being broken); scape short, 1.9× as long as its apical width; F1 slightly curved, 6.0× as long as its apical width, 1.1× as long as F2.

Mesosoma (Fig. 13A, B): 2.4× as long as its height. Mesoscutum not elevated above pronotum in lateral view. Pronotum with weak transverse carinae; mesoscutum flattened, coarsely rugose, with irregularly scattered fine setae, with a nearly smooth posteromedial area. Notauli indistinct. Mesoscutellum slightly convex to nearly flattened, ca. as long as its basal width, finely transversely puncticulate. Propodeum not areolate, with an incomplete median sulcus that is branched laterally giving off irregular oblique ridges. Mesopleuron coarsely rugose above, smooth with some fine punctures ventrally; sternaulus deep, nearly straight, extending along the entire ventral margin of mesopleuron.

Wings (Figs 13D, 14A): Fore wing 4.3× as long as its maximum width; metacarpus slightly longer than pterostigma (1.17×); pterostigma 4.7× as long as its maximum

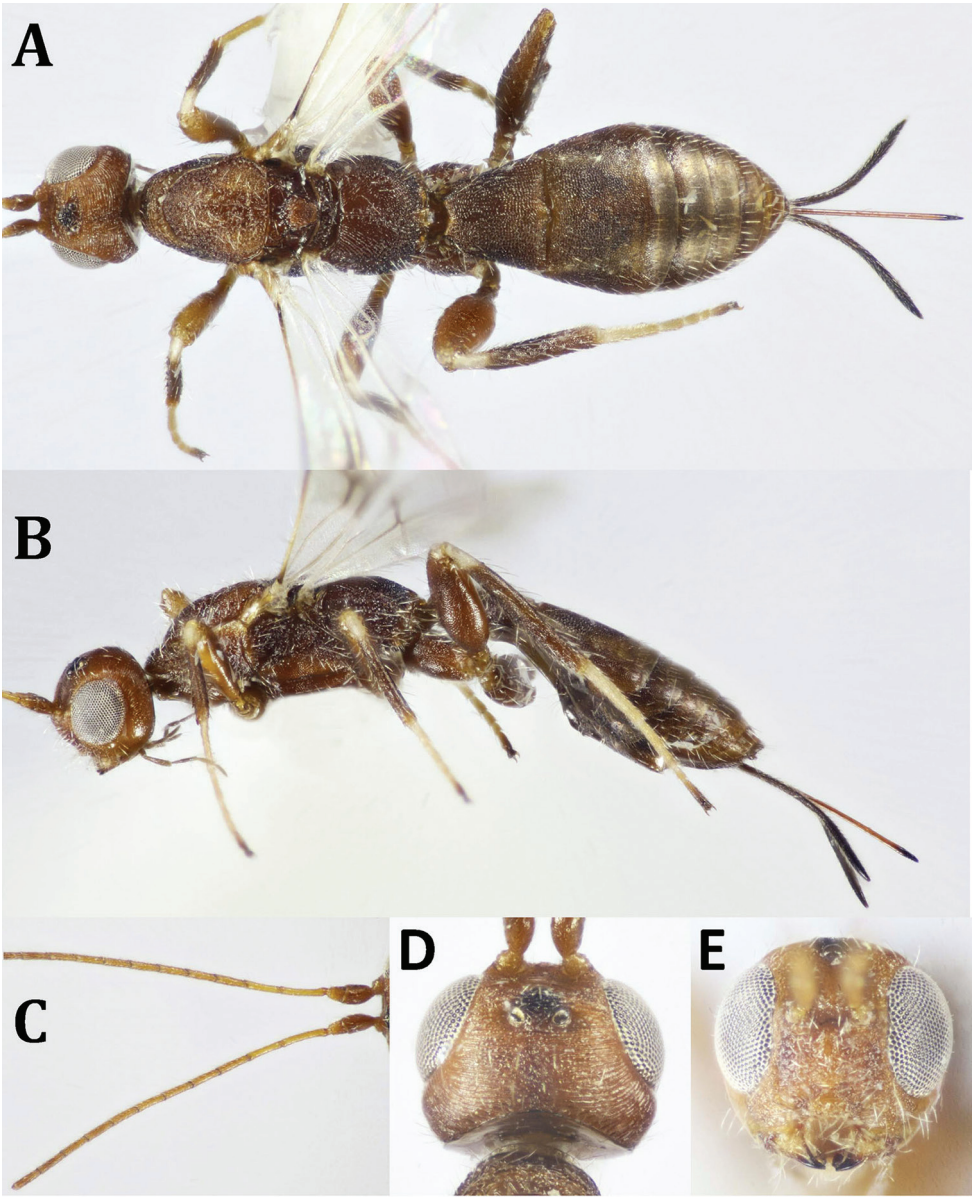

Figure 12. *Mimodoryctes arabicus* Edmardash, Gadallah & Soliman, sp. nov. ♀: **A** dorsal habitus **B** lateral habitus **C** antenna (part) **D** head, dorsal view **E** head, frontal view.

width; r arising from middle of pterostigma; 2-SR 1.5× r; 2-SR 0.3× SR1; m-cu distinctly antefurcal; vein 1cu-a postfurcal; distance between cu-a to 1-M 2.0× as long as cu-a; vein M+CU distinctly curved away from 1–1A; 1-CU1 0.4× 2-CU1; r-m not tubular, with wide bulla; 2-SR+M present. Hind wing with three hamuli on R1; vein SC+R 0.7× as long as vein C+SC+R; vein M+CU slightly longer than vein 1M (1.14×); vein m-cu interstitial, directed towards wing base.

Legs (Figs 13C, 14B–D): Hind coxa 2.4× as long as its maximum width, with a small rounded tubercle basoventrally, finely alutaceous, with a medio-ventral smooth and shiny area extending subbasally to apex; hind femur 2.6× as long as its maximum width, finely alutaceous, with some fine long hairs; outer edge of hind tibia with fine, long outstanding setae, ca. as long as tibial maximum width; hind tarsus ca. as long as hind tibia; hind basitarsus 0.7× as long as second-fifth tarsomeres combined.

Metasoma (Fig. 14E): slightly longer than head and mesosoma combined (1.1×). T1 distinctly gradually widened from base to apex, without spiracular protuberance, without basal carina; apical width of T1 3.0× its basal width, 1.2× as wide as its median length. T2 1.2× as wide as its middle length, with very weak median, slightly wavy, sulcus, 3.1× as long as T3. T1 and T2 (except posterior half of T2) densely granulose; posterior half of T2 and rest of tergites are smooth and shiny. Ovipositor distinctly shorter than metasoma, Ovipositor sheath 0.5× metasomal length, 1.7× T1 length.

Color (Figs 12A–C, E): Body dark reddish brown, with head and antennal flagellomeres lighter in color; palpi reddish brown. Legs dark reddish brown, except for pale yellow to ivory bases of tibiae and tarsi (except dark brown telotarsi). Wings hyaline, with slight infuscation under metacarpus as well as veins linings; veins dark brown with the following veins are pale: M+CU1 (except apically), 1-M, apical two-thirds of 2-CU1, m-cu. In hind wing, only 1r-m and distal half of 1-M are dark brown, rest of veins are pale.

Recognition. The most important character separating the new species, *M. arabicus*, from the Algerian species *M. proprius* Belokobylskij is the presence of vein r-m of fore wing (Fig. 14A) (absent in *M. proprius*). Other characters can be summarized as follows: vertex transversely strigated without dense granulations between the striae (Fig. 12D) (in *M. proprius* dense granulations between striae could be seen); malar space relatively short, 0.6× basal width of mandible (Fig. 13A) (longer in *M. proprius*, 0.9× basal width of mandible); mesosoma 2.4× as long as high (Fig. 13A) (twice as long as high in *M. proprius*); propodeum with curved striations especially laterally (Fig. 13B) (densely striated in *M. proprius*); metasomal T1 and T2 densely rugulose-striated (Fig. 14E) (densely striated longitudinally in *M. proprius*); T4–6 finely sculptured at base (Fig. 14E) (in *M. proprius* the larger part of T3 with fine granulation, T4–6 with very weak granulation at base); body color dark reddish brown, including the legs except for bases of tibiae and all tarsi pale yellowish (Fig. 12A, B) (in *M. proprius*, body pale reddish brown, yellow in places, with the legs same as body with all tibiae yellowish at bases and apices); hind wing vein M+CU 1.2× 1-M (1.4× in *M. proprius*).

Remark. The absence or presence of vein r-m of the fore wing has been found to be a polymorphic character for four genera: *Afrospathius* Belokobylskij & Quicke, *Leluthia* Cameron, *Pareucorystes* Tobias, and *Platydoryctes* Barbalho & Pentiado-Dias. However, this character has not yet been recorded in *Mimodoryctes* Belokobylskij (see Belokobylskij (2001)), and this was later confirmed in Belokobylskij et al. (2004) in their phylogenetic study of the doryctine genera based solely on morphological

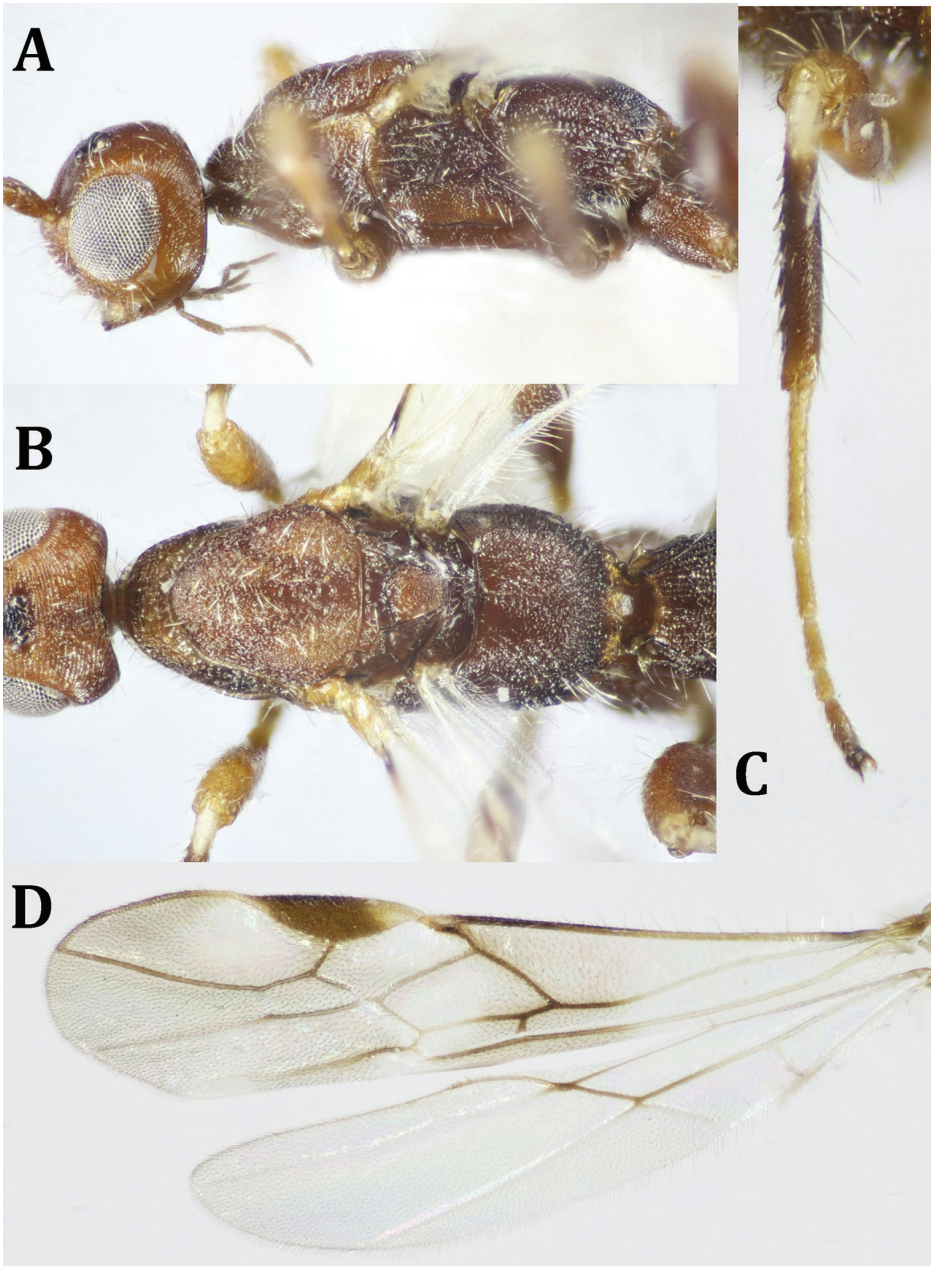

Figure 13. *Mimodoryctes arabicus* Edmardash, Gadallah & Soliman, sp. nov. ♀: **A** head and mesosoma, lateral view **B** head (part) and mesosoma, dorsal view **C** fore leg (fore tibial spines indicated) **D** fore and hind wings.

evidence. However, in the absence of other reliable diagnostic characters, the situation is considered in the present study to be the same as in the above-mentioned four genera.

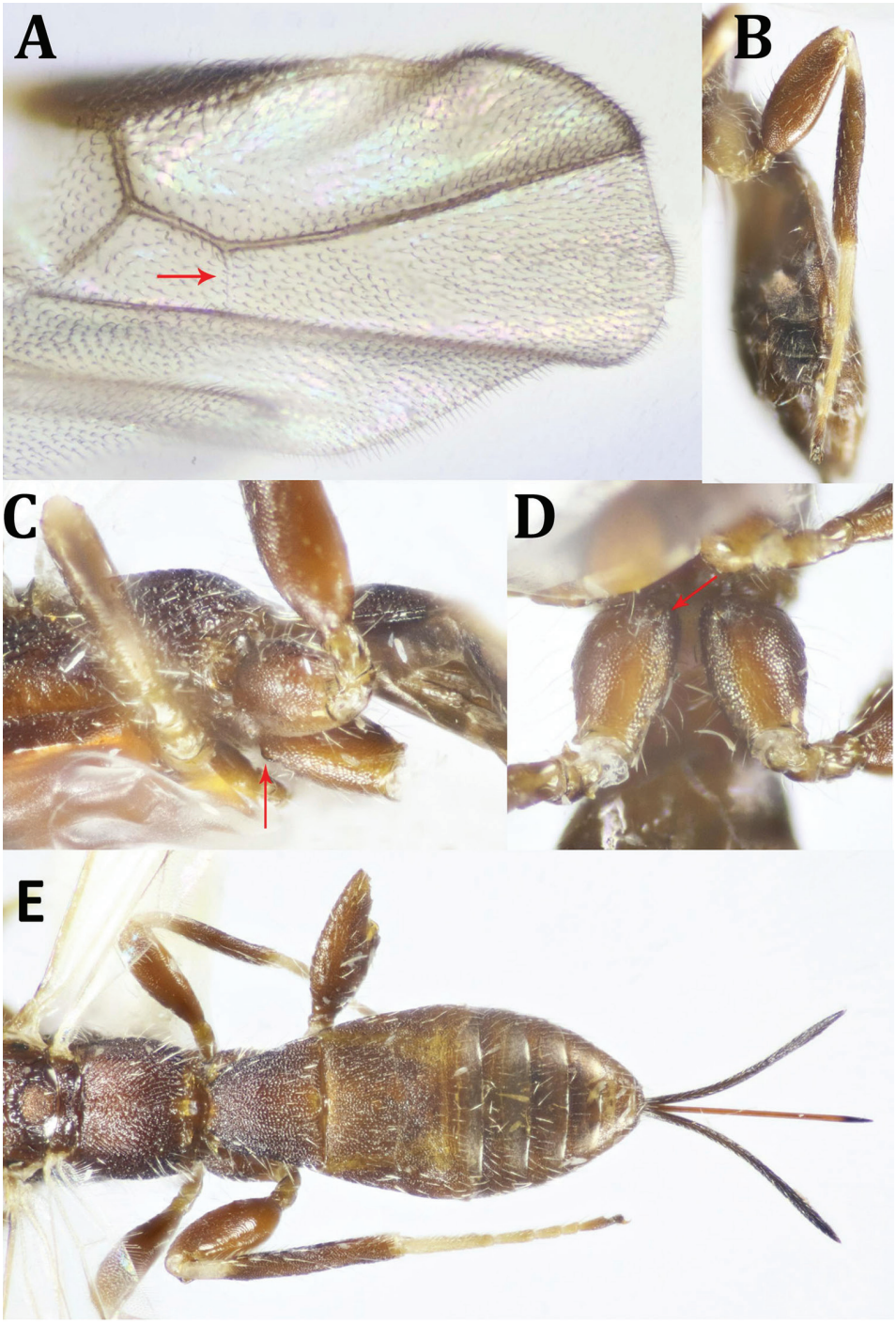

Figure 14. *Mimodoryctes arabicus* Edmardash, Gadallah & Soliman, sp. nov. ♀: **A** fore wing (part), presence of r-m indicated **B** hind leg and metasoma (part), lateral view **C** hind coxa, lateral view (basoventral tubercle indicated) **D** hind coxae, ventral view (basoventral tubercle indicated) **E** propodeum and metasoma, dorsal view.

***Mimodoryctes proprius* Belokobylskij, 2001**
Figures 15 (A–D), 16 (A–E)

Mimodoryctes proprius Belokobylskij, 2001: 750, ♀.

Re-description. Body length: 3.6 mm; length of fore wing: 2.75 mm.

Head (Fig. 15C, D): 1.4× as wide as its median length, somewhat angulate behind eye in frontal view, roundly narrowed after eyes in dorsal view. Transverse eye diameter ca. twice as long as temple in dorsal view. Vertex with transverse curved striations with rugosity between striae (Fig. 15D). Face densely punctate, with fine, inwardly directed whitish setae, as well as thicker and shorter sparse setae on vertex. Temple gently rounded behind eyes, ca. 0.5× eye height. Ocelli small, ocellar triangle equilateral; POL 1.1× OD, 2.4× OOL. Eyes 1.2× as high as its width, glabrous. Malar space 0.4× as long as eye height, 1.6× as long as basal width of mandible. Face slightly wider than eye height (1.1×); hypostomal depression of moderate size, rounded, its width as long as its distance from eye edge. Antenna slender, with apex missing, 18-segmented, appearing shorter than body; scape 1.9× as long as its apical width, slightly longer dorsally than ventrally, F1 slightly curved along outer side, 6.3× as long as its apical width, slightly longer than F2 (1.2×); F3 straight, slightly longer than F4 (1.2×).

Mesosoma (Fig. 16A): 3.0× as long as its height. Mesoscutum gently and roundly elevated above pronotum. Pronotum with weak transverse carinae on the disc, without any processes, deeply concave posteriorly; mesoscutum flattened, sparsely setose, finely granulose anteriorly and laterally, coarsely rugose medially; notauli hardly seen; scuto-scutellar sulcus in the form of oval longitudinal depressions separated by carinae. Mesoscutellum ca. as long as its basal width, finely granulose on the disc, rugose laterally, sparsely setose apically. Propodeum without distinct areas, finely granulose at base, rest of it coarsely obliquely reticulate-rugose, sparsely setose laterally. Mesopleuron sparsely, superficially punctate above, finely granulose below, sternaulus superficially finely punctate, with row of 3–4 fine setae.

Wings (Fig. 16B). Fore wing 3.7× as long as its maximum width. Metacarpe 1.1× as long as pterostigma. Pterostigma 4.3× as long as its width; r released from the middle of pterostigma; 2-SR ca. as long as r; r-m absent, m-cu distinctly prefurcal; distance between cu-a to 1-M 0.1× cu-a length; 1-CU1 0.4× as long as 2-CU1; M+CU1 straight to slightly curved; 2-SR+M present, unsclerotized. Hind wing m-cu prefurcal.

Legs (Fig. 16C, D). Hind coxa 1.35× as long as its maximum width, densely alutaceous, with a small rounded tubercle basoventrally; hind femur 2.7× as long as its maximum width, finely alutaceous. Outer edge of hind tibia with a row of widely separated spines; hind tarsus slightly longer than hind tibia, 1.1×; hind basitarsus 0.8× as long as 2^{nd} -5^{th} tarsomeres combined.

Metasoma (Fig. 16E). 0.95× as long as head and mesosoma combined. T1 gradually widened from base to apex, 1.3× as wide as its middle length, without median longitudinal carina, with dense, close longitudinal striae, granulose in between; T2 distinctly broader than T1, 1.3× as wide its median length, longitudinally striated at anterior 0.7 length, followed by small, finely granulated area, then smooth at posterior

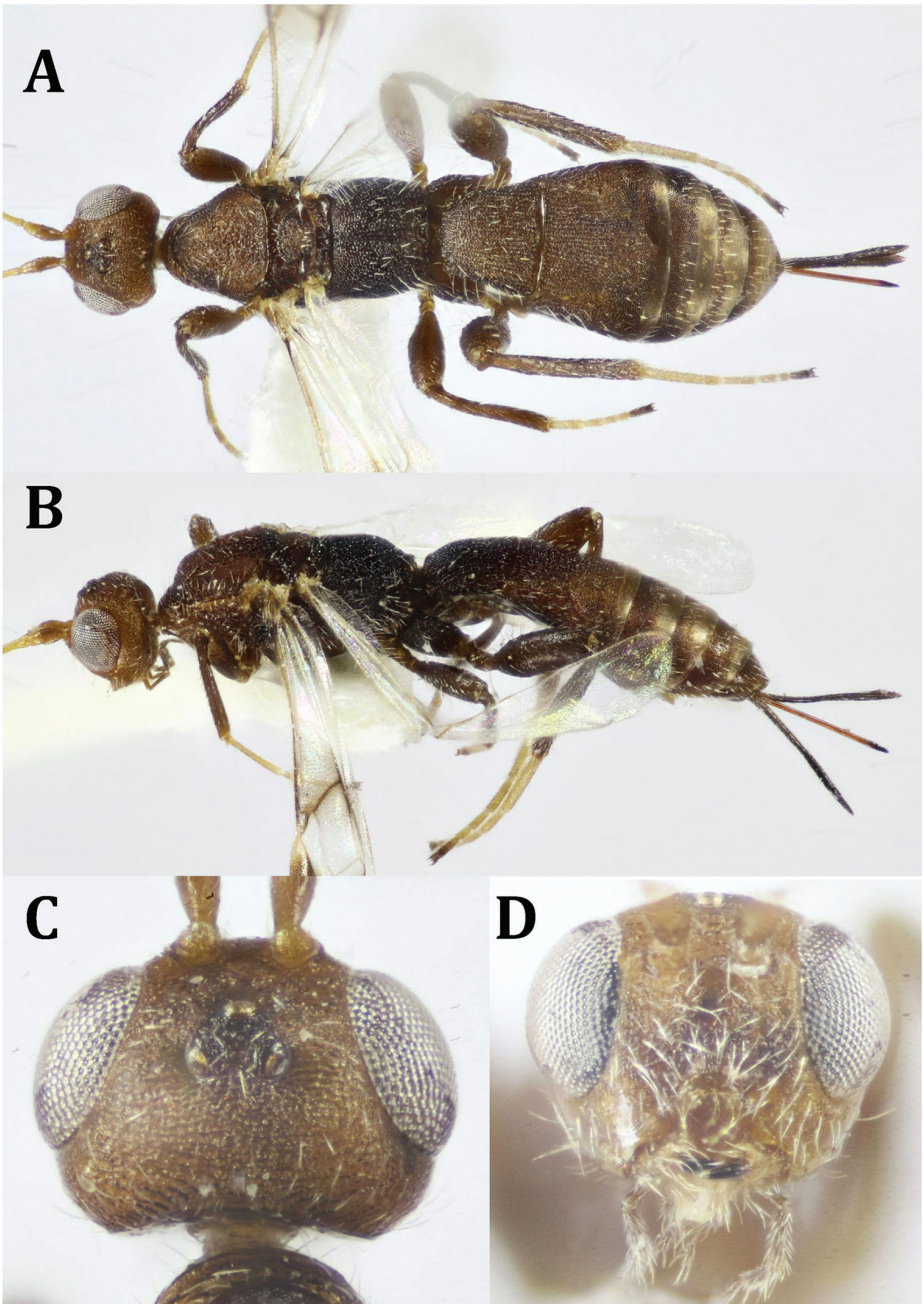

Figure 15. *Mimodoryctes proprius* Belokobylskij, ♀: **A** dorsal habitus **B** lateral habitus **C** head, dorsal view **D** head, frontal view.

margin, with very weak, hardly seen transverse curved sulcus medially; T1 0.7× as long as T2. Rest of tergites finely alutaceous, and smooth apically. Metasomal tergites sparsely setose. Ovipositor 0.4× as long as metasomal length, 1.8× as long as T1.

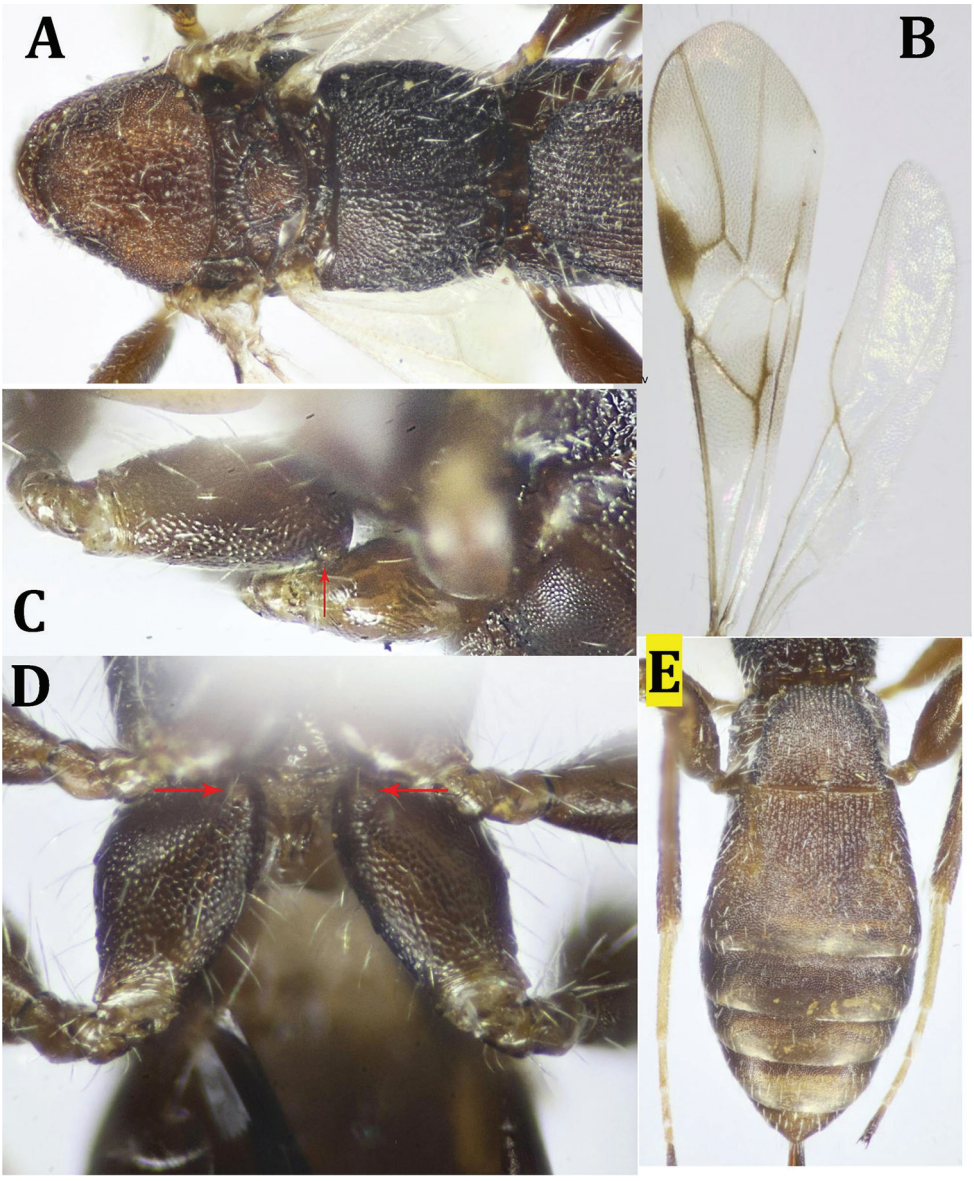

Figure 16. *Mimodoryctes proprius* Belokobylskij, ♀: **A** mesosoma and T1 (part) **B** fore and hind wings **C** hind coxa, lateral view (basoventral tubercle indicated) **D** hind coxae, ventral view (basoventral tubercle indicated) **E** metasoma, dorsal view.

Color (Figs 15A, B, 16B). Body dark brown, with somewhat lighter head (face) and mesoscutum; eyes whitish. Legs dark brown, with yellowish tarsi (except dark brown to black telotarsi). Ovipositor red, black at tip; ovipositor sheath black. Fore wing with dark brown pterostigma, whitish at base; veins dark, with M+CU1 (except dark apically), 1-SR+M, m-cu and 2-SR+M, apical half of 2-CU1 membranous.

Material examined. 2♀, Kingdom of Saudi Arabia, Jazan, Farasan Islands, Al-Kosar; 16°40'5.75"N, 42°08'51.62"E, 25.I.2017; leg. Abu El-Ghiet & El-Sheikh; LT [KSMA].

Intraspecific variation. The Saudi Arabian specimen differs from the Algerian one in the following: Vertex with transverse curved striation with rugosity between , frons and face coarsely rugose, weakly striated below eyes; temples weakly concentrically striated (vertex, frons densely striated, temple densely granulate); POL 1.6× OD, 0.95× OOL (1.3× OD, 0.75× in *proprius*); malar space 0.9× basal width of mandible (1.1× in *M. proprius*); ovipositor sheath 0.5× as long as metasomal length, 1.8× as long as T1 (0.35× metasomal length, 1.5× T1 in *M. proprius*).

General distribution. Algeria (Belokobylskij, 2001), Saudi Arabia (Farasan Islands) (new record).

Discussion

Saudi Arabia is a large arid land, covering the major part of the Arabian Peninsula, with an area of ca. 2,250,000 km^2 (Aldhebiani and Howladar 2015). It is characterized by different ecosystems and is considered as one of the richest areas of biodiversity in the Arabian Peninsula, as its flora is formed by a mixture of Afrotropical, Oriental, and South Palaearctic (Mediterranean) elements (Aldhebiani and Howladae 2015).

From a biogeographical point of view, the position of Saudi Arabia is on the frontier between the Palaearctic and Afrotropical regions, as the Arabian Desert being a strong ecological barrier. The Farasan Archipelago (east of the Saudi Arabia-Yemen border) is considered to be more closely related to the Afrotropical region, with a high floristic diversity in relation to other parts of Saudi Arabia (Alwelaie et al. 1993; El-Demerdash 1996; Alfarhan et al. 2002).

In the Afrotropical region, the subfamily Doryctinae is represented by 234 species in 39 genera (Yu et al. 2016). Only three doryctine species are reported to occur in the Arabian Peninsula, *Rhaconotus arabicus*, *Zombrus anisopus* (Saudi Arabia) (Marshall 1900; Fahringer 1930; Fischer 1980; Belokobylskij 2001), and *Doryctophasmus ferrugineus* (United Arab Emirates, Yemen) (Belokobylskij 2015). In the present study, six doryctine species are added to the Arabian Peninsula fauna and Saudi Arabia (Farasan Archipelago), of which *Mimodoryctes arabicus* Edmardash, Gadallah & Soliman, and most probably *Neoheterospilus* sp. (until being confirmed by the collection of females) are new species. Most of the collected species are exclusively Afrotropical. This is closely correlated with the floristic composition of the area under study (Farasan Islands) as has been reported by many authors (e.g., Alwelaie et al. 1993; El-Demerdash 1996; Alfarhan et al. 2002).

In the present study, *Hecabalodes anthaxiae* Wilkinson, 1929 is recorded from Saudi Arabia, a species not recorded anywhere since it was originally described from Sudan (Wilkinson 1929).

The absence or presence of vein r-m of the fore wing has been found to be a polymorphic character for only four genera: *Afrospathius* Belokobylskij & Quicke, *Leluthia* Cam-

eron, *Pareucorystes* Tobias, and *Platydoryctes* Barbalho & Pentiado-Dias. However, this character is absent in *Mimodoryctes* Belokobylskij (see Belokobylskij (2001)), and this was also confirmed in Belokobylskij et al. (2004) in their phylogenetic study of the doryctine genera based solely on morphological evidence. However, in the absence of other reliable diagnostic characters, the situation is considered in the present study to be the same as in the above-mentioned four genera. On the other hand, the number of segments in maxillary and labial palps can also be hardly counted especially in dry specimens, because the basal first and sometimes second segments can be very short and are very difficult to see separately in dry specimens (Belokobylskij, pers. comm.), and in our opinion, this character should also be considered as a polymorphic character for this genus.

Because of the rich biodiversity of Saudi Arabia, more species of this subfamily and others are expected to occur. Therefore, further collections and studies are needed to clarify the distribution of this group of wasps in other parts of this large country.

Acknowledgements

Sincere gratitude to Sergey Belokobylskij and Kees van Achterberg for their valuable suggestions and assistance and for critical reviews of the manuscript. Thanks also to Andrew Polaszek (UK) for confirming the identification of *Rhaconotus carinatus*. Sincere thanks to Adrian Pont and Andrew Polaszek (London) for their linguistic revision of different parts of the paper.

The authors are grateful to Saudi Wildlife Authority (SWA) officials in Farasan Islands National Park for the support and facilities provided during the field work. Sincere appreciation also extended to Deanship of Scientific Research in Jazan University for its funding of this research project no. 37/7/00014.

References

Aldhebiani AY, Howladar SM (2015) Floristic diversity and environmental relations in two valleys, South West Saudi Arabia. International Journal of Science and Research 4(2): 1916–1925. https://www.ijsr.net/get_abstract.php?paper_id=SUB151587

Alfarhan AH, Al Turki AT, Thomas J, Basahy RA (2002) Annotated list to the flora of Farasan Archipelago, Southern Red Sea, Saudi Arabia. Teckholmia 22(1): 1–33. https://doi.org/10.21608/taec.2002.12388

Alwelaie AN, Chaudary SA, Alwetaid Y (1993) Vegetation of some Red Sea islands of the Kingdom of Saudi Arabia. Journal of Arid Environment 24: 287–296. https://doi.org/10.1006/jare.1993.1025

Belokobylskij SA (1983) To the knowledge of the genera *Heterospilus* Hal. and *Dendrosotinus* Tel. (Hymenoptera, Braconidae) of the USSR fauna. Proceedings of the All-Union Entomological Society 65: 168–186.

Belokobylskij SA (1992) On the classification and phylogeny of the braconid wasps subfamilies Doryctinae and Exothecinae (Hymenoptera: Braconidae). I. Classification, 1. Entomo-

logicheskoe Obozrenie 71: 900–928 (in Russian); Entomological Review 72: 109–137. https://ci.nii.ac.jp/naid/10011409279/

Belokobylskij SA (1994) The species of the genus *Heterospilus* Haliday, 1836 (Hymenoptera: Braconidae) from Vietnam. Tropical Zoology 7: 11–23. https://doi.org/10.1080/03946975.1994.10539237

Belokobylskij SA (1995) Principal evolutionary transformations of morphological structures in subfamilies Doryctinae and Exothecinae (Hymenoptera: Braconidae). Entomologicheskoe Obozrenie 74: 153–176. http://www.zin.ru/labs/insects/Hymenopt/Personalia/Belokobylskij/pdf/074-1995e.pdf

Belokobylskij SA (2001) New taxa of the braconid subfamilies Doryctinae and Exothecinae (Hymenoptera, Braconidae) from the Western Palaearctic region. Entomological Review 81(7): 749–766. http://www.zin.ru/labs/insects/Hymenopt/Personalia/Belokobylskij/pdf/112-2001e.pdf

Belokobylskij SA (2006) *Neoheterospilus* gen. n., a new genus of the tribe Heterospilini (Hymenoptera: Braconidae, Doryctinae) with highly modified ovipositor and a worldwide distribution. Insect Systematics and Evolution 37: 149–178. https://doi.org/10.1163/187631206788831119

Belokobylskij SA (2015) Review of species of the Old World genus *Doryctophasmus* Enderlein, 1912 (Hymenoptera: Braconidae: Doryctinae). Zootaxa 3985(4): 541–564. https://doi.org/10.11646/zootaxa.3985.4.4

Belokobylskij SA, Maeto K (2008) Doryctinae (Hymenoptera: Braconidae) of Ogasawara Islands (Japan). Annales Zoologici (Warszawa) 58(1): 125–166. https://doi.org/10.3161/067.058.0107

Belokobylskij SA, Zaldívar-Riverón A, Quicke DLJ (2004) Phylogeny of the genera of the parasitic wasps, subfamily Doryctinae (Hymenoptera: Braconidae) based on morphological evidence. Zoological Journal of the Linnean Society 142: 369–404. https://doi.org/10.1111/j.1096-3642.2004.00133.x

Braet Y (2016) Key to the Genera of Doryctinae of the World. http://www.doryctinaekey.myspecies.info

Cameron P (1910) On some Asiatic species of the subfamilies Spathiinae, Doryctinae, Rhogadinae, Cardiochilinae and Macrocentrinae in the Royal Berlin Zoological Museum. Wiener Entomologische Zeitschrift 29: 93–100. https://doi.org/10.5962/bhl.part.23337

Chen XX, van Achterberg C (2019) Systematics, phylogeny, and evolution of the braconid wasps: 30 years of progress. Annual Review of Entomology 64: 1–24. https://doi.org/10.1146/annurev-ento-011118-111856

de Macêdo MV, Monteiro RT (1989) Seed predation by a braconid wasp, *Allorhogas* sp. (Hymenoptera). Journal of the New York Entomological Society 97: 358–362. https://www.jstor.org/stable/25009780

Dowton M, Austin AD, Antolin MF (1998) Evolutionary relationships among the Braconidae (Hymenoptera: Ichneumonoidea) inferred from partial 16S rDNA gene sequences. Insect Molecular Biology 7: 129–150. https://doi.org/10.1046/j.1365-2583.1998.72058.x

El-Demerdash MA (1996) The vegetation of the Farasan Islands, Red Sea, Saudi Arabia. Journal of the Vegetation Science 7: 81–88. https://doi.org/10.2307/3236419

Fahringer J (1930) Opuscula braconologica. Band 3. Palaearktischen Region. Liefrung 1–2. Opuscula braconologica, 1–160.

Fischer M (1968) Über gezüchtete Raupenwespen (Hymenoptera: Braconidae). Pflanzenschutz Berichte 37(7/8/9): 97–140.

Fischer M (1980) Taxonomische Untersuchungen über Doryctinae aus der *Odontobracon* Verwandtschaft (Hymenoptera, Braconidae). Annalen des Naturhistorischen Museums in Wien 83: 547–572. https://www.jstor.org/stable/41768825

Foerster A (1863) Synopsis der Familien und Gattungen der Braconiden. Verhandlingen des Naturhistorischen Vereines der Pruessischen Rheinlande und Westphalens 19: 226–288.

Harris RA (1979) A glossary of surface sculpturing. Occasional Papers in Entomology 28: 1–31. http://agris.fao.org/agris-search/search.do?recordID=US201300583954

Hedqvist KJ (1965) Braconidae from the Cape Verde Islands. Commentationes Biologicae, Helsinki 28: 1–28.

Giraud J (1869) Observations hyménoptèrologiques. Annales de la Société Entomologique de France (4) 9: 469–488.

Mandura AS, Saifullah SM, Khafaji AK (1987) Mangrove ecosystem of southern Red Sea Coast of Saudi Arabia. Proceedings of Saudi Biological Society 10: 165–193.

Marsh PM (1991) Description of a phytophagous doryctine braconid from Brazil (Hymenoptera: Braconidae: Doryctinae). Proceedings of the Entomological Society of Washington 93(1): 92–95. https://www.cabdirect.org/cabdirect/abstract/19921158253

Marsh PM (1993) Descriptions of new Western Hemisphere genera of the subfamily Doryctinae (Hymenoptera: Braconidae). Contributions of the American Entomological Institute 28(1): 1–58. http://www.sidalc.net/cgi-bin/wxis.exe/?IsisScript=oet.xis&method=post&formato=2&cantidad=1&expresion=mfn=026854

Marsh PM (1997) Doryctinae. In: Wharton RA, Marsh PM, Sharkey MJ (Eds) Manual of the New World Genera of the Family Braconidae (Hymenoptera). International Society of Hymenopterists. Special Publication No.1, 207–233.

Marsh PM (2002) The Doryctinae of Costa Rica (excluding the genus *Heterospilus*). Memoirs of the American Entomological Institute 70: 1–319. http://www.sidalc.net/cgibin/wxis.exe/?IsisScript=oet.xis&method=post&formato=2&cantidad=1&expresion=mfn=024700

Marsh PM, de Macêdo MV, Pimental MCP (2000) Descriptions and biological notes on two new phytophagous species of the genus *Allorhogas* from Brazil (Hymenoptera: Braconidae: Doryctinae). Journal of the Hymenoptera Research 9(2): 292–297. https://www.biodiversitylibrary.org/page/2858335

Marsh PM, Wild AL, Whitfield JB (2013) The Doryctinae (Braconidae) of Costa Rica: genera and species of the tribe Heterospilini. ZooKeys 347: 1–474. https://www.ncbi.nlm.nih.gov/pmc/articles/PMC3822444/

Marshall TA (1888) Les Braconides. In: André E (Ed.) Species des Hyménoptères d'Europe et d'Algérie. Beaune and Gray, Paris, 4, 609 pp.

Marshall TA (1900) Les Braconides (Supplément). In: André E (Ed.) Species des Hyménoptères d'Europe et d'Algerie. Paris-Tome 5 bis, 369 pp.

Muoftah IA (1990) Farasan: People, Sea and History. Jizan Cultural Club, Jizan.

Papp J (1987) Braconidae (Hymenoptera) from Korea. VIII. Acta Zoologica Hungarica 33: 157–175. https://pascalfrancis.inist.fr/vibad/index.php?action=getRecordDetail&idt=8333549

Polaszek A, Fitton MG, Bianchi G, Huddleston T (1994) The parasitoids of the African white rice borer, *Maliarpha separatelle* Ragonot (Lepidoptera: Pyralidae). Bulletin of the Entomological Research 84: 65–90. https://doi.org/10.1017/S0007485300032247

Quicke DLJ (2015) The Braconid and Ichneumonid Parasitoid Wasps: Biology, Systematics, Evolution and Ecology. Hoboken, N.J. Wiley Blackwell, 681 pp. https://doi.org/10.1002/9781118907085

Quicke DLJ, Ficken LC, Fitton MG (1993) New diagnostic ovipositor characters for doryctine wasps (Hymenoptera: Braconidae). Journal of the Natural History 26: 1035–1046. https://doi.org/10.1080/00222939200770611

Ramírez WB, Marsh PM (1996) A review of the genus *Psenobolus* (Hymenoptera: Braconidae) from Costa Rica, an inquiline fig wasp with brachypterous males, with description of two new species. Journal of the Hymenoptera Research 5: 64–72. http://repositorio.sibdi.ucr.ac.cr:8080/jspui/bitstream/123456789/11873/1/RBW0004.pdf

Ruthe JF (1854) Beiträge zur Kenntnis der Braconiden. Stettiner Entomologische Zeitung 15: 343–355.

Sharanowski BJ, Dowling APG, Sharkey MJ (2011) Molecular phylogenetics of Braconidae (Hymenoptera: Ichneumonoidea), based on multiple nuclear genes, and implications for classification. Systematic Entomology 36: 549–572. https://doi.org/10.1111/j.1365-3113.2011.00580.x

Sharkey MJ, Wharton RA (1997) Morphology and terminology. In: Wharton RA, Marsh PM, Sharkey MJ (Eds) Manual of the New World Genera of the Family Braconidae (Hymenoptera). International Society of Hymenopterists. Special Publication No.1, 19–63.

Shaw MR (1995) Observations on the adult behaviour and biology of *Histeromerus mystacinus* Wesmael (Hymenoptera: Braconidae). Entomologist 114(1): 1–13.

Shaw MR (1997) The genus *Heterospilus* Haliday in Britain with description of a new species and remarks on related taxa (Hymenoptera: Braconidae: Doryctinae). Zoologische Mededelingen Leiden 71(5): 33–41. http://repository.naturalis.nl/document/149389

Shaw SR, Edgerly JS (1985) A new braconid genus (Hymenoptera) parasitizing web-spinners (Embiidina) in Trinidad. Psyche 92: 505–511. https://doi.org/10.1155/1985/54285

Shenefelt RD, Marsh PM (1976) Pars 13. Braconidae 9, Doryctinae. In: Vecht Van der, Shenefelt RD (Eds) Hymenopterorum Catalogus (nova editio). Dr W. Junk, The Hague, 1263–1424. https://ci.nii.ac.jp/naid/10011409284/

Shi QX, Yang JQ, Chen JH (2002) A new species of *Heterospilus* Haliday (Hymenoptera: Braconidae) from China. Entomological Journal of East China 11(2): 3–5. https://europepmc.org/article/cba/383682

Strumia F, Dawah H (2019) An overview of the Chrysididae (Hymenoptera) of the Red Sea Farasan Archepelago (Saudi Arabia). Journal of the Insect Biodiversity 9(1): 1–17. https://doi.org/10.12976/jib/2019.09.1.1

Tang P, Belokobylskij SA, He JH, Chen XX (2013) *Heterospilus* Haliday (Hymenoptera: Braconidae, Doryctinae) from China with a key to species. Zootaxa 3683(3): 201–246. https://doi.org/10.11646/zootaxa.3683.3.1

Telenga NA (1941) Family Braconidae, subfamily Braconinae (continuation) and Sigalphinae. Fauna USSR. Hymenoptera 5(3): 1–466.

Tobias VI, Belokobylskij SA, Kotenko AG (1995) Keys to the insects of the European part of the USSR. Akademia Nauk SSSR, Zoologicheskii Institut, 908 pp. https://www.cabdirect.org/cabdirect/abstract/19961104913

van Achterberg C (1993) Illustrated key to the subfamilies of the Braconidae (Hymenoptera: Ichneumonoidea). Zoologische Verhandelingen 283: 1–189. https://ci.nii.ac.jp/naid/10008879101/

van Achterberg C, Polaszek A (1996) The parasites of cereal stem borers (Lepidoptera: Cossidae, Crambidae, Noctuidae, Pyralidae) in Africa, belonging to the family Braconidae (Hymenoptera: Ichneumonoidea). Zoologische Verhandelingen 204: 1–123. https://ci.nii.ac.jp/naid/10008879101/

van Achterberg C, Walker AK (1998) 17 Braconidae In: Polaszek A (Ed.) African Stem Borers – Economic importance, taxonomy, natural enemies and control. CAB International, Wallingford, 137–185, 448–483. http://www.sidalc.net/cgibin/wxis.exe/?IsisScript=UACHBC.xis&method=post&formato=2&cantidad=1&expresion=mfn=091907

van Achterberg C, Marsh PM (2002) Revision of the genus *Psenobolus* Reinhard (Hymenoptera: Braconidae: Doryctinae). Zoologische Mededelingen Leiden 76(1): 1–25. https://repository.naturalis.nl/pub/217457/ZM76_001-026.pdf

Wilkinson DS (1929) New parasitic Hymenoptera and notes on other species. Bulletin of Entomological Research 20(1): 103–114. https://doi.org/10.1017/S000748530002099X

Yu DSK, van Achterberg C, Horstmann K (2016) Taxapad 2016, Ichneumonoidea 2015. Taxapad database on flash-drive, Ottawa.

Zaldívar-Riverón A, Mori M, Quicke DLJ (2006) Systematics of the cyclostome subfamilies of braconid parasitic wasps (Hymenoptera: Ichneumonoidea): A simultaneous molecular and morphological Bayesian approach. Molecular Phylogenetics and Evolution 38(1): 130–145. https://doi.org/10.1016/j.ympev.2005.08.006

Zaldívar-Riverón A, Belokobylskij SA, Leon RV, Martínez J, Brinceno R, Quicke DLJ (2007) A single origin of gall association in a group of parasitic wasps with disparate morphologies. Molecular Phylogenetics and Evolution 44(3): 981–992. https://doi.org/10.1016/j.ympev.2007.05.016

Zaldívar-Riverón A, Belokobylskij SA, Leon RV, Martínez J, Brinceno R, Quicke DLJ (2008) Molecular phylogeny and historical biogeography of the cosmopolitan parasitic wasp subfamily Doryctinae (Hymenoptera: Braconidae). Invertebrate Systematics 22(3): 345–363. https://doi.org/10.1071/IS07028

Zaldívar-Riverón A, Martínez J, Belokobylskij SA, Pedraza-Lara C, Shaw SR, Hanson PE, Varela-Hernandez F (2014) Systematics and evolution of gall formation in the plant-associated genera of the wasp subfamily Doryctinae (Hymenoptera: Braconidae). Systematic Entomology 39(4): 633–659. https://doi.org/10.1111/syen.12078

ZooKeys 977: 75–100 (2020)
doi: 10.3897/zookeys.977.57875
https://zookeys.pensoft.net

RESEARCH ARTICLE

A peer-reviewed open-access journal
ZooKeys
Launched to accelerate biodiversity research

Taxonomic notes on the genus *Campiglossa* Rondani (Diptera, Tephritidae, Tephritinae, Tephritini) in India, with description of three new species

Karamankodu Jacob David[1], David Lawrence Hancock[2], Santhamma Salini[1], Ramasamy Gandhi Gracy[1], Kandiyil Sachin[1]

1 *National Bureau of Agricultural Insect Resources, Bangalore-560024, Karnataka, India* **2** *60 South Street, Carlisle, Cumbria CA1 2EP, UK*

Corresponding author: Karamankodu Jacob David (davidkj.nbaii@gmail.com)

Academic editor: M. De Meyer | Received 21 August 2020 | Accepted 11 September 2020 | Published 22 October 2020

http://zoobank.org/14C6E040-62AE-4B5B-BFDD-D62EFED4E594

Citation: David KJ, Hancock DL, Salini S, Gracy RG, Sachin K (2020) Taxonomic notes on the genus *Campiglossa* Rondani (Diptera, Tephritidae, Tephritinae, Tephritini) in India, with description of three new species. ZooKeys 977: 75–100. https://doi.org/10.3897/zookeys.977.57875

Abstract

Three new species of *Campiglossa* Rondani are described from India: adults of both sexes and third instar larvae of *C. ialong* David, Salini & Hancock, **sp. nov.** and *C. sherlyae* David & Hancock, **sp. nov.**, plus an adult female of *C. shaktii* David, Sachin & Hancock, **sp. nov.**, are described and illustrated. Postabdominal structures, cephalopharyngeal skeleton, and anterior and posterior spiracles of *C. gemma* (Hering, 1939) and *C. sororcula* (Wiedemann, 1830) are illustrated. DNA barcode sequences of *C. ialong* **sp. nov.**, *C. sherlyae* **sp. nov.**, and *C. gemma* were obtained and reported. Records of *C. absinthii* (Fabricius, 1805) and *C. iracunda* (Hering, 1938) are regarded as misidentifications of *C. lyncea* (Bezzi, 1913) and *C. shaktii* **sp. nov.**, respectively, and excluded from the Indian fauna. A key to the known species of *Campiglossa* from India is provided. Results of preliminary phylogenetic analysis using COI revealed that *C. ialong* **sp. nov.** is paraphyletic to the *Campiglossa misella* group and C. *C. sherlyae* **sp. nov.** is a sister species of *C. deserta*.

Keywords

Asteraceae, *Conyza*, *Dioxyna*, northeast India, *Sonchus*, Western Ghats

Introduction

Campiglossa Rondani is one of the most speciose genera in the subfamily Tephritinae with nearly 200 described species (Norrbom et al. 1999; Han and Ro 2019). They are characterised by an elongate proboscis, a predominantly spinulose preglans area of the phallus, and bases of the antennae widely separated by a space 0.5–1 times the width of the scape (Korneyev 1999). *Campiglossa* is predominantly a Palaearctic genus but has representatives in other zoogeographic regions. Most species are associated with host plants of the family Asteraceae. The Afrotropical fauna was revised by Munro (1957) and the Palaearctic fauna by Korneyev (1990) and Merz (1992). Han and Ro (2019) synonymised *Homoeotricha* Hering and *Dioxyna* Frey with *Campiglossa* based on their analysis employing the mtCOI marker, but study of related genera is required before precise generic limits can be determined. The Indian fauna was studied by Bezzi (1913), Agarwal et al. (1989), and Hancock and McGuire (2002). Although Agarwal and Sueyoshi (2005) listed eight species of *Campiglossa* from India, Hancock (2008) regarded report of *C. iracunda* (Hering, 1938) from India as a misidentification, while record of *C. absinthii* (Fabricius, 1805) is also regarded as a misidentification, as discussed below. Three new species of *Campiglossa* encountered in India during surveys for fruit flies are described here. Postabdominal structures and larvae of *C. gemma* (Hering, 1939) and *C. sororcula* (Wiedemann, 1830) from southern India are described and illustrated along with taxonomic notes on the four other recorded Indian species. As types of these four species were not available for study, detailed redescriptions or diagnoses are not included.

Material and methods

Specimens deposited in NBAIR were examined for the study. Following are the acronyms used in the text:

NBAIR ICAR – National Bureau of Agricultural Insect Resources, Bangalore, India
NPC National Pusa Collection, Indian Agricultural Research Institute, New Delhi, India
ZSI Zoological Survey of India, Kolkata, India

Collections were made by sweep netting and rearing infested flowers of host plants belonging to family Asteraceae. Images of specimens were taken using a Leica DFC 420 camera mounted on a Leica M205A stereozoom microscope; images of genitalia were taken using an 8 MP camera temporarily attached to a Leica DM 1000 compound research microscope. Multiple images were stacked and combined to a single image using Combine ZP (Hadley 2011). Line drawings were made using a drawing tube attached to a Leica DM 1000 compound microscope. Measurements of male and

female genitalia were taken using Leica Automontage Software, LAS 3.4. Terminology adopted here follows White et al. (1999). Singular form is used for all paired organs and setae in the text (e.g., one postpronotal lobe seta means one pair of postpronotal lobe setae). Ratios have been calculated as per Han and Ro (2019).

DNA isolation and partial gene sequencing of COI

To isolate the genomic DNA, the hind and mid legs (one each) of individual insects were used and the DNA isolation was carried out using the Qiagen DNeasy Blood & Tissue Kit method following the manufacturer's protocol. After obtaining the DNA, the quality and quantity were estimated using nanodrop-BioRad. PCR amplification of partial gene sequences of mitochondrial COI gene was carried out by using the universal COI primers (Hebert et al. 2004). PCR amplification was performed for a total volume of 30 µL, containing 2 µl DNA extract (20 ng), 1 µl (2mol) of each primer, 1 µl dNTP mixture (2.5 mmol for each), 2.5 µL 10x Taq PCR reaction buffer, 3 µL 25 mM $MgCl_2^+$, and 1 unit of Taq DNA polymerase using a thermal cycler (BioRad iCycler) with the PCR cycle as follows: initial step at 94 °C for 1 minute and 35 cycles of the following: denaturing 95 °C for 30 seconds, annealing 51 °C for 30 seconds, extension at 72 °C for 45 seconds and 4 °C thereafter (Ball and Armstrong 2008). The PCR products size varied from 650 to 680 bp; the amplified products were confirmed by running on 1.5% agarose gel with 250 bp ladder and visualized in INGENIUS gel dock. The amplified products were purified using Qiagen PCR purification Kit by following the manufacturer's instructions and the purified samples were sequenced using Sanger's method. The sequences were annotated using NCBI Blast tools and submitted to NCBI GenBank Database where accession numbers were obtained (*C. ialong* sp. nov. – MT169786; *C. sherlyae* sp. nov. – MT019895; *C. gemma* – MT169785; *C. sororcula* – MT019889)

Construction of molecular phylogeny tree

The molecular phylogeny of *Campiglossa* was constructed using the software MEGAX (Kumar et al. 2018). A total of 18 DNA barcode sequences were used for this analysis including the outgroup *Tephritis conura* Loew, in which four were from India and another 14 were downloaded from NCBI database. *Campiglossa* from Oriental, Palaearctic, and Nearctic regions were included in the analysis. The evolutionary relationship was inferred using the maximum likelihood method. The General Time Reversible model (Nei and Kumar 2000) was used with uniform rate of substitution. The bootstrap consensus tree inferred from 1000 replicates was taken to represent the evolutionary history of the taxa analyzed (Felsenstein 1985). Branches corresponding to partitions reproduced in less than 50% bootstrap replicates were collapsed. Initial tree(s) for the heuristic search were obtained automatically by applying the maximum parsimony method. This analysis involved 18 nucleotide sequences. Codon positions included were 1^{st} + 2^{nd} + 3^{rd}.

Results

Key to species of *Campiglossa* Rondani from India

1 Scutellum with one pair of distinct setae, the apical pair absent or vestigial; wing pattern reticulate with dark markings pale and diffuse ..... ***C. sororcula* (Wiedemann)**

– Scutellum with two pairs of setae, the apicals distinct; wing with dark markings distinct **2**

2 All femora yellow or yellowish orange with no trace of brown or black colour **3**

– All femora predominantly black/brown **5**

3 Apex of cell r_{4+5} without a hyaline spot, apical scutellar seta as long as basal, spermatheca elongate and tubular, aculeus tip broad with preapical indentations ..... ***C. gemma* (Hering)**

– Apex of cell r_{4+5} with a hyaline spot, apical scutellar seta shorter than basal, spermatheca oval or round, aculeus tip pointed with or without preapical indentation **4**

4 Pterostigma with two yellow or hyaline spots, aculeus tip with preapical indentation, spermathecae round .... ***C. shaktii* David, Sachin & Hancock, sp. nov.**

– Pterostigma with a single hyaline spot, aculeus tip pointed without preapical indentation, spermathecae oval ..... ***C. ialong* David, Salini & Hancock, sp. nov.**

5 Posterior notopleural seta black; cell r_{2+3} with one hyaline marginal spot **6**

– Posterior notopleural seta white; cell r_{2+3} with two hyaline marginal spots ... **7**

6 Base of the cell r_{2+3} in wing usually with three round hyaline spots before the crossvein r-m (distribution: Kashmir) ..... ***C.producta* (Loew)**

– Base of the cell r_{2+3} in wing predominantly black or brown with single prominent hyaline spot near the crossvein r-m (distribution: southern India)..... ***C. sherlyae* David & Hancock, sp. nov.**

7 Wing with hyaline discal spots between apices of veins R_1 and Cu_1 large and often crossing cells; pterostigma with a single, medial hyaline spot..... ***C. lyncea* (Bezzi)**

– Wing with hyaline discal spots between veins R_1 and Cu_1 small and rounded, not crossing cells; pterostigma with two (small or large) hyaline spots..... **8**

8 Hyaline spots in pterostigma very small and rounded; abdomen with two submedian yellow spots each on tergites 1+2 to 6, scutum with longitudinal stripes ..... ***C. kumaonensis* Agarwal et al.**

– Hyaline spots in pterostigma large and quadrate; abdomen with two median black spots on each abdominal tergite except tergite 1+2; scutum without longitudinal stripes ..... ***C. cribellata* Bezzi**

Taxonomy

Genus *Campiglossa* Rondani

Campiglossa Rondani, 1870: 121. Type species *Tephritis irrorata* Fallen, by original designation.

Diagnosis. antennae widely separated by 0.5–1× width of scape; proboscis elongate and geniculate; scutum with dorsocentral setae placed near transverse suture; posterior notopleural seta black, brown, yellow, or white; apical scutellar seta often shorter than basals; epandrium elongate and usually with a lateral surstylar flange; preglans area of phallus spinulose; glans of phallus with elongate tubular acrophallus; aculeus tip often with preapical indentations; spermatheca tubular, oval or round, and spinulose (Korneyev 1990; Merz 1994).

Campiglossa ialong David, Salini & Hancock, sp. nov.

http://zoobank.org/ECA22E62-C83C-458E-8CC7-9830831F6E99
Figures 1–11

Diagnosis. Medium-sized fly (3.74–4.25 mm), body grey, pollinose, with white setulae; scutum without prominent stripes; abdomen with submedian black markings; wing with reticulate pattern.

Description. Male (body length, 3.74–4.25 mm; wing length, 3.76–4.04 mm).

***Head*:** Slightly higher than long (head ratio 0.83–0.86); frons fulvous (frons-head ratio 0.38–0.40), with a medial band of pruinosity from ocellar triangle to lunule leaving two dark fuscous lateral bands devoid of pruinosity; two frontal setae (three in a few specimens); two subequal orbital setae (posterior one white); well-developed proclinate ocellar seta (0.7 length of medial vertical seta); lateral vertical seta white; medial vertical seta black; paravertical seta white; postocular setae intermixed black and white. Scape, pedicel, and flagellomere concolorous with frons; pedicel plus flagellomere shorter than face; arista bare; face concave with raised epistomal margin; gena and occiput fulvous. Eye ratio 0.64–0.69; gena-eye ratio 0.13–0.18; antenna-head ratio 0.45–0.47; arista-antenna ratio 1.20–1.45.

***Thorax*:** Scutum grey pollinose, with three faint stripes and well-developed chaetotaxy (all setae black); one postpronotal lobe seta, one presutural supra-alar seta, one anterior notopleural seta, one posterior notopleural seta, one dorsocentral seta near transverse suture, placed anterior of postsutural supra-alar seta and posterior notopleural seta, one presutural supra-alar seta, one postalar seta, one intra-alar seta, one prescutellar acrostichal seta. Anepisterum grey with single black anepisternal seta in line with posterior notopleural seta; anepisternum covered with tiny white setulae; thick white setulae posteriorly near phragma; anepimeron without any black setae, with thick stub-

Figure 1. Habitus (male) of *Campiglossa ialong* David, Salini & Hancock, sp. nov.

by white setulae anteriorly; katepisternum with single black seta posterior to phragma in dorsal region; anatergite and katatergite grey without any setulae; haltere pale yellow. Scutellum flat, yellow with sparse white setulae; two scutellar setae; apical scutellar seta 2/3 length of basal scutellar seta. Mediotergite grey, without setulae.

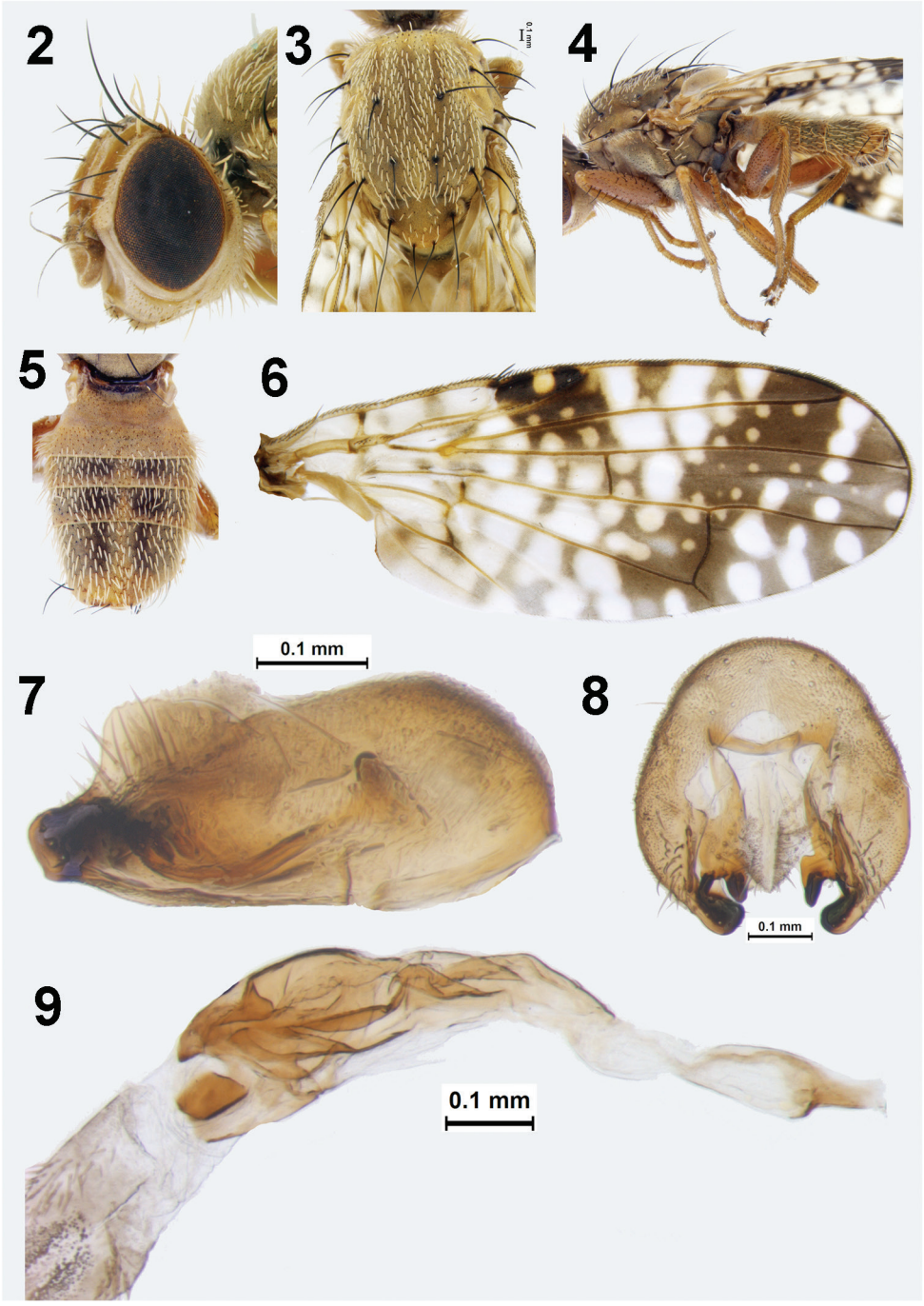

Figures 2–9. *Campiglossa ialong* David, Salini & Hancock, sp. nov. **2** head **3** thorax (dorsal view) **4** thorax (lateral view) and legs **5** abdomen **6** wing **7** epandrium and surstyli (lateral view) **8** epandrium and surstyli (posterior view) **9** glans of phallus.

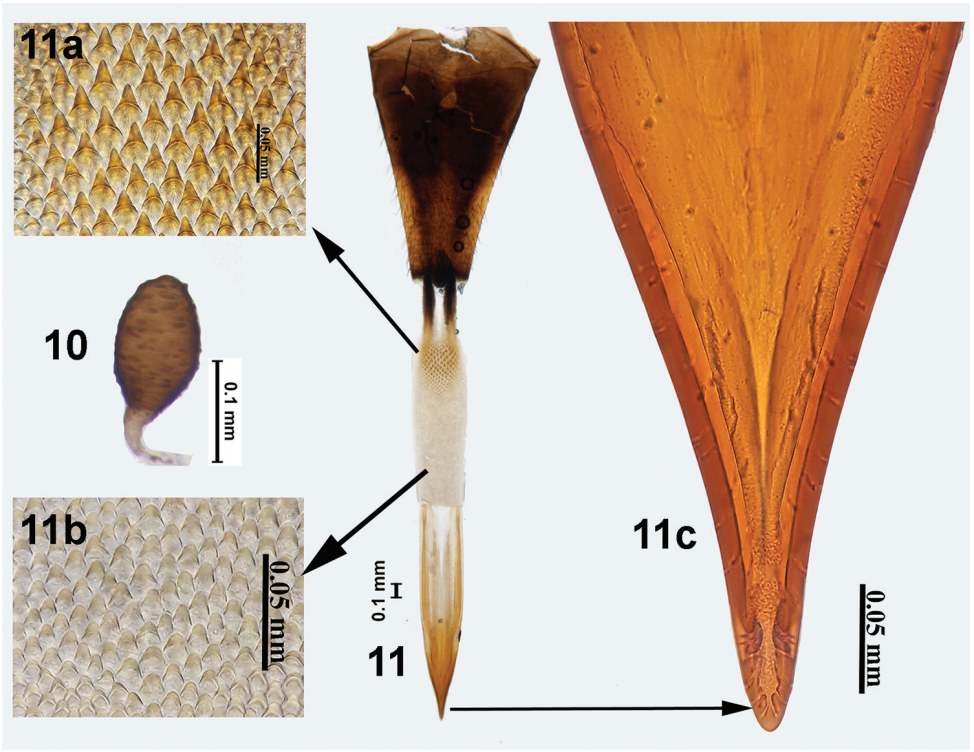

Figures 10, 11. *Campiglossa ialong* David, Salini & Hancock, sp. nov. **10** spermatheca **11** ovipositor **11a** spicules on proximal end of eversible membrane **11b** spicules on distal end of eversible membrane **11c** aculeus tip.

***Legs*:** All segments unicolorous, yellowish orange; fore femur with single row of five or six stout ventral setae, two rows of dorsal setae; mid and hind femur covered with tiny black setulae. Mid tibia with four apical spines, one elongate, the others all 1/4 length of prominent spine.

***Wing*:** Reticulate pattern, with hyaline and yellow spots; basal 1/3 hyaline with faint brown markings; apical 2/3 dark brown with numerous hyaline and yellow spots. Cell bc hyaline; cell c hyaline with two faint brown markings; pterostigma dark brown with a medial, yellow spot/patch; apex of cell r_1 and r_{2+3} black without any hyaline spots; cell r_{2+3} with a preapical dumbbell-shaped spot. Cell r_1 with three broad hyaline patches and irregular yellow spots or patches; cell r_{2+3} hyaline only in basal portion, rest brown to black with irregular yellow spots and, broad hyaline markings that are extensions of the hyaline markings from cell r_1 and preapical dumbbell-shaped spot (separate spots in a few specimens). Cell br predominantly hyaline, with irregular brown markings; cell r_{4+5} predominantly black or brown with an apical hyaline spot, two preapical spots, numerous yellow spots, and a broad basal hyaline spot. Cells bm and bcu hyaline; basal 2/3 of cell dm largely hyaline, with narrow basal and submedial brown

transverse bands, apical 1/3 brown with hyaline spots; cell m with four broad irregular markings; cell cu_2 and anal lobe predominantly hyaline with irregular brown markings.

***Abdomen*:** Grey pollinose, with white setulae; tergites 1+2 broad, with reduced pruinosity; tergites 3–5 with broad, submedian, quadrate patches; tergite 5 is 2–2.25× broader than tergites 3 and 4, with apical black setae. Sternites grey; posterior margin of sternite 5 with shallow concavity.

***Male genitalia*:** Epandrium elongate, tapering towards surstylar end (lateral view) without clear demarcation between surstylus and epandrium. Lateral surstylar flange as high as epandrium, serrate throughout its entire length; apex of lateral surstylus without clear demarcation of anterior and posterior lobes; proctiger hyaline, microtrichose. Epandrium oval in outline (caudal view); medial surstylus well developed with prensisetae. Phallus elongate (1.34 mm); preglans area strongly spinulose; basal lobe absent; glans of phallus sclerotised, 1/2 length of phallus (0.78 mm), with well-developed, elongate, tubular acrophallus.

***Female*:** Similar to male except larger (body length 4.56–5.23 mm; wing length 4.14–4.62 mm). Oviscape shining black (1.66 mm); taeniae short (0.25 of total length of eversible membrane); spicules on anterior end of eversible membrane (1.30 mm) conical with pointed apex, whereas spicules of distal end conical with blunt apex. Aculeus elongate (1.38 mm) with pointed tip, devoid of preapical indentations. Spermatheca dark brown, oval, with transverse striations.

Type material. Holotype ♂, INDIA: Meghalaya, Mihmyntdu, Ialong, 25.476°N, 92.226°E, 13.x.2019, Salini S. Paratypes: 21♂♂, 7♀♀, same data as above except for two males with collector's name David K.J. 1 larva on slide (III instar), same data as above (NBAIR).

DNA barcode. GenBank accession number MT169786 (1♂, INDIA: Meghalaya, Mihmyntdu, Ialong, 25.476°N, 92.226°E, 24.x.2019, K.J. David).

Etymology. The specific epithet is a noun in apposition and refers to the type locality.

Third instar larva (Figs 12–14). Larva short, stout (3.22–3.51 mm), whitish to dull white. Mouthhook pointed with a well-developed preapical tooth as long as apical mouthhook; ventral apodeme 2× broader than mouthhook; mandibular neck not prominent; dorsal apodeme pointed dorsally; labial sclerite elongate; pharyngeal sclerite 2.5× longer than broad; hypopharyngeal bridge reduced; parastomal bar prominent; dorsal bridge pointed anteriorly; ventral bridge of hypopharyngeal sclerite pointed anteriorly; anterior sclerite not well developed; dorsal cornua undivided; ventral cornua with two branches. Anterior spiracle weakly sclerotised, with six tubules. Posterior spiracle with spiracular slits oval, slightly longer than wide, devoid of transverse striations; spiracles separated by distance equal to the length of each slit; dorsal and ventral spiracular bundle with 2–6 single hairs; lateral spiracular bundle with 4–6 single hairs.

Remarks. *Campiglossa ialong* is most similar to *C. iracunda* (Hering) in appearance but with only one hyaline spot at the apex of cell R_{2+3}, as in *C. siamensis* (Hardy 1973). However, the black posterior notopleural seta differs from *C. siamensis*, which has a brown or yellowish seta. As per the phylogenetic tree (Fig. 51), it is paraphyletic with the *misella* group.

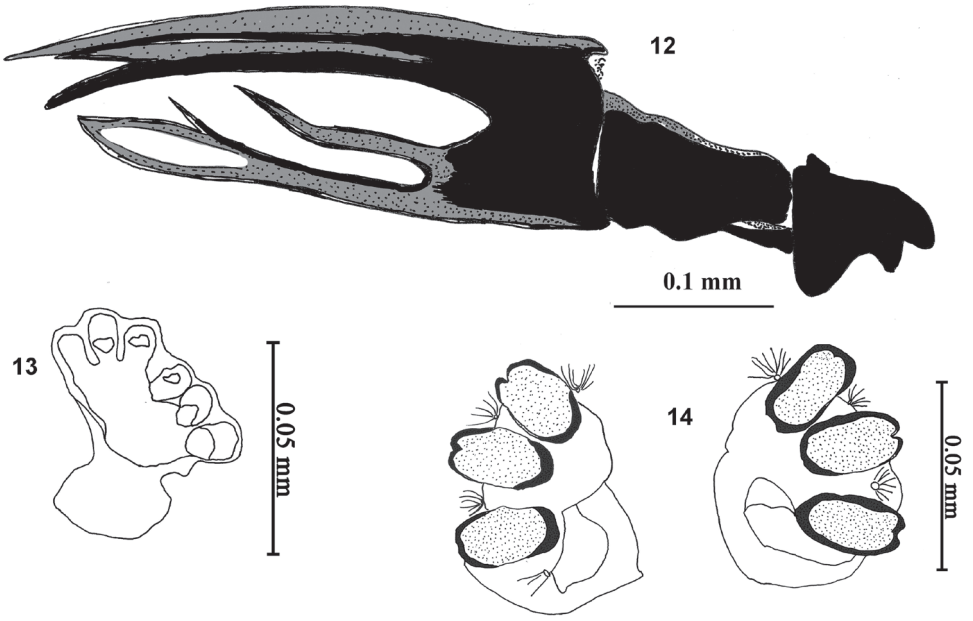

Figures 12–14. Larval morphology of *Campiglossa ialong* David, Salini & Hancock, sp. nov. **12** cephalopharyngeal skeleton **13** anterior spiracle **14** posterior spiracles.

***Campiglossa shaktii* David, Sachin & Hancock, sp. nov.**
http://zoobank.org/BC902BFB-A5BE-45F1-9543-F2C66F81391D
Figures 15–22

Diagnosis. Medium-sized fly (4.42–4.85 mm), body predominantly grey pollinose, with white setulae; scutum without prominent stripes; abdomen uniformly grey without submedian black markings; wing with reticulate pattern.

Description. Female (body length 4.40–4.66 mm; wing length 4.30–4.70 mm).

***Head*:** Slightly higher than long (head ratio 0.84–0.94), frons fulvous (frons-head ratio 0.42– 0.45), with a medial band of pruinosity from ocellar triangle to lunule leaving two dark fuscous lateral bands devoid of pruinosity; two frontal setae; two orbital setae; posterior one white, shorter than anterior; well-developed proclinate ocellar seta (0.7 length of medial vertical seta) longer than orbital and frontal setae; lateral vertical seta white; medial vertical seta black; paravertical white; postocular setae intermixed black and white. Scape, pedicel, and flagellomere concolorous with frons; pedicel plus flagellomere shorter than face; arista bare; face concave with raised epitsomal margin; gena and occiput fulvous. Eye ratio 0.65–0.72; gena-eye ratio 0.17–0.19; antenna-head ratio 0.39–0.42; arista-antenna ratio 1.34–1.49.

***Thorax*:** Scutum grey pollinose with three faint stripes and well developed chaetotaxy (all setae black); one postpronotal lobe seta, one presutural supra-alar seta, one anterior notopleural seta, one posterior notopleural seta, one dorsocentral setae

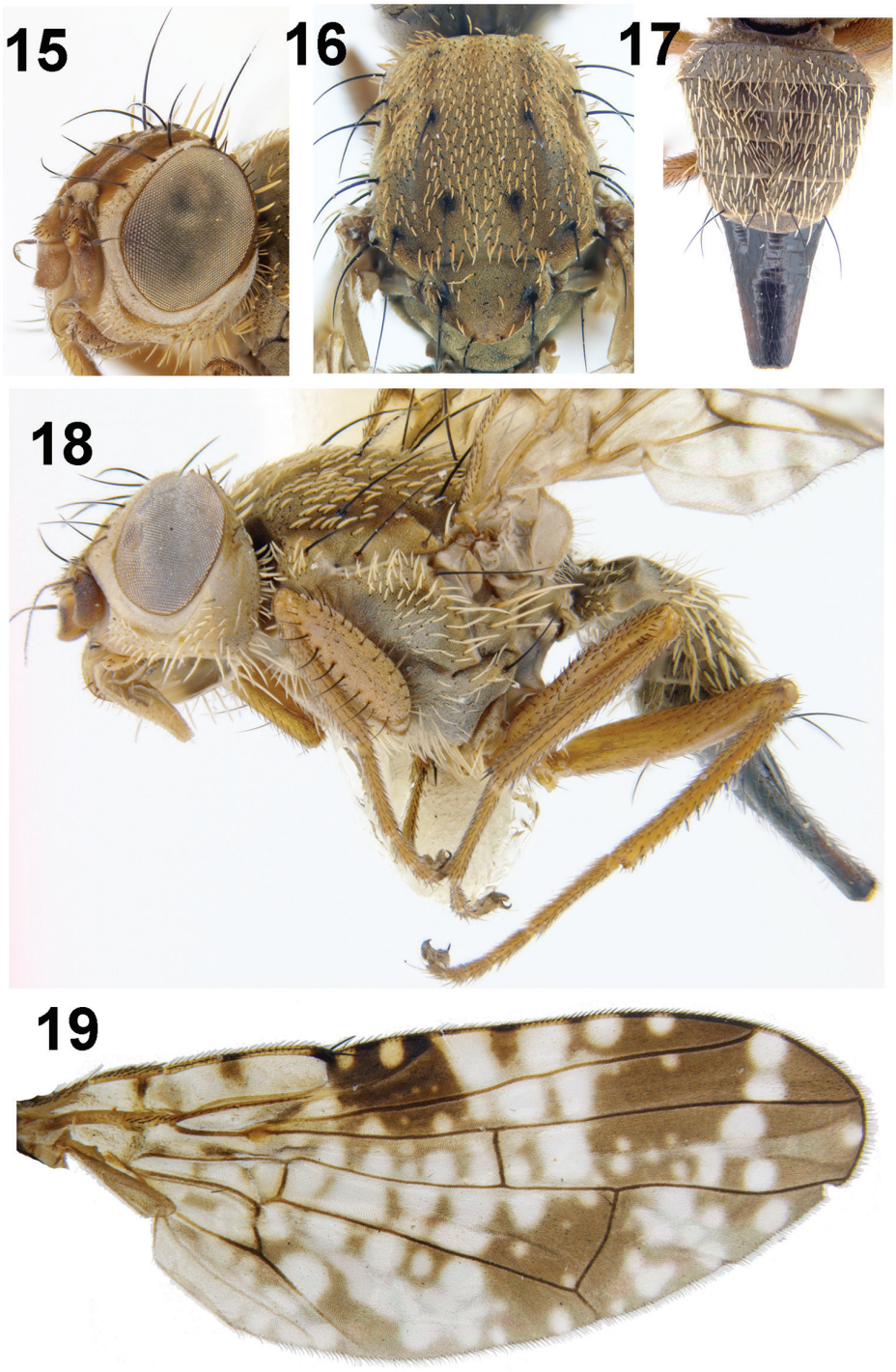

Figures 15–19. *Campiglossa shaktii* David, Sachin & Hancock, sp. nov. **15** head **16** thorax (dorsal view) **17** abdomen **18** thorax (lateral view) and legs **19** wing.

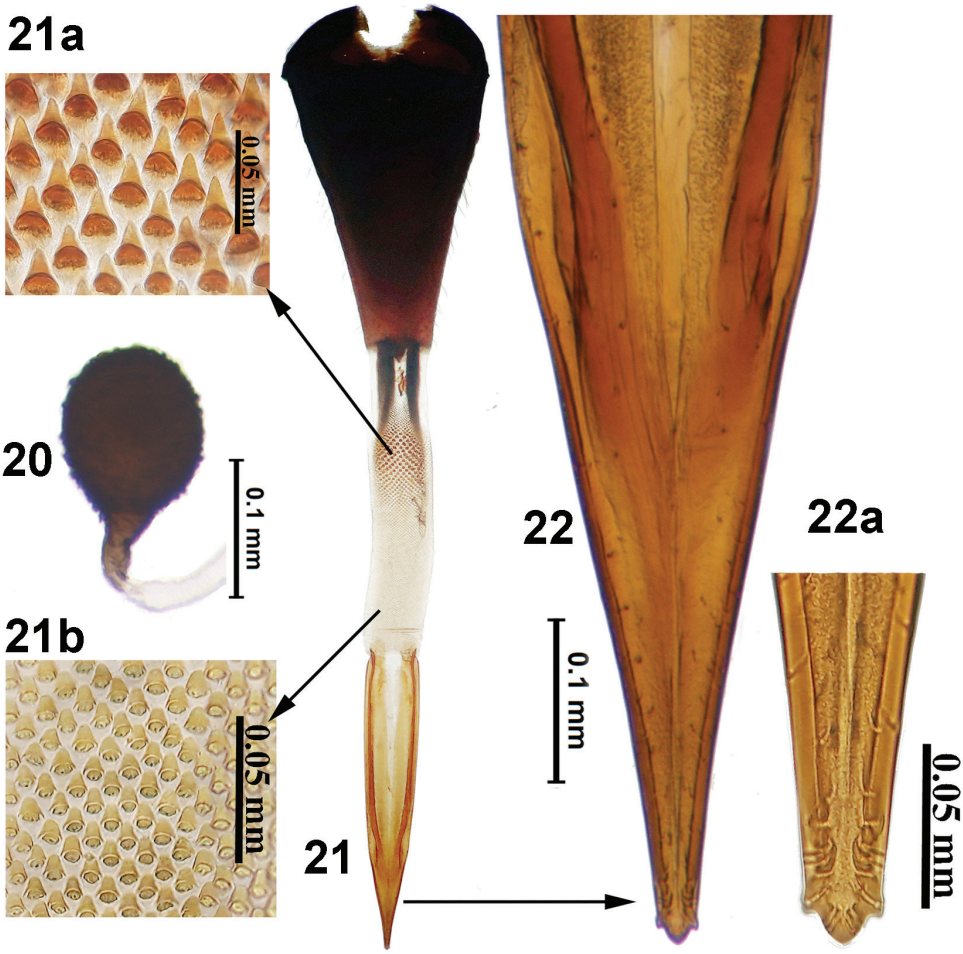

Figures 20–22. *Campiglossa shaktii* David, Sachin & Hancock, sp. nov. **20** spermatheca **21** ovipositor **21a** spicules on proximal end **21b** spicules on distal end of eversible membrane **22** aculeus **22a** aculeus tip.

near transverse suture, placed anterior of postsutural supra-alar seta and posterior notopleural seta, one presutural supra-alar seta, one postalar seta, one intra-alar seta, one prescutellar acrostichal seta. Anepisternum grey, with a single black anepisternal seta in line with posterior notopleural seta; anepisternum covered with white setulae in posterior half; elongate setae near phragma; anepimeron without any black setae, with thick, stubby, white setulae anteriorly; katepisternum with single black setae posterior to phragma; anatergite and katatergite grey, without any setulae; haltere pale yellow. Scutellum flat, grey, with sparse, white setulae; two pairs of scutellar setae; apical scutellar seta 2/3 length of basal scutellar seta. Mediotergite grey, without setulae.

***Legs*:** All segments unicolorous, yellowish orange; fore femur with single row of six or seven stout ventral setae, two rows of dorsal setae; mid and hind femur covered

with tiny black setulae. Tibiae and tarsi with rows of spines; mid tibia with four apical spines, one elongate, the others all 1/4 length of prominent spine.

***Wing*:** Reticulate pattern, with hyaline and yellow spots; cell bc hyaline with a brown spot on humeral crossvein; cell c hyaline with a single brown patch medially; pterostigma dark brown, with two round, yellow spots, the one closer to apex of vein Sc smaller compared to distal one; apex of cell r_1 and r_{2+3} black, without any hyaline spots. Cell r_1 with three broad, hyaline patches and irregular yellow spots; cell r_{2+3} dark basally, with two faint yellow spots or markings and with a preapical dumbbell-shaped spot. Cell br predominantly hyaline, with irregular brown markings; cell r_{4+5} predominantly black or brown, with a small apical hyaline spot, three preapical spots arranged in a triangle, numerous yellow spots, and hyaline basally. Cells bm and bcu hyaline; cell dm basally broadly hyaline with three narrow, transverse, brown bands to level of r-m crossvein; apically brown with hyaline spots; cell m with diffuse hyaline markings; cell cu_2 and anal lobe predominantly hyaline with irregular brown markings.

***Abdomen*:** Grey pollinose with white setulae; tergite 1 with reduced pruinosity; tergites grey without dark markings; oviscape glossy black and equal in length to tergites 4–6.

***Female genitalia*:** Oviscape dark brown to black (1.59 mm); eversible membrane as long as oviscape, with taeniae short (0.3 mm); spicules on proximal end of eversible membrane (1.44 mm) conical, well sclerotised, whereas spicules at distal end broadly conical and weakly sclerotised. Aculeus tip trilobed, with preapical indentation. Spermatheca black, round, spinose.

Type material. Holotype ♀, INDIA: Sikkim, Lachung, 08.vi.2012, Shakti K. Singh. Paratypes: 1♀, same data as holotype (NBAIR).

Etymology. This species is named after its collector, Shakti Kumar Singh.

Remarks. This species is undoubtedly the '*Paroxyna*' or '*Campiglossa*' *iracunda* of previous authors (Kapoor et al. 1979; Kapoor 1993; Agarwal and Sueyoshi 2005), the identity of which was discussed by Hancock (2008) and regarded as a misidentification.

Campiglossa sherlyae David & Hancock, sp. nov.

http://zoobank.org/A53ED0F8-DD7A-4A8F-A59F-B42B1F1C20C0
Figures 23–28

Diagnosis. Small fly (male 2.50–2.90 mm; female 2.80–3.36 mm); body grey pollinose, without prominent stripes; abdomen grey with submedian black markings; wing with reticulate pattern.

Description. Female (body length 2.80–3.36 mm; wing length 2.50–3.00 mm).

***Head*:** Nearly as long as high (head ratio 0.95–0.96), frons fulvous (frons-head ratio 0.40–0.41), with two frontal setae, two orbital setae (posterior orbital seta white), postocellar and postvertical seta white; lateral vertical seta white; medial vertical seta black; ocellar seta black and longer than frontal and orbital setae; postocular setae intermixed

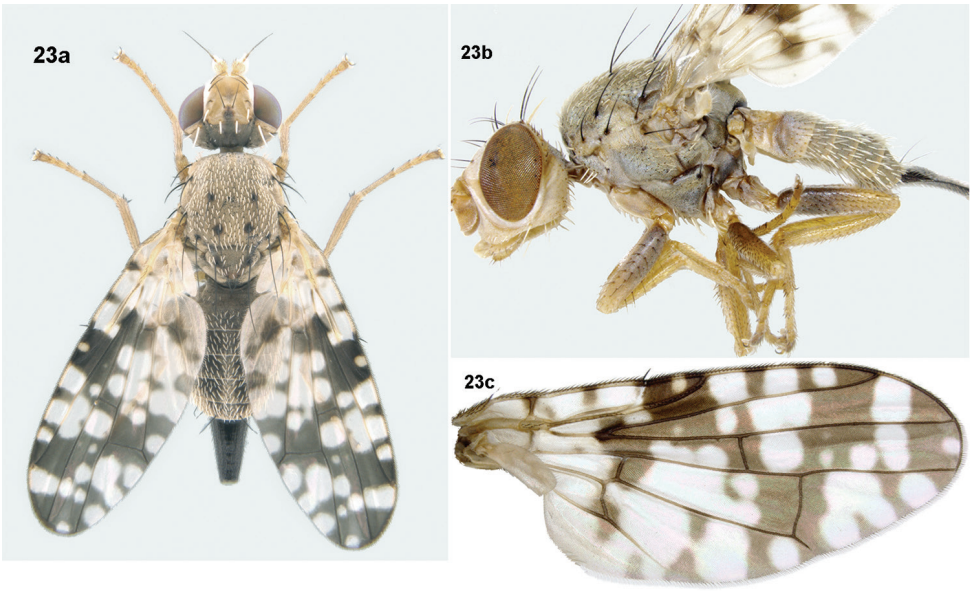

Figure 23. *Campiglossa sherlyae* David & Hancock, sp. nov. **23a** habitus (dorsal) **23b** habitus (lateral) **23c** wing.

black and white. Scape, pedicel, and flagellomere concolorous with frons; pedicel plus flagellomere shorter than face; arista bare; face concave, with raised epistomal margin; gena and occiput fulvous. Eye ratio 0.70–0.79; gena-eye ratio 0.14–0.15; antenna-head ratio 0.44–0.50; arista-antenna ratio, 1.22–1.38.

***Thorax*:** Scutum grey pollinose, without stripes and chaetotaxy well-developed (all setae black); one postpronotal lobe seta, one presutural supra-alar seta, one anterior notopleural seta, one posterior notopleural seta, one dorsocentral seta near transverse suture, placed anterior of postsutural supra-alar seta and posterior notopleural seta, one presutural supra-alar seta, one postalar seta, one intra-alar seta, one prescutellar acrostichal seta. Anepisterum grey, with single black anepisternal seta in line with posterior notopleural seta; anepisternum covered with white setulae; anepimeron without any black setae; katepisternum with single black seta posterior to phragma, anatergite, and katatergite grey without any setulae; haltere pale yellow. Scutellum flat, grey, with sparse white setulae; two scutellar setae; apical scutellar seta 1/2 length of basal scutellar seta. Mediotergite grey, without setulae.

***Legs*:** All femora with extensive black markings (0.75 of all femora with black markings), all other segments fulvous; fore femur with single row of four or five stout ventral setae, two rows of eight or nine dorsal setae; mid and hind femur covered with tiny black setulae. Tibiae and tarsi with rows of spines; mid tibia with four subequal apical spines.

***Wing*:** Reticulate pattern with hyaline and yellow spots; cell bc hyaline with a brown streak on humeral crossvein; cell c hyaline, with a single brown band medially;

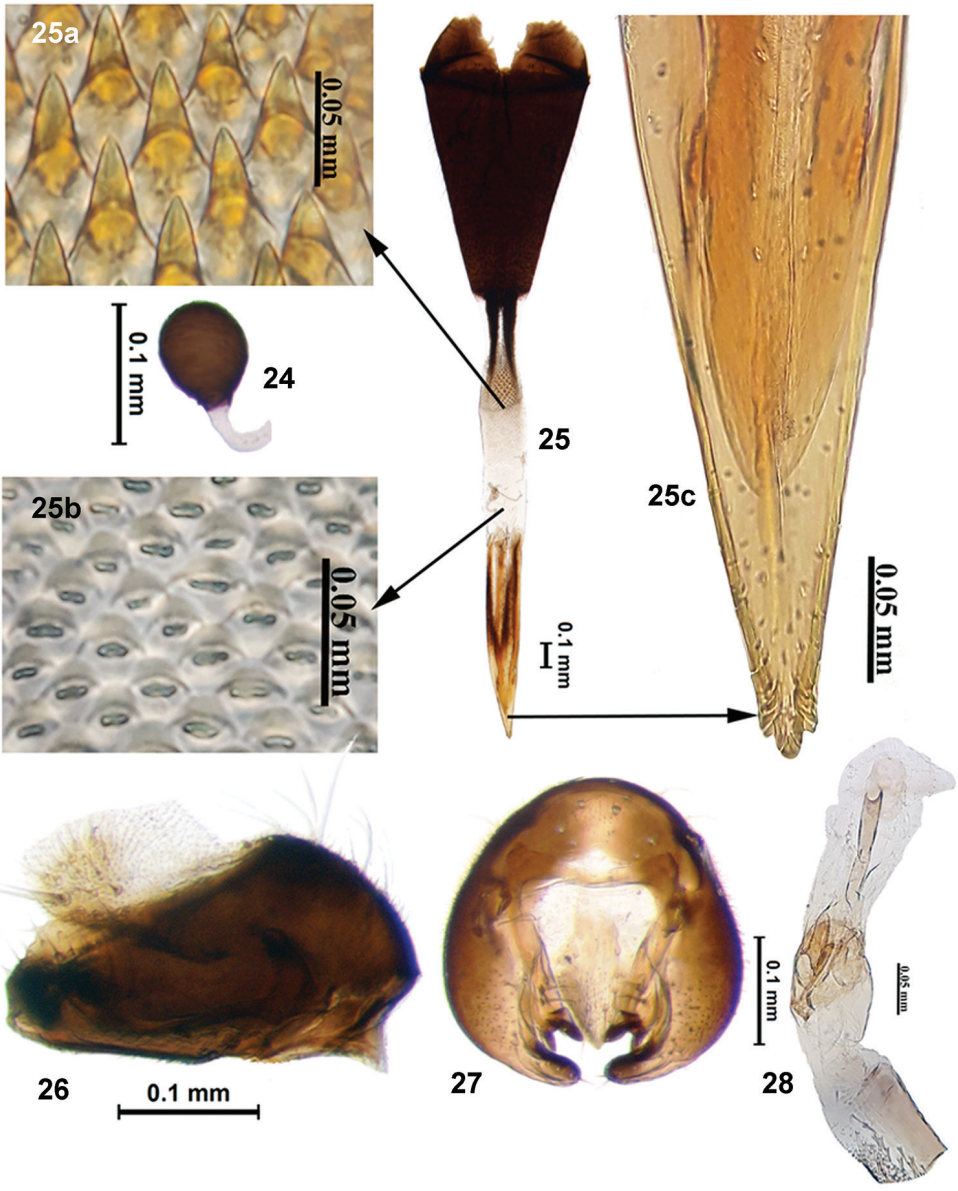

Figures 24–28. *Campiglossa sherlyae* David & Hancock, sp. nov. **24** spermatheca **25** ovipositor **25a** spicules on proximal end of eversible membrane **25b** spicules on distal end of eversible membrane **25c** aculeus tip **26** epandrium and surstyli (lateral view) **27** epandrium and surstyli (posterior view) **28** glans of phallus.

pterostigma dark brown, with a single hyaline spot, apex of cell r_1 and r_{2+3} without hyaline spot. Cell r_1 with three broad, hyaline patches, cell r_{2+3} with three broad, hyaline markings. Cell br hyaline basally and with a broad preapical hyaline patch; cell r_{4+5} with five uneven, hyaline spots (basal and subapical larger than medial and apical spot);

apex of cell r_{4+5} with small hyaline spot. Cells bm and bcu hyaline; cell dm predominantly hyaline with base and apex brown; cell m with a broad, hyaline mark (formed by fusion of three spots) and a preapical spot; cell cu_2 predominantly hyaline, with brown streaks and apical hyaline spot; apex of cell bcu with brown patch.

***Abdomen*:** Grey pollinose, with white setulae. Tergite 1 with reduced pruinosity; tergites grey with submedian markings on tergites 3–6; oviscape black and equal in length to tergites 4–6.

***Male postabdomen*:** Epandrium well sclerotised, without clear delineation between epandrium and lateral surstylus; proctiger hyaline, with densely arranged setae anteriorly; surstylar flange prominent, with serrated edge; epandrium and surstyli oval in outline in posterior view; medial surstylus with well-developed apical prensisetae. Phallus, excluding glans, 1.2 mm long; glans of phallus with well-developed tubular acrophallus.

***Female postabdomen*:** Oviscape black (1.02 mm), not longer than the combined length of last three abdominal segments. Eversible membrane (0.85 mm) with well-developed taeniae; spicules on proximal end of eversible membrane elongate and conical; distal end with broad conical spicules. Aculeus (0.89 mm) with tip trilobed. Spermatheca round, brown, granulose.

Type material. Holotype ♀, INDIA, Karnataka, Bangalore, Attur, 23.ix.2013, David, K. J. Paratypes: 3♂♂, 1♀, INDIA, Karnataka, Bangalore, Attur, 23.ix.2013, David K.J.; 4♂♂, 4♀♀, INDIA, Karnataka, Tumkur, Kunigal, 04.xii.2013, David K.J.; 1♂, INDIA, Karnataka, Bangalore, Attur, 09.xii.2013, David K.J.; 1♀, INDIA, Karnataka, Bangalore, Hebbal, 02.i.2014, David K.J.; 1♂, 1♀, INDIA, Karnataka, Bangalore, Attur, 08.xii.2014, Prabhu G.; 1♂, 2♀♀, INDIA, Karnataka, Bangalore, Attur, 13.x.2016, Prabhu G.; 1♂, 1♀, INDIA, Karnataka, Bangalore, Attur, 16.x.2016, Prabhu G.; 1♀, INDIA, Karnataka, Tumkur, Devarayanadurga, 04.iv.2017, Prabhu G.; 1♀, INDIA, Karnataka, Bangalore, Attur, 12.xii.2017, Prabhu G.; 1 larva in slide (III instar): INDIA: Karnataka, Bangalore, Attur, 18.xi.2013, Prabhu G. (NBAIR).

DNA barcode. NCBI GenBank accession number MT019895 (1♂, INDIA: Karnataka, Bangalore, Attur, 03.ix.2019, Sachin, K.).

Etymology. The species is named after the late Sherly Joseph, in memory of the first author's sister.

Third instar larva (Figs 29–31). Larva short (3.88–4.14 mm), fusiform, creamy white. Mouthhook pointed with a well-developed preapical tooth as long as the apical mouthhook; ventral apodeme broader than mouthook; mandibular neck not prominent; dorsal apodeme pointed dorsally, conical; labial sclerite elongate; hypopharyngeal sclerite longer than broad; hypopharyngeal bridge reduced; parastomal bar reaching midway of hypopharyngeal sclerite; ventral bridge of hypopharyngeal sclerite pointed anteriorly; anterior sclerite present; dorsal cornua undivided; ventral cornua with two branches. Anterior spiracle weakly sclerotised with six tubules. Posterior spiracle with spiracular slits oval, slightly longer than wide, devoid of transverse striations; spiracles separated by a distance twice the length of each slit; dorsal and ventral spiracular bundle absent; lateral spiracular bundle with three single hairs.

Host plant. Flowers of *Sonchus* sp. (Asteraceae).

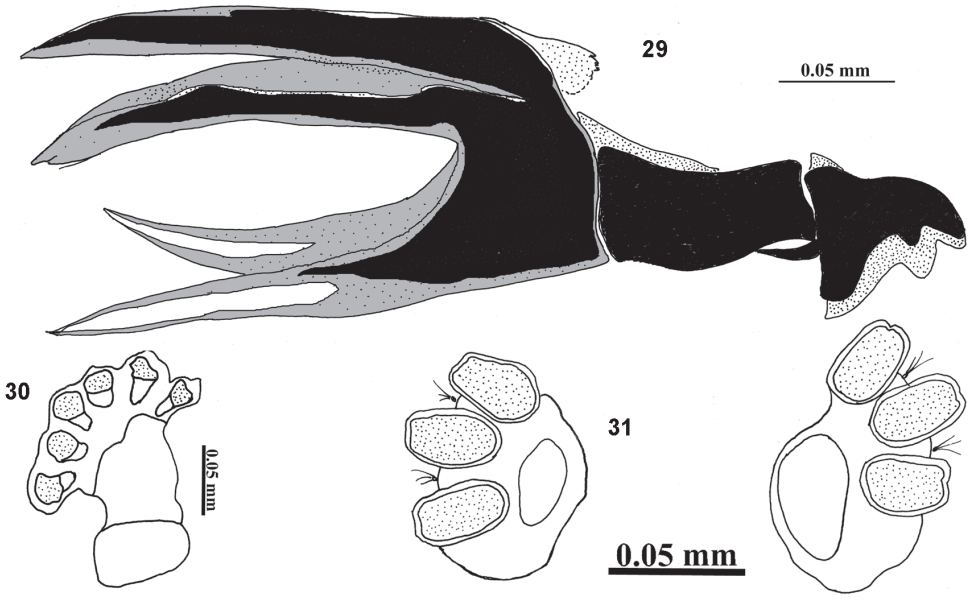

Figures 29–31. III instar larva of *Campiglossa sherlyae* David & Hancock, sp.nov. (Hering) **29** cephalopharyngeal skeleton **30** anterior spiracle **31** posterior spiracles.

Remarks. This species belongs in the *producta* group and is known only from Karnataka. It was misidentified as *C. deserta* (Hering, 1939) by Hancock and McGuire (2002) and their Indian record of a female from Mudigere, Karnataka, is *C. sherlyae*. Other records listed by Hancock and McGuire (2002) from Thailand and Vietnam appear to have been properly identified as *C. deserta*, which is a species widespread in China (including Guangxi Province), Korea, and Japan. *Campiglossa sherlyae* is very similar to *C. producta* and *C. deserta*, differing from *C. producta* in possessing predominantly black or brown base of cell r_{2+3} in wing with a prominent spot near crossvein r-m, and from *C. deserta* in lacking a hyaline base to cell r_{2+3} and in having *Sonchus* rather than *Lactuca* as its host plant. The phylogenetic tree (Fig. 51) shows that this species and Korean samples of *C. deserta* are closely related but with a 2% divergence based on a NCBI-GenBank sequence similarity search (BLAST), along with differences in morphological characters and host plant, suggest they are distinct.

Notes on other Indian species

***Campiglossa gemma* (Hering, 1939)**
Figures 32–37

Paroxyna gemma Hering, 1939: 183. Type locality: Kodaikanal, Tamil Nadu, India.

Material examined. 10♂♂, 4♀♀, INDIA, Tamil Nadu, HRS Kodaikanal, 01.iv.2012, David K.J.; 1♂, INDIA, Tamil Nadu, Kodaikanal, 02.iv.2012, Salini S.; 1♂, INDIA,

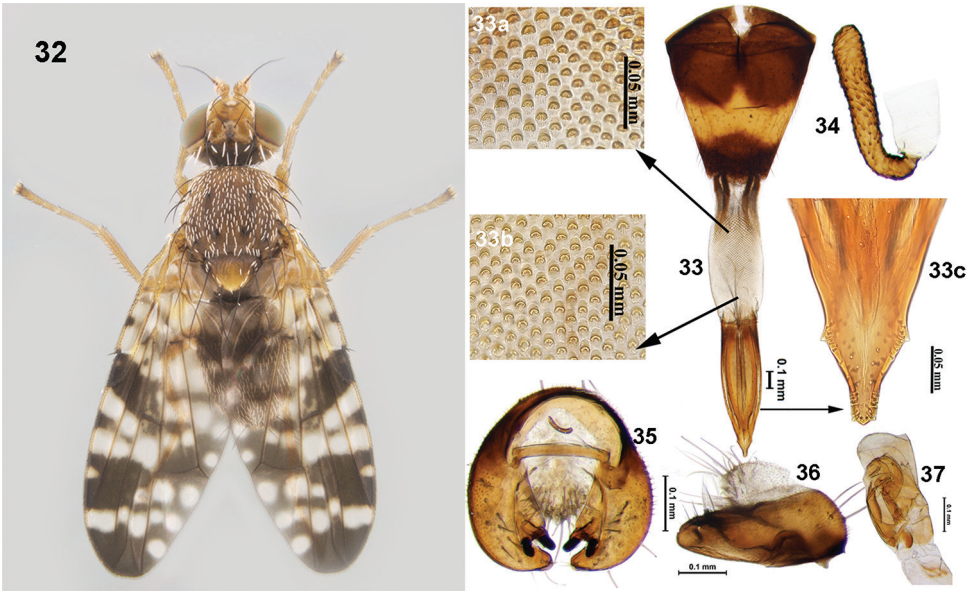

Figures 32–37. *Campiglossa gemma* (Hering) **32** habitus (dorsal view) **33** ovipositor **33a** spicules on proximal end of eversible membrane **33b** spicules on distal end of eversible membrane **33c** aculeus tip **34** spermatheca **35** epandrium and surstyli (posterior view) **36** epandrium and surstyli (lateral view) **37** glans of phallus.

Tamil Nadu, Shenbaganur, 02.iv.2014, Veenakumari K.; 2♂♂, INDIA: Tamil Nadu, Dindigul, Thandikudi, 08.xii.2019, Sachin, K., 2♂♂ same data as above except for the collector, K.J. David; 2♂♂, 2♀♀, INDIA: Tamil Nadu, HRS Kodiakanal, 10.xii. 2019, K.J. David; 2♂♂, 3♀♀, same data as above except K. Sachin, 1 larva in slide (III instar): INDIA: Tamil Nadu, HRS Kodiakanal, 10.xii. 2019, K.J. David, (NBAIR).

Description. Medium-sized fly (male 3.24–3.92 mm; female 4.49–4.83mm) with grey pollinose body, yellow legs, and reticulate wing pattern. Head slightly higher than long; frons fulvous with two frontal setae, two orbital setae (posterior orbital seta white), postocellar and postvertical seta white, lateral vertical seta white, medial vertical seta black, ocellar seta black longer than frontal and orbital seta. Scutum grey pollinose, with postpronotal lobe and notopleuron pale yellow, and well-developed chaetotaxy; posterior notopleural seta white. Scutellum with two pairs of scutellar setae; apical setae as long as basal setae. Legs fulvous, without any black markings. Wing with reticulate pattern; pterostigma black, without any hyaline spot or marking; apex of cell r_{2+3} and r_{4+5} without hyaline spot. Abdomen grey pollinose, without any markings.

***Male postabdomen*:** Epandrium elongate, without clear delineation between epandrium and surstylus; lateral surstylar flange lacking, proctiger hyaline, as high as epandrium. Epandrium and surstyli oval in outline (posterior view), medial surstylus with well-developed prensisetae. Phallus 1.58 mm long, with well sclerotised glans (Fig. 37).

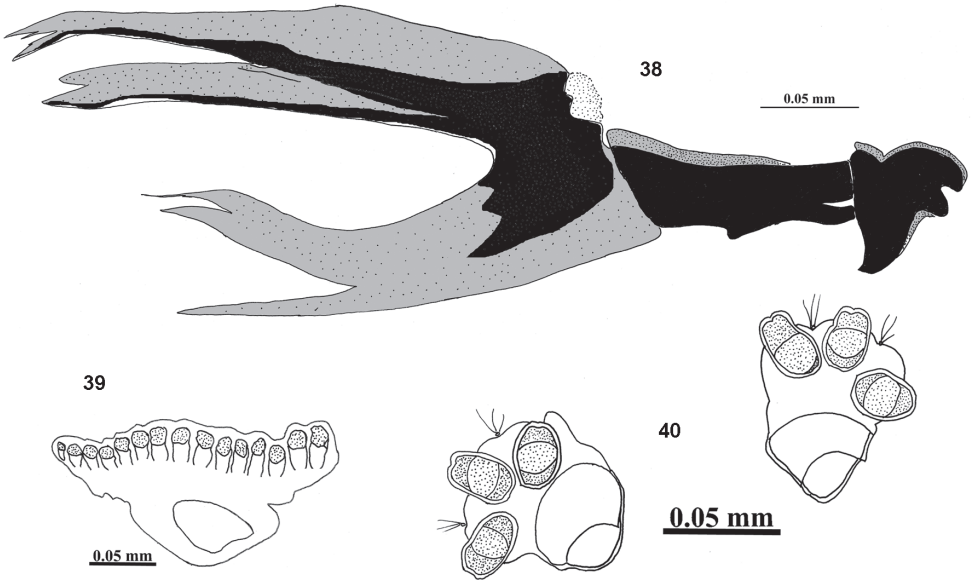

Figures 38–40. III instar larvae of *Campiglossa gemma* (Hering) **38** cephalopharyngeal skeleton **39** anterior spiracle **40** posterior spiracles.

***Female postabdomen*:** Oviscape brown (0.98 mm), with a median yellow band; eversible membrane (0.78 mm) with spicules on distal and proximal end an inverted U-shaped; distal spicules smaller compared to proximals; aculeus broad, with two preapical indentions (0.77 mm); spermatheca elongate, tubular, with striations.

DNA barcode. GenBank accession number MT169785 (1♀, INDIA: Tamil Nadu, Kodaikanal HRS, 3.x.2019, K.J.David).

Third instar larva (Figs 38–40). Larva short (2.66 mm), oblong, dull creamy white, with a black triangular marking posterodorsally. Mouthhook pointed with a well-developed preapical tooth as long as apical mouthhook; ventral apodeme broader than mouthook; mandibular neck not prominent; dorsal apodeme pointed posteriorly; labial sclerite elongate; hypopharyngeal sclerite 4× longer than broad; hypopharyngeal bridge pointed posteriorly; parastomal bar reaching beyond middle of hypopharyngeal sclerite; ventral bridge of hypopharyngeal sclerite not prominent; anterior sclerite present; dorsal cornua undivided; ventral cornua with two branches. Anterior spiracle weakly sclerotised with 15 tubules. Posterior spiracle with spiracular slits oval, slightly longer than wide, devoid of transverse striations; spiracles separated by a distance more than twice length of each slit; dorsal and ventral spiracular bundle absent in specimen examined; lateral spiracular bundle with three unbranched hairs.

Host plant. Flowers of *Conyza* sp. (Asteraceae).

Remarks. This species is known only from Tamil Nadu and western Karnataka (Kemmangundi) in southwestern India (this study; Hancock and McGuire 2002). Although there is some slight variation in wing markings, the examined specimens are

consistent with Hering's (1939) original description and most are from the type locality. In the phylogenetic tree, *C. gemma* is placed as a sister group to all the included *Campiglossa* species (Fig. 51). This might be due to the low taxon sampling or, alternatively, the species may belong to another genus, which should only be considered after a thorough study of other *Campiglossa* species and related groups.

***Campiglossa sororcula* (Wiedemann, 1830)**
Figures 41–47

Trypeta sororcula Wiedemann, 1830: 509. Type locality: Tenerife, Canary Islands.

Material examined. 2♂, INDIA, Tamil Nadu, Ooty, Emerald, 17.ii.2016, Prabhu G., 1♀, INDIA, Karnataka, Bengaluru, Attur, 08.xi.2016, Prabhu G., 1♂, INDIA, Karnataka, Bengaluru, Attur, 16.v.2017, Prabhu G., 1♂1♀, INDIA, Karnataka, Bengaluru, Attur, 04.vii.2017, Prabhu G., 1♀, INDIA, Karnataka, Bengaluru, Attur, 07.viii.2018, Prabhu G., 1♀, INDIA, Karnataka, Bengaluru, Attur, 16.viii.2018, Prabhu G., 1♀, INDIA, Karnataka, Bengaluru, Attur, 21.iii.2018, Prabhu G., 2♀3♂, INDIA, Karnataka, Bengaluru, G.K.V.K, 17.vi.2019, Sachin K., 2♀2♂, INDIA, Kerala, Palakkad, Nelliyampathy, 11.xii.2019, David K.J., 3♂, INDIA, Kerala, Palakkad, Nelliyampathy, 11.xii.2019, Sachin K., 4♂, INDIA, Karnataka, Bangalore, Attur, 18.ii.2020, Maruthi K.V., 1 larva in slide (III instar): INDIA: Karnataka, Bangalore, Attur, 12.vii. 2019, Sachin, K., (NBAIR)

Description. Small fly (male 2.37–2.94 mm; female 3.0–3.39 mm) with grey pollinose body, yellow legs, and reticulate wing pattern. Head longer than high, frons with two frontal setae, two orbital setae (posterior orbital seta white), postocellar, postvertical seta white, lateral vertical seta white, medial vertical seta black, ocellar seta black and longer than frontal and orbital seta. Scutum grey pollinose with postpronotal lobe and notopleuron pale yellow and well-developed chaetotaxy, posterior notopleural seta black. Scutellum with two scutellar setae. Legs with fulvous black patches on mid and hind femur. Wing with reticulate pattern; pterostigma black without any hyaline spot or marking; apex of cell r_{4+5} with a hyaline spot. Abdomen grey pollinose; tergites 3–5 with a pair of quadrate, submedian, black markings.

***Male postabdomen*:** Epandrium elongate, without clear delineation between epandrium and surstylus; lateral surstylar flange lacking; proctiger hyaline, shorter than epandrium. Epandrium and surstyli circular in outline in posterior view; medial surstylus with well-developed prensisetae. Phallus 1.05 mm long, with well sclerotised glans (0.25 mm) (Fig. 44).

***Female postabdomen*:** Oviscape black (0.81 mm); eversible membrane (0.57 mm) with spicules on distal and proximal end inverted conical; distal spicules smaller compared with proximals; aculeus pointed (0.65 mm), without preapical indentions; spermatheca oval, with striations.

DNA barcode. GenBank accession number MT019889 (1♀, INDIA: Karnataka, Bangalore, Attur, 29.v.2019, K. Sachin.)

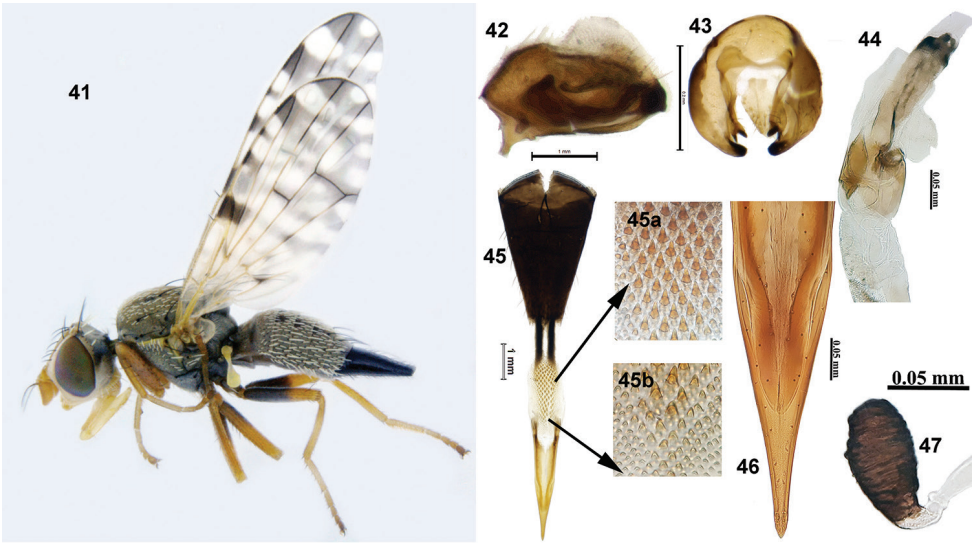

Figures 41–47. *Campiglossa sororcula* (Wiedemann) **41** habitus (lateral) **42** epandrium (lateral view) **43** epandrium (posterior view) **44** glans of phallus **45** ovipositor **45a** spicules on proximal end of eversible membrane **45b** spicules on distal end of eversible membrane **46** aculeus **47** spermatheca.

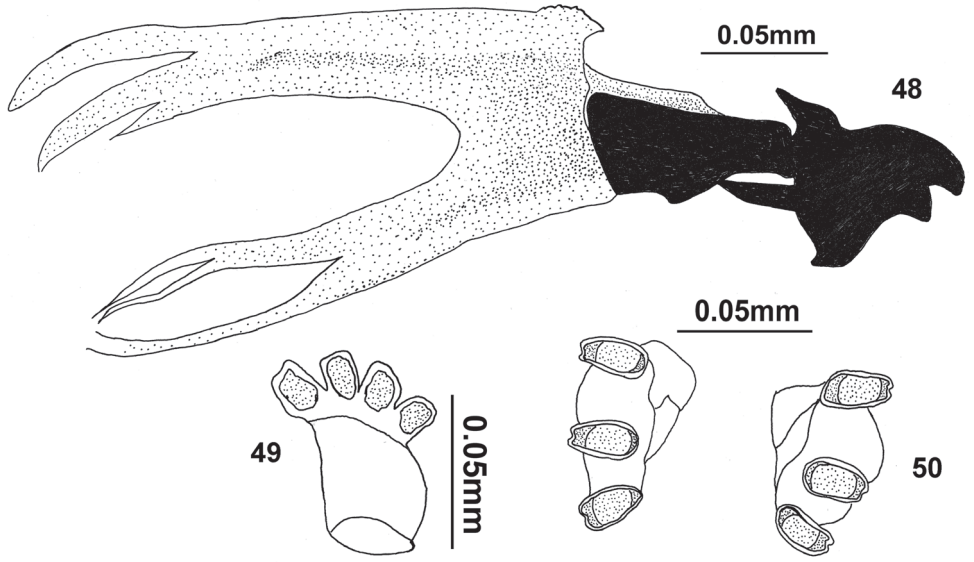

Figures 48–50. Third instar larva of *Campiglossa sororcula* (Wiedemann) **48** cephalopharyngeal skeleton **49** anterior spiracle **50** posterior spiracles.

Third instar larva (Figs 48–50). Larva short (3.08 mm), elongate, fusiform, creamy white. Mouthhook pointed, with a well-developed preapical tooth as long as the apical mouthhook; ventral apodeme broader than mouthook; mandibular neck not prominent;

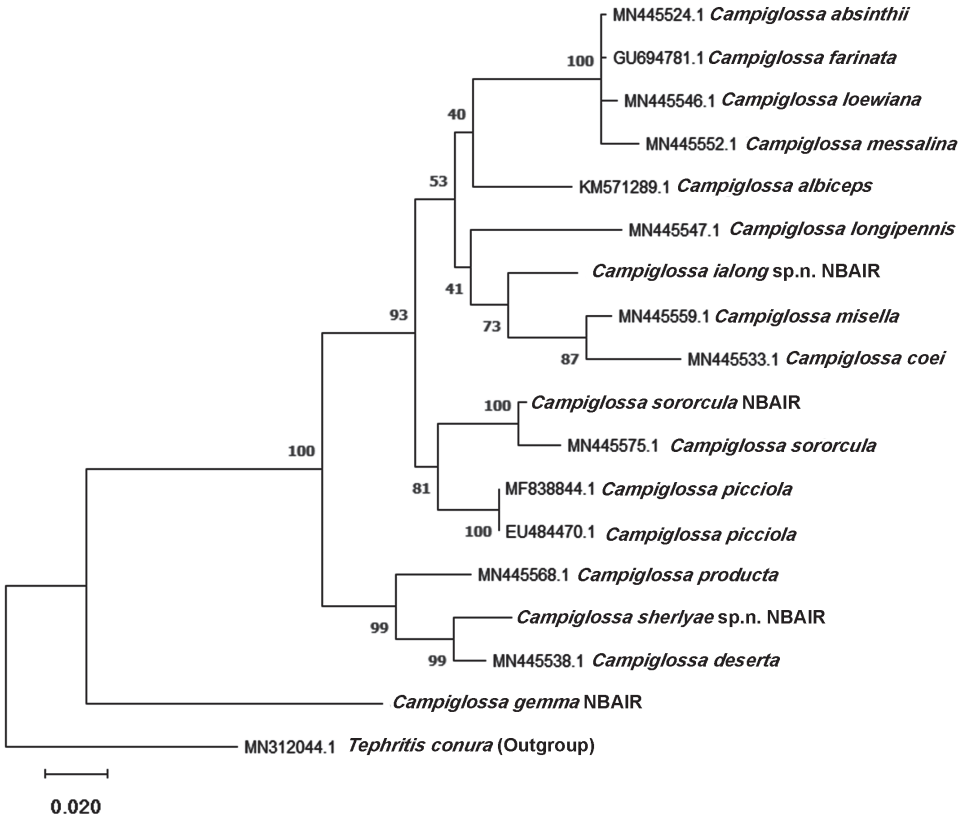

Figure 51. Maximum likelihood phylogram of 17 *Campiglossa* and one *Tephritis* (outgroup) DNA barcode sequences using General Time Reversible model. The number at each node is the boostsrap value based on ML analysis.

dorsal apodeme dagger-shaped, pointed posteriorly; labial sclerite elongate; hypopharyngeal sclerite 2–2.5× longer than broad; hypopharyngeal bridge pointed posteriorly; parastomal bar reaching beyond the middle of hypopharyngeal sclerite; ventral bridge of hypopharyngeal sclerite not prominent; anterior sclerite not prominent; dorsal cornua divided apically; ventral cornua with two branches. Anterior spiracle weakly sclerotised, with four tubules. Posterior spiracle with spiracular slits oval, slightly longer than wide, devoid of transverse striations; spiracles separated by a distance as equal to length of each slit; dorsal, ventral, and lateral spiracular bundle absent in specimen examined.

Host plants recorded during the study: flowers of *Bidens pilosa* L. and *Cosmos sulphureus* Cav. (Asteraceae).

Remarks. This species occurs commonly from southern Europe to Africa, Asia, and Australia, and has been introduced into Hawaii (Norrbom et al. 1999). Bezzi (1913), Hancock and McGuire (2002), Agarwal and Sueyoshi (2005), and David and Ramani (2011) recorded it from various locations in India, where it is widespread. Leg colour in many populations is variable (Hardy and Drew 1996); in India, the femora

are generally yellow with a black basal patch on mid and hind femora. Vestigial apical scutellar setae have been observed in some Australian populations (Hardy and Drew 1996), but Indian specimens lack the apical pair.

Campiglossa cribellata Bezzi, 1913

Campiglossa cribellata Bezzi, 1913: 161. Type locality: Kurseong, E. Himalayas, West Bengal, India.

Remarks. This species belongs in the *irrorata* group and was illustrated by Bezzi (1913) and Kapoor (1993). It is known only from the eastern Himalayas in India and Nepal (Bezzi 1913; Kapoor et al. 1979b). The host plant is unknown. The holotype, deposited in ZSI, is damaged (Banerjee, D; Diptera Section, ZSI, pers. comm.) and was not available on loan; hence, a detailed diagnosis and redescription are not included here.

Campiglossa kumaonensis Agarwal, Grewal, Kapoor, Gupta & Sharma, 1989

Campiglossa kumaonensis Agarwal, Grewal, Kapoor, Gupta & Sharma, 1989: 90. Type locality: between Naini Tal and Ranikhet, Uttar Pradesh, India.

Remarks. This species is provisionally included in the *irrorata* group and was illustrated by Agarwal et al. (1989) and Kapoor (1993). It is distinguished from *C. cribellata* by the reduced hyaline wing markings (particularly in the pterostigma and cell r_1) and the more elongate wing. This species is known only from the type locality. The holotype, deposited in NPC, could not be traced and might have been lost or misplaced; hence, a diagnosis and redescription are not included here. Its unusual wing shape suggests that placement in *Campiglossa* requires confirmation.

Campiglossa lyncea (Bezzi, 1913)

Tephritis lyncea Bezzi, 1913: 165. Type locality: Darjeeling, E. Himalayas, West Bengal, India.

Remarks. *Campiglossa lyncea* is distinguished from other Indian species by its mostly black femora, white posterior notopleural seta, two hyaline marginal spots in cell $r_{2+3,}$ and large, often coalesced, hyaline discal spots. This species is known only from northern India and includes the record of *C. absinthii* Fabricius, 1805 from Solan, Himachal Pradesh (Agarwal and Sueyoshi 2005), which was misidentified as the synonym *C. parvula* (Loew, 1862) by Kapoor et al. (1979a) and Kapoor (1993). The illustration of *C. parvula* by Kapoor (1993) closely matches *C. lyncea* of Bezzi (1913), whereas the

figure of *C. lyncea* in Kapoor's (1993) publication is copied from Hardy (1973) and is neither this species nor Indian. Hence, Hardy's (1973) Vietnamese records, considered to be conspecific with Kapoor's (1993) figure of '*C. lyncea*' by Hancock (2008), are also excluded. The syntypes of *C. lyncea*, deposited in ZSI, are damaged (Banerjee, D; Diptera Section, ZSI, pers. comm.) and were not available on loan. Hence, a detailed diagnosis and redescription are not included.

Campiglossa producta (Loew, 1844)

Trypeta producta Loew, 1844: 399. Type locality: Turkey.

Remarks. This species was recorded from India by Hancock and McGuire (2002), based on two males and two females from Gulmarg, Kashmir. However, given the complexity of this group, additional material is required for confirmation. Elsewhere, it is widespread from Western Europe to Central Asia, including Afghanistan (Agarwal and Sueyoshi 2005).

Acknowledgements

The first author is grateful to Dr. N. Bakthavatsalam, The Director, ICAR-National Bureau of Agricultural Insect Resources, Bangalore, India for the facilities and Science and Engineering Research Board (SERB), Department of Science and Technology, Government of India (CRG/2018/003247) for the financial support. We thank Dr Ho-Yeon Han, Yonsei University, South Korea, for the critical review of the manuscript and suggestions for its improvement.

References

Agarwal ML, Grewal JS, Kapoor VC, Gupta SK, Sharma SK (1989) Three new species of fruit flies (Diptera: Tephritidae) from India. Journal of Insect Science 2(2): 88–94.

Agarwal ML, Sueyoshi M (2005) Catalogue of Indian fruit flies (Diptera: Tephritidae). Oriental Insects 39: 371–433. https://doi.org/10.1080/00305316.2005.10417450

Ball SL, Armstrong KF (2008) Rapid, one-step DNA extraction for insect pest identification by using DNA barcodes. Journal of Economic Entomology101: 523–532. https://doi.org/10.1093/jee/101.2.523

Bezzi M (1913) Indian trypaneids (fruit-flies) in the collection of the Indian Museum, Calcutta. Memoirs of the Indian Museum 3: 53–175.

Felsenstein J (1985) Confidence limits on phylogenies: An approach using the bootstrap. Evolution 39: 783–791. https://doi.org/10.1111/j.1558-5646.1985.tb00420.x

Hadley A (2011) Combine ZP. http://www.hadleyweb.pwp.blueyonder.co.uk/ [Accessed on: 2019-7-12]

Han HY, Ro KE (2019) DNA barcoding reveals a species group of the genus *Campiglossa* (Diptera, Tephritidae, Tephritinae) with recognition of a new species from East Asia and previously unknown females of *Campiglossa coei* (Hardy). ZooKeys 899: 1–36. https://doi.org/10.3897/zookeys.899.46779

Hancock DL (2008) Systematic notes on some species in the fruit fly Tribe Tephritini (Diptera: Tephritidae: Tephritinae) in the Asian and Pacific Regions. Australian Entomologist 35(2): 77–72.

Hancock DL, McGuire DJ (2002) New species and records of non-dacine fruit flies (Insecta: Diptera: Tephritidae) from South and South-east Asia. Steenstrupia 27(1): 1–17.

Hardy DE (1973) The fruit flies (Tephritidae–Diptera) of Thailand and bordering countries. Pacific Insects Monograph 31: 1–353, pls 1–8.

Hardy DE, Drew RAI (1996) Review of the Australian Tephritini (Diptera: Tephritidae). Invertebrate Taxonomy 10(2): 213–405. https://doi.org/10.1071/IT9960213

Hering EM (1939) Neue Trypetiden der Erde. Verhandlunger Siebenter Internationaler Kongress für Entomologie, Berlin (1938)1: 165–190.

Kapoor VC (1993) Indian Fruit Flies (Insecta: Diptera: Tephritidae). International Science Publisher, New York, viii + 228 pp.

Kapoor VC, Agarwal ML, Grewel JS (1979a) Three new records of fruit flies from India with a note on wing venation of *Sphenella sinensis* (Dipt.: Teph.). Journal of the Natural History Museum, Nepal 3(4): 147–149.

Kapoor VC, Malla YK, Ghosh K (1979b) On a collection of fruit flies (Diptera: Tephritidae) from Kathmandu Valley, Nepal. Oriental Insects 13(1-2): 81–85. https://doi.org/10.1080/00305316.1979.10433545

Korneyev VA (1990) A review of *Sphenella* and *Paroxyna* series of genera (Diptera, Tephritidae, Tephritinae) of the Eastern Palaearctic. Nasekomye Mongolii [Insects of Mongolia] 11395–470. [In Russian, with English summary]

Korneyev VA (1999) Phylogeny of the subfamily Tephritinae: relationships of the tribes and subtribes. In: Aluja M, Norrbom AL (Eds) Fruit Flies (Tephritidae): Phylogeny and Evolution of Behavior. CRC Press, Boca Raton, Florida, 549–580. https://doi.org/10.1201/9781420074468.sec6

Kumar S, Stecher G, Li M, Knyaz C, Tamura K (2018) MEGA X: Molecular Evolutionary Genetics Analysis across computing platforms. Molecular Biology and Evolution 35: 1547–1549. https://doi.org/10.1093/molbev/msy096

Merz B (1992) Revision der west palaearktischen Gattungen und Arten der *Paroxyna*-Gruppe und Revision der Fruchtfliegen der Schweiz (Diptera, Tephritidae). PhD thesis, Zürich Switzerland: Eidgenössischen Technischen Hochschule Zürich, 341 pp.

Merz B (1994) Diptera Tephritidae. Insecta Helvetica Fauna 10: i–vii, 1–198.

Munro HK (1957) Trypetidae. In: Ruwenzori Expedition, 1934–1935. Vol. 2, No. 9. British Museum (Natural History), London, 853–1054.

Nei M, Kumar S (2000) Molecular Evolution and Phylogenetics. Oxford University Press, 333 pp.

Norrbom AL, Carroll LE, Thompson FC, White IM, Freidberg A (1999) Systematic database of names. In: Thompson FC (Ed.) Fruit Fly Expert Identification System and Systematic Information Database. A Resource for Identification and Information on Fruit Flies and Maggots, with Information on Their Classification, Distribution and Documentation. Myia 9: 65–251.

Rondani C (1870) Ortalidinae Italicae collectae, distinctae et in ordinum dispositae. Dipterologiae Italicae prodromus. Pars VII. Fasc. 4 (sect. 1) [concl.]. Bollettino della Societa Entomologica Italiana 2: 105–133.

White IM, Headrick DH, Norrbom AL, Carroll LE (1999) Glossary. In: Aluja M, Norrbom AL (Eds) Fruit Flies (Tephritidae): Phylogeny and Evolution of Behaviour. CRC Press, Boca Raton, Florida, 881–924. https://doi.org/10.1201/9781420074468.sec8

ZooKeys 977: 101–161 (2020)
doi: 10.3897/zookeys.977.55693
https://zookeys.pensoft.net

RESEARCH ARTICLE

A peer-reviewed open-access journal
ZooKeys
Launched to accelerate biodiversity research

Multiple data revealed two new species of the Asian horned toad *Megophrys* Kuhl & Van Hasselt, 1822 (Anura, Megophryidae) from the eastern corner of the Himalayas

Shengchao Shi[1,2,3], Meihua Zhang[1], Feng Xie[1], Jianping Jiang[1], Wulin Liu[4], Li Ding[1], Li Luan[5], Bin Wang[1]

1 *CAS Key Laboratory of Mountain Ecological Restoration and Bioresource Utilization & Ecological Restoration Biodiversity Conservation Key Laboratory of Sichuan Province, Chengdu Institute of Biology, Chinese Academy of Sciences, Chengdu 610041, China* **2** *Key Laboratory of Bio-Resource and Eco-Environment of Ministry of Education, College of Life Sciences, Sichuan University, Chengdu 610065, Sichuan, China***3** *University of Chinese Academy of Sciences, Beijing 100049, China* **4** *Forestry Survey and Design Research Institute of the Tibet Autonomous Region, Lhasa 850000, China* **5** *Chengdu Survey and Design Research Institute of China Electric Power Construction Group Co., Ltd., Chengdu 610041, China*

Corresponding author: Bin Wang (wangbin@cib.ac.cn); Jianping Jiang (jiangjp@cib.ac.cn)

Academic editor: A. Ohler | Received 22 June 2020 | Accepted 4 September 2020 | Published 22 October 2020

http://zoobank.org/E2A644A7-15F5-4052-AB1B-2DC062A3F308

Citation: Shi S, Zhang M, Xie F, Jiang J, Liu W, Li Ding1, Luan L, Wang B (2020) Multiple data revealed two new species of the Asian horned toad *Megophrys* Kuhl & Van Hasselt, 1822 (Anura, Megophryidae) from the eastern corner of the Himalayas. ZooKeys 977: 101–161. https://doi.org/10.3897/zookeys.977.55693

Abstract

Multiple disciplines can help to discover cryptic species and resolve taxonomic confusions. The Asian horned toad genus *Megophrys sensu lato* as a diverse group was proposed to contain dozens of cryptic species. Based on molecular phylogenetics, morphology, osteology, and bioacoustics data, the species profiles of *Megophrys* toads in the eastern corner of Himalayas in Medog County, Tibet Autonomous Region, China was investigated. The results indicated that this small area harbored at least four *Megophrys* species, i.e., *M. medogensis*, *M. pachyproctus*, *Megophrys zhoui* **sp. nov.**, and *Megophrys yeae* **sp. nov.**, the latter two being described in this study. Additionally, the mitochondrial DNA trees nested the low-middle-elevation and high-elevation groups of *M. medogensis* into a monophyletic group, being in discordance with the paraphyletic relationship between them revealed in the nuclear DNA trees. The findings highlighted the underestimated biodiversity in Himalayas, and further indicated that the *Megophrys* toads here have been probably experienced complicated evolutionary history, for example, introgression between clades or incomplete lineage sorting and niche divergences in microhabitats. Anyway, it is urgent for us to explore the problems because these toads are suffering from increasing threats from human activities and climatic changes.

Keywords
Multiple data, taxonomy, molecular phylogenetic analyses, morphology, introgression

Introduction

Species are the basic units of biodiversity, and species taxonomy is central to biodiversity explorations, further contributing to evolutionary biology, conservation biology and other categories of biological studies (Queiroz 2007; Condon et al. 2008; Wheeler et al. 2012). Increasing numbers of studies have advocated integrative taxonomy mainly because the findings from different disciplines would improve rigor (Dayrat 2005; Pante et al. 2014; Gómez Daglio and Dawson 2019). Integrative taxonomy has strongly promoted the discovery of cryptic species either in the understudied taxa (Larsen 2001; Bickford et al. 2007; Burns et al. 2008; Yoder et al. 2005) or in well-studied biomes (Rissler and Apodaca 2007; Stockman and Bond 2007). It could also resolve the taxonomic confusions like through demonstration of conspecificity of described species (Petrusek et al. 2008; Seifert 2009). And finally, multiple disciplines may further bring out clues for understanding the evolutionary processes of species for example in cases of disagreement among disciplines (DeSalle and Giddings 1986; Degnan and Rosenberg 2009; Thielsch et al. 2017).

The Asian horned toad *Megophrys sensu lato* Kuhl and Van Hasselt, 1822 (Anura, Megophryidae Bonaparte, 1850) widely inhabit mountain forests in the tropical and subtropical regions of Asia, ranging from India to south-central China and south to the Sundas and the Philippines (Frost 2020). The generic classifications of the group have been controversial for a long time (e.g., Tian and Hu 1983; Dubois 1987; Rao and Yang 1997; Lathrop 1997; Jiang et al. 2003; Delorme et al. 2006; Fei et al. 2009; Fei and Ye 2016; Chen et al. 2016; Mahony et al. 2017; Liu et al. 2018; Frost 2020). Most recent phylogenetic studies, however, clustered all members of the group into a monophyletic group (Chen et al. 2016; Mahony et al. 2017; Liu et al. 2018; Li et al. 2018; Liu et al. 2020; Wang et al. 2020), which was defined as one big genus *Megophrys sensu lato* by Mahony et al. (2017). The genus currently contains 95 species, of which, noticeably, 39 species were discovered in this decade (Frost 2020; Liu et al. 2020; Wang et al. 2020). What's more, molecular phylogenetic studies still put forward dozens of cryptic species in the group (Chen et al. 2016; Liu et al. 2018). Misleading taxonomic judgements without precise and adequate comparisons and insufficient field work often hinder the discovery of cryptic diversity in the group (Mahony et al. 2018; Liu et al. 2018). Hence, comprehensive examinations with multiple data (e.g., molecular phylogenetic, morphological, and bioacoustics data) are needed for describing new taxon and furtherly recognizing underestimated species diversity in this diverse group.

Himalaya Mountains holds high level of biodiversity, and with increasingly deep surveys, species diversity in this region was indicated to be much underestimated. For example, just in Medog County, Tibet Autonomous Region, China in the eastern corner of Himalayas, several new frog or toad species has been found in recent years (e.g.,

Jiang et al. 2012; Jiang et al. 2016a, b, c). In Medog County, two *Megophrys* species has been recorded, i.e., *M. pachyproctus* Huang, 1981 and *M. medogensis* Fei, Ye and Huang 1983. Nevertheless, for ca. four decades, there have been only incomplete morphological reports (e.g., Fei et al. 2009; Fei and Ye 2016) or separate molecular data for them (Chen et al. 2016; Liu et al. 2018) but no detailed evaluation on taxonomic profiles of their populations especially using multiple disciplines. According to the hypothesis "lots of cryptic species in *Megophrys*" (Chen et al. 2016; Liu et al. 2018), it is expected that the toad populations in this high-profile biodiversity hotspot may contain cryptic species.

In recent years, we conducted a series of field surveys in Medog County, Tibet Autonomous Region, China, and collected a series of specimens of *Megophrys sensu lato*. Based on molecular phylogenetic, morphological, osteological and bioacoustics data, we will explore the species composition of the Asian horned toad *Megophrys* in Medog County, Tibet Autonomous Region, China in the eastern corner of Himalayas. Our multiple-data comparisons proposed that the specimens contained two undescribed species. Herein we describe them as two new species.

Materials and methods

Sampling

A total of 50 *Megophrys* specimens was collected from nine sites in Medog County, Tibet Autonomous Region, China (Fig. 1; for voucher numbers see Table 1, Suppl. material 1: Tables S1, S2). The specimens were identified as four species, i.e., *M. medogensis*, *M.* cf. *pachyproctus*, and the two undescribed species (*Megophrys zhoui* sp. nov. and *Megophrys yeae* sp. nov.) based on morphology. *Megophrys* cf. *pachyproctus* was defined because the specimens were collected from the type locality of *M. pachyproctus* (a stream in Gelin village, Medog County), and they are morphologically similar to the holotype of *M. pachyproctus* although with some morphological differences. For caution, we regarded *M. pachyproctus* and *M.* cf. *pachyproctus* as two groups in the following analyses and descriptions. In addition, for comparison, we also divided *M. medogensis* specimens into two groups, i.e., high-elevation group (above ca. 2100 m a.s.l.) and low-middle-elevation group (500–1600 m). The high-elevation group contained five tadpoles collected from 80k and Gedang village, and the low-middle-elevation group contained five adult males, six adult females, and four tadpoles from the urban area of Medog town, Bari village, Beibeng village, Gelin village and Didong village (Fig. 1; Tables 1, Suppl. material 1: Tables S1, S2). Sex and maturity of each toad were determined by direct observation of advertisement calls or inspection of vocal sac openings and gonads. The tadpoles were identified based on their phylogenetic positions after representatives of the population with almost identical morphology were sequenced.

In the field, after taking photographs, the toads and tadpoles were euthanized using isoflurane, and then the specimens were fixed in 75% ethanol. Tissue samples

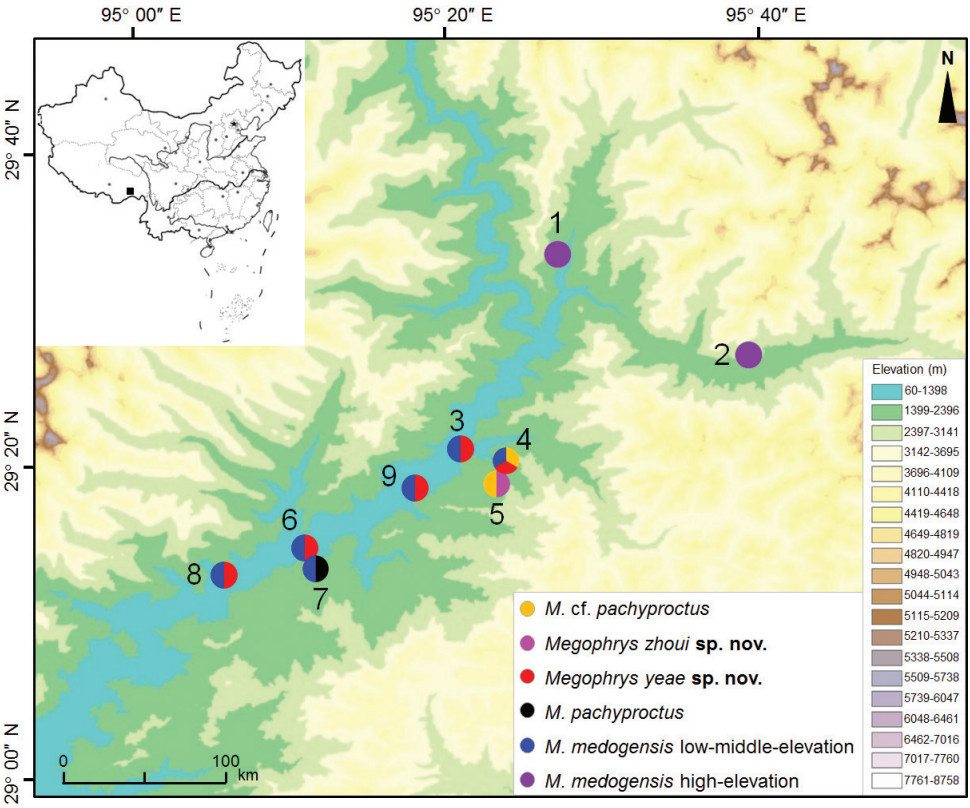

Figure 1. Distributional localities for specimens of the *Megophrys* species used in this study in Medog County, Tibet Autonomous Region, China. **1** 80k **2** Gedang village **3** vicinity of Medog urban area **4** Bari village **5** vicinity of Renqingbeng Temple **6** Beibeng village **7** Gelin village **8** Didong village **9** Yarang village. Species were denoted as different color.

were taken and preserved separately in 95% ethanol prior to fixation. Specimens collected in this work were deposited in Chengdu Institute of Biology, Chinese Academy of Sciences (CIB, CAS). The Animal Care and Use Committee of Chengdu Institute of Biology, CAS provided full approval for this research (Number: CIB2016012301). Field work was approved by the Management Office of the Administration of Yarlung Zangbo Grand Canyon National Nature Reserve (YLZB000342).

Molecular phylogenetic analyses

Total genomic DNA was extracted from each specimen collected in this study using QIAamp DNA Mini Kit (QIAGEN, Hilden, Germany), following manufacturer instructions. Three mitochondrial genes (12S rRNA, 16S rRNA, and COI) and two nuclear protein-coding genes (RAG1 and CXCR-4) were amplified and sequenced. Primer sequences were retrieved from literatures for 12S (Sumida et al. 2000), 16S

Table 1. Sampling information and GenBank accession numbers of samples used in the molecular analyses.

ID	Species	Voucher number	Locality	12S	16S	COI	RAG1	CXCR-4
1	*M. medogensis* low-middle elevation	CIB022017061502	Gelin, Medog, Tibet, China	/	MN963236	MN964296	MN984365	/
2		CIB022017060801	Beibeng, Medog, Tibet, China	/	MN963245	MN964287	MN984356	/
3		CIB022017060904	Didong, Medog, Tibet, China	/	MN963244	MN964288	MN984357	/
4		CIB022017061808	Bari, Medog, Tibet, China	/	MN963225	MN964306	MN984376	/
5		CIB022017061810	Bari, Medog, Tibet, China	/	MN963223	MN964308	MN984378	/
6		CIB022017061801	Bari, Medog, Tibet, China	/	MN963230	MN964301	MN984371	/
7		CIB022017061604	Beibeng, Medog, Tibet, China	/	MN963232	MN964299	MN984369	/
8		CIB022017061601	Beibeng, Medog, Tibet, China	/	MN963235	MN964297	MN984366	/
9		CIB022017061602	Beibeng, Medog, Tibet, China	/	MN963234	MN964298	MN984367	/
10		CIB022017061603	Beibeng, Medog, Tibet, China	/	MN963233	/	MN984368	/
11		CIB022017061501	Gelin, Medog, Tibet, China	/	MN963237	MN964295	MN984364	/
12		CIB022017061404DD	Didong, Medog, Tibet, China	/	MN963240	MN964292	MN984361	/
13		CIB022017061406MT	Suburb Medog, Tibet, China	/	MN963239	MN964293	MN984362	/
14		CIBMT1710104	Bari, Medog, Tibet, China	/	MN963212	MN964317	MN984385	/
15		CIBMT1710101	Yadong, vicinity of suburb Medog, Tibet, China	/	MN963213	MN964316	MN984384	/
16		KIZ06621	Beibeng, Tibet, China	/	KX811767	KX812082	KX812197	/
17	*M. medogensis* unknown elevation	SYSa002932	Motuo, Tibet, China	MH406458	MH406725	MH406177	MH404950	/
18	*M. glandulosa*	SYSa003795	Jingdong County, Yunnan, China	MH406493	MH406760	MH406219	MH404995	/
19	*M. medogensis* high elevation	CIB022017062002	80K, Medog, Tibet, China	/	MN963219	MN964310	/	/
20		CIB022017062003	80K, Medog, Tibet, China	/	MN963218	MN964311	/	/
21		CIBMT1710106	Gutang (Gedang), Medog, Tibet, China	/	MN963211	MN964318	MN984386	/
22		CIBMT1710107	Gutang (Gedang), Medog, Tibet, China	/	MN963210	MN964319	MN984387	/
23		CIBMT1710112	80K, Medog, Tibet, China	MN963176	MN963209	MN964320	MN984388	/
24	*M. medogensis* unknown elevation	SYSa002934	Motuo, Tibet, China	MH406459	MH406726	MH406178	MH404952	/
25	*M. mangshanensis*	KIZ021786	Nanling National Forest Park, Guangdong, China	/	KX811790	KX812079	KX812194	/
26	*M. maosonensis*	ROM 16679	Tam Dao, Vinh Phuc, Vietnam	/	KX811784	KX812081	KX812196	/
27	*M. periosa*	BNHS 6055 [SDBDU 2009.793]	28°12'33.96"N, 94°59'10.02"E	MH647522	MH647522	MH647529	MH647553	MH647537
28	*M. himalayana*	BNHS 6050 [SDBDU 2009.1227]	27°4'56.52"N, 92°34'50.22"E	MH647526	MH647526	/	MH647554	MH647538
29	*M. flavipunctata*	SDBDU 2009.297	East Khasi Hills dist, Meghalaya, India	KY022307	KY022307	MH647536	KY022352	KY022330
30	*M. robusta*	SDBDU 2011.1057	Darjeeling, West Bengal, India	KY022314	KY022314	/	KY022365	KY022343
31	*M. oreocrypta*	SDBDU 2009.1104	West Garo Hills dist, Meghalaya, India	KY022306	KY022306	/	KY022351	KY022329
32	*M. major*	SDBDU 2007.229	Kohima dist, Nagaland, India	MH647514	MH647514	/	MH647550	MH647540
33	*M. zhangi*	KIZ014278	Zhangmu, Tibet, China	/	KX811765	KX812084	KX812200	/
34	*M. monticola* middle elevation	SDBDU 2011.420	Darjeeling dist, West Bengal, India	MH647510	MH647510	/	KY022359	KY022337
35	*M. monticola* high elevation	SDBDU 2011.1047	Darjeeling dist, West Bengal, India	KY022312	KY022312	/	KY022358	KY022336
36		ZSI11401	Kabi, North district, Sikkim, India	/	KX894667	/	/	/
37	*M. lekaguli*	FMNH 265955	Pang Si Da, Sa Kaeo, Thailand	KY022214	KY022214	/	KY022241	KY022177

ID	Species	Voucher number	Locality	12S	16S	COI	RAG1	CXCR-4
38	*M. auralensis*	NCSM 79599	Aural, Kampong Speu, Cambodia	/	KX811807	/	/	/
39	*M. takensis*	FMNH 261711	Khlong Lan National Park, Kampaeng, Thailand	KY022215	KY022215	/	KY022246	KY022183
40	*M.* cf. *parva*	KIZ048507	Tongbiguan Nature Reserve, Yunnan, China	/	KX811796	KX812071	KX812180	/
41	*M. zunhebotoensis*	RGK 0041	Nagaland, India	KY022322	KY022322	/	KY022367	KY022345
42	*M. serchhipii*	SDBDU 2009.612	Tripura, India	KY022323	KY022323	/	KY022366	KY022344
43	*M. ancrae*	SDBDU 2009.727	27°29.833'N 96°23.467'E	KY022318	KY022318	/	KY022350	KY022328
44	*M. oropedion*	SDBDU 2009.299	Mawphlang, Mawphlang Sacred Forest, East Khasi Hills, Meghalaya, India	KY022317	KY022317	/	KY022360	KY022338
45	*M. megacephala*	ZSI A 11213	East Khasi Hills, northern Meghalaya, India	KY022315	KY022315	/	KY022357	KY022335
46	*M. aceras*	LSUHC 7038	Tremengor Forest, Perak, Peninsular Malaysia, Malaysia	/	GQ995534	/	/	/
47	*M. longipes*	IABHU 21101	Genting highland, Malaysia	/	AB530656	/	/	/
48	*Megophrys yeae* sp. nov.	CIB201706MT01	Didong, Medog, Tibet, China	MN963172	MN963217	MN964312	MN984380	/
49		CIB201706MT02	Beibeng, Medog, Tibet, China	MN963173	MN963216	MN964313	MN984381	/
50		CIB201706MT03	Suburb of Medog, Tibet, China	MN963174	MN963215	MN964314	MN984382	/
51		CIB022017061102	Didong, Medog, Tibet, China	MN963162	MN963243	MN964289	MN984358	/
52		CIB022017061407b	Beibeng, Medog, Tibet, China	MN963165	MN963238	MN964294	MN984363	MN984402
53		CIB022017061804	Bari, Medog, Tibet, China	MN963167	MN963229	MN964302	MN984372	MN984403
54		CIB022017061809	Bari, Medog, Tibet, China	MN963171	MN963224	MN964307	MN984377	/
55		CIB022017061811	Bari, Medog, Tibet, China	/	MN963222	MN964309	MN984379	/
56		CIB022017061103	Didong, Medog, Tibet, China	MN963163	MN963242	MN964290	MN984359	/
57		CIB022017061104	Didong, Medog, Tibet, China	MN963164	MN963241	MN964291	MN984360	/
58		CIB022017061606	Beibeng, Medog, Tibet, China	MN963166	MN963231	MN964300	MN984370	/
59		CIBMT171064	Yadong, vicinity of suburb Medog, Tibet, China	MN963187	MN963198	/	MN984399	/
60		CIBMT171065	Yarang, Medog, Tibet, China	MN963188	MN963197	/	MN984400	/
61		CIBMT171066	Yarang, Medog, Tibet, China	MN963189	MN963196	/	MN984401	/
62		KIZ010978	Beibeng, Tibet, China	/	KX811908	KX812153	KX812265	/
63		KIZ011175	Beibeng, Tibet, China	/	KX811909	KX812154	KX812266	/
64	*M. vegrandis*	SDBDU 2009.1272 /ZSI A 11605	27°06.067'N 92°31.642'E	KY022305	KY022305	/	KY022349	KY022327
65	*Megophrys* cf. *pachyproctus*	CIBMT171053	Renqinbeng, Medog, Tibet, China	MN963178	MN963207	MN964322	MN984390	/
66		CIBMT171060	Renqinbeng, Medog, Tibet, China	MN963185	MN963200	MN964329	MN984397	/
67		CIBMT171062	Renqinbeng, Medog, Tibet, China	MN963186	MN963199	MN964330	MN984398	/
68		CIB022017061813	Bari, Medog, Tibet, China	/	MN963220	/	/	/
69		CIBMT171054	Renqinbeng, Medog, Tibet, China	MN963179	MN963206	MN964323	MN984391	/
70		CIBMT171052	Renqinbeng, Medog, Tibet, China	MN963177	MN963208	MN964321	MN984389	/
71		CIB201706MT04	Bari, Medog, Tibet, China	MN963175	MN963214	MN964315	MN984383	/
72		CIB022017061805	Bari, Medog, Tibet, China	MN963168	MN963228	MN964303	MN984373	MN984404
73		CIB022017061806	Bari, Medog, Tibet, China	MN963169	MN963227	MN964304	MN984374	MN984405
74		CIB022017061807	Bari, Medog, Tibet, China	MN963170	MN963226	MN964305	MN984375	MN984406
75		CIB022017061812	Bari, Medog, Tibet, China	/	MN963221	/	/	/

ID	Species	Voucher number	Locality	12S	16S	COI	RAG1	CXCR-4
76	*Megophrys* cf. *pachyproctus*	CIBMT171055	Renqinbeng, Medog, Tibet, China	MN963180	MN963205	MN964324	MN984392	/
77		CIBMT171056	Renqinbeng, Medog, Tibet, China	MN963181	MN963204	MN964325	MN984393	/
78		CIBMT171057	Renqinbeng, Medog, Tibet, China	MN963182	MN963203	MN964326	MN984394	/
79		CIBMT171058	Renqinbeng, Medog, Tibet, China	MN963183	MN963202	MN964327	MN984395	/
80		CIBMT171059	Renqinbeng, Medog, Tibet, China	MN963184	MN963201	MN964328	MN984396	/
81	*M. xianjuensis*	CIBXJ190503	Xianju, Zhejiang, China	/	MN563758	MN563774	/	/
82	*M. lishuiensis*	WYF00169	Lishui, Zhejiang, China	/	KY021418	/	/	/
83	*M. shunhuangensis*	HNNU16SH02	Shunhuang Mountains, Hunan, China	MK836034	MK836037	/	/	/
84	*M. brachykolos*	SYSa002258	Hong Kong, China	MF667851	KJ560403	MH406120	MH404888	/
85	*M. kuatunensis*	SYSa003449	Guadun, Fujian, China	MF667850	MF667881	MH406206	MH404982	/
86	*M. dongguanensis*	SYSa001971/ CIB110006	Mt. Yinping, Dongguan City, Guangdong, China	/	MK524097	MK524128	/	/
87	*M. nankunensis*	SYSa004498	Mt. Nankun, Huizhou City,Guangdong, China	/	MK524108	MK524139	/	/
88	*M. wugongensis*	SYSa002610	Wugongshan Scenic Area, Anfu County, Jiangxi, China	/	MK524114	MK524145	/	/
89	*M. ombrophila*	NJFU2015201 KRM15	Mt. Wuyi, Fujian, China	KX856422	KX856401	/	/	/
90	*M. obesa*	SYSa002271	Heishiding, Guangdong, China	MH406410	KJ579121	MH406123	MH404891	/
91	*M. lini*	SYSa002381	Mt. Jinggang, Jiangxi, China	MF667842	MF667874	MH406135	MH404903	/
92	*M. nanlingensis*	SYSa001959	Nanling Nature Reserve, Shaoguan City, Guangdong, China	/	MK524111	MK524142	/	/
93	*M. cheni*	SYSa002126	Taoyuandong, Hunan, China	MH406389	MH406659	MH406096	MH404864	/
94	*M. insularis*	SYSa002169	Nan'ao Island, Guangdong, China	MH406393	MH406663	MH406103	MH404871	/
95	*M. jinggangensis*	SYSa004824	Mt. Sifang, Hunan, China	MH406590	MH406857	MH406319	MH405100	/
96	*M. caudoprocta*	SYSa004281	Zhangjiajie, Hunan, China	MH406528	MH406795	MH406257	MH405036	/
97	*M. tuberogranulatus*	SYSa004310	Zhangjiajie, Hunan, China	MH406534	MH406801	MH406263	MH405042	/
98	*M. wushanensis*	SYSa003008	Mt. Wu, Hubei, China	MH406465	MH406732	MH406184	MH404959	/
99	*M. leishanensis*	SYSa002213	Mt. Leigong, Guizhou, China	MH406403	MH406673	MH406113	MH404881	/
100	*M. acuta*	SYSa002276	Heishiding, Guangdong, China	MH406413	KJ579124	MH406126	MH404894	/
101	*M. boettgeri*	SYSa004149	Mt. Wuyi, Fujian, China	MF667847	MF667878	MH406247	MH405026	/
102	*M. huangshanensis*	SYSa002703	Huangshan, Anhui, China	MF667854	MF667883	MH406161	MH404929	/
103	*M. liboensis*	GNUG20150813001	Libo Country, Guizhou, China	MF285242	MF285253	/	/	/
104	*M. jiulianensis*	SYSa002107	Mt. Jiulian, Ganzhou City, Jiangxi, China	/	MK524099	MK524130	/	/
105	*M. mufumontana*	SYSa006390 CIB110012	Mt. Mufu, Pingjiang County, Hunan, China	/	MK524104	MK524135	/	/
106	*M. baolongensis*	KIZ019216	Baolong, Chongqing, China	/	KX811813	KX812093	KX812202	/
107	*M. sangzhiensis*	SYSa004306	Zhangjiajie, Hunan, China	MH406530	MH406797	MH406259	MH405038	/
108	*M. spinata*	SYSa002226	Mt. Leigong, Guizhou, China	MH406405	MH406675	MH406115	MH404883	/
109	*M. binlingensis*	SYSa005313	Wawu Shan, Sichuan, China	MH406625	MH406892	MH406354	MH405137	/
110	*M. wuliangshanensis*	SYSa003924	Mt. Wuliang, Yunnan, China	MH406504	MH406771	MH406230	MH405007	/
111	*M. jingdongensis*	SYSa003928	Mt. Wuliang, Yunnan, China	MH406506	MH406773	MH406232	MH405009	/
112	*M. daweimontis*	KIZ048997	Dawei Shan, Yunnan, China	/	KX811867	KX812125	KX812248	/

ID	Species	Voucher number	Locality	12S	16S	COI	RAG1	CXCR-4
113	*M. omeimontis*	KIZ025765	Emei Shan, Sichuan, China	/	KX811884	KX812136	KX812223	/
114	*M. binchuanensis*	KIZ019441	Jizu Shan, Yunnan, China	/	KX811849	KX812112	KX812219	/
115	*M. rubrimera*	AMS R177676	Sa Pa, Lao Cai, Vietnam	/	MF536419	/	/	/
116	*M. jiangi*	CIBKKS20180722006	Kuankuosui Nature Reserve, Guizhou, China	/	MN107743	MN107748	/	/
117	*M. minor*	SYSa003209	Dujiangyan, Sichuan, China	MF667825	MF667862	MH406194	MH404969	/
118	*M. hansi*	AMCC 144729	Thua Tien Hue, A Luoi District, A Roang Commune, Viet Nam	KY022204	KY022204	/	KY022229	KY022165
119	*M. microstoma*	KU KUH 311601	Shiwan Dashang Nature Reserve, Guangxi, China	KY022200	KY022200	/	KY022234	KY022170
120	*M. gerti*	AMCC 106456	Quang Nam, Tra My Dist., Tra Don Commune, Viet Nam	KY022201	KY022201	/	KY022231	KY022167
121	*M. synoria*	FMNH 262778	Mondolkiri, Cambodia	KY022198	KY022198	/	KY022235	KY022171
122	*M. elfina*	ZMMU NAP-02658	Chu Pan Fan Mt, Chu Yang Sin N.P., Dak Lak Prov., Vietnam	KY425389	KY425389	/	/	/
123	*M. palpebralespinosa*	FMNH 258098	Phou Dendin National Biodiversity Conservation Area, Phongsaly, Laos	KY022209	KY022209	/	KY022238	KY022174
124	*M. intermedia*	FMNH 258093	Xe Kong, Kaleum District, Xe Sap National Biodiversity Conservation Area, Laos	KY022196	KY022196	/	KY022221	KY022157
125	*M. carinense*	CAS 243791	Khotama Camp, Yephyu, Dawei, Tanintharyi, Myanmar	KY022197	KY022197	/	KY022219	KY022155
126	*M. lancip*	MZB:Amp:22233	Ngarip, Ulubelu, Lampung, Sumatra, Indonesia	/	KY679891	/	/	/
127	*M. montana*	LSUMZ 81916	Sukabumi, Java, Indonesia	/	KX811927	KX812163	KX812281	/
128	*M. chuannanensis*	SYSa004926	Hejiang County, Sichuan, China	MH406635	MH406901	MH406364	MH405147	/
129	*M. feae*	SYSa003912	Jingdong County, Yunnan, China	MH406633	MH406899	MH406362	MH405145	MH450011
130	*M. popei*	SYSa001864	Taoyuandong, Hunan, China	MH406632	KM504256	MH406361	MH405144	/
131	*M. gigantica*	SYSa003883	Ailao Shan, Yunnan, China	MH406499	MH406766	MH406225	MH405001	MH450010
132	*M. wawuensis*	SYSa005311	Wawu Shan, Sichuan, China	MH406624	MH406891	MH406353	MH405136	/
133	*M. nankiangensis*	CIB ZYC517	Nanjiang, Sichuan, China	/	KX811900	/	/	/
134	*M. shapingensis*	KIZ014512	Liziping Nature Reserve, Sichuan, China	/	KX811904	KX812060	KX812274	/
135	*M. dringi*	UNIMAS 8948	Gunung Mulu, Sarawak, Malaysia	/	KJ831316	/	/	/
136	*M. nasuta*	MBH 5357	Bengkulu, Sumatra, Indonesia	KY022185	KY022185	/	KY022225	KY022161
137	*M. kalimantanensis*	FMNH 236525	Crocker Range National Park, Tenom Dist, Sabah, Borneo, Malaysia	DQ283342	DQ283342	/	/	/
138	*M. kobayashii*	UNIMAS 8148	Gunung Kinabalu National Park, Sabah, Malaysia	/	KJ831313	/	/	/
139	*M. baluensis*	voucher not preserved	Kinabalu, Borneo	DQ642146	DQ642121	/	/	/
140	*M. stejnegeri*	KU 314303	Pasonanca Natural Park, Zamboanga City, Philippines	/	KX811922	KX812052	KX812172	/
141	*M. edwardinae*	FMNH 273694	Bintulu, Sarawak, Malaysia	/	KX811918	KX812050	KX812168	/
142	*M. ligaya*	ZMMU NAP-05015	Palawan, Philippines	/	KX811919	KX812051	KX812169	/
143	*Leptolalax alpinus*	SYSa003927	Jingdong County, Yunnan, China	MH406639	MH406905	MH406368	MH405151	/
144	*Leptobrachium* cf. *rakhinensis*	SDBDU 2009.49	Trishna Wildlife Sanctuary, South Dist, Tripura state, India	KY022304	KY022304	/	KY022347	KY022325

(Simon et al. 1994), COI (Che et al. 2011), RAG1 (Mauro et al. 2004; Fu et al. 2007), and CXCR-4 (Biju and Bossuyt 2003) genes. PCR amplifications for mitochondrial genes were performed in a 30 μl volume reaction with the following conditions: an initial denaturing step at 95 °C for 4 min; 36 cycles of denaturing at 95 °C for 40 s, annealing at 55 °C (for 12S and 16S)/52 °C (for COI) for 40 s and extending at 72 °C for 70 s, and a final extending step of 72 °C for 10 min. Amplifications of nuclear genes were according to Mahony et al. (2017). PCR products were sequenced with both forward and reverse primers same as used in PCR. Sequencing was conducted using an ABI3730 automated DNA sequencer in Sangon Biotechnologies Co., Ltd. (Shanghai, China). New sequences were uploaded to GenBank (see Table 1).

For phylogenetic comparisons, corresponding sequences of *Megophrys* species were downloaded from GenBank especially for their holotypes and/or topotypes for which comparable sequences were available (Table 1). Corresponding sequences of one *Leptobrachium rakhinensis* and one *Leptobrachella khasiorum* (Table 1) were also downloaded and used as outgroups according to previous studies (Mahony et al. 2017; Chen et al. 2016).

Sequences were assembled and aligned using BioEdit v. 7.0.9.0 (Hall 1999) with default settings, and were further revised manually if necessary. To avoid bias in alignments, GBLOCKS v. 0.91.b (Castresana 2000) with default settings was used to extract regions of defined sequence conservation from the length-variable 12S and 16S fragments. The protein-coding gene (COI, RAG1, and CXCR-4) sequences were translated to amino acid sequences in MEGA v. 7.0 (Kumar et al. 2016), adjusted for open reading frames, and checked to ensure absence of premature stop codons. No-sequenced fragments were treated as missing data. At last, for phylogenetic analyses, two datasets were obtained, i.e., three-mitochondrial genes concatenated dataset of 12S+16S+COI and two-nuclear genes concatenated dataset of RAG1+CXCR-4.

Phylogenetic analyses were conducted on each dataset using maximum likelihood (ML) and Bayesian Inference (BI) methods, implemented in PhyML v. 3.0 (Guindon et al. 2010) and MrBayes v. 3.2 (Ronquist et al. 2012), respectively. For the phylogenetic analyses, each gene was regarded as one partition, and the best evolutionary model for each partition were chosen under the Bayesian Inference Criteria (BIC) using jModelTest v. 2.1.3 (Darriba 2012). The analyses selected GTR + I + G model for each mitochondrial gene, and HKY + I for each nuclear gene. For the ML tree, branch supports were drawn from 10000 non-parametric bootstrap replicates. In BI analyses, the parameters for each partition were unlinked, and branch lengths were allowed to vary proportionately across partitions. Two runs each with four Markov chains were simultaneously run for 80 million generations with sampling every 1000 generations. The first 25% of trees were removed as the "burn-in" stage followed by calculations of Bayesian posterior probabilities at stationarity, and the 50% majority-rule consensus of the post burn-in trees sampled. Finally, genetic distance between species with uncorrected *p*-distance model on the 16S gene was estimated using MEGA.

Morphological analyses

In total, 38 adult specimens of four species (the two undescribed species, *M. medogensis*, and *M.* cf. *pachyproctus*) were measured (Suppl. material 1: Table S1). The terminology and methods followed Mahony (2011). Measurements were taken with a dial caliper to the nearest 0.1 mm. Twenty-two characters of adult specimens were measured:

EL eye length (horizontal distance between the anterior and posterior borders of orbit);
EN eye-nostril length (distance from front of eye to the center of nostril);
FAL forearm length (distance from elbow to wrist);
FIIIW finger III width (largest width of tip of finger III);
FIVW finger IV width (largest width of tip of finger IV);
FOL foot length (distance from the proximal end of the inner metatarsal tubercle to the tip of the fourth digit);
HAL hand length (distance from wrist to tip of third digit);
HL head length (distance from the rear of the mandible to the tip of the snout);
HLL hindlimb length;
HW head width (distance between the posterior angles of jaw);
IBE internal back of eyes (the shortest distance between the posterior borders of the orbits);
IFE internal front of eyes (shortest distance between the anterior borders of orbits);
IMT ength of the inner metatarsal tubercle;
IN internarial distance (shortest distance between two nostrils);
IUE inter upper eyelid width (shortest distance between upper eyelids);
SHL shank length (distance from knee to ankle);
SL snout length (distance from tip of snout to anterior border of the orbit);
SN nostril-snout length (distance from center of the nostril to tip of the snout);
SVL snout-vent length (distance from the tip of the snout to the posterior edge of the vent);
TFOL tarsal-foot length (distance from heel to the tip of the fourth digit);
TL thigh length (distance from cloaca to knee);
TYD largest tympanum diameter;
TYE tympanum-eye distance (distance from the anterior border of the tympanum to the posterior orbital border);
UEW maximum upper eyelid width.

Thirteen tadpoles of four groups (i.e., *Megophrys yeae* sp. nov., *M.* cf. *pachyproctus*, and two elevation groups of *M. medogensis*) were measured (Suppl. material 1: Table S2). The stages of tadpoles were identified following Gosner (1960). Seventeen morphometric characters of tadpoles were measured:

BH maximum body height;
BL body length (distance from tip of snout to trunk-tail junction);

BW maximum body width;
ED maximum eye diameter;
IND internasal distance (distance between center of two naris);
LF maximum height of lower tail fin;
NE naris-eye distance (distance from center of naris to anterior corner of eye);
ODW oral disc width (largest width of oral disc);
PP interpupilar distance;
RN rostro-narial distance (distance from tip of snout to center of naris);
SS snout-spiracle distance (distance from tip of snout to opening of spiracle);
SU snout-upper fin distance (distance from snout to beginning of upper tail fin);
TAL tail length (distance between posterior side of opening of cloaca to tip of tail);
TMH maximum tail muscle width;
TMW maximum tail muscle height;
TOL total length;
UF maximum height of upper tail fin.

For morphometric comparisons, the corresponding morphometric data of the holotype and two topotypes of *M. vegrandis* were retrieved from Mahony et al. (2013), and that of the allotype and one paratype of *M. pachyproctus* from Huang and Fei (1981). To reduce the impact of allometry, the correct value from the ratio of each measurement to SVL was calculated and then log-transformed for the following morphometric analyses. Mann-Whitney *U* test was used to test the significance of difference on each character between different species in each gender group. In the analyses for male group, 13 characters of 28 individuals of five species (*Megophrys yeae* sp. nov., *M.* cf. *pachyproctus*, *M. pachyproctus*, *M. medogensis*, and *M. vegrandis*) were included, and for female, 26 characters of 13 individuals of four species (*Megophrys yeae* sp. nov., *Megophrys zhoui* sp. nov., *M.* cf. *pachyproctus*, and *M. medogensis*) were included. The significance level was set at 0.05. The analyses were carried out in R (R Development Core Team 2008).

The two undescribed species were compared with each other as well with other congeners of *Megophrys sensu lato* on morphology. Comparative morphological data were obtained from literatures (Table 2). In addition, the holotype of *M. pachyproctus* and topotypes of *M. medogensis* were also examined for comparisons (Suppl. material 1: Tables S1, S2).

Bioacoustics

We recorded advertisement calls of three species: six males (CIB022017061804, CIB022017061101–CIB022017061103, CIBMT171064, and one unvouchered individual) of *Megophrys yeae* sp. nov., three males (CIB022017061805–CIB022017061807) of *M.* cf. *pachyproctus*, and three unvouchered males of *M. medogensis* (Suppl. material 1: Table S3). Each calling individual was recorded at a distance between 0.5–1.0 m using a Philip VTR6900 digital voice recorder with a build-in microphone with sampling rate 96 kHz. Temperature was recorded using HTC-1 hygro-

Table 2. References utilized for morphological characters of congeners of the genus *Megophrys*.

No.	Species	Literature obtained
1	*Megophrys aceras* Boulenger, 1903	Bourret 1942; Munir et al. 2018
2	*Megophrys acuta* Wang, Li, and Jin, 2014	Li et al. 2014
3	*Megophrys ancrae* Mahony, Teeling, and Biju, 2013	Mahony et al. 2013
4	*Megophrys angka* Wu, Suwannapoom, Poyarkov, Chen, Pawangkhanant, Xu, Jin, Murphy, and Che, 2019	Wu et al. 2019
5	*Megophrys auralensis* Ohler, Swan, and Daltry, 2002	Ohler et al. 2002
6	*Megophrys baluensis* Boulenger, 1899	Boulenger 1899, 1908
7	*Megophrys baolongensis* Ye, Fei, and Xie, 2007	Ye et al. 2007; Fei and Ye 2016
8	*Megophrys binchuanensis* Ye and Fei, 1995	Ye et al. 1995; Fei and Ye 2016
9	*Megophrys binlingensis* Jiang, Fei, and Ye, 2009	Fei et al. 2009
10	*Megophrys boettgeri* Boulenger, 1899	Boulenger 1908; Fei et al. 2009
11	*Megophrys brachykolos* Inger and Romer, 1961	Inger et al. 1961; Fei et al. 2009; Li et al. 2014
12	*Megophrys carinense* Boulenger, 1889	Boulenger 1908; Bourret 1942
13	*Megophrys caudoprocta* Shen, 1994	Shen 1994; Shen et al. 2013
14	*Megophrys cheni* Wang and Liu, 2014	Wang et al. 2014
15	*Megophrys chuannanensis* Fei, Ye, and Huang, 2001	Fei and Ye 2001; Fei et al. 2009
16	*Megophrys damrei* Mahony, 2011	Mahony 2011
17	*Megophrys daweimontis* Rao and Yang, 1997	Rao and Yang 1997; Fei and Ye 2016
18	*Megophrys dongguanensis* Wang and Wang, 2019	Wang et al. 2019
19	*Megophrys dringi* Inger, Stuebing, and Tan, 1995	Inger et al. 1995; Oberhummer et al. 2014
20	*Megophrys edwardinae* Inger, 1989	Inger et al. 1989
21	*Megophrys elfina* Poyarkov, Duong, Orlov, Gogoleva, Vassilieva, Nguyen, Nguyen, Nguyen, Che, and Mahony, 2017	Poyarkov et al. 2017
22	*Megophrys fansipanensis* Tapley, Cutajar, Mahony, Nguyen, Dau, Luong, Le, Nguyen, Nguyen, Portway, Luong, and Rowley, 2018	Tapley et al. 2018
23	*Megophrys feae* Boulenger, 1887	Boulenger 1908; Fei et al. 2009
24	*Megophrys feii* Yang, Wang, and Wang, 2018	Yang et al. 2018
25	*Megophrys flavipunctata* Mahony, Kamei, Teeling, and Biju, 2018	Mahony et al. 2018
26	*Megophrys gerti* Ohler, 2003	Poyarkov et al. 2017
27	*Megophrys gigantica* Liu, Hu, and Yang, 1960	Liu et al. 1960; Fei et al. 2009
28	*Megophrys glandulosa* Fei, Ye, and Huang, 1990	Fei et al. 1990; Fei et al. 2009; Fei and Ye 2016
29	*Megophrys hansi* Ohler, 2003	Ohler 2003
30	*Megophrys himalayana* Mahony, Kamei, Teeling, and Biju, 2018	Mahony et al. 2018
31	*Megophrys hoanglienensis* Tapley, Cutajar, Mahony, Nguyen, Dau, Luong, Le, Nguyen, Nguyen, Portway, Luong, and Rowley, 2018	Tapley et al. 2018
32	*Megophrys huangshanensis* Fei and Ye, 2005	Fei and Ye 2005, 2016; Fei et al. 2009
33	*Megophrys insularis* Wang, Liu, Lyu, Zeng, and Wang, 2017	Wang et al. 2017a
34	*Megophrys intermedia* Smith, 1921	Smith 1921
35	*Megophrys Jiangi* Liu, Li, Wei, Xu, Cheng, Wang and Wu, 2020	Liu et al. 2020
36	*Megophrys jingdongensis* Fei and Ye, 1983	Fei at al. 1983, 2009; Fei and Ye 2016
37	*Megophrys jinggangensis* Wang, 2012	Wang et al. 2012
38	*Megophrys jiulianensis* Wang, Zeng, Lyu, and Wang, 2019	Wang et al. 2019
39	*Megophrys kalimantanensis* Munir, Hamidy, Matsui, Iskandar, Sidik, and Shimada, 2019	Munir et al. 2019
40	*Megophrys kobayashii* Malkmus and Matsui, 1997	Malkmus and Matsui 1997
41	*Megophrys koui* Mahony, Foley, Biju, and Teeling, 2017	Yang 1991
42	*Megophrys kuatunensis* Pope, 1929	Pope 1929; Fei et al. 2009; Tapley et al. 2017
43	*Megophrys lancip* Munir, Hamidy, Farajallah, and Smith, 2018	Munir et al. 2018
44	*Megophrys leishanensis* Li, Xu, Liu, Jiang, Wei, and Wang, 2019 "2018"	Li et al. 2018a
45	*Megophrys lekaguli* Stuart, Chuaynkern, Chan-ard, and Inger, 2006	Stuart et al. 2006a
46	*Megophrys liboensis* Zhang, Li, Xiao, Li, Pan, Wang, Zhang, and Zhou, 2017	Zhang et al. 2017
47	*Megophrys ligayae* Taylor, 1920	Taylor 1920
48	*Megophrys lini* Wang and Yang, 2014	Wang et al. 2014
49	*Megophrys lishuiensis* Wang, Liu and Jiang, 2017	Wang et al. 2017b
50	*Megophrys longipes* Boulenger, 1886	Boulenger 1908; Bourret 1942
51	*Megophrys major* Boulenger, 1908	Boulenger 1908

No.	Species	Literature obtained
52	*Megophrys mangshanensis* Fei and Ye, 1990	Fei et al. 1990; Fei and Ye 2016
53	*Megophrys maosonensis* Bourret, 1937	Bourret 1942
54	*Megophrys medogensis* Fei, Ye, and Huang, 1983	Fei at al. 1983, 2009; Fei and Ye 2016; This paper
55	*Megophrys megacephala* Mahony, Sengupta, Kamei, and Biju, 2011	Mahony et al. 2011
56	*Megophrys microstoma* Boulenger, 1903	Fei et al. 2009
57	*Megophrys minor* Stejneger, 1926	Stejneger 1926; Li et al. 2014; Fei and Ye 2016
58	*Megophrys montana* Kuhl and Van Hasselt, 1822	Munir et al. 2018
59	*Megophrys monticola* Günther, 1864	Mahony et al. 2018
60	*Megophrys mufumontana* J. Wang, Lyu, and Y.Y. Wang, 2019	Wang et al. 2019
61	*Megophrys nankiangensis* Liu and Hu, 1966	Fei et al. 2009
62	*Megophrys nankunensis* Wang, Zeng, and. Wang, 2019	Wang et al. 2019
63	*Megophrys nanlingensis* Lyu, J. Wang, Liu, and Y.Y. Wang, 2019	Wang et al. 2019
64	*Megophrys nasuta* Schlegel, 1858	Mahony et al. 2018
65	*Megophrys obesa* Wang, Li, and Zhao, 2014	Li et al. 2014
66	*Megophrys ombrophila* Messenger and Dahn, 2019	Messenger et al. 2019
67	*Megophrys omeimontis* Liu, 1950	Fei et al. 2009; Fei and Ye 2016
68	*Megophrys oreocrypta* Mahony, Kamei, Teeling, and Biju, 2018	Mahony et al. 2018
69	*Megophrys oropedion* Mahony, Teeling, and Biju, 2013	Mahony et al. 2013
70	*Megophrys pachyproctus* Huang, 1981	Huang and Fei 1981 Huang et al. 1998; This paper
71	*Megophrys palpebralespinosa* Bourret, 1937	Bourret 1942
72	*Megophrys parallela* Inger and Iskandar, 2005	Inger and Iskandar 2005
73	*Megophrys parva* Boulenger, 1893	Boulenger 1908; Deuti et al. 2017
74	*Megophrys periosa* Mahony, Kamei, Teeling, and Biju, 2018	Mahony et al. 2018
75	*Megophrys popei* Zhao, Yang, Chen, Chen, and Wang, 2014	Zhao et al. 2014
76	*Megophrys robusta* Boulenger, 1908	Boulenger 1908; Mahony et al. 2018
77	*Megophrys rubrimera* Tapley, Cutajar, Mahony, Chung, Dau, Nguyen, Luong, and Rowley, 2017	Tapley et al. 2017
78	*Megophrys sangzhiensis* Jiang, Ye, and Fei, 2008	Jiang et al. 2008
79	*Megophrys serchhipii* Mathew and Sen, 2007	Mathew and Sen 2007
80	*Megophrys shapingensis* Liu, 1950	Liu et al. 1950; Fei et al. 2009
81	*Megophrys shuichengensis* Tian and Sun, 1995	Tian and Sun 1995; Fei et al. 2009
82	*Megophrys shunhuangensis* Wang, Deng, Liu, Wu, and Liu, 2019	Wang et al. 2019a
83	*Megophrys spinata* Liu and Hu, 1973	Fei et al. 2009; Fei and Ye 2016
84	*Megophrys stejnegeri* Taylor, 1920	Taylor 1920
85	*Megophrys synoria* Stuart, Sok, and Neang, 2006	Stuart et al. 2006b
86	*Megophrys takensis* Mahony, 2011	Mahony 2011
87	*Megophrys tuberogranulata* Shen, Mo and Li, 2010	Mo et al. 2010
88	*Megophrys vegrandis* Mahony, Teeling, Biju, 2013	Mahony et al. 2013
89	*Megophrys wawuensis* Fei, Jiang, and Zheng, 2001	Fei et al. 2009
90	*Megophrys wugongensis* J. Wang, Lyu, and Y.Y. Wang, 2019	Wang et al. 2019
91	*Megophrys wuliangshanensis* Ye and Fei, 1995	Fei et al. 2009; Fei and Ye 2016
92	*Megophrys wushanensis* Ye and Fei, 1995	Fei et al. 2009; Fei and Ye 2016
93	*Megophrys xianjuensis* Wang, Wu, Peng, Shi, Lu and Wu, 2020	Wang et al. 2020
94	*Megophrys zhangi* Ye and Fei, 1992	Ye and Fei 1992; Fei et al. 2009; Fei and Ye 2016
95	*Megophrys zunhebotoensis* Mathew and Sen, 2007	Mathew and Sen 2007

thermograph. All callings were recorded between a relatively concentrated temperature range of 17–25 °C. Calls were analyzed using Raven Pro© v.1.5 beta software (http://www.birds.cornell.edu/raven) with fast-Fourier transform (FFT) of 512 points, 50% overlap, and 188 Hz grid-spacing using Hanning windows. Sonograms and spectrograms were presented in figures using Praat (Boersma 2001) after de-noised using Audition 3. Terminology of advertisement call analyses and description followed Köhler et al. (2017). Call duration (ms), intercall interval (ms), number of calls per call group,

call repetition rate (calls/s), number of pulses per call, and dominant frequency (kHz) were applied in measurement. To compare acoustic characteristics between the species, one-way ANOVA was conducted with LSD post hoc.

Skull scanning. The holotype CIB201706MT02 of *Megophrys yeae* sp. nov., holotype CIBMT171053 of *Megophrys zhoui* sp. nov., and the adult male CIB022017061805 of *M.* cf. *pachyproctus* were scanned. For comparisons, the holotype NWIPB 770650 of *M. pachyproctus* and the adult male topotype CIB022017061406 of *M. medogensis* were also scanned. In the high-resolution X-ray scanner (Quantum GX micro-CT Imaging System, PerkinElmer®), the specimens were scanned along the coronal axis at an image resolution of 1024× 1024 pixels. Segmentation and three-dimensional reconstruction of the CT images were made using VG57 Studio Max 2.2 (Volume Graphics, Heidelberg, Germany). Terminology of skull description follows Fei and Yei (2016).

Results

Phylogenetic analyses

Aligned sequence matrix of mitochondrial DNA and nuclear DNA contained 2890 bp and 2058 bp, respectively. ML and BI analyses based on the mitochondrial DNA matrix resulted in essentially consistent topologies (Fig. 2A), and all analyses on nuclear DNA matrix also obtained generally consistent topologies (Fig. 2B), though some relationships were not r|solved in these trees.

All samples of *Megophrys sensu lato* were strongly clustered into a clade in all trees. In all trees, each of the two new species was well supported as an independent clade, and all of them were then clustered into a big clade also containing *M.* cf. *pachyproctus* and *M. vegrandis*. In all trees, in this clade, *M.* cf. *pachyproctus* was indicated to be at the basal position. In mitochondrial DNA trees, the relationships of other three species were supported as (*Megophrys zhoui* sp. nov. (*M. vegrandis*, *Megophrys yeae* sp. nov.)), but in nuclear DNA trees, as (*M. vegrandis* (*Megophrys yeae* sp. nov., *Megophrys zhoui* sp. nov.)). This clade with the four species was phylogenetically far from the clade containing all samples of *M. medogensis* in all trees. As note, in nuclear DNA trees, *M. medogensis* was resolved as a monophyletic group because the high-elevation and low-middle-elevation groups of *M. medogensis* were nested into one clade, but in mitochondrial DNA trees, the low-middle-elevation group of *M. medogensis* was clustered as a clade sister to *M. robusta*, being paraphyly with the clade in comprising of the high-elevation group of *M. medogensis*.

Genetic distance among samples of each new species is below 0.4%, much lower than the interspecific distance of *Megophrys* (mean: 10.5%; range: 0.8%–26.1%; Suppl. material 1: Table S4). Genetic distance between *Megophrys zhoui* sp. nov. and other congeners was at least 4.0% (*Megophrys zhoui* sp. nov. vs. *M. vegrandis*), and that between *Megophrys yeae* sp. nov. and other congeners was at least 5.4% (*Megophrys yeae*

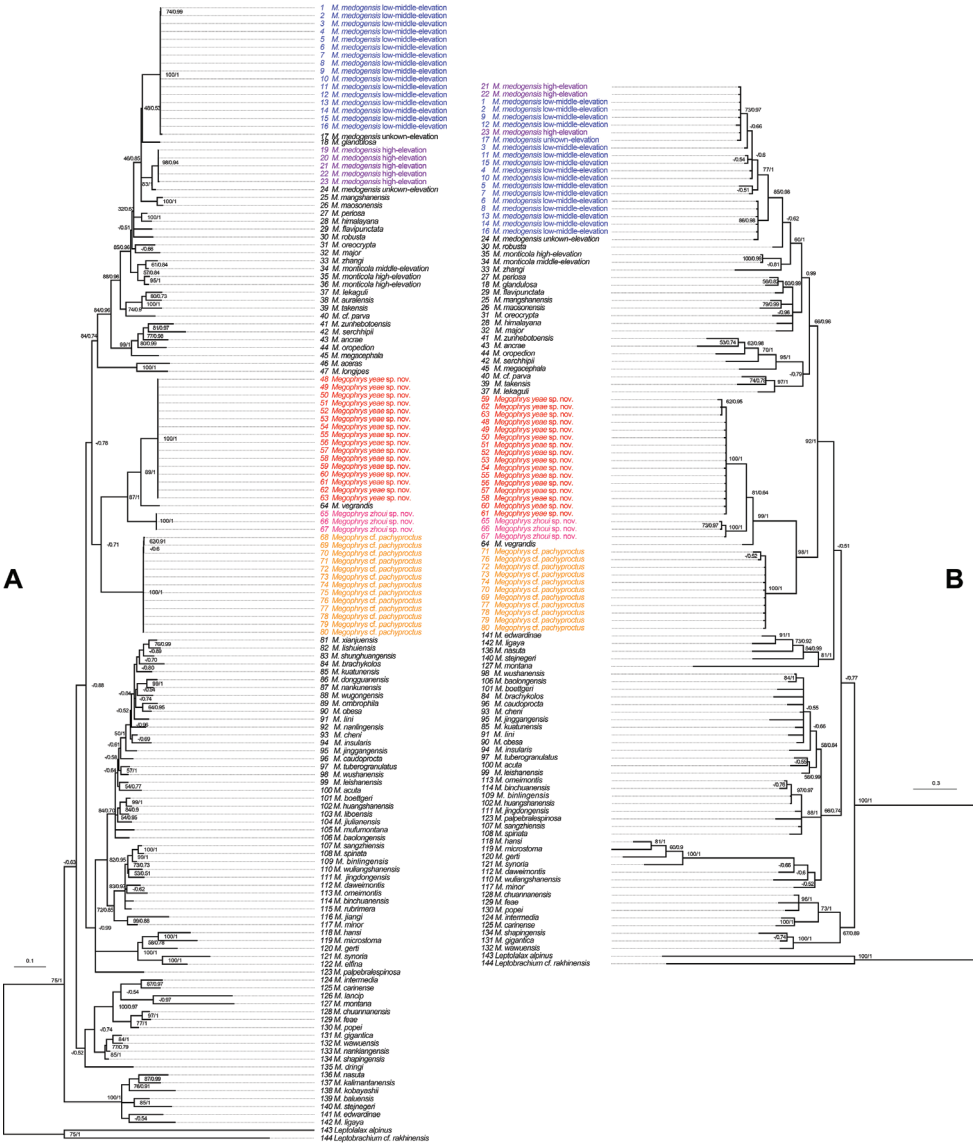

Figure 2. Phylogenetic trees respectively based on the mitochondrial DNA and nuclear DNA. **A** Maximum Likelihood (ML) tree based on the mitochondrial DNA **B** ML tree based on the nuclear DNA. ML bootstrap support/Bayesian posterior probability was denoted beside node. Samples 1–144 refer to Suppl. material 1: Table S1.

sp. nov. vs. *M. vegrandis*). As note, genetic distance between the low-middle-elevation and high-elevation groups of *M. medogensis* was 5.0% on 16S gene. These values were much higher than interspecific genetic distance between many pairs of *Megophrys* species (Suppl. material 1: Table S4).

Morphological analyses

On many morphometric characters, the two new species were significantly different from each other as well from *M. vegrandis*, *M. medogensis*, and *M. pachyproctus* (Table 3). In male, ten characters were significantly different at least between one pair of spe-

Table 3. Morphometric comparisons between the *Megophrys* species from the eastern corner of Himalayas. P-value is resulted from Mann-Whitney *U* test on each character between species. Significant level at 0.05 (* P-value < 0.05). Abbreviation for species name: MCP, *M.* cf. *pachyproctus*; MZ, *Megophrys zhoui* sp. nov.; MY, *Megophrys yeae* sp. nov.; MP, *M. pachyproctus*; MM, *M. medogensis*; and MV, *M. vegrandis*. See abbreviations for the morphological characters in Materials and methods section.

Sex	Character	MCP vs. MY	MCP vs. MZ	MCP vs. MM	MCP vs. MP	MCP vs. MV	MZ vs. MY	MZ vs. MM	MY vs. MP	MY vs. MM	MP vs. MV	MM vs. MV
Female	**SVL**	0.133	0.133	0.016*	/	/	0.333	0.095	/	0.095	/	/
	HW	0.133	0.267	0.016*	/	/	0.333	0.095	/	0.095	/	/
	HL	1.000	0.267	0.032*	/	/	1.000	0.571	/	0.190	/	/
	SL	0.533	0.267	0.032*	/	/	0.333	0.095	/	1.000	/	/
	SN	1.000	0.267	1.000	/	/	0.333	0.190	/	0.857	/	/
	EN	0.800	1.000	0.286	/	/	1.000	0.570	/	1.000	/	/
	IN	1.000	0.267	0.286	/	/	1.000	1.000	/	0.857	/	/
	EL	0.133	1.000	1.000	/	/	0.667	1.000	/	0.095	/	/
	IUE	0.533	0.533	0.111	/	/	1.000	1.000	/	1.000	/	/
	UEW	0.533	0.533	0.730	/	/	1.000	1.000	/	1.000	/	/
	IFE	0.800	0.267	0.111	/	/	1.000	0.950	/	0.571	/	/
	IBE	0.133	0.133	1.000	/	/	0.667	0.190	/	0.190	/	/
	TYD	0.533	0.133	0.032*	/	/	0.333	0.095	/	0.095	/	/
	TYE	0.800	0.133	0.016*	/	/	0.667	0.095	/	0.095	/	/
	FAL	0.133	0.800	0.286	/	/	0.333	0.381	/	0.095	/	/
	HAL	0.133	1.000	0.016*	/	/	0.333	0.095	/	0.095	/	/
	FIL	1.000	0.133	0.016*	/	/	0.333	0.095	/	0.095	/	/
	FIIL	0.133	0.533	0.016*	/	/	0.333	0.095	/	0.381	/	/
	FIIIL	0.133	0.267	0.286	/	/	0.333	1.000	/	0.095	/	/
	FIVL	1.000	0.533	0.730	/	/	0.333	0.381	/	0.381	/	/
	TL	0.133	0.533	0.413	/	/	0.333	0.571	/	1.000	/	/
	SHL	0.533	0.800	0.730	/	/	0.333	0.857	/	0.857	/	/
	TFOL	1.000	0.133	0.730	/	/	0.333	0.857	/	1.000	/	/
	FOL	1.000	0.267	1.000	/	/	0.333	0.571	/	1.000	/	/
	FIIIW	0.133	0.133	0.556	/	/	0.333	0.095	/	0.095	/	/
	FIVW	0.133	0.133	0.730	/	/	0.333	0.095	/	0.095	/	/
Male	**SVL**	0.001*	/	0.476	0.533	0.029*	/	/	/	0.005*	0.643	0.038*
	HW	0.446	/	1.000	0.533	0.486	/	/	/	0.180	0.286	0.067
	HL	0.599	/	0.038*	1.000	0.057	/	/	/	0.005*	0.143	0.171
	SL	0.521	/	0.610	0.533	0.200	/	/	/	0.125	0.286	0.067
	IN	0.262	/	0.257	1.000	0.686	/	/	/	1.000	1.000	0.352
	EL	0.262	/	0.380	0.533	0.886	/	/	/	0.000*	0.710	0.670
	UEW	0.133	/	0.190	1.000	0.029*	/	/	/	0.180	0.710	0.010*
	TYD	0.262	/	0.380	0.533	0.343	/	/	/	0.018*	1.000	0.010*
	FAL	0.002*	/	0.010*	1.000	0.029*	/	/	/	0.000*	0.710	0.010*
	HAL	0.133	/	0.010*	0.800	0.029*	/	/	/	0.000*	0.710	0.010*
	SHL	0.684	/	0.010*	0.533	0.343	/	/	/	0.102	0.710	0.914
	TFOL	0.212	/	0.171	1.000	0.343	/	/	/	0.964	0.643	0.171
	FOL	0.020*	/	1.000	0.533	0.886	/	/	/	0.007*	1.000	0.762

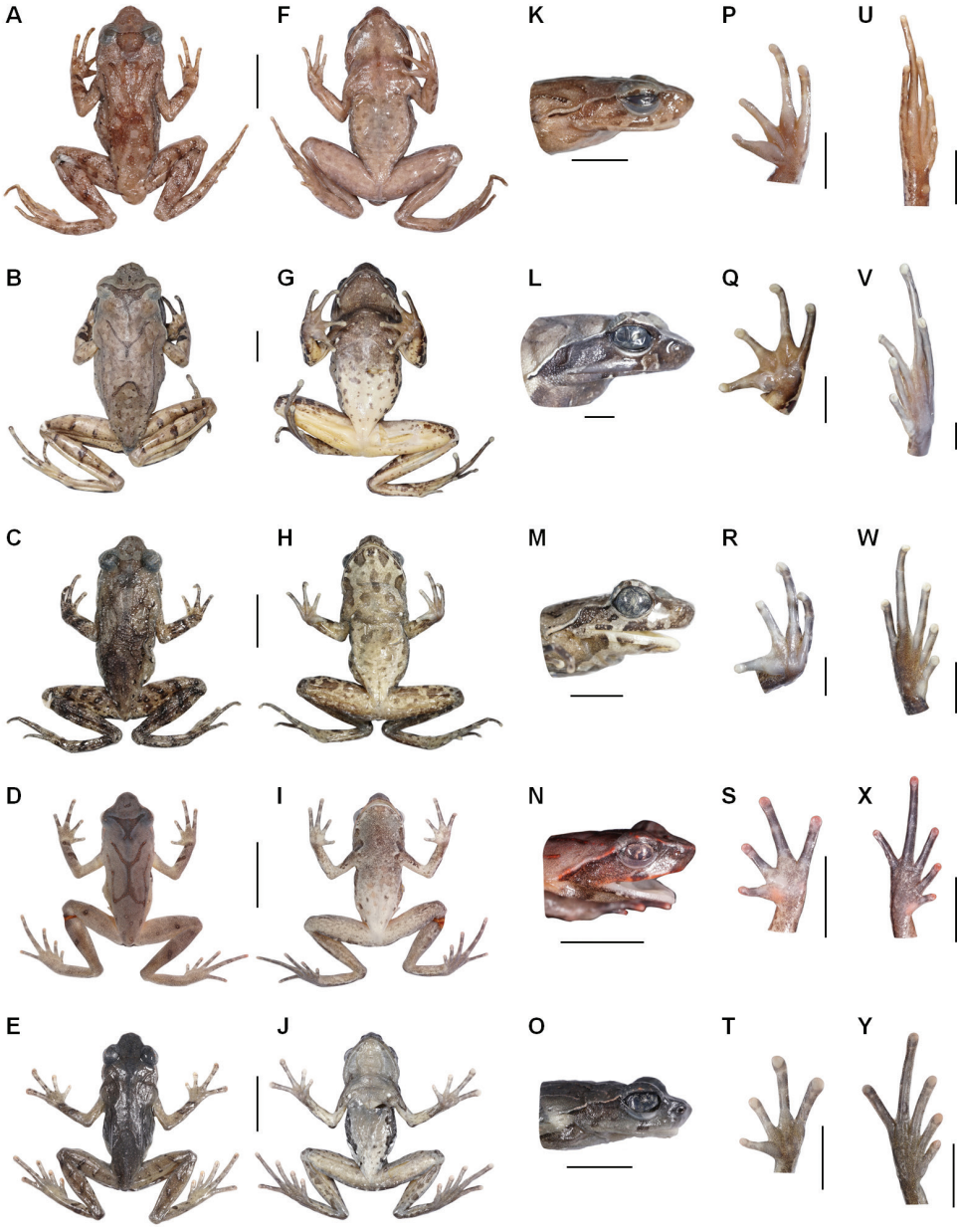

Figure 3. Photos of specimens of *Megophrys* species in Medog. **A–E** dorsal views of adult male holotype NWIPB770650 of *M. pachyproctus*, adult male topotype CIB022017061406 of *M. medogensis*, adult male CIB022017061805 of *M.* cf. *pachyproctus*, adult male holotype CIBMT171053 of *Megophrys zhoui* sp. nov., and adult male holotype CIB201706MT02 of *Megophrys yeae* sp. nov., respectively **F–J** ventral views of the specimens, respectively **K–O** lateral view of head of the specimens, respectively **P–T** ventral view of hand of the specimens, respectively **U–Y** ventral view of foot of the specimens, respectively. Scale bar for body view equal to 10 mm, and for partial view 5 mm.

Table 4. Comparisons of advertisement calls between three *Megophrys* species in Medog. P-value is resulted from Mann-Whitney *U* test on each character between species. Significant level at 0.05 (* P-value < 0.05). Abbreviation for species names: MCP, *M.* cf. *pachyproctus*; MY, *Megophrys yeae* sp. nov.; and MM, *M. medogensis*.

Call character	MCP	MY	MM	P-value		
	Mean ± SD (range)	Mean ± SD (range)	Mean ± SD (range)	MH vs. MY	MH vs. MM	MY vs. MM
Number of individuals	6	3	3	/	/	/
Total number of calls analyzed	3.2 ± 2.6 (1–8)	5.0 ± 2.6 (2–7)	5.3 ± 3.5 (2–9)	/	/	/
Call repetition rate (calls/s)	3.0 ± 0.7 (1.9–4.1)	0.9 ± 0.2 (0.7–1.1)	1.2 ± 0.9 (0.6–2.2)	0.024*	1	0.048*
Calls/call group	68.9 ± 46.7 (10.3–109.3)	10.8 ± 3.3 (7.1–13.3)	4.3 ± 1.6 (2.8–6.0)	0.229	0.1	0.057
Call duration (ms)	139 ± 39 (99–212)	746 ± 221 (491–889)	176 ± 61 (121–241)	0.024*	0.1	0.381
Intercall interval (ms)	218 ± 81 (146–370)	580 ± 122 (493–720)	205 ± 514 (153–254)	0.024*	0.1	0.905
Pulses/call	9.2 ± 0.6 (8.5–9.9)	42.1 ± 2.0 (40.6–44.4)	17.1	0.024*	0.5	0.286
Dominant frequency (kHz)	4.7 ± 0.3 (4.4–5.2)	3.2 ± 0.1 (3.2–3.3)	2.5 ± 0.1 (2.4–2.6)	0.024*	0.1	0.024*
Temperature (°C)	17–25	17–21	19–20	/	/	/

cies, i.e., SVL, HL, SL, EL, UEW, TYD, FAL, HAL, SHL, and FOL (all P-values < 0.05; Table 3); and in female, 14 characters were significant different at least between one pair of species, i.e., SVL, HW, HL, SL, IFE, IBE, TYD, TYE, FAL, HAL, FIL, FIIIL, FIIIW, and FIVW (all P-values < 0.05; Table 3).

On morphology, the two new species could be identified from each other as well as from their congeners by a series of characters (for morphological differences between the five groups of *Megophrys* species from Medog County see Suppl. material 1: Table S5; Fig. 3). Detailed comparisons on morphological characters between the new species and other congeners were demonstrated in detail in the sections for describing the new species.

Bioacoustics comparisons. The advertisement calls of *Megophrys yeae* sp. nov., *M.* cf. *pachyproctus*, and *M. medogensis* were obviously different (Fig. 4; Tables 4; Suppl. material 1: Table S3). *Megophrys yeae* sp. nov. vocalizes continuous fast short calls in high-frequency, *M. medogensis* vocalizes sparse relatively deep calls in moderate speed, and as for *M.* cf. *pachyproctus*, the calls are moderate in frequency and repetition rate, but distinctly longer (call duration 491–889 ms) than the former two species (Fig. 4; Tables 4; Suppl. material 1: Table S3).

Skull comparisons. Skulls of the four toad species in Medog were different on many aspects (Fig. 5; Suppl. material 1: Table S5). In general, the skulls of these five species are weakly ossified except for *M. medogensis*. Skulls of them differ from each other on the following characters: premaxillary and maxillary teeth, nasal bones contact with sphenethmoid or not, texture and shape of sphenethmoid, the shape of frontoparietal, opening of anterior fontanelle and sagittal suture, front part of anterior process parasphenoid, relatively position of exoccipitals with the line connecting conjunctions of quadratojugal and mandible, and columella auris (Fig. 5; Suppl. material 1: Table S5).

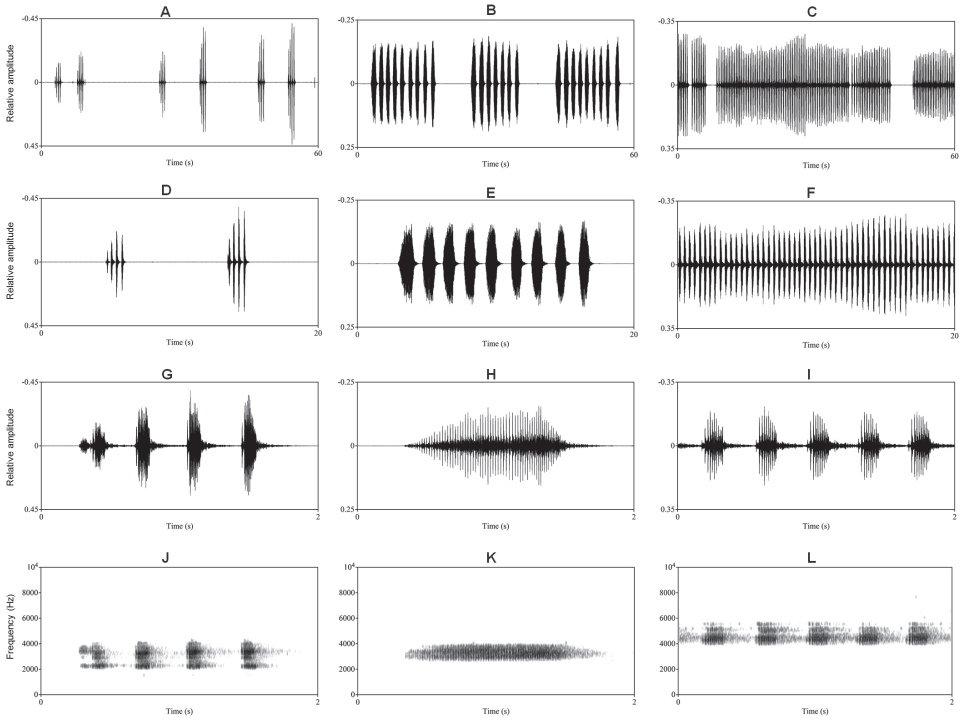

Figure 4. Visualization of advertisement calls of three *Megophrys* species from Medog. **A–C** visualizations of 60 seconds waveform of relative amplitude over time for *M. medogensis* (one unvouchered individual recorded in the vicinity of Medog urban area), *M.* cf. *pachyproctus* (CIB022017061807), and *Megophrys yeae* sp. nov. (paratype CIB022017061804), respectively **D–F** visualizations of 20 seconds waveform of relative amplitude over time **G–I** visualizations of two seconds waveform of relative amplitude for the species, respectively **J–L** visualizations of two seconds waveform of spectrogram for the species, respectively.

Taxonomic accounts

Megophrys pachyproctus Huang, 1981

Figs 3A, F, K, P, U, 5A, F, Suppl. material 2: Fig. S5C; Tables 1, Suppl. material 1: Tables S1, S2, S5

Megophrys pachyproctus Huang, 1981* in Huang & Fei, 1981: 211–212. Holotype: NWIPB 770650, by original designation. Type locality: Gelin, Medog (29°11'N, 95°10'E), Xizang, China; altitude 1530 m, China.

Specimens examined. Holotype: adult male NWIPB 770650.

Description of holotype. (Fig. 3A, F, K, P, U; Suppl. material 1: Table S1). Measurements in mm. Adult male. Body moderate, SVL 35.7; a large swollen arc-shaped

* For detailed comparisons, we re-described *M. pachyproctus* mainly based on the holotype NWIPB 770650 and added our skull information for it.

protuberance present on vent beyond cloaca and visible on both dorsal and lateral view, its length 6.8 (measured dorsally), width 4.7, and thickness 2.7.

Head wider than long (HW/HL 1.13); snout blunt in dorsal view, obtusely protruding beyond mandible in lateral view; rostral appendage absent; canthus rostralis well developed, loreal region concave; dorsal surface of snout slightly concave; nostril oval, slightly closer to snout than eye (EN/SN 1.04); eyes lager than twice tympanum (EL/TYD 2.24); eye-tympanum distance smaller than tympanum diameter (TYE/TYD 0.86); tympanum oval, obliquely orientated, upper 1/3 concealed with supratympanic ridge; interorbital space flat, wider than upper eyelids (UEW/IUE 0.89); pineal ocellus not visible; vomerine ridges well developed, acutely angled, enlarged at ends where bearing several vomerine teeth; maxillary teeth present; tongue notched posteriorly, medial lingual process absent.

Forearm moderately long and wide; fingers long and thin, without webbing and lateral fringes; subarticular tubercles absent; inner and outer metacarpal tubercles small and oval, weakly connected at lower half; finger relative lengths I < II < IV < III; base of finger I strong, larger than base of finger II; tips of fingers slightly swollen and rounded (FIIIW 0.8), without pads.

Hindlimbs relatively thin and long; thighs ca. equal length of shanks and feet; toes long and thin, relative lengths I < II < V < III < IV; tips of toes rounded; toes rudimentary webbed; lateral fringes narrow; continuous dermal ridges present under toes; outer metatarsal, and subarticular tubercles absent; inner metatarsal tubercle distinct, rounded, separate from base of toe I at a distance nearly twice its diameter; tips of toes rounded.

Dorsal surface of head and body relativity rough, densely scattered with small granules; temporal region and upper corner of mandible scattered small granules; tympanum border slightly raised; upper eyelid without pointed edge; supratympanic ridges extend from posterior upper eyelid border to region above forearm insertions, not curving above tympanum, rear part thicker than front; flanks densely covered with small granules and scattered several larger tubercles; two longitudinal ridges on dorsolateral body distinct, nearly parallel, extending from above shoulder to nearby groin; parietoscapular-sacral ridges forming a "> <" configuration, composed by rows of small tubercles, dorsal surface of forearm thighs and shanks with several rows of small tubercles transversely arranged; dorsal upper arm and other dorsal surfaces of hindlimbs covered with dense small granules; ventral surface of body and limbs smooth; pectoral glands small (diameter 0.8) and rounded, close to axilla on chest; femoral glands small (diameter 1.0) and rounded, closer to outer edge of knee than to cloaca.

Coloration of holotype in preservative. (Fig. 3A, F, K, P, U). Dorsal and lateral surface of body, dorsal surface of head mostly tan; a brown triangle present between eyes, little lighter in center, anterior corners reach to near out edge of upper eyelids; indistinct "X"-shaped markings on dorsum, with small tubercles in center; darker brown stripe along with dorsolateral ridges; tubercles on flanks white, edged with dark patches; lateral surface of head tan with brown stripes radiating from orbit to upper mandible and upper eyelid; iris dark brown; a brown stripe extending from posterior corner of orbit under former half supratympanic ridges to behind tympanum, a clear thin dark stripe under edges of supratympanic ridges after tympanum, no long white stripe present on upper lip; dorsal and lateral surface of limbs mostly tan, two broad brown transverse bands on

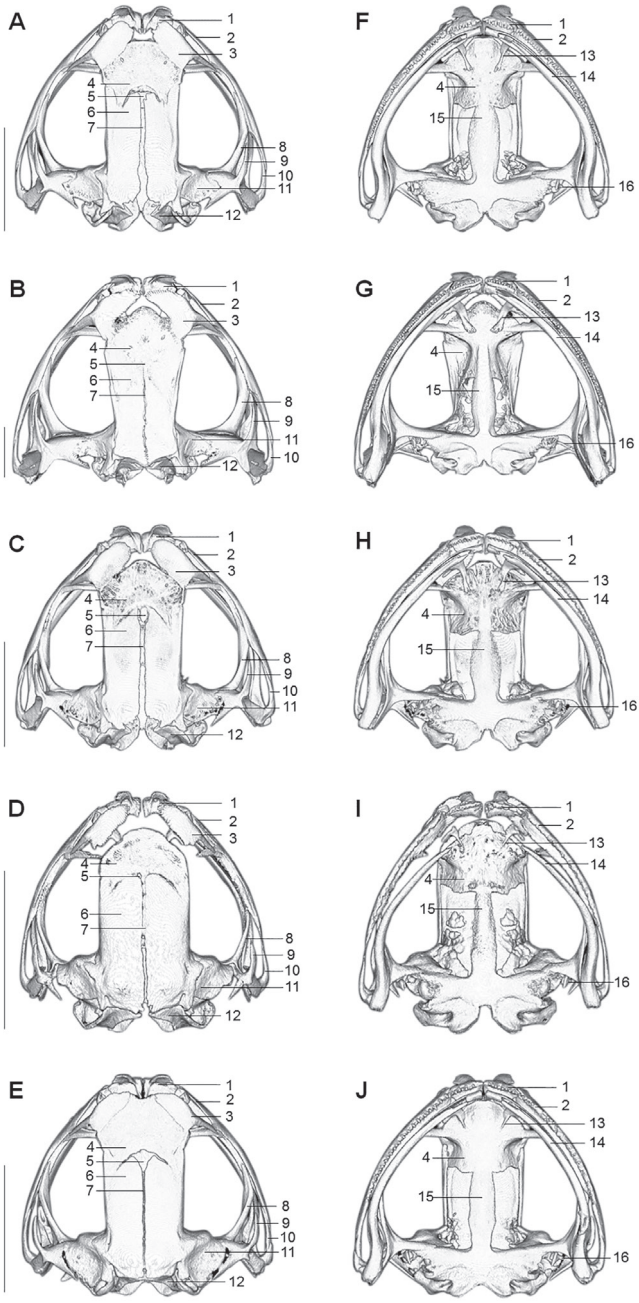

Figure 5. Skull of *Megophrys* species in Medog. **A–E** dorsal views of adult male holotype NWIPB770650 of *M. pachyproctus*, adult male topotype CIB022017061406 of *M. medogensis*, adult male CIB022017061805 of *M.* cf. *pachyproctus*, adult male holotype CIBMT171053 of *Megophrys zhoui* sp. nov., and adult male holotype CIB201706MT02 of *Megophrys yeae* sp. nov., respectively **F–J** ventral views of the specimens, respectively. Key to skull: 1 premaxillary; 2 maxillary; 3 nasal; 4 sphenethmoid; 5 anterior fontanelle; 6 frontoparietal; 7 sagittal suture; 8 pterygoid; 9 squamosal; 10 quadratojugal; 11 prootic; 12 exoccipital; 13 vomerine ridge; 14 mandible; 15 anterior process of parasphenoid; 16 columella auris. Scale bar equal to 5 mm.

forearms, and four thin indistinct transverse bands on dorsal thighs and shanks; dorsal tarsal pale gray with three indistinct transverse bands, outer three fingers with tan blotches; gular region and chest dusty tan with a short longitudinal brown stripe in middle of throat; two light patches on edges of jaw corresponding anterior corners of eyes and front edge of brown stripe at posterior end of jaw; and one brown stripe extending from posterior end of jaws to base of forearms on both sides; abdomen dusty tan, with a dozen darker patches on middle and upper abdomen, large longitudinal dark patches present on ventral lateral abdomen hardly present; ventral surface of forelimbs and hindlimbs dusty tan mottled with light patches; pectoral and femoral glands light tan.

Coloration of holotype in life. According to Huang and Fei (1981): dorsum brown or dark brown; two to four dark colored transverse bands present on forearms; and four to five dark colored transverse bands present on thighs and shanks; places around cloaca, groin, and anterior, posterior, ventral thigh orange; tips of fingers and toes light red; ventral surfaces of tarsi, metatarsus, and toes grayish brown or black-brown; lateral and ventral surface with lots of grayish black spots; a longitudinal short grayish black stripe present on middle throat; granules on dorsal surface of body and limbs light red.

Skull. (Fig. 5A, F). Description based on scan of the holotype. Skull weakly ossified, width 1.12× of length; maxillary overlapping with the quadratojugal; premaxillary and maxillary teeth strong, most tooth closely positioned with others, 9/9 teeth present on left/right premaxillary, no teeth present on mandible; vomerine ridge well developed, two vomerine teeth present on enlarged posterior end of each vomerine ridge; nasal process of premaxilla protruding beyond skull; nasal bones separated from each other, inner edge mostly contact with sphenethmoid; sphenethmoid relatively smooth with few small pits on both dorsal and ventral surface, the middle one third of front edge not contacting nasal bones and truncate, separated from premaxilla; frontoparietal divided by a distinctly opening sagittal suture, sagittal suture slightly wider posteriorly; anterior fontanelle small, only slightly wider than sagittal suture; front and rear part of frontoparietal almost equally wide; posterior edge of exoccipitals posterior to the line connecting conjunctions of quadratojugal and mandible; pterygoid moderate; anterior process of squamosal slender and sharp, tip closer to the junction of pterygoid and quadratojugal than its base, posterior process present; prootic relatively smooth, separated from exoccipitals; anterior process of parasphenoid in shape of fusiform, anterior part not raised above sphenethmoid, conjunction of parasphenoid anterior process meet with sphenethmoid moderate, width ca. three quarters of the constriction near its base; columella auris short.

Variations. See for morphometric variation within the three types (two adult males and one adult female) in Suppl. material 1: Table S1. According to the photo of dorsal view of the only adult male paratype NPIB 770651 presented by Fei and Yei (2016), the adult male paratype resemble the holotype in general, also has a distinct swollen arc-shaped protuberance present on end of body beyond cloaca, but different in color on dorsal body darker, and not having distinguishable "X"-shaped markings on dorsum. The adult female allotype NPIB 770652 do not have a distinct projection on vent, and the coloration on dorsal and ventral surface of body lighter than males.

Secondary sexual characters. Male with gray nuptial pad on inner side of the first finger, spines on nuptial pad dense and small; single subgular vocal sac; vocal sac

opening small, slit like; a distinct fatty swollen rounded projection present on the end of body beyond cloaca.

Distribution and natural history. According to Huang and Fei (1981), this species was first collected at elevation 1530 m in the type locality, Gelin, Medog, Xizang, China; two adult males were found on shrubs emitting continuous calls sounds like "gazhi...gazhi...gazhi..." to the human ear; the female was found on the road near a brook.

Comparisons. *Megophrys pachyproctus* differs from all other known congeners except *M. koui* and *M. caudoprocta* by having a distinct protuberance above vent, and further differs from the latter two species in protuberance above vent being swollen and arc-shaped (vs. not). For comparisons with subsequent undescribed species covered in this paper, refer to relevant morphological comparison sections for those species.

Remarks. *Megophrys pachyproctus* was originally described by Huang and Fei (1981) with description and figures of the holotype, measurements of types, secondary sexual characters, and brief natural history. And then were translated into English and measurements of snout length, internasal space, interorbital space, eyelid width, diameter of eye, tympanum, and tibia width were supplemented by Huang et al. (1998). Fei et al. (2009) provided illustration of the holotype. Fei et al. (2010) and Fei and Ye (2016) provided colored drawings of the holotype and the paratype (NPIB) 770651, and colored photos of dorsal and lateral views of one living topotype from Medog (photographs by Ke Jiang). The topotype possess expanded fingertips with small disk and two large longitudinal dark patches on ventral lateral abdomen (while the holotype of *M. pachyproctus* does not have these character), and not having a distinct swollen arc-shaped protuberance present above vent (while the holotype of *M. pachyproctus* possess). Li et al. (2010) provided similar photos of a living specimen and measurements of seven specimens from Maniwong and Yarang, Medog, under the name *M. pachyproctus*. The body length of these specimens ranges from 26.1 mm to 27.9 mm, and Li et al. (2010) cited the body length of the male types of *M. pachyproctus* as 25.3 mm to 36.2 mm, which should be 35.3 mm to 36.2 mm (Huang and Fei 1981). These specimens with small body size, expanded fingertips with small disk, and two large longitudinal dark patches on ventral lateral abdomen turn out to be mostly similar with *Megophrys yeae* sp. nov. (see description of *Megophrys yeae* sp. nov.). We suggest reexamination of these specimens should be taken. Saikia and Sinha (2018) reported *M. pachyproctus* from Southern Xizang (27.547681°N, 93.897555°E, 1855 m), provided description, measurements (body length 37.8), and a photo of dorsal view of the single male voucher specimen V/A/NERC/1352. But the photo does not present an arc-shaped swelling above vent (Saikia and Sinha 2018: fig. 3A) as the holotype. We suggest further examination should be made to confirm the identification of the specimen. This species was also reported new range in Lao Cai and Ha Tinh Province, Vietnam (Orlov et al. 2002; Nguyen et al. 2005). Since *Megophrys* inhibits astonishing cryptic species biodiversity, and species like *M. pachyproctus* thought to be widespread from Southwest China to Vietnam confirmed to be another species (Chen et al. 2016; Tapley et al. 2017; Liu et al. 2018), records from Vietnam where more than 1000 km from type locality should be questioned and specimens should be reexamined.

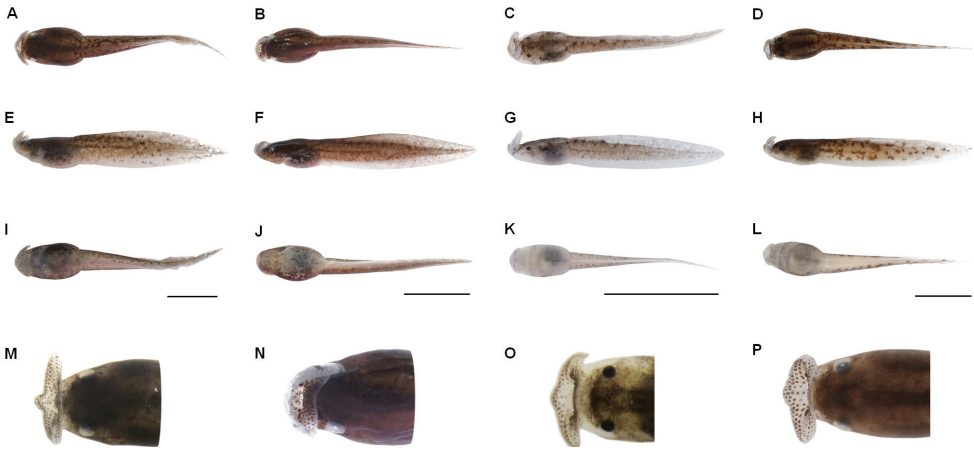

Figure 6. Tadpole specimens of four groups of three *Megophrys* species from Medog. **A–D** dorsal views of the low-middle-elevation tadpole CIBMT20170621 of *M. medogensis* (Goser stage 35), the high-elevation tadpole CIBMT171001 of *M. medogensis* (stage 27), tadpole CIBMT20170611 of *M.* cf. *pachyproctus* (stage 25), tadpole CIBMT170604 of *Megophrys yeae* sp. nov. (stage 35), respectively **E–H** lateral views of the tadpoles, respectively **I–L** ventral views of the tadpoles, respectively. M–P dorsal views of head of the tadpoles, respectively. Scale bar for body view equal to 10 mm, and for head view 2 mm.

Megophrys medogensis Fei et al., 1983

Figs 3B, G, L, Q, V, 4A, D, G, J, 5B, G, 6A, B, E, F, I, J, M, N, 10A–C, E, F, Suppl. material 2: Figs S1, S5A–H; Tables 1–4, Suppl. material 1: Table S1–S5

Megophrys omeimontis medogensis Fei, Ye and Huang (1983)[**]: 49–52.

Specimens examined. Five adult females and six adult males from Medog (Suppl. material 1: Table S1).

Holotype description. Refer to Fei et al. (1983) for holotype description, Mahony et al. (2018) for picture of holotype CIB 73II0015, Fei et al. (2009) and Fei and Ye (2016) for description of coloration and picture of topotypes.

Skull. (Fig. 5B, G). Description based on sequenced adult male topotype CIB022017061406. Skull well ossified, width 1.21× length; maxillary overlapping with the quadratojugal; premaxillary and maxillary teeth well developed, and closely positioned with others, 11/13 teeth present on left/right of premaxillary; vomerine ridge robust; few vomerine teeth strong, present on posterior end of vomerine ridge; nasal process of premaxilla protruding beyond skull; nasal bones separated, posterior one third of inner edge contact with sphenethmoid; frontoparietal distinctly wider in front than rear; sphenethmoid relatively smooth with few small pits on dorsal and ventral surface, the middle half of front edge not contacting nasal bones and pro-

** For detailed comparisons, we supplied morphology description of skull and tadpole for *M. medogensis* mainly based on the specimens collected in this study and added bioacoustics data for this species.

truding forward, separated from premaxilla; frontoparietal not divided, sagittal suture occlusive; anterior fontanelle occlusive; front part of frontoparietal distinctly wider than rear; posterior edge of exoccipitals anterior to the line connecting conjunctions of quadratojugal and mandible; pterygoid robust; anterior process of squamosal slender, tip much closer to the junction of pterygoid and quadratojugal than its base, posterior process present; prootic relatively smooth, separated from exoccipitals; anterior process of parasphenoid in shape of fusiform, the front part raise above sphenethmoid from ventral view, the conjunction with sphenethmoid with width equals the constriction near base of anterior process of parasphenoid; columella slender and long.

Secondary sexual characters. Adult female generally with larger body size. Average body length females 79.7 mm (n = 5, 75.7–85.5 mm), male 65.3 mm (n = 6, 63.1–68.7 mm). Males with brown nuptial pads on fingers I and II, spines on nuptial pad dense; single subgular vocal sac.

Tadpole. (Fig. 6A, B, E, F, I, J, M, N; Suppl. material 1: Table S2). For low-middle-elevation tadpoles of *M. medogensis*, description was based on tadpole CIBMT20170621 (stage 35) which shared the same pond of sequenced tadpole CIBMT022017061808 in Bari village. They are similar on morphology. For coloration at stage 26, description based on sequenced specimen CIBMT1710101 from Yadong village. Measurements in mm. For stage 35, body 13.3, elongated; head slightly narrower than trunk, oral disk large, funnel like, 1.2× body width; three rows of short oval submarginal papillae on lower lip; middle of lower lip protruding forward, with five rounded papillae longitudinal arranged from the tip middle lower lip to oral cavity; corner of mouth with six papillae arranged in a transverse row on both sides; three transverse rows of short oval papillae on upper lip; keratodonts absent; nares closer to eyes than tip of snout (RN/NE 1.6); eyes round, positioned dorsolaterally; internarial distance (IND 3.0) 61% of the interpupilar distance (PP 4.9); spiracle mostly in left side of body, in right-handed helix from ventral view; spiracular tube not protruding beyond body wall, positioned 60% of the distance between tip of the snout and trunk-tail junction, and below the horizontal mid trunk line; tail accounts 69% of total length; dorsal fin arise above trunk-tail junction, 35% of maximum body height; ventral fin connected to the trunk, with lesser height, 27% of maximum body height; anal siphon opens medially; maximum tail muscle height 72% of maximum body height, maximum tail muscle strong, width 53% of maximum body width; 12 small curves present on both lateral side of tail muscle. For stage 26, dorsal fin arises behind trunk-tail junction. For stage 43, clear "X" and "l_l" skin ridges have present on dorsum, limbs are well developed. For high-elevation tadpoles of *M. medogensis*, description mostly based on sequenced tadpole CIBMT171001 (at stage 27), coloration based on sequenced tadpoles CIBMT1710106 and CIBMT1710112, collected from Gedang, Medog, Tibet Autonomous Region, China (29.463916°N, 95.769507°E, 2142 m). Body 9.5, elongated; head slightly narrower than trunk; oral disk moderate, funnel like, positioned anterior-dorsal, width equal with body width; 5 transverse rows of short oval papillae on upper lip; keratodonts absent; nares much closer to eyes than tip of snout (RN/NE 2.2); eyes round, positioned dorsolaterally; internarial distance

(IND1.9) 61% of the interpupil distance (PP 3.2); spiracle barely visible from ventral view; the spiracular tube not protruding beyond body wall, positioned 63% of the distance between tip of the snout and trunk-tail junction, and below the horizontal mid trunk line; tail accounts 72% of total length; dorsal fin arise above anal siphon opens, 40% of maximum body height; ventral fin connected to the trunk, with lesser height than dorsal fin, 37% of maximum body height; anal siphon opens medially; tail muscle relatively weak, maximum height 72% of maximum body height, width only 44% of maximum body width; eleven small curves present on both lateral side of tail muscle.

Coloration of tadpoles. Low-middle-elevation tadpoles. In preservation (based on CIBMT20170621; Fig. 6A, B, E, F): dorsal body brown; lips semitransparent, papillae on lips brown; dorsal tail light brown, marbled with deep brown markings; lateral side of tail densely covered with tiny brown pigment spots, also mottled with small light colored patches, and scattered with deep brown pigments piles; fins semitransparent; ventral surface of body semitransparent, sparsely covered with brown pigments. In live: dorsal and lateral body generally in light yellow-brown; lateral side of tail mottled with light colored patches; ventral body without white patches; iris brown.

High elevation tadpoles (Fig. 6I, J, M, N). In preservation: dorsal body and tail with brown pigmentation; lateral body brown, skin coloration lighter below spiracular tube, with clear white patches; lateral tail muscle brown mottled with dense tiny white dots; upper and lower fin semitransparent brown, lower fin colored lighter; no dark patches on lateral and dorsal tail; ventral body semitransparent white, stained with light brown pigments; lips semitransparent white, papillae brown. When alive, dorsal body and tail basically deep brown, mottled with copper pigmentation, especially dense on body; lateral body brown, with cream-white patches near abdomen; lateral tail brown, scattered with tiny white pigment spots, no dark brown patches on tail; ventral surface of body semitransparent brown, covered with small white pigments; iris brown.

Bioacoustics. (Fig. 4A, D, G, J; Suppl. material 1: Tables 4; Suppl. material 2: Fig. S3). A total of 16 call groups and 62 calls were analyzed. Average dominant frequency of calls low, 2.5 kHz (2.3–3.0 kHz); call repetition rate moderate, average 1.2 calls per seconds; call interval short, average 153–254 ms; call groups with average 10.8 calls; call duration long (average 746 ms), and with lots of notes (average 42.1). To the human ear, the call sound like "ga ga ga...".

Distribution and natural history. The species is currently known with certainty from the type locality in Medog County, and its distribution elevation was recorded between 680–2200 m (Fei et al. 1983, 2012, Fei and Ye, 2016; this study). This species was recorded in or near small mountain streams of tropical rain forests, sit on rocks, leaf litter, and sometimes bare soil. Calls heard between 11 June to 5 August (this study; Fei et al. 2019). Four in five females recorded during 11 June to 18 June were gravid. Males start calling before dusk under dense vegetation. Normally, two or more males call in small groups along stream banks, spacing themselves ca. 3–5 meters from each other. Sequenced tadpoles in metamorphosis were recorded on 18 June, in small mountain stream pond at 1560 m. Tadpoles of two other species of *Megophrys* share the same ponds. See description in following. Breeding season is supposed to including early June and may last to early August.

Comparison. Refer to Mahony et al. (2018) for comparison with other species of *M. major* group. *M. medogensis* differs from *M. pachyproctus* by much larger body size (SVL 57.2–68.7 in 21 males vs. 35.3–35.7 in two males in the latter), absence of large protuberance above vent (vs. present in the latter), skin relatively smooth (vs. rough in the latter), frontoparietal distinctly wider in front than rear (vs. almost equally wide in the latter), sagittal suture occlusive (vs. distinctly open in the latter), and columella auris long (vs. short in the latter). For comparisons with species studied in this paper, refer to relevant morphological comparison sections for those species.

Megophrys* cf. *pachyproctus

Figs 3C, H, M, R, W, 4B, E, H, K, 5C, H, 6C, G, K, O, 7, 10C, D, H, I, Suppl. material 2: Figs S2, S5B, S5F; Tables 1, 3, 4, Suppl. material 1: Tables S1, S2, S3, S5

Megophrys cf. *pachyproctus* Huang, 1981[***]

Specimens examined. Four adult males, CIB022017061805 (Figs 3C, H, M, R, W, 5C, H, 7), CIB201706MT04, CIB022016061806, CIB022017061807, collected from Bari village, Medog County, Tibet Autonomous Region, China (29.32947°N, 95.36016°E, 1780 m) by SC Shi and L Ding, on 18 June 2017. One adult male (CIBMT171056), four adult females in gravidity (CIBMT171052, CIBMT171057, CIBMT171058, CIBMT171054), and one male toadlet (CIBMT171059) were collected from vicinity of Renqingbeng Temple (29.304832°N, 95.361682°E, 2003 m) by SC Shi on 26 October 2017.

Description of the representative (referred) specimen. Adult male, CIB022017061805 (Figs 3C, H, M, R, W, 5C, H, 7). Measurements in mm. Body stout, relatively small size (SVL 34.8); protuberance beyond cloaca small, barely visible from ventral view, not swollen.

Head moderately large, wider than long (HW 12.3, HL 11.0, IFE 6.5, IBE 10.4); snout rounded in dorsal view, slightly projecting in profile, protruding beyond lower jaw; rostral appendage absent (SL 4.6); canthus rostralis blunt; loreal region concave, dorsal surface of snout slightly concave; nostril oval, nearly in the middle of distance from snout to eye (SN 2.2, EN 2.3), distance between nostrils almost equal to distance between upper eyelids (IN 3.9, IUE 3.8); tympanum smaller than half of eyes (EL 4.5, TYD 1.8); eye-tympanum distance subequal to tympanum diameter (TYE 1.7); tympanum irregular rounded, upper 1/3 conceal with supratympanic ridge; interorbital space flat, larger than upper eyelid (UEW 3.2); pineal ocellus not visible; vomerine ridges distinct, orientation of two ridges acutely angled, enlarged at ends where bearing several vomerine teeth; maxillary teeth present; tongue notched posteriorly, medial lingual process absent.

Forearm moderately long and wide, similar size of upper arms, shorter than hand (FAL 7.5, HAL 9.6); fingers long and thin, with rudimentary webbing; narrow lateral fringes present on finger III, indistinct on other fingers; subarticular tubercles absent;

[***] For detailed comparisons between these all related species, we independently described specimens of *M.* cf. *pachyproctus* in detail.

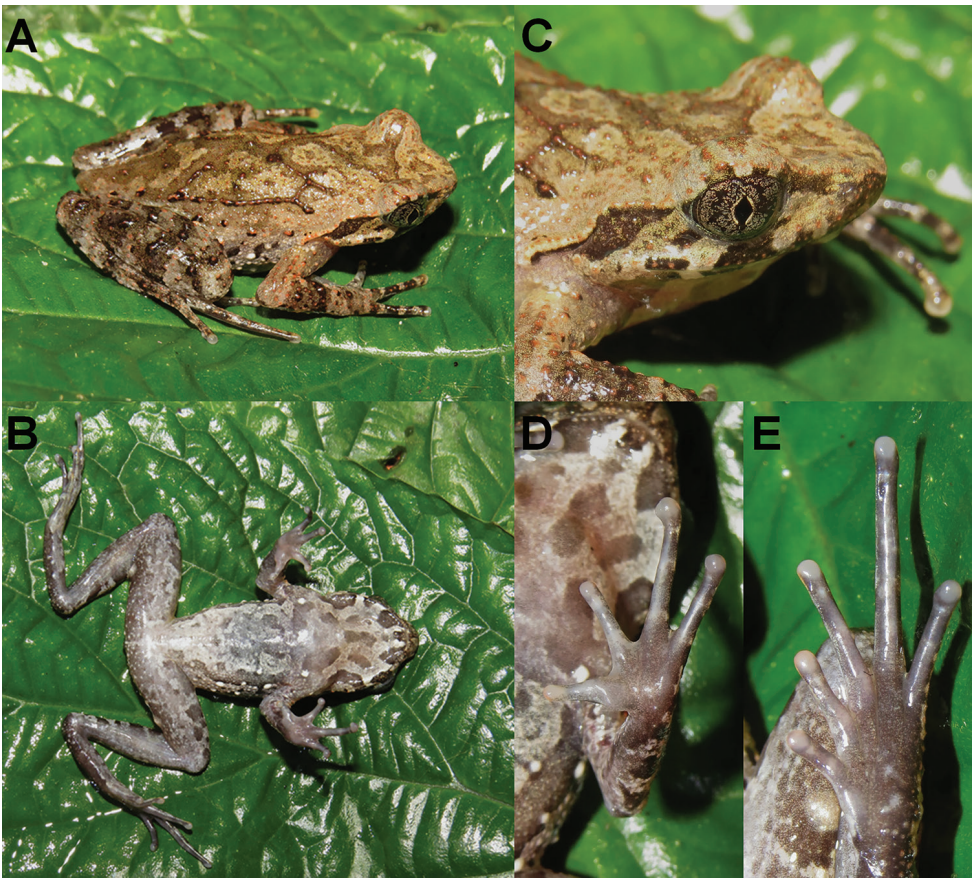

Figure 7. The adult male CIB022017061805 of *M.* cf. *pachyproctus* in life. **A** dorsolateral view of body **B** ventral view of body **C** dorsolateral view of head **D** ventral view of hand **E** ventral view of foot.

inner and outer metacarpal tubercles mostly fused, large, with the size of base of finger I; finger length formula I < II < IV < III; base of finger I strong, larger than base of finger II; tips of fingers slightly swollen, without pads (FIIIW 1.1).

Hindlimbs thin and long; tibio-tarsal articulation reaches middle eye; thighs shorter than shanks but longer than feet (TL 16.5, SHL 17.2, FOL 15.2, TFOL 24.0); toes long and thin, relative lengths I < II < V < III < IV, rudimentary webbed, with narrow lateral fringes, tips rounded, dermal ridges continuously present on ventral surface; subarticular tubercles absent; outer metatarsal tubercle tiny and rounded; inner metatarsal tubercle distinct (IMT 1.6), nearly oval, partially fused with toe I.

Skin. Dorsal surface of head and body rough, densely scattered with small granules; temporal region and upper corner of mandible with rough granules; tympanum ring slightly raised; several small granules on edges of upper eyelids; supratympanic ridges extend from posterior upper eyelids to above forearm insertions, curving above tympanum, rear part thicker than the front; skin on flanks smoother than

skin on dorsum, with several large warts and lesser granules; dorsolateral ridges distinct, irregularly stretch from above shoulder to near groin; a transverse skin ridge between upper eyelids; a near "V"-shaped skin ridge between shoulders, connected with the right dorsolateral ridge by a short skin ridge, a tubercle present near the end of "V"-shaped skin ridge; two oblique skin ridges connected with dorsolateral ridges at posterior; dorsal surface of upper arm covered with small granules in three rows from shoulder to elbow; small granules on dorsum of lower arm, hand, and hindlimbs, four transverse rows of granules on thighs and shanks; ventral surface of body and limbs smooth; pectoral glands small and rounded, with the size of first fingertip, close to axilla on chest; femoral glands small, closer to outer edge of knee than to cloaca.

Coloration in preservative. (Fig. 3C, H, M, R, W). Dorsal surface of head gray; dorsal surface of body pale gray; a darker gray triangle bet between eyes, little lighter in center, anterior corners reach to near out edge of upper eyelids; area around dorsal skin ridges darker, no clear "X"-shaped markings on dorsum; tubercles on flanks white and edged with dark patches on one side; lateral surface of head mottled with pale gray and grayish white; a dark stripe extend from behind upper eyelid to behind corners of the mouth, thicker in the middle, and covers tympanum entirely; no long white stripe present on upper lip; two dark strips from eyes to upper lips, two short dark bands on upper lips before eyes; iris dark covered with silver pigments radiated from pupil; dorsal and lateral surface of limbs pale gray with darker transverse bands, one or two broad dark brown transverse bands on forearms, and four indistinct transverse bands on dorsal thighs and shanks, dorsal tarsal pale gray with three indistinct transverse bands, dorsal surface of fingers and toes also covered with several darker transverse bands; gular and chest dusty white; edge of lower mandible white with five brown patches, the pair corresponding to places between nasals and eyes are largest; a short longitudinal light brown stripe present in middle of throat, two pairs of faint brown patches beside the short longitudinal light brown stripe; a brown stripes extending from posterior end of jaws to base of forearms on both sides; skin around pectoral glands faint brown, three medium size faint brown patches present on dusty white upper abdomen, lower abdomen cream-white reticulated with dusty brown pigments, no large longitudinal dark patches present on ventral lateral abdomen; ventral surface of forelimbs and hindlimbs dusty brown, mottled with several irregular brown patches; pectoral and femoral glands cream-white; nuptial pad grayish black.

Coloration in life. (Fig. 7). Markings as described in preservative; flanks, lateral sides of head, dorsal surface of head, body, and limbs light brown in general with orange-red granules; tympanum and stripes under eyes brown; several cream-white dots present on flanks; two dark brown transverse bands present on forearms; four dark brown transverse bands present on thighs, shanks, and tarsi; ventral surface of head, and abdomen grayish white basically, two large longitudinal brown present on lateral sides of abdomen; chest, ventral surface of hand, thigh, and feet flesh colored; skins around cloaca, on groin, and anterior, posterior and ventral thigh without orange

patches; iris dark brown reticulated with dense golden pigments, pupil edged with diamond-shaped golden ring; nuptial pad gray.

Skull. (Fig. 5C, H). Skull weakly ossified, width 1.15× of length; maxillary overlapping with the quadratojugal; premaxillary and maxillary teeth weakly developed, most tooth separated from others by a distinct gap, 10/10 teeth present on left/right premaxillary, teeth absent on mandible; vomerine ridge moderate, few vomerine teeth weak, present on enlarged posterior end of vomerine ridge; nasal process of premaxilla protruding beyond skull; nasal bones separated from each other, half connected with sphenethmoid; sphenethmoid rough with curves and pits on dorsal and ventral surface, middle one third of front edge free from nasal bones, and protruding forward, separated from premaxilla; frontoparietal divided by a distinctly open sagittal suture , slightly wider posteriorly; anterior fontanelle small, slightly wider sagittal suture; front and rear part of frontoparietal almost equally wide; posterior edge of exoccipitals posterior to the line connecting conjunctions of quadratojugal and mandible; pterygoid moderate; anterior process of squamosal slender and sharp, tip closer to the junction of pterygoid and quadratojugal than its base, posterior process present; front part of prootic smooth, rear part rough, separated from exoccipitals; anterior process of parasphenoid in shape of fusiform, anterior part not raised above sphenethmoid, conjunction of parasphenoid anterior process meet with sphenethmoid narrow, width ca. half the constriction near its base; columella auris short.

Variation. (Suppl. material 2: Fig. S2). The topotypes have the following differences: tympanum diameter/eye diameter ratio varies from 0.40 to 0.60 for adults, 0.36 for the juvenile CIBMT171059; skin ridges between dorsolateral ridges on dorsum vary in configuration, i.e., "> <" (CIB022016061806) and ">" (CIB022017061807); and specimen CIB022017061807 with orange-red patches on groin, and flanks stained with orange-red. The three skulls similar in morphology (e.g., premaxillary and maxillary teeth weak; the nasal bones half connected with sphenethmoid; the sphenethmoid rough and protruding forward; tip of anterior process of parasphenoid narrow), but possessing following variation: vomerine teeth only present on left vomerine ridge of CIBMT171056; sagittal suture of CIBMT171056 partially occlusive near the center.

Secondary sexual characters. Adult female with larger body size, average 1.17× of males. Male with gray nuptial pad on inner first finger, spines on nuptial pad dense and small; single subgular vocal sac; vocal sac opening small, slit like; lineae musculinae absent.

Bioacoustics. (Fig. 4B, E, H, K; Tables 4; Suppl. material 1: Table S3). A total of 15 call groups and 82 calls were analyzed. Average dominant frequency of calls moderate, 3.2 kHz (3.2–3.3 kHz); call repetition rate moderate, average 0.9 calls per seconds; call interval long, average 493–720 ms; call groups with average 10.8 calls; call duration long (average 746 ms), and with lots of notes (average 42.1). To human ears, sound like pebbles hitting ground continuously.

Tadpole. (Fig. 6C, G, K, O; Suppl. material 1: Table S2). Description based on measurements and observation of tadpole specimen CIBMT20170611 at stage 25. Measurements in mm. Body 6.1, elongated; head slightly narrower than trunk; oral disk large, funnel like, positioned anterior-dorsal, width 1.6× of body width; 4 rows

of oval submarginal papillae on middle lower lip, 3 rows of oval submarginal papillae on both sides of upper lips; all these papillae range towards oral cavity; keratodonts absent; nares much closer to eyes than tip of snout (RN/NE 3.8); eyes round, positioned dorsolaterally; internarial distance (IND1.4) 85% of the interpupil distance (PP 1.63); spiracle mostly in left side of body, in right-handed helix from ventral view, the spiracular tube not protruding beyond body wall, positioned 63% of the distance between tip of the snout and trunk-tail junction, and below the horizontal mid trunk line; tail accounts 68% of total length; dorsal fin arise above trunk-tail junction, 38% of maximum body height; ventral fin connected to the trunk, with lesser height than dorsal fin, 31% of maximum body height; anal siphon opens medially; maximum tail muscle height 72% of maximum body height, maximum tail muscle width 53% of maximum body width; eleven small curves present on both lateral side of tail muscle.

When alive, dorsal body and tail basically with yellow-brown pigmentation; two golden spots in size of eyes present on dorsolateral mid body. In preservation, dorsal body, and most part of lateral tail with brown pigmentation; ventral body and tail fin semitransparent; lateral body and tail with pigmentation, but lower fin and ventral body barely pigmented.

Comparison. By having relative smaller body size (males 33.6–36.6, n = 5; females 40.6–42.8, n = 4; measurements in mm), *Megophrys* cf. *pachyproctus* differs from *M. medogensis* (males 57.2–68.7, n = 21), *M. caudoprocta* (males 70.8–81.3, n = 4); *M. hoanglienensis* (males 37.4–47.6, n = 11), *M. jingdongensis* (males 53.0–56.5, n = 3), *M. liboensis* (males 61.6–62.9, n = 4), *M. omeimontis* (males 56.0–59.5, n = 10), *M. aceras* (males 55.8–62.4, n = 6); *M. ancrae* (males 39.1–45.3, n = 8), *M. damrei* (male 57.1, n = 1), *M. flavipunctata* (males 56.9–68.4, n = 4), *M. glandulosa* (males 76.3–81.0, n = 10), *M. himalayana* (males 68.0–73.5, n = 6), *M. lekaguli* (males 55.6–66.6, n = 8), *M. major* (males 71.6–87.5, n = 12), *M. mangshanensis* (male 62.5, n = 1), *M. maosonensis* (male 77, n = 1), *M. megacephala* (males 45.9–53.4, n = 12), *M. monticola* (males 38.4–49.5, n = 17), *M. periosa* (males 71.3–93.8, n = 12), *M. robusta* (males 73.5–83.1, n = 6), *M. longipes* (male 47, n = 1; female 65, n = 1), *M. oreocrypta* (female 94.9, n = 1), *M. serchhipii* (male 37.1, n = 1), and *M. takensis* (males 47.3–53.0, n = 3).

By having relative larger body size (males 33.6–36.6, n = 5; females 40.6–42.8, n = 4; measurements in mm), *Megophrys* cf. *pachyproctus* differs from *M. zunhebotoensis* (male 30.0, n = 1; female 39.0, n = 1), *M. rubrimera* (males 26.7–30.5, n = 8), and *M. angka* (males 31.2–32.1, n = 2).

By tympanum present distinctly, *Megophrys* cf. *pachyproctus* differs from *M. gigantica*, *M. nankiangensis*, and *M. shapingensis* (vs. absent or concealed in the latter).

By vomerine ridge and teeth present, *Megophrys* cf. *pachyproctus* differs from *M. wawuensis* (vs. absent in the latter).

By maxillary teeth present, *Megophrys* cf. *pachyproctus* differs from *M. elfina*, *M. gerti*, *M. hansi*, *M. koui*, *M. microstoma*, and *M. synoria* (vs. absent in the latter).

By hind limbs long and head not wide and flat, *Megophrys* cf. *pachyproctus* differs from *M. carinense*, *M. chuannanensis*, *M. feae*, *M. intermedia*, and *M. popei* (vs. hind limbs short and head flat wide in the latter).

By lacking a single, wide and flat palpebral projection on the edge of the upper eyelid, *Megophrys* cf. *pachyproctus* differs from *M. lancip*, *M. montana*, *M. parallela*, *M. baluensis*, *M. edwardinae*, *M. kobayashii*, *M. ligayae*, *M. nasuta*, and *M. kalimantanensis* (vs. present in the latter).

By lacking rostral appendage, *Megophrys* cf. *pachyproctus* differs from *M. stejnegeri* (vs. having less rostral appendage in the latter).

By lacking a distinct horn-like tubercle at edge of upper eyelid, *Megophrys* cf. *pachyproctus* differs from *M. dringi* (vs. present in the latter).

By vomerine teeth present, *Megophrys* cf. *pachyproctus* differ from *M. vegrandis*, *M. baolongensis*, *M. binchuanensis*, *M. binlingensis*, *M. boettgeri*, *M. brachykolos*, *M. cheni*, *M. kuatunensis*, *M. lini*, *M. lishuiensis*, *M. minor*, *M. obesa*, *M. palpebralespinosa*, *M. sangzhiensis*, *M. shuichengensis*, *M. spinata*, *M. tuberogranulata*, *M. wuliangshanensis*, *M. wushanensis*, *M. ombrophila*, *M. leishanensis*, *M. wugongensis*, *M. mufumontana*, *M. feii*, *M. auralensis*, and *M. huangshanensis*, *M. angka*, *M. shunhuangensis*, *M. jiangi*, and *M. xianjuensis* (vs. absent in the latter).

By relatively finger lengths I < II < IV < III and nuptial pads present only on finger I, *Megophrys* cf. *pachyproctus* differs from *M. nanlingensis* (vs. relatively finger lengths II < I < IV < III, nuptial pads and nuptial spines invisible in males during breeding season in the latter).

By toes with rudimentary webbing, *Megophrys* cf. *pachyproctus* differs from *M. serchhipii* (vs. at least one fourth webbed in the latter).

By toes with narrow lateral fringes, *Megophrys* cf. *pachyproctus* differs from *M. binchuanensis*, *M. cheni*, *M. jingdongensis*, *M. lini*, *M. rubrimera*, *M. shuichengensis*, *M. spinata*, *M. feii*, *M. vegrandis*, and *M. glandulosa* (vs. wide in the latter).

By dorsal skin rough but without spines, *Megophrys* cf. *pachyproctus* differs from the following species: *M. vegrandis* (vs. smooth); *M. medogensis* (vs. smooth with small granules); *M. daweimontis* (vs. smooth); *M. fansipanensis* (vs. smooth with small granules); *M. oropedion* (vs. smooth with small granules); *M. parva* (vs. smooth); *M. zhangi* (vs. smooth); and *M. jiulianensis* (vs. dorsal skin rough with spines).

By snout rounded in dorsal view and nuptial pad only present only on finger I, *Megophrys* cf. *pachyproctus* differs from *M. dongguanensis* (vs. snout pointed, nuptial pads present on the first two fingers in the latter).

Megophrys cf. *pachyproctus* further differs from *M. medogensis* by the following characters: nuptial pads only present on finger I in males (vs. on the first two fingers in the latter); dorsal skin rough (vs. relatively smooth in the latter); vomerine ridge moderate, vomerine teeth weak (vs. both strong in the latter).

By having following characters of skull, *Megophrys* cf. *pachyproctus* differs from *M. medogensis*: skull weakly ossified, opening of anterior fontanelle present, sagittal suture distinctly open (vs. skull well ossified, opening of anterior fontanelle and sagittal suture occlusive in the latter); frontoparietal front equals rear (vs. distinctly wider in the latter); sphenethmoid rough with curves and pits, middle front edge protruding (vs. relatively smooth with few pits, truncate in the latter); exoccipitals posterior to the

line connecting conjunctions of quadratojugal and mandible (vs. anterior in the latter); and columella auris short (vs. long in the latter).

By having following characters of bioacoustics, *Megophrys* cf. *pachyproctus* differs from *M. medogensis* (Tables 3, Suppl. material 1: Table S5): call duration significantly much longer (491–889 ms vs. 121–241 ms; $P < 0.001$); dominant frequency significantly higher (3.2–3.3kHz vs. 2.3–3.0 kHz; $P < 0.01$); and call intervals significantly longer (493–720 ms vs. 153–254 ms; $P < 0.001$).

Megophrys cf. *pachyproctus* very resemble *M. pachyproctus* on morphology, but differs from the latter in the following characters: protuberance beyond cloaca small, barely visible from ventral view, not swollen (vs. protuberance present on vent beyond cloaca large, swollen, arc-shaped, can be seen on both dorsal and lateral view in the latter); inner metatarsal tubercle distinct partially fused with toe I (vs. inner metatarsal tubercle separate from base of toe I at a distance nearly twice its diameter in the latter). *Megophrys* cf. *pachyproctus* further differs from *M. pachyproctus* by having the following characters on skull morphology: premaxillary and maxillary teeth weak, separated from others by gaps (vs. strong, closely positioned with others in the latter); inner edge of nasal bones half contact with sphenethmoid (vs. mostly in the latter); sphenethmoid rough with curves and pits, middle front edge protruding (vs. relatively smooth with few pits, truncate in the latter); and conjunction of parasphenoid anterior process meet with sphenethmoid narrow, width ca. half the constriction near its base (vs. moderate, ca. three quarters in the latter).

Distribution and natural history. This group is currently known at elevation from 1560 m to 2003 m in Medog County, Tibet Autonomous Region, China. It inhabits mountain streams of subtropical forests. During June, males call on branches and leaves of bushes near mountain stream with a distance at least three meters from others, where covered with dense broad leaf forests (Figs 10C, D, H, I, Suppl. material 2: Fig. S5B, S5F). Females collected during October were gravid with well-developed eggs, and also found on leaves of floor vegetation like *Elatostema* species and ferns near small mountain streams. Distribution elevation overlap with *M. medogensis* at 1560 m, where a small stream pond was found to have tadpoles of three *Megophrys* species on 18 June, including *M. medogensis* (at stage 42), *Megophrys* cf. *pachyproctus* (at stages 26–27), and *Megophrys yeae* sp. nov. (at stages 28–35). *Theloderma* sp. and *Amolops medogensis* Li and Rao, 2005 were recorded at the same habitat.

***Megophrys zhoui* sp. nov.**

http://zoobank.org/8E90115E-03A7-440A-9A57-60F8D8489492

Figs 3D, I, N, S, X, 5D, I, 8, 10D, J, Suppl. material 2: Figs S3, S5B; Tables 1, 3, Suppl. material 1: Tables S1, S5

Holotype. (Figs 3D, I, N, S, X, 8). Adult male CIBMT171053, collected from vicinity of Renqingbeng Temple, Medog County, Tibet Autonomous Region, China (29.304832°N, 95.361682°E, 2003 m) by SC Shi on 26 October 2017.

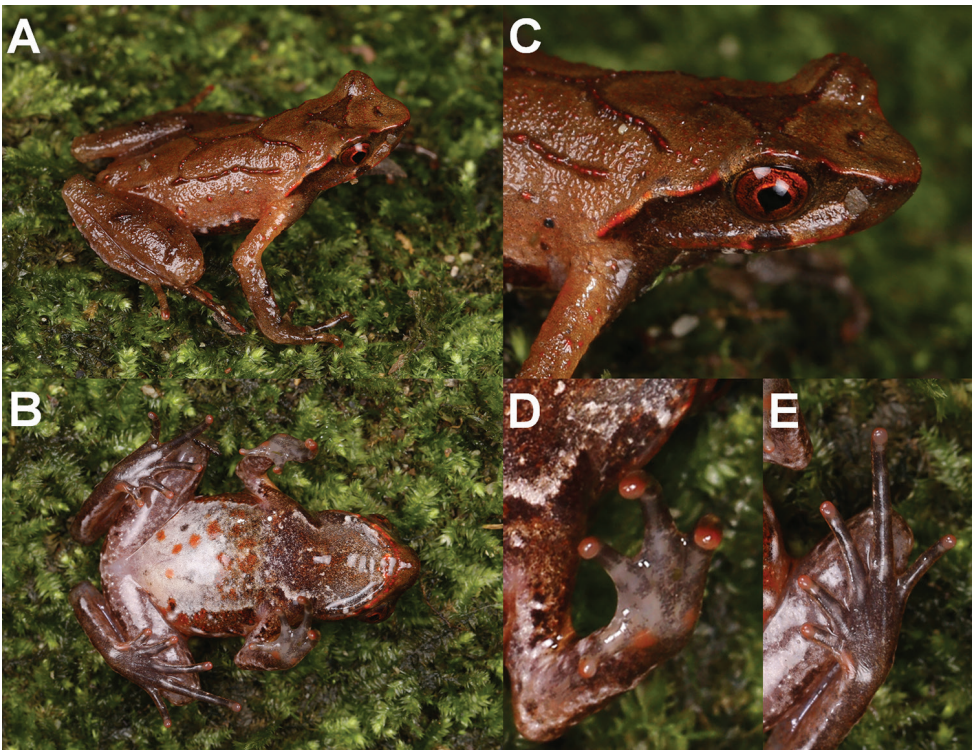

Figure 8. The holotype adult male CIBMT171053 of *Megophrys zhoui* sp. nov. in life. **A** dorsolateral view of body **B** ventral view of body **C** dorsolateral view of head **D** ventral view of hand **E** ventral view of foot.

Paratypes. (Suppl. material 2: Fig. S3). Two adult gravid females CIBMT171060 and CIBMT171062, collected along with the holotype.

Etymology. The specific name is in honor of Professor Zhou Kai-Ya, for his contribution to Chinese amphibian research.

Suggested vernacular name. Zhou's horned toad (English), Zhou Shi Jiao Chan (周氏角蟾, Chinese).

Diagnoses. *Megophrys zhoui* sp. nov. is assigned to the genus *Megophrys sensu lato* based upon molecular phylogenetic analyses and the following morphological characters: canthus rostralis well-developed; supratympanic fold distinct; axillary glands small and tit-like, on sides of the breast; head length more than 25% of body size; upper jaw protruding beyond the margin of the lower jaw; no skin fold on back of head; maxillary teeth present; tympanum distinct; hind legs long and thin.

Megophrys zhoui sp. nov. is distinguished from its congeners by a combination of following characters: body small (male 23.0, n = 1; females 23.5–23.9, n = 2); vomerine ridge weak, vomerine teeth absent; tympanum present, moderate; base of finger I in similar size with finger II, relative finger lengths I < II < IV < III, fingertips not expanded into small pads; toes with narrow lateral fringes or absent; inner metatarsal tubercle long oval, positioned on base of toe I; dorsal skin relatively smooth; protuberance beyond

cloaca indistinct, barely visible from ventral view, not swollen; skull weakly ossified, premaxillary and maxillary teeth weak; skull wider slightly than long; nasal bones not contact with sphenethmoid.

Holotype description. (Figs 3D, I, N, S, X, 8). Measurements in mm. Adult male, with well-developed testes; body slender, extremely small (SVL 23.0); protuberance beyond cloaca small, not visible from ventral view, not swollen.

Head moderate, longer than wide (HW 7.8, HL 8.3, IFE 4.5, IBE 7.2); snout near rounded in dorsal view, slightly protruding beyond lower jaw; rostral appendage absent (SL 3.6); canthus rostralis blunt; loreal region slightly concave, dorsal surface of snout slightly concave; nostril oval, closer to eye than tip of snout (SN 1.8, EN 1.4); distance between nostrils approximate distance between upper eyelids (IN 3.0, IUE 2.7); eyes twice size of tympanum (EL 2.7, TYD 1.3); pupils diamond, inferior angle slightly concave; eye-tympanum distance subequal with tympanum diameter (TYE 1.1); tympanum rounded, upper 1/3 conceal with supratympanic ridge; interorbital space flat, wider than upper eyelids (UEW 2.3); pineal ocellus not visible; two arcuate vomerine ridges present, orientation of two ridges acutely angled, not enlarged at posterior ends, shortest distance between two ridges equal to length of vomerine ridges; vomerine teeth absent; maxillary teeth present; tongue weakly notched behind, medial lingual process absent.

Forearm slender, not wider than upper arms, shorter than hand (FAL 5.2, HAL 7.1); fingers thin, without rudimentary webbing; subarticular tubercles absent; inner and outer metacarpal tubercles indistinct; base of finger I equal wide with base of finger II; finger relative length I < II < IV < III; tips of fingers slightly swollen, without pads (FIIIW 0.5).

Hindlimbs thin and long, tibio-tarsal articulation reaches middle eye; thighs shorter than shanks but longer than feet (TL 11.5, SHL 12.5, FOL10.9, TFOL 16.7); toes slender, relative length I < II < V < III < IV, rudimentary webbed, without lateral fringes, tips slightly swollen, no dermal ridges on ventral surface; subarticular tubercles absent; outer metatarsal tubercle absent; inner metatarsal tubercle long oval (IMT 1.1), positioned on base of toe I.

Dorsal surface of head and body basically smooth, with skin ridges formed by small disconnected granules; lateral surface of head smooth, tympanum ring not raised; two small granules on out edges of upper eyelid; supratympanic ridges nearly straight, extend from behind upper eyelids to above forearm insertions, rear part not thicker than the front; flanks smoother than dorsum, with several small tubercles one or two × size of nostril; skin on head scattered with tiny granules, some lager granules form a triangle between eyes; a "Y"-shaped skin ridges present between shoulders, but posterior part connected the middle of a "W"-shaped skin ridge on dorsum; several larger granules on rear dorsum behind the "W"; dorsal surface of arm smooth, scattered with tiny granules; dorsal hand and feet smooth; dorsal thighs and shanks smooth, with several larger granules; ventral surface of body and limbs smooth; pectoral glands tiny, barely visible, close to axilla on chest; pectoral glands small and rounded, slightly larger than fingertips; closer to outer edge of knee than to cloaca.

Coloration of holotype in preservative. (Fig. 3D, I, N, S, X). Dorsal surface of body and limbs covered with dense gray pigments; larger granules on body and limbs light colored; a brown triangle present between eyes on head; markings on dorsum, and larger granules on dorsal thighs and shanks with brown fringes around; one broad brown transverse bands present on finger II, III and IV; two narrow transverse short bands present on lower arms; one or two faint brown transverse bands on dorsal toes. Lateral side of head pale gray mostly; skin on upper jaw between nostril and below eyes colored lighter; eyes dark with silver dense fiber around pupils and radiate on iris; supratympanic ridge light colored; chest, ventral surface of head, arms and shanks and feet covered with dense smoky gray pigments; abdomen ivory stained with smoky pigments, and scattered with several dark dots; several small ivory patches present on ventral margin of mandible; a darker brown patches with light colored inner edges extend from posterior end of jaws to ventral surface of upper arms on both sides; ventral surface hand mostly with smoky gray pigments, but base of finger I and II ivory; a brown stripe present on ventrolateral body; ventral surface of thighs smoky gray; tips of digits light colored; pectoral and femoral glands ivory.

Coloration of holotype in life. (Fig. 8). Dorsal body and limbs orange-brown, granules on body orange-red; markings on dorsal body as described above; lateral head basically brown; supratympanic ridge orange; temporal region under supratympanic ridge dark brown; upper lips and canthus rostralis stained with orange; dark patches present on upper lips under eyes; iris orange-red, brighter around pupils. Flanks with several larger orange dots, ventrolateral trunk with white pigments and larger white dots. Throat, chest, arms orange-brown, mottled with dense white pigments; chin stained with orange, several small white patches present on lower lips; brown patches from posterior end of jaws to ventral surface of upper arms edged with white at inner side; upper abdomen orange-brown, stained with several faint orange dots; lower abdomen white, scattered with several clean orange dots; both lateral sides of abdomen with broad brown strips; ventral surface of thighs and shanks flesh brown, with several white tiny granules around cloaca; ventral hand with dense gray-brown pigments, base of finger I and II fleshy; inner and outer metacarpal tubercle, and tips of fingers light orange; ventral feet brown; inner metatarsal tubercle, tips of toes light orange.

Skull. (Fig. 5D, J). Skull weakly ossified, width equal to length; maxillary overlapping with the quadratojugal; premaxillary and maxillary teeth weak, barely visible; teeth absent on mandible; vomerine ridge weak, vomerine teeth absent; nasal process of premaxilla protruding beyond skull; nasal bones separated from each other, completely disconnected with sphenethmoid; sphenethmoid relatively smooth with several small pits on dorsal surface and ventral surface, the front edge of sphenethmoid rounded and protruding forward, separated from premaxilla; frontoparietal partially divided by a narrowly opening sagittal suture; anterior fontanelle almost occlusive; front and rear part of frontoparietal almost equally wide; posterior edge of exoccipitals posterior to the line connecting conjunctions of quadratojugal and mandible; pterygoid moderate; anterior process of squamosal slender and sharp, tip in the middle

of the distance from the base to the junction of pterygoid and quadratojugal, posterior process present; prootic relatively smooth, separated from exoccipitals; anterior process of parasphenoid in shape of narrow trapezoid, anterior part not raised above sphenethmoid, conjunction of anterior process of parasphenoid with width ca. two thirds of the constriction near the base; columella auris short.

Variation. (Suppl. material 2: Fig. S3). Paratypes resemble the holotype in general but with following differences: for CIBMT171060, narrow fringes present on toes, tympanum slightly larger than half eyes, orange granules on dorsum form an "X"-shaped skin ridge and a pair of nearly parallel ridges on dorsolateral trunk, and ventral surface less brown and more orange; for CIBMT171060, a broad "X" pattern present on dorsum, and parallel skin ridges on dorsolateral trunk do not make contact with skin ridges between the left parallel ridge.

Secondary sexual characters. Male with single subgular vocal sac; nuptial pad not observed in October; lineae musculinae absent.

Distribution and natural history. The species is currently only discovered from type locality Renqingbeng Temple area at elevation 2003 m in Medog County, Tibet Autonomous Region, China, inhabits small streams in subtropical forests (Fig. 10D, J; Suppl. material 1: Table S5B). All three individuals were found on short herds or ferns beside small mountain stream at a distance shorter than 0.5 m to the ground (Fig. 10J). Females were found to be gravid during October, but eggs not well developed. Advertisement calls not head in October. Several gravid females of *Megophrys* cf. *pachyproctus* were collected from the same small stream with types of *Megophrys zhoui* sp. nov. on the same night. *Theloderma* sp. and *Amolops nyingchiensis* Jiang, Wang, Xie, Jiang, and Che, 2016 were recorded at the same habitat.

Comparison. By body relatively smaller (male 23.0, n = 1; females 23.5–23.9, n = 2 measurements in mm), *Megophrys zhoui* sp. nov. differs from *M. pachyproctus* (males 35.3–35.7, n = 2; female 35.8, n = 1), *Megophrys* cf. *pachyproctus* (males 33.6–36.6, n = 5; females 40.6–42.8, n = 4), *M. medogensis* (males 57.2–68.7, n = 21), *M. acuta* (males 27.1–33.0, n = 10), *M. baolongensis* (males 41.8–45.0, n = 5), *M. binchuanensis* (males 32.0–36.0, n = 4), *M. binlingensis* (males 45.1–51.0, n = 3), *M. boettgeri* (males 34.5–37.8, n = 20), *M. brachykolos* (males 33.7–39.3, n = 5), *M. caudoprocta* (males 70.8–81.3, n = 4), *M. cheni* (males 26.2–29.5, n = 15), *M. daweimontis* (males 34–37, n = 18), *M. fansipanensis* (males 30.9–44.3, n = 13), *M. hoanglienensis* (males 37.4–47.6, n = 11), *M. insularis* (males 36.8–41.2, n = 5), *M. jingdongensis* (males 53.0–56.5, n = 3), *M. jinggangensis* (males 35.1–36.7, n = 2), *M. kuatunensis* (males 26.2–31.4, n = 18), *M. liboensis* (males 61.6–62.9, n = 4), *M. lini* (males 34.1–39.7, n = 20), *M. lishuiensis* (males 30.7–34.7, n = 13), *M. minor* (males 34.5–41.2, n = 4), *M. obesa* (male 35.6, n = 1; females 37.5–41.2, n = 6), *M. omeimontis* (males 56.0–59.5, n = 10), *M. palpebralespinosa* (male 36, n = 1; female 41, n = 1), *M. rubrimera* (males 26.7–30.5 n = 8), *M. sangzhiensis* (male 54.7, n = 1), *M. shuichengensis* (males 102.0–118.3, n = 7), *M. spinata* (males 47.2–54.4, n = 18), *M. tuberogranulata* (males 33.2–39.6, n = 9), *M. wuliangshanensis* (males 27.3–31.6, n = 10), *M. wushanensis* (males 30.4–35.5, n = 10), *M. ombrophila* (males 27.4–34.5, n = 5), *M. leishanensis* (males 32.1–42.3, n = 10), *M. dongguanensis*

(males 30.2–39.3, n = 9), *M. nankunensis* (males 29.9–34.9, n = 11), *M. jiulianensis* (males 30.4–33.9, n = 9), *M. nanlingensis* (males 30.5–37.3, n = 10), *M. wugongensis* (males 31.0–34.1, n = 4), *M. mufumontana* (males 30.1–30.8, n = 2), *M. feii* (males 24.5–25.1, n = 4; female 28.2–28.9, n = 2), *M. vegrandis* (males 27.5–30.6, n = 4), *M. aceras* (males 55.8–62.4, n = 6); *M. ancrae* (males 39.1–45.3, n = 8), *M. auralensis* (males 76.7, n = 1), *M. damrei* (male 57.1, n = 1; female 69.1, n = 1), *M. flavipunctata* (males 56.9–68.4, n = 4), *M. glandulosa* (males 76.3–81.0, n = 10), *M. himalayana* (males 68.0–73.5, n = 6), *M. huangshanensis* (males 36.0–41.6, n = 4), *M. katabhako* (males 35.4–37.0, n = 3), *M. lekaguli* (males 55.6–66.6, n = 8), *M. longipes* (male 47, n = 1; female 65, n = 1), *M. major* (males 71.6–87.5, n = 12), *M. mangshanensis* (male 62.5, n = 1; female 73.0, n = 1), *M. maosonensis* (male 77, n = 1; female 94, n = 1), *M. megacephala* (males 45.9–53.4, n = 12), *M. monticola* (males 38.4–49.5, n = 17), *M. periosa* (males 71.3–93.8, n = 12), *M. robusta* (males 73.5–83.1, n = 6), *M. longipes* (male 47, n = 1; female 65, n = 1), *M. oreocrypta* (female 94.9, n = 1), *M. oropedion* (males 32.8–39.2, n = 7), *M. parva* (males 35.6–50.6, n = 5), *M. periosa* (males 71.3–93.8, n = 12), *M. robusta* (males 73.5–83.1, n = 6), *M. sanu* (males 39.0–46.7, n = 5), *M. serchhipii* (male 37.1, n = 1), *M. takensis* (males 47.3–53.0, n = 3), *M. zhangi* (males 32.5–37.2, n = 3), *M. zunhebotoensis* (male 30.0, n = 1; female 39.0, n = 1), *M. angka* (males31.2–32.1, n = 2), *M. shunhuangensis* (males 30.3–33.7, n = 10), *M. jiangi* (males 34.4–39.2, n = 9), and *M. xianjuensis* (males 31.0–36.3, n = 7).

By tympanum distinct moderate, larger than half eye diameter, *Megophrys zhoui* sp. nov. differs from *M. gigantica*, *M. nankiangensis*, *M. shapingensis*, and *M. wawuensis* (vs. tympanum absent, concealed or very small in the latter).

By maxillary teeth present, *Megophrys zhoui* sp. nov. differs from *M. elfina*, *M. gerti*, *M. hansi*, *M. koui*, *M. microstoma*, and *M. synoria* (vs. absent in the latter).

By hind limbs long and head not wide and flat, *Megophrys zhoui* sp. nov. differs from *M. carinense*, *M. chuannanensis*, *M. feae*, *M. intermedia*, and *M. popei* (vs. head wide flat and hind limbs short in the latter).

By lacking a single, wide and flat palpebral projection on the edge of the upper eyelid, *Megophrys zhoui* sp. nov. differs from *M. lancip*, *M. montana*, *M. parallela*, *M. baluensis*, *M. edwardinae*, *M. kobayashii*, *M. ligayae*, *M. nasuta*, and *M. kalimantanensis* (vs. present in the latter).

By lacking rostral appendage, *Megophrys zhoui* sp. nov. differs from *M. stejnegeri* (vs. having less rostral appendage in the latter).

By lacking a distinct horn-like tubercle at edge of upper eyelid, *Megophrys zhoui* sp. nov. differs from *M. dringi* (vs. present in the latter).

By vomerine ridge weak, *Megophrys zhoui* sp. nov. differs from *M. pachyproctus*, *M. medogensis*, and *Megophrys* cf. *pachyproctus* (vs. vomerine ridge stronger in the latter); differs from *M. vegrandis*, *M. baolongensis*, *M. binchuanensis*, *M. boettgeri*, *M. kuatunensis*, *M. lishuiensis*, *M. wuliangshanensis*, *M. wushanensis*, *M. ombrophila*, *M. leishanensis*, *M. feii*, *M. huangshanensis*, *M. shunhuangensis*, and *M. jiangi* (vs. absent in the latter).

By vomerine teeth absent, *Megophrys zhoui* sp. nov. differs from *Megophrys* cf. *pachyproctus*, *M. pachyproctus*, *M. medogensis*, *M. caudoprocta*, *M. daweimontis*, *M. fansipanensis*, *M. hoanglienensis*, *M. insularis*, *M. jingdongensis*, *M. jinggangensis*, *M. liboensis*, *M. omeimontis*, *M. rubrimera*, *M. dongguanensis*, *M. nankunensis*, *M. jiulianensis*, *M. nanlingensis*, *M. aceras*, *M. ancrae*, *M. damrei*, *M. flavipunctata, M. glandulosa*, *M. himalayana*, *M. katabhako*, *M. lekaguli*, *M. longipes*, *M. major*, *M. mangshanensis*, *M. maosonensis*, *M. megacephala*, *M. monticola*, *M. oreocrypta*, *M. oropedion*, *M. parva*, *M. periosa*, *M. serchhipii*, *M. takensis*, *M. zhangi*, and *M. zunhebotoensis* (vs. present in the latter).

By toes with narrow lateral fringes or absent, *Megophrys zhoui* sp. nov. differs from *M. binchuanensis*, *M. cheni*, *M. jingdongensis*, *M. lini*, *M. rubrimera*, *M. shuichengensis*, *M. spinata*, *M. feii*, *M. vegrandis*, and *M. glandulosa* (vs. wide in the latter).

By dorsal skin relatively smooth, *Megophrys zhoui* sp. nov. differs from *M. pachyproctus*, *Megophrys* cf. *pachyproctus*, *M. insularis*, *M. jinggangensis*, *M. tuberogranulata*, *M. wuliangshanensis*, *M. leishanensis*, *M. dongguanensis*, *M. jiulianensis*, *M. nanlingensis*, *M. wugongensis*, *M. mufumontana*, and *M. feii* (vs. rough in the latter).

By tympanum moderate (TYD/EL 0.40–0.60, n = 9), *Megophrys zhoui* sp. nov. differs from species with large tympanum: *M. brachykolos* (0.70–0.75, n = 7); *M. jinggangensis* (0.73–0.88, n = 5), and *M. takensis* (0.71–0.77, n = 4).

By fingertips not expanded into small pads, *Megophrys zhoui* sp. nov. differs from *M. vegrandis*, *M. ancrae*, and *M. feii* (vs. fingertips with small pads in the latter).

By the following characters, *Megophrys zhoui* sp. nov. differs from *M. pachyproctus*: protuberance beyond cloaca small, not visible from ventral view, not swollen (vs. protuberance present on vent beyond cloaca large, swollen, arc-shaped, visible on both dorsal and lateral view in the latter); and inner metatarsal tubercle long oval, positioned on base of toe I (vs. inner metatarsal tubercle rounded, separate from base of toe I at a distance nearly twice its diameter in the latter).

By having following differences on skull morphology, *Megophrys zhoui* sp. nov. differs from *M. pachyproctus*: premaxillary and maxillary teeth weak, barely visible or separated from others by gaps (vs. strong, closely positioned with others in the latter); nasal bones not contact with sphenethmoid (vs. mostly in the latter); and middle front edge of sphenethmoid protruding (vs. truncate in the latter).

By base of finger I in similar size with finger II, relative finger lengths I < II < IV < III, *Megophrys zhoui* sp. nov. differs from *M. medogensis* (vs. base of finger I distinctly larger than finger II, relative finger lengths II < I < IV < III in the latter).

By having following differences on skull, *Megophrys zhoui* sp. nov. differs from *M. medogensis*: skull weakly ossified, opening of anterior fontanelle present, sagittal suture narrowly or wide open (vs. skull well ossified, opening of anterior fontanelle and sagittal suture occlusive in the latter); premaxillary and maxillary teeth weak, barely visible or separated from others by gaps (vs. strong, closely positioned with others in the latter); frontoparietal front equals rear (vs. distinctly wider in the latter); exoccipitals posterior to the line connecting conjunctions of quadratojugal and mandible (vs. anterior); and columella auris short (vs. long in the latter).

By base of finger I similar in size with finger II, nasal bones not in contact with sphenethmoid, and texture of sphenethmoid relatively smooth with several small pits, *Megophrys zhoui* sp. nov. differs from *Megophrys* cf. *pachyproctus* (vs. base of finger I larger than the base of finger II, nasal bones mostly contact with sphenethmoid, and sphenethmoid rough with curves and pits in the latter).

***Megophrys yeae* sp. nov.**

http://zoobank.org/983FA221-7721-49AE-B8F7-568383A19D18

Figs 3E, J, O, T, Y, 4C, F, I, L, 5E, J, 6D, H, L, P, 9, 10A, C, G, Suppl. material 2: Figs S4, S5A, S5B, S5E, S5F; Tables 1–4, Suppl. material 1: Tables S1–S3, S5

Holotype. (Figs 3E, J, O, T, Y, 4C, F, I, L, 9). CIB201706MT02, adult male, collected in Beibeng village, Medog County, Tibet Autonomous Region, China (29.24292°N, 95.18561°E, 870 m), at 1:40 h on 15 June 2017 by SC Shi and L Ding.

Paratypes. Thirteen specimens (eleven males and two females) from Medog County, Tibet Autonomous Region, China. Four adult males (CIB201706MT01, CIB022017061102, CIB022017061103, and CIB022017061104) collected in Didong village (29.22508°N, 95.12463°E, 670 m) on 11 June 2017 by SC Shi and L Ding. One adult female (CIB201706MT03) collected on 13 June 2017 in Medog urban neighborhood (29.32213°N, 95.31324°E, 907 m) by SC Shi and L Ding. One adult female (CIBMTXC-201701-043) and one adult male (CIBMTXC-201701-044) collected on 28 May 2017 in Medog City neighborhood by F Xie and DW Yang. Two adult males (CIB022017061606 and CIB022017061407) collected in the same location of holotype by SC Shi and L Ding. One male (CIB022017061804) collected in Bari village (29.32947°N, 95.36016°E, 1780 m) at 21:01 18 June 2017 by S.C. Shi. Two adult males (CIBMT171065 and CIBMT171066) collected on 10 and 24 October 2017 in Yarang village (29.29485°N, 95.28126°E, 795 m) by F Xie and DW Yang. One adult male (CIBMT171064) collected at 23:54, 25 October 2017 in Yadong village in the vicinity of Medog city suburb (29.32654°N, 95. 34397°E, 1073 m) by SC Shi and B Wang.

Etymology. The specific name *yeae* is in honor of Professor Ye Chang-Yuan, for her contribution to Chinese amphibian research and inspiration for younger generations of Chinese herpetologists.

Suggested vernacular name. Ye's horned toad (English), Ye Shi Jiao Chan (叶氏角蟾, Chinese).

Diagnoses. *Megophrys yeae* sp. nov. is assigned to the genus *Megophrys sensu lato* based on molecular phylogenetic analyses and the following morphological characters: canthus rostralis well-developed; a tiny horn'-like tubercle at edge of upper eyelid present; supratympanic fold distinct; axillary glands small and tit-like, on sides of the breast; oral disc of tadpoles funnel-like; mouth of tadpoles lacking transverse rows of teeth; head length more than 25% of body size; upper jaw protruding beyond the margin of the lower jaw; no skin fold on back of head; maxillary teeth present; tympanum distinct; hind legs long and thin.

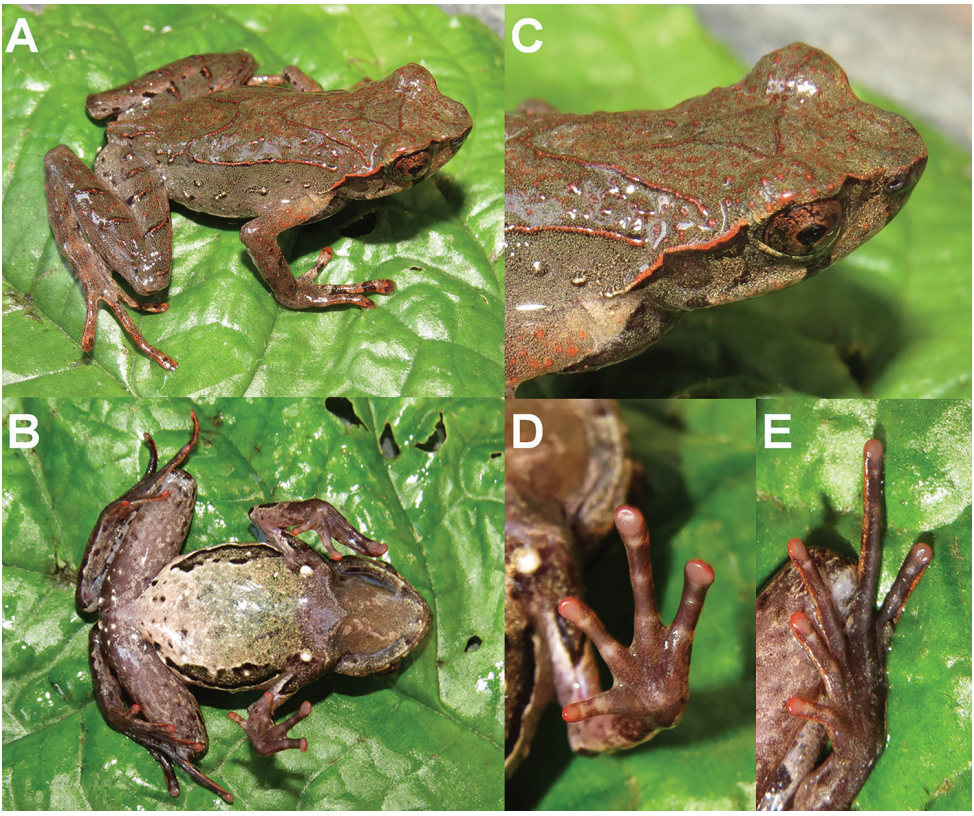

Figure 9. The holotype adult male CIB201706MT02 of *Megophrys yeae* sp. nov. in life. **A** dorsolateral view of body **B** ventral view of body **C** dorsolateral view of head **D** ventral view of hand **E** ventral view of foot.

Megophrys yeae sp. nov. is distinguished from its congeners by a combination of following characters: body relatively small (males 23.8–29.1 mm, n = 12; females 27.9–31.3 mm, n = 2); vomerine ridge weak, vomerine teeth absent; base of first finger weak, size equal to the base of second finger, tips of fingers II-IV flat, expand to small pad; foot of males shorter (FOL 10.8–12.6 mm, n = 12); dorsal skin being relatively smooth; protuberance beyond cloaca small, not visible from ventral view, not swollen; nuptial pad absent; skull weakly ossified, wider than long; premaxillary and maxillary teeth weak, separated from others by gaps; texture of sphenethmoid smooth, without curves and pits; anterior fontanelle opening large, sagittal suture occlusive; advertisement call short and fast (duration 99–212 ms, repetition rate 1.9–4.1 call/s, intervals, n = 6), and dominant frequency high (4.4–5.2 kHz, n = 6).

Description of holotype. (Figs 3E, J, O, T, Y, 4C, F, I, L, 9). Measurements in mm. Adult male. Body small and slender (SVL 27.5); protuberance beyond cloaca small, not visible from ventral view, not swollen.

Head moderate, wider slightly than long (HW 9.8, HL 9.0, IFE 5.1, IBE 8.7); snout rounded in dorsal view, slightly projecting in profile, protruding beyond lower

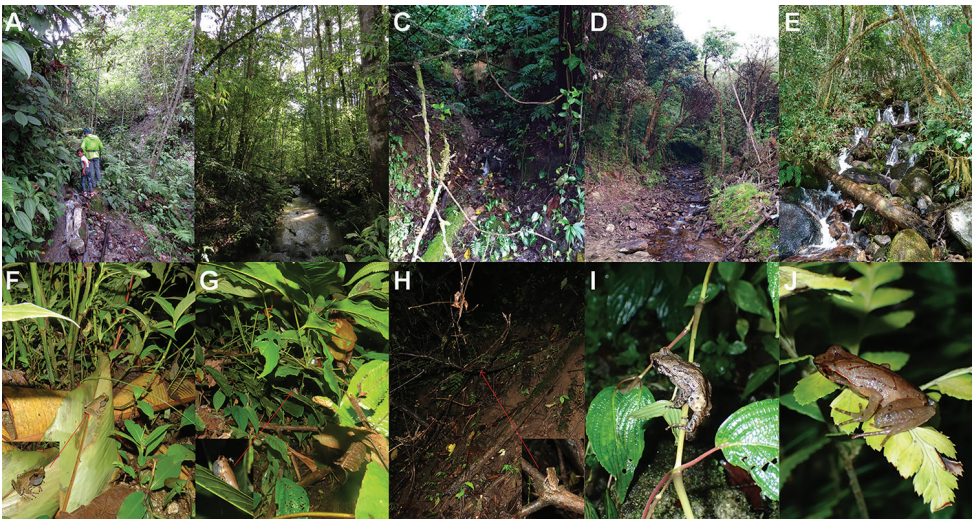

Figure 10. Microhabitats of *Megophrys* toads in the field in Medog. **A** stream at elevation 850 m in Didong village, harboring the low-middle-elevation *M. medogensis* and *Megophrys yeae* sp. nov. **B** a stream at 1530 m in Gelin village, hosting the low-middle-elevation *M. medogensis* and *M. pachyproctus* **C** a stream at 1780 m in Bari village, harboring low-middle-elevation *M. medogensis*, *M.* cf. *pachyproctus* and *Megophrys yeae* sp. nov. **D** a stream at 2003 m in the vicinity of Renqingbeng Temple, hosting *M.* cf. *pachyproctus* and *Megophrys zhoui* sp. nov. **E** a stream at 2142 m in Gedang village, hosting *M. medogensis* **F** one adult male of low-middle-elevation *M. medogensis* calling on a dead leaf on the tropical forest ground nearby a stream in Didong village **G** the adult male paratype CIB022017061102 of *Megophrys yeae* sp. nov. calling on a leaf of dense bushes under tropical forest, ca. 0.5 m above a stream in Didong village **H** the adult male CIB022017061806 of *M.* cf. *pachyproctus* calling on a branch of dead bush, ca. 0.5 m above ground under subtropical forest in Bari village **I** the gravid female CIBMT171054 of *M.* cf. *pachyproctus* precariously climbing up onto a stem of herb, ca. 0.3 m above a tiny stream under subtropical forest in Renqingbeng **J** the adult male holotype CIBMT171053 of *Megophrys zhoui* sp. nov. sitting on a split of a fern leaf in a small stream under subtropical forest in the vicinity of Renqingbeng Temple.

jaw, rostral appendage absent (SL 3.6); loreal region vertical and concave; canthus rostralis blunt; dorsal surface of snout slight concave; nostrils oval, nearly in the middle of distance from snout to eye(SN 1.9, EN 2.0); distance between nostrils (IN 3.2) almost equal with the shortest distance between upper eyelids (IUE 3.1); tympanum small, rounded, diameter (TYD 1.6) less than half of eye length (EL 3.8 mm), upper one third of tympanum anulus merge with supratympanic fold (Figure 5C); eye-tympanum distance (TYE 1.6) equal to tympanum diameter; pupil near oval, with a gap at lower edge; visible pineal ocellus absent; vomerine ridges weak, interval longer than its length, vomerine teeth absent; tongue feebly notched behind, hardly visible, with no medial lingual process.

Forearm long and slim, forearm length (FAL 7.0) 25% of body length, slightly shorter than hand (HAL 8.3), not enlarged relative to the upper arm; relative finger lengths I < II < IV < III; base of first finger weak, size equal to the base of second fin-

ger; tips of finger I rounded, slightly swollen, tips of fingers II-IV flat and expanded, forming small oval pads (FIIIW 1.2, FIVW 1.3), pads without grooves and distinctively larger than terminal phalanges; fingers rudimentary webbed, with ventral callous ridges and narrow lateral fringes; subarticular and supernumerary tubercles absent, palmar tubercles indistinct.

Hindlimbs long and thin, tibio-tarsal articulation reaches area between nostril and eye; heels meet when thighs are positioned at right angles to the body, shank (SHL 14.1) slightly longer than thigh (TL 12.3) and feet (FOL 12.5, TFOL 19.7); toes thin, rudimentary webbed, with ventral callous ridges and narrow fringes; relatively toes lengths I < II < V < III < IV; tips of toes flat and slightly dilated, without grooves, slightly larger than terminal phalanges; inner metatarsal tubercle weak (IMT 1.9) and elliptical, outer metatarsal tubercle, subarticular and supernumerary tubercles absent.

Dorsal body and head relatively smooth, with tiny tubercles scattered on dorsal part of body and limbs; tiny tubercles on most of dorsum form a large "W" skin ridge from behind supratympanic fold curve to ca. one third distance left of groin, a "V" between shoulders ahead of "W", and a triangle between eyes; edges of snout, eyelids, especially supratympanic fold and flanks scattered with larger tubercles; supratympanic fold thin, extend from rear of eyelid, curves down above tympanum to shoulder; small tubercles on dorsal thigh and shank arranged in several transversal rows. Ventral surface of body smooth; a granular line present on ventrolateral side of belly, interrupted on left side; several small glandular tubercles present around cloaca; pectoral glands small, as large as tips of finger II, raised slightly, close to axilla; single femoral gland on ventral thigh small and slightly raised, closer to knee than cloaca.

Coloration of holotype in life. (Fig. 9). Dorsal head and body light brown, tiny tubercles scattered on dorsum and head orange-red; skin ridges edged with faint brown, forming a barely visible "X" pattern on dorsum and triangular on head; skin ridges on thigh edged with narrow black-brown; supratympanic fold orange-red; one short black vertical bar on each side of upper lips beneath the eyes; tympanum pale gray; a black streak under supratympanic fold; tubercles on flanks edged with small dark blotches; two thin ambiguous transverse dark band on dorsal forearms; fingers II-IV with transverse dark band on dorsal surface; dorsal surface of fingers and toes colored with orange-red; flanks light brown; throat pale dusty gray; chest mottled gray stained with light purple between axillary glands; two pale gray streaks from lower place of joins of jaws extend to half of ventral upper arm; abdomen ivory, mottled gray on upper part, several small dark dots scattered rear; a large dark streaks present on both lateral sides of abdomen, from behind axilla to near groin, bordering the creamy white ventrolateral granular line on belly; groin not colored with red; ventral surfaces of thighs light purple mottled with tiny smoky white pigments; small glandular tubercles around cloaca and ivory; ventral surface of shanks and arms with large dark patches; palm and ventral surfaces of foot purplish gray; tips of digits orange edges; pectoral glands and femoral glands creamy white; iris orange-bronze.

Coloration of holotype in preservative. (Fig. 3E, J, O, T, Y). Dorsal body gray, triangle on head and "X" pattern on dorsum barely visible; tubercles on dorsum, dorsal surface of head and limbs light gray; tympanum brown, a black streak under supratym-

panic fold; vertical bar beneath the eyes pale gray; tubercles on flanks edged with small black blotches; tubercles rows on dorsal thigh and shank with dark edges more or less; dorsal surface of forelimbs and hindlimbs dark gray with several ambiguous transverse dark bands; fingers II, III and IV with transverse dark band on dorsal surface; tips of digits light colored; throat, chest, and upper abdomen dusty gray, lower part of abdomen off-white; two dark streaks from lower place of joins of jaws extend to half of ventral upper arm; several small dark patches scattered on lower abdomen; two large dark streaks on lateral sides of abdomen; ventral surface of lower arm whitish, with a pale gray patches connected to hand; palm and ventral surface of foot dusty gray, with light colored fingertips; ventral surface of thigh dusty gray, femoral glands and glandular tubercles around cloaca white; ventral surface of shank dusty gray with several large pale gray patches; iris mottled copper.

Skull. (Fig. 5E, J). Skull rather small and weakly ossified, width 1.16× of length; maxillary overlapping with the quadratojugal; premaxillary and maxillary teeth moderately developed, independent with each other, 10/7 teeth present on left/right premaxillary, teeth absent on mandible; vomerine ridge weak, vomerine teeth absent; nasal process of premaxilla protruding beyond skull; nasal bones separated, posterior edges completely contact with sphenethmoid; sphenethmoid smooth on both dorsal and ventral surface, without curves and pits, the front edge of sphenethmoid concave, in contact with premaxillary; frontoparietal not divided, sagittal suture occlusive; anterior fontanelle opening large, triangular, width approximately the same as nasal bones; the front and rear part of frontoparietal almost equally wide; posterior edge of exoccipitals posterior to the line connecting conjunctions of quadratojugal and mandible; pterygoid moderate; anterior process of squamosal slender and sharp, tip closer to the junction of pterygoid and quadratojugal than its base, posterior process present; prootic relatively smooth, separated from exoccipitals; anterior process of parasphenoid in shape of narrow trapezoid, anterior part not raised above sphenethmoid, conjunction of anterior process of parasphenoid with width approximately the same as the constriction near the base; columella auris short.

Variation (Suppl. material 2: Fig. S4; Suppl. material 1: Table S1). Two female specimens with no lateral fringes on toes. A distinct brown "X" marking on dorsum and a clear triangular on head present on CIB022017061407, CIBMT171064. Abdomens of CIB201706MT01, CIB022017061103 with dark patches on both sides instead of two large streaks. Overall coloration of CIB022017061102, CIB022017061103, CIB022017061103, CIB201706MT01 lighter, without visible "X" marking on dorsum. The "W" skin ridges on dorsum of CIBMT171065 and CIBMT171066 shattered into short disconnected bars. The tympanum of CIBMT171065 not merged with supratympanic fold. The ventrolateral line varies among individuals, in some (e.g., CIB201706MT01) it is interrupted and short, in others (e.g., CIBMT171066) it is simply formed by two separated granules.

Secondary sexual characters. An internal single subgular vocal sac present in male. Vocal openings present at rear of part the mouth. Calling males without nuptial pad on finger.

Advertisement call. (Fig. 4C, F, I, L; Tables 4; Suppl. material 1: Table S3). A total of 19 call groups and 176 calls were analyzed. *Megophrys yeae* sp. nov. has a high dominant frequency (average 4.7 kHz, range 4.4–5.2 kHz). Calls frequent, average calls per seconds 3.0, vary from 1.9 to 4.1; average intercall interval 218 ms, vary from 649 ms to 119 ms when ambient temperatures vary from 17 °C to 25 °C. The number of calls in each call group average 68.9, range from 5 to 187. Calls short, duration average 139 ms, range from 89 ms to 246 ms. Pules per call average 9.2, vary from 7 to 12. To human ears, sound like cricket.

Tadpole. (Fig. 6D, H, L, P; Suppl. material 1: Table S2). Stages 28–35. Body length range from 10.2–11.4 mm, elongated and slender; oral disk funnel like; positioned anterior-dorsal, large, width average 1.4 (1.1–1.5) × of maximum body width, with five nearly parallel rows of oval submarginal papillae on middle lower lip, three rows of oval submarginal papillae on both sides of upper lips, both submarginal papillae rows on upper and lower lips rows pointing towards oral cavity, smaller outer sides; nares oval and are closer to the eye than to the snout (RN/NE average 2.2, 1.8–2.6); internarial distance average 69% (64–78%) of the interorbital distance; eyes positioned dorsolaterally, the pupils rounded; spiracle in right-handed helix from ventral view, spiracular tube not protruding beyond body wall, positioned 53% (47–57%) of the distance between tip of the snout and trunk-tail junction, and opens laterally; the tail makes up average 69% (67–72%) of the total body length; dorsal fin arise behind trunk-tail junction, average 35% (30–41%) of maximum body height; the basal tail width average 60% (48–65%) of the maximal trunk width; keratodonts absent.

Coloration of tadpoles in life: dorsal body brown with dense copper pigments; dorsal tail brown, scattered with copper pigments; lateral tail above lower fin mottled with copper patches; ventral surface of body, and lower fin semi-transparent; iris light brown. Coloration in preservative: dorsal body brown; dorsal tail light brown scattered with brown patches; lateral sides of body brown; lateral tail semitransparent brown, muscle scattered with a lot of distinct brown patches; fins semitransparent stained with little brown, no pigments on lower fin except latter 1/3; ventral body semitransparent white, with tiny gray pigments scattered on throat and chest; ventral tail off-white; lips semitransparent white, papillae brown.

Distribution and natural history. This species is currently known from five localities in Medog County, Tibet Autonomous Region, China (Fig. 1). All calling males recorded on June and October were found on herb leaves near or upon small stream in tropical forest (Fig. 10A, C, G; Suppl. material 2: Fig. S5A, B, E, F). Eggs in adult female (CIB201706MT03) are in two different development stage: pure yellow eggs with diameter of 1.1 mm, and semitransparent eggs with size half or less of the former. A total of 45 larger yellow eggs were counted, smaller semitransparent eggs more than 70. Thus, breeding season is suggested including June to October, and this species may lay eggs more than once during one season. The new species was recorded at elevation between 670 m to 1780 m. On 18 June 2017, four males of *Megophrys pachyproctus* (CIB201706MT04–CIB022016061806, CIB022017061807) were calling in the same stream where one male (CIB022017061804) of the new species was calling to-

gether at nearest distance ca. 3 meters in Bari Village (29.32947°N, 95.36016°E, 1780 m). From its habitat, other amphibians like *Megophrys medogensis*, *Megophrys* cf. *pachyproctus*, *Odorrana zhaoi* Li, Lu, and Rao, 2008, *Amolops medogensis*, and *Huangixalus translineatus* Wu, 1977 were also recorded.

Comparison. By body relatively smaller (males 23.8–29.1, n = 12; females 27.9–31.3, n = 2; measurements in mm), *Megophrys yeae* sp. nov. differs from *M. pachyproctus* (males 35.3–35.7, n = 2; female 35.8, n = 1), *Megophrys* cf. *pachyproctus* (males 33.6–36.6, n = 5; females 40.6–42.8, n = 4), *M. medogensis* (males 57.2–68.7, n = 21), *M. baolongensis* (males 41.8–45.0, n = 5), *M. binchuanensis* (males 32.0–36.0, n = 4), *M. binlingensis* (males 45.1–51.0, n = 3), *M. boettgeri* (males 34.5–37.8, n = 20), *M. brachykolos* (males 33.7–39.3, n = 5), *M. caudoprocta* (males 70.8–81.3, n = 4), *M. daweimontis* (males 34–37, n = 18), *M. fansipanensis* (males 30.9–44.3, n = 13), *M. hoanglienensis* (males 37.4–47.6, n = 11), *M. insularis* (males 36.8–41.2, n = 5), *M. jingdongensis* (males 53.0–56.5, n = 3), *M. jinggangensis* (males 35.1–36.7, n = 2), *M. liboensis* (males 61.6–62.9, n = 4), *M. lini* (males 34.1–39.7, n = 20), *M. lishuiensis* (males 30.7–34.7, n = 13), *M. minor* (males 34.5–41.2, n = 4), *M. obesa* (male 35.6, n = 1; females 37.5–41.2, n = 6), *M. omeimontis* (males 56.0–59.5, n = 10), *M. palpebralespinosa* (male 36, n = 1; female 41, n = 1), *M. sangzhiensis* (male 54.7, n = 1), *M. shuichengensis* (males 102.0–118.3, n = 7), *M. spinata* (males 47.2–54.4, n = 18), *M. tuberogranulata* (males 33.2–39.6, n = 9), *M. wushanensis* (males 30.4–35.5, n = 10), *M. leishanensis* (males 32.1–42.3, n = 10), *M. dongguanensis* (males 30.2–39.3, n = 9), *M. nankunensis* (males 29.9–34.9, n = 11), *M. jiulianensis* (males 30.4–33.9, n = 9), *M. nanlingensis* (males 30.5–37.3, n=10), *M. wugongensis* (males 31.0–34.1, n = 4), *M. mufumontana* (males 30.1–30.8, n = 2), *M. aceras* (males 55.8–62.4, n = 6); *M. ancrae* (males 39.1–45.3, n = 8), *M. auralensis* (males 76.7, n = 1), *M. damrei* (male 57.1, n = 1; female 69.1, n = 1), *M. flavipunctata* (males 56.9–68.4, n = 4), *M. glandulosa* (males 76.3–81.0, n = 10), *M. himalayana* (males 68.0–73.5, n = 6), *M. huangshanensis* (males 36.0–41.6, n = 4), *M. katabhako* (males 35.4–37.0, n = 3), *M. lekaguli* (males 55.6–66.6, n = 8), *M. longipes* (male 47, n = 1; female 65, n = 1), *M. major* (males 71.6–87.5, n = 12), *M. mangshanensis* (male 62.5, n = 1; female 73.0, n = 1), *M. maosonensis* (male 77, n = 1; female 94, n = 1), *M. megacephala* (males 45.9–53.4, n = 12), *M. monticola* (males 38.4–49.5, n = 17), *M. periosa* (males 71.3–93.8, n = 12), *M. robusta* (males 73.5–83.1, n = 6), *M. longipes* (male 47, n = 1; female 65, n = 1), *M. oreocrypta* (female 94.9, n = 1), *M. oropedion* (males 32.8–39.2, n = 7), *M. parva* (males 35.6–50.6, n = 5), *M. periosa* (males 71.3–93.8, n = 12), *M. robusta* (males 73.5–83.1, n = 6), *M. sanu* (males 39.0–46.7, n = 5), *M. serchhipii* (male 37.1, n = 1), *M. takensis* (males 47.3–53.0, n = 3), *M. zhangi* (males 32.5–37.2, n = 3), *M. zunhebotoensis* (male 30.0, n = 1; female 39.0, n = 1), *M. angka* (males 31.2–32.1, n = 2), *M. shunhuangensis* (males 30.3–33.7, n = 10), *M. jiangi* (males 34.4–39.2, n = 9), and *M. xianjuensis* (males 31.0–36.3, n = 7).

By tympanum distinct moderate, *Megophrys yeae* sp. nov. differs from *M. gigantica*, *M. nankiangensis*, *M. shapingensis*, and *M. wawuensis* (vs. absent, concealed or very small in the latter).

By maxillary teeth present, *Megophrys yeae* sp. nov. differs from *M. elfina*, *M. gerti*, *M. hansi*, *M. koui*, *M. microstoma*, and *M. synoria* (vs. absent in the latter).

By hind limbs long and head not wide and flat, *Megophrys yeae* sp. nov. differs from *M. carinense*, *M. chuannanensis*, *M. feae*, *M. intermedia*, and *M. popei* (vs. head wide flat and hind limbs short in the latter).

By lacking a single, wide and flat palpebral projection on the edge of the upper eyelid, *Megophrys yeae* sp. nov. differs from *M. lancip*, *M. montana*, *M. parallela*, *M. baluensis*, *M. edwardinae*, *M. kobayashii*, *M. ligayae*, *M. nasuta*, and *M. kalimantanensis* (vs. present in the latter).

By lacking rostral appendage, *Megophrys* yeae sp. nov. differs from *M. stejnegeri* (vs. having less rostral appendage in the latter).

By lacking a distinct horn-like tubercle at edge of upper eyelid, *Megophrys yeae* sp. nov. differs from *M. dringi* (vs. present in the latter).

By vomerine ridge weak, *Megophrys yeae* sp. nov. differs from *M. pachyproctus*, *M. medogensis*, and *Megophrys* cf. *pachyproctus* (vs. stronger in the latter); differs from *M. vegrandis*, *M. baolongensis*, *M. binchuanensis*, *M. boettgeri*, *M. kuatunensis*, *M. lishuiensis*, *M. wuliangshanensis*, *M. wushanensis*, *M. ombrophila*, *M. leishanensis*, *M. feii*, *M. huangshanensis*, *M. shunhuangensis*, *M. jiangi*, and *M. xianjuensis* (vs. absent in the latter).

By vomerine teeth absent, *Megophrys yeae* sp. nov. differs from *Megophrys* cf. *pachyproctus*, *M. pachyproctus*, *M. medogensis*, *M. caudoprocta*, *M. daweimontis*, *M. fansipanensis*, *M. hoanglienensis*, *M. insularis*, *M. jingdongensis*, *M. jinggangensis*, *M. liboensis*, *M. omeimontis*, *M. rubrimera*, *M. dongguanensis*, *M. nankunensis*, *M. jiulianensis*, *M. nanlingensis*, *M. aceras*, *M. ancrae*, *M. damrei*, *M. flavipunctata*, *M. glandulosa*, *M. himalayana*, *M. katabhako*, *M. lekaguli*, *M. longipes*, *M. major*, *M. mangshanensis*, *M. maosonensis*, *M. megacephala*, *M. monticola*, *M. oreocrypta*, *M. oropedion*, *M. parva*, *M. periosa*, *M. serchhipii*, *M. takensis*, *M. zhangi*, and *M. zunhebotoensis* (vs. present in the latter).

By tips of fingers II-IV flat, expand to small pad, *Megophrys yeae* sp. nov. differs from *Megophrys* cf. *pachyproctus*, *Megophrys zhoui* sp. nov., *M. pachyproctus*, *M. acuta*, *M. binlingensis*, *M. brachykolos*, *M. cheni*, *M. lini*, *M. minor*, *M. obesa*, *M. palpebralespinosa*, *M. sangzhiensis*, *M. shuichengensis*, *M. spinata*, *M. tuberogranulata*, *M. wugongensis*, *M. mufumontana*, *M. auralensis*, and *M. robusta* (vs. expanded pads on fingertips absent in the latter).

By foot of males shorter (FOL 10.8–12.6 mm, n = 12), tympanum relatively smaller (males TD/EL 0.36–0.46, n = 12), and toes with narrow lateral fringes, *Megophrys yeae* sp. nov. further differs from *M. vegrandis* (vs. FOL 13.2–13.8 mm, n = 4, $P < 0.001$; TYD/EL 0.44–0.56, n = 4, $P < 0.03$; and fringes on toes wide in the latter).

By dorsal skin being relatively smooth, *Megophrys yeae* sp. nov. differs from *M. feii* (vs. dorsal skin rough in the latter).

Megophrys yeae sp. nov. differs from *M. medogensis* by the following characters: nuptial pad absent (vs. present in the latter); and base of first finger weak, size equal to the base of second finger, relative finger lengths I < II < IV < III (vs. base of finger I strong, larger than base of finger II, relative finger lengths II < I < IV < III in the latter).

By having following differences on skull morphology, *Megophrys yeae* sp. nov. differs from *M. medogensis*: skull weakly ossified, opening of anterior fontanelle large (vs. skull well ossified, opening of anterior fontanelle occlusive in the latter); premaxillary and maxillary teeth weak, separated from others by gaps (vs. strong, closely positioned with others in the latter); texture of sphenethmoid smooth, without curves and pits (vs. relatively smooth, with few pits in the latter); frontoparietal front equals rear (vs. distinctly wider in the latter); exoccipitals posterior to the line connecting conjunctions of quadratojugal and mandible (vs. anterior); and columella auris short (vs. long in the latter).

By having following differences on bioacoustics, *Megophrys yeae* sp. nov. differs from *M. medogensis*: dominant frequency significantly higher (4.4–5.2 kHz vs. 2.3–3.0 kHz in the latter; $P < 0.001$); call significantly faster (repetition rate average 3.0, vary from 1.9 to 4.1 vs. average 1.2 vary from 0.6 to 2.2 in the latter); and call intervals significantly longer (493–720 ms vs. 153–254 ms in the latter; $P < 0.001$).

By having the following characters, *Megophrys yeae* sp. nov. differs from *M. pachyproctus*: lacking a swollen protruding beyond cloaca (vs. present in the latter); nuptial pad absent (vs. present in the latter); and base of first finger weak, size equal to the base of second finger (vs. base of finger I strong, larger than base of finger II in the latter).

By having the following characters on skull morphology, *Megophrys yeae* sp. nov. differs from *M. pachyproctus*: premaxillary and maxillary teeth weak, separated from others by gaps (vs. strong, closely positioned with others in the latter); texture of sphenethmoid smooth, without curves and pits (vs. relatively smooth, with few pits in the latter); anterior fontanelle opening large (vs. occlusive in the latter); and sagittal suture occlusive (vs. distinctly open in the latter).

By having the following characters, *Megophrys yeae* sp. nov. differs from *Megophrys* cf. *pachyproctus*: nuptial pad absent (vs. present on finger I in the latter); and base of first finger weak, size equal to the base of second finger (vs. strong, larger than base of finger II in the latter).

By having following characters on skull morphology, *Megophrys yeae* sp. nov. differs from *Megophrys* cf. *pachyproctus*: texture of sphenethmoid smooth, without curves and pits (vs. rough, with curves and pits in the latter); anterior fontanelle opening large (vs. small, width equals sagittal suture in the latter); and sagittal suture occlusive (vs. distinctly open in the latter).

By having the following acoustical characters, *Megophrys yeae* sp. nov. differs from *Megophrys* cf. *pachyproctus*: call significantly shorter (99–212 ms, $n = 6$ vs. 491–889 ms, $n = 3$ in the latter; $P < 0.001$); dominant frequency much higher (4.4–5.2 kHz, $n = 6$ vs. 3.2–3.3 kHz, $n = 3$ in the latter; $P < 0.001$); call intervals significantly shorter (146–370 ms, $n = 6$, vs. 493–720 ms, $n = 3$ in the latter; $P < 0.001$); and calls significantly faster (call repetition rate1.9–4.1 call/s, $n = 6$, vs. 0.7–1.1call/s, $n = 3$ in the latter; $P < 0.01$).

By having following characters on skull morphology, *Megophrys yeae* sp. nov. differs from *Megophrys zhoui* sp. nov.: texture of sphenethmoid smooth, without curves and pits (vs. relatively smooth, with several small pits in the latter); and sagittal suture occlusive (vs. narrowly or wide open in the latter).

Discussion

Similar to our surveys, only relatively few herpetologists have conducted field work in the eastern corner of Himalayas, mainly in Medog County, China (e.g., Huang and Fei 1981; Fei et al. 1983; Li et al. 2010; Jiang et al. 2012; Jiang et al. 2016a, b, and c). Several factors probably hindered the discoveries of the three new *Megophrys* species described here. First, in this region, *M. medogensis*, especially its tadpoles, are almost sympatric with all other related species' tadpoles at extensive elevations even in the microhabitats, probably arousing the judgement of "one population with one species". Moreover, the related species were superficially similar morphologically, easily misleading the identifications if made without detailed examination, especially for the first identification in the field. Of course, the third was insufficient expeditions. Chen et al. (2016) recognized two specimens KIZ010978 and KIZ011175 from Medog County as *M. pachyproctus* without reporting their morphological information. But in our phylogenetic trees, these two specimens were deeply nested into the *Megophrys yeae* sp. nov. clade (Fig. 2). Additionally, our results suggested that *Megophrys yeae* sp. nov. differs distinctly from *M. pachyproctus* on morphology (Figs 3, 5; Tables 1, 2). Hence, we propose that the two specimens were misidentified in this literature and that they should be classified as *Megophrys yeae* sp. nov. Similarly, Liu et al. (2018) treated one sample SYSa002934 from Medog County as *M. pachyproctus*. Our analyses, however, nested this sample into the *M. medogensis* clade (Fig. 2). *Megophrys pachyproctus* and *M. medogensis* should be classified as different species groups based on their morphology: the much larger body size of *M. medogensis* in the large-body-size clade (*M. major* complex proposed in Mahony et al. 2018), also indicating that the two species should be phylogenetically distinct. In any case, all these specimens should be reexamined.

By the protruding vent, *M. pachyproctus* differs from almost all species of *Megophrys* except *M. caudoprocta* and *M. koui*. The protruding vent of *M. caudoprocta* includes an elongated urostyle that slightly exceed ischium (Shen et al. 2013: fig. 1). However, the protruding vent of *M. pachyproctus* is a swelling and the urostyle does not exceed the vent. Furthermore, according to Yang and Rao (2008), the specimens of *Megophrys* (*Ophryophyne*) from the type locality (Zhushihe, Mengla, Yunnan Province, China) of *M. koui* vary in the presence of protruding vent while they share other morphological characters (identical skin ridge patterns and horn on outer edge of upper eyelid). Furthermore, *M. pachyproctus* was described based only on two males and one female. All these observations increase the uncertainty of whether the swelling protrusion can be used as a diagnostic character of *M. pachyproctus*. Our specimens *M.* cf. *pachyproctus* from Renqinbeng and Bari differ from the holotype of *M. pachyproctus* from Gelin mostly in the following characters: protuberance beyond cloaca small, barely visible from ventral view, not swollen (vs. protuberance present on vent beyond cloaca large, swollen, arc-shaped, visible on both dorsal and lateral view in the latter); and inner metatarsal tubercle distinct partially fused with toe I (vs. separate from base of toe I at a distance nearly twice its diameter in the latter). But *M.* cf. *pachyproctus* is similar to *M. pachyproctus* on many other morphological characters (e.g., body measurements,

skin texture and skin ridges, and most characters on skull; Suppl. material 1: Table S5). For the moment, only one specimen (the holotype) of *M. pachyproctus* was examined, and there is no available molecular evidence from samples from Gelin; therefore, it is not prudent to erect a new name while there are still enigmas. Thus, we temporally treat these specimens from Renqingbeng and Bari as *M.* cf. *pachyproctus.* Further sampling at Gelin would help to resolve this problem in the future.

In this work, we classified samples of *M. medogensis* as low-middle-elevation group (682–1560 m) and high-elevation group (> 2100 m), because these samples phylogenetically clustered into two lineages based on mitochondrial DNA dataset but formed a single lineage when based on nuclear DNA dataset. The discordance indicates introgression between these two groups. The tadpoles of high-elevation group are morphologically different from the low-middle-elevation group: body coloration deep brown with copper pigmentation vs. body yellow-brown without copper pigmentation; tail muscle weaker (TMW/BW 44%) than the latter (TMW/BW 53–57%); lateral tail without dark patches vs. present. The morphological comparisons between adults of the two groups were not applicable in this work because no adults of the high-elevation groups were collected. The scenario of phylogenetical discordance between different gene datasets was also found in *M. monticola* (Mahony et al. 2018). The mechanism of two discovered cases of introgression from southeastern Himalayan is fascinating for further study. Note that the phylogenetically sister species of *Megophrys* in this region (i.e., *Megophrys yeae* sp. nov., *Megophrys zhoui* sp. nov., and *M. vegrandis* being genetically closer; Fig. 2) are distributed in different sites or altitudes, i.e., *Megophrys zhoui* sp. nov. just lives above 2000 m near the Renqingbeng Temple in Medog County, *Megophrys yeae* sp. nov. has a larger range but in some other sites at elevations between 500–1800 m (Figs 1, 10, and Suppl. material 2: Fig. S5) in Medog, and *M. vegrandis* has been just found at 1110 m in a southwestern locality away from the type localities of the first two relatives (Mahony et al. 2013). This case fits the "micro-endemism" model (Liu et al. 2018; Wang et al. 2019) for separating closely related species. On the other hand, the more "phylogenetically distant" species are often sympatric in microhabitat, such as tadpoles of *Megophrys* cf. *pachyproctus* and *Megophrys yeae* sp. nov. in the same pond, and *M. medogensis* with *Megophrys* cf. *pachyproctus*, *Megophrys zhoui* sp. nov., and *Megophrys yeae* sp. nov. in the same stream, indicating the "sympatric but phylogenetically distant" model. These biogeographical patterns have often been found in *Megophrys* (Mahony et al. 2018; Liu et al. 2018; Wang et al. 2019), indicating a complicated picture of biogeographical history of this taxonomically diverse toad group.

Separations of the horned toad species in Medog are also likely reflected on their different behaviors. Although being sympatric even in the same stream at elevations between 1500–1800 m in Bari village (Fig. 1), *M. medogensis* prefers tropical and subtropical forest floor (Fig. 10F), while *Megophrys yeae* sp. nov. is typically found calling on the leaves of tall dense plants (Fig. 10G), and *Megophrys* cf. *pachyproctus* calls on the branches of bushes (Fig. 10H). It is interesting that *Megophrys* cf. *pachyproctus* possess unique long calls, making a distinctly contrast with *Megophrys yeae* sp. nov. in the same stream which emit short calls (Fig. 4B, C; Table 3). The distinct calling patterns

especially in the two "standing-upper" species probably prevent their calls overlapping in the upper space. This kind of "so-small-microhabitat" niche divergences may be also related with phenotype differences between them. The "floor" toad *M. medogensis* presents bigger body size, while the two "standing-on-plants or leaves" species have a pale body. Probably for further isolations, *Megophrys* cf. *pachyproctus* with relatively moderate body size prefers relative harder branches, vines, or stem of plants (Fig. 10H, I), while the sympatric species *Megophrys yeae* sp. nov. and *Megophrys zhoui* sp. nov. often stand on soft leaves and/or grass by their lighter body (Fig. 10G, J), even developing finger pads for climbing like tree frogs (Table 2; Fei et al. 2009). It is fascinating on exploring how their behaviors with corresponding morphological characteristics have been evolved to fitting corresponding environments.

The discoveries of the new species indicate a much-underestimated biodiversity in the Himalayan Mountains. Yet, the amphibians in the region are suffering from obvious threats in their habitats, for example, the ongoing construction of roads, towns, and houses, the use of pesticide chemicals for farming, and increasing activities of tourists. And, we also still have a poor understanding of the influences of local and/or global climatic changes. Undoubtedly, it is urgent to investigate their population status for the conservation of these extraordinary toads.

Acknowledgements

We thank Dengwei Yang, Yin Qi, Bo Cai, Guocheng Shu, and Yong Huang for their assistance in the field. We are grateful to the Administration of Yarlung Zangbo Grand Canyon National Nature Reserve for issuing relevant permits for our field work. We are grateful to the editor Nathalie Yonow who provided many suggestions on language and descriptions. This research is supported by the Second Tibetan Plateau Scientific Expedition and Research Program (STEP) (Grant Nos.: 2019QZKK05010503 and 2019QZKK0501), Project supported by the biodiversity investigation, observation and assessment program (2019–2023) of Ministry of Ecology and Environment of China (2019HJ2096001006), and China Biodiversity Observation Networks (Sino BON–Amphibian & Reptile).

References

Bickford D, Lohman DJ, Sodhi NS, Ng PKL, Meier R, Winker K, Ingram KK, Das I (2007) Cryptic species as a window on diversity and conservation. Trends in Ecology and Evolution 22: 148–155. https://doi.org/10.1016/j.tree.2006.11.004

Biju SD, Bossuyt F (2003) New frog family from India reveals an ancient biogeographical link with the Seychelles. Nature 425(6959): 711–714. https://doi.org/10.1038/nature02019

Boersma P (2001) Praat, a system for doing phonetics by computer. Glot International 5: 341–345.

Bonaparte CLJL (1850) Conspectus Systematum Herpetologiae et Amphibiologiae. Brill EJ, Editio altera reformata, Lugduni Batavorum, Leiden, 1 pl.

Boulenger GA (1886) Description of a new frog of the genus *Megalophrys*. Proceedings of the Zoological Society of London 1885: 1–850.

Boulenger GA (1887) Description of a new frog of the genus *Megalophrys*. Annali del Museo Civico di Storia Naturale di Genova Serie 2, 4: 512–513.

Boulenger GA (1889) Description of a new batrachian of the genus *Leptobrachium*, obtain by M. L. Burma. Annali del Museo Civico di Storia Naturale di Genova. Serie 2, 7: 748–750.

Boulenger GA (1899a) Descriptions of three new reptiles and a new batrachian from Mount Kina Balu, North Borneo. Annals and Magazine of Natural History, Series 7(4):1–453. https://doi.org/10.1080/00222939908678228

Boulenger GA (1899b) On a collection of reptiles and batrachians made by Mr. J. D. La Touche in N.W. Fokien, China. Proceedings of the Zoological Society of London 1899: 159–172.

Boulenger GA (1903) Report on the batrachians and reptiles. Annandale, N., and H. C. Robinson eds., Fasciculi Malayenses. Anthropological and Zoological Results of an Expedition to Perak and the Siamese Malay States 1901–1903 undertaken by Nelson Annandale and Herbert C. Robinson under the auspices of the University of Edinburgh and the University of Liverpool. Volume 2, Zoology Part 1: 131–176.

Boulenger GA (1908) A revision of the oriental pelobatid batrachians (genus *Megophrys*). Proceedings of the Zoological Society of London 78(2): 407–430. https://doi.org/10.1111/j.1096-3642.1908.tb01852.x

Bourret R (1937) Notes herpétologiques sur l'Indochine française. XIV. Les batraciens de la collection du Laboratoire des Sciences Naturelles de l'Université. Descriptions de quinze espèces ou variétés nouvelles. Annexe au Bulletin Général de l'Instruction Publique Hanoi 1937: 5–56.

Bourret R (1942) Les Batraciens de l'Indochine. Institut Océanographique de l'Indochine, Hanoi 190–207.

Burns JM, Janzen DH, Hajibabaei M, Hallwachs W, Hebert PDN (2008) DNA barcodes and cryptic species of skipper butterflies in the genus *Perichares* in Area de Conservation Guanacaste, Costa Rica. Proceedings of the National Academy of Sciences of the United States of America 105: 6350–6355. https://doi.org/10.1073/pnas.0712181105

Castresana J (2000) Selection of conserved blocks from multiple alignments for their use in phylogenetic analysis. Molecular Biology and Evolution 17(4): 540–552. https://doi.org/10.1093/oxfordjournals.molbev.a026334

Che J, Chen H, Yang J, Jin J, Jiang K, Yuan Z (2011) Universal COI primers for DNA barcoding amphibians. Molecular Ecology Resources 12(2): 247–258. https://doi.org/10.1111/j.1755-0998.2011.03090.x

Chen JM, Zhou WW, Poyarkov Jr NA, Stuart BL, Brown RM, Lathrop A, Wang YY, Yuan ZY, Jiang K, Hou M, Chen HM, Suwannapoom C, Nguyen SN, Duong TV, Papenfuss TJ, Murphy RW, Zhang YP, Che J (2016) A novel multilocus phylogenetic estimation reveals unrecognized diversity in Asian horned toads, genus *Megophrys* sensu lato (Anura: Megophryidae). Molecular Phylogenetics and Evolution 106: 28–43. https://doi.org/10.1016/j.ympev.2016.09.004

Condon MA, Scheffer SJ, Lewis ML, Swensen SM (2008) Hidden Neotropical diversity: greater than the sum of its parts. Science 320: 928–31. https://doi.org/10.1126/science.1155832

Dayrat B (2005) Towards integrative taxonomy. Biological Journal of the Linnean Society 85: 407–415. https://doi.org/10.1111/j.1095-8312.2005.00503.x

Queiroz KD (2007) Species concepts and species delimitation. Systematic Biology 56: 879–886. https://doi.org/10.1080/10635150701701083

Darriba D, Taboada GL, Doallo R, Posada D (2012) Jmodeltest 2: more models, new heuristics and parallel computing. Nature Methods 9(8): 772. https://doi.org/10.1038/nmeth.2109

Degnan JH, Rosenberg NA (2009) Gene tree discordance, phylogenetic inference and the multispecies coalescent. Trends in Ecology and Evolution 24: 332–340. https://doi.org/10.1016/j.tree.2009.01.009

Delorme M, Dubois A, Grosjean S, Ohler A (2006) Une nouvelle ergotaxinomie des Megophryidae (Amphibia, Anura). Alytes 24: 6–21.

DeSalle R, Giddings LV (1986) Discordance of nuclear and mitochondrial DNA phylogenies in Hawaiian Drosophila. Proceedings of the National Academy of Sciences of the United States of America 83(18): 6902–6906. https://doi.org/10.1073/pnas.83.18.6902

Dubois A (1987 "1986") Miscellanea taxinomica batrachologica (I). Alytes 5: 7–95.

Fei L, Ye CY (2001) The Colour Handbook of the Amphibians of Sichuan, Science Press, Beijing, China, 138–151. [In Chinese]

Fei L, Ye CY (2005) Two new species of Megophryidae from China. In: Fei et al. (Ed.) The Key and Illustration of Chinese. Sichuan Publishing House of Science and Technology, Chongqing, China, 253–255. [In Chinese]

Fei L, Ye CY (2016) Amphibians of China, Volume 1. Science Press, Beijing, 611–735.

Fei L, Ye CY, Huang YZ (1983) Two new subspecies of *Megophrys omeimontis* Liu from China (Amphibia, Pelobatidae). Acta Herpetologica Sinica/Liangqi paxing dongwu yanjiu New Series 2(2): 49–52. [In Chinese with English abstract]

Fei L, Ye C Y, Huang Y Z (1990) Keys to Chinese amphibians. Chongqing Branch, Publishing House of Science and Technology Literation Publishing House, Chongqing, 1–364.

Fei L, Ye C Y, Jiang JP (2010) Colored Atlas of Chinese Amphibians. Sichuan Publishing Group, Chengdu, 135–247. [In Chinese]

Fei L, Hu SQ, Ye CY, Huang YZ (2009) Fauna Sinica. Amphibia. Volume 2. Anura. Science Press, Beijing, 328–481. [In Chinese]

Frost DR (2020) Amphibian Species of the World: an Online Reference. Version 6.0. Electronic Database. American Museum of Natural History, New York. [Accessed on 31 Aug 2020]

Fu JZ, Weadick CJ, Bi K (2007) A phylogeny of the high-elevation Tibetan megophryid frogs and evidence for the multiple origins of reversed sexual size dimorphism. Journal of Zoology 273: 315–325. https://doi.org/10.1111/j.1469-7998.2007.00330.x

Gómez Daglio L, Dawson MN (2019) Integrative taxonomy: ghosts of past, present and future. Journal of the Marine Biological Association of the United Kingdom 99: 1237–1246. https://doi.org/10.1017/S0025315419000201

Gosner KL (1960) A simplified table for staging anuran embryos and larvae with notes on identification. Herpetologica 16(3): 183–190.

Guindon S, Dufayard JF, Lefort V, Anisimova M, Hordijk W, Gascuel O (2010) New algorithms and methods to estimate maximum-likelihood phylogenies: assessing the performance of PhyML 3.0. Systematic Biology 59(3): 307–321. https://doi.org/10.1093/sysbio/syq010

Günther ACLG (1864) The reptiles of British India. The Ray Society, London, 452 pp.

Hall TA (1999) BIOEDIT: a user-friendly biological sequence alignment editor and analysis program for Windows 95/98/NT. Nucleic Acids Symposium Series 41(41): 95–98.

Hu SQ, Zhao EM, Liu CC. 1966. A herpetological survey of the Tsinling and Ta-Pa Shan region. Acta Zoologica Sinica 18: 57–89. [In Chinese]

Hu SQ, Zhao EM, Liu CC (1973) A survey of amphibians and reptiles in Kweichow province, including a herpetofaunal analysis. Acta Zoologica Sinica 19: 149–181. [In Chinese]

Huang CM, Lathrop A, Murphy RW (1998) Translations of "Two new species of amphibian in Tibet" Huang and Fei 1981 and "Description of two new species of the genus *Megophrys*" Fei, Ye, and Huang 1995. Smithsonian Herpetological Information Service 118: 1–20. https://doi.org/10.5479/si.23317515.118.3

Huang YZ, Fei L (1981) Two new species of amphibians from Xizang. Acta Zootaxonomica Sinica 6: 211–15. [in Chinese with English abstract]

Inger RF (1989) Four new species of frogs from Borneo. Malayan Nature Journal 42: 229–243.

Inger RF, Romer JD (1961) A new pelobatid frog of the genus *Megophrys* from Hong Kong. Fieldiana. Zoology 39(46): 533–538. https://doi.org/10.5962/bhl.title.3373

Inger RF, Stuebing RB, Lian TF (1995) New species and new records of Anurans from Boreno. Raffles Bulletin of Zoology, Singapore 43(1): 115–131.

Inger RF, Iskandar DT (2005) A collection of amphibians from West Sumatra, with description of a new species of *Megophrys* (Amphibia: Anura). Raffles Bulletin of Zoology. Singapore 53: 133–142.

Jiang JP, Yuan FR, Xie F, Zheng ZH (2003) Phylogenetic relationships of some species and genera in megophryids inferred from partial sequences of mitochondrial 12S and 16S rRNA genes. Zoological Research 24: 241–248.

Jiang JP, Ye CY, Fei L (2008) A new horn toad *Megophrys sangzhiensis* from Hunan, China (Amphibia, Anura). Zoological Research 29(2): 219–222. https://doi.org/10.3724/SP.J.1141.2008.00219 [In Chinese with English abstract]

Jiang K, Rao DQ, Yuan SQ, Wang JS, Li PP, Hou M, Che M, Che J (2012) A new species of the genus *Scutiger* (Anura: Megophryidae) from southeastern Tibet, China. Zootaxa 3388: 29–40. https://doi.org/10.11646/zootaxa.3388.1.3

Jiang K, Wang K, Xie J, Zou DH, Liu WL, Jiang JP, Li C, Che J (2016a) A new species of the genus *Amolops* (Amphibia: Ranidae) from southeastern Tibet, China. Zoological Research 37: 31–40.

Jiang K, Wang K, Zou DH, Yan F, Li PP, Che J (2016b) A new species of the genus *Scutiger* (Anura: Megophryidae) from Medog of southeastern Tibet, China. Zoological Research 37: 21–30.

Jiang K, Yan F, Wang K, Zou DH, Li C, Che J (2016c) A new genus and species of treefrog from Medog, southeastern Tibet, China (Anura, Rhacophoridae). Zoological Research 37: 15–20.

Köhler J, Jansen M, Rodríguez A, Kok P, Toledo LF, Emmrich M, Glaw F, Haddad CFB, Rödel MO, Vences M (2017) The use of bioacoustics in anuran taxonomy: theory, terminology,

methods and recommendations for best practice. Zootaxa 4251(1): 1–124. https://doi.org/10.11646/zootaxa.4251.1.1

Kuhl H, Van Hasselt JC (1822) Uittreksels uit breieven van de Heeren Kuhl en van Hasselt, aan de Heeren C. J. Temminck, Th. van Swinderen en W. de Haan. Algemeene Konst-en Letter-Bode 7: 99–104.

Kumar S, Stecher G, Tamura K (2016) MEGA7: Molecular Evolutionary Genetics Analysis Version 7.0 for Bigger Datasets. Molecular Biology and Evolution 33(7): 1870. https://doi.org/10.1093/molbev/msw054

Larsen K (2001) Morphological and molecular investigation of polymorphism and cryptic species in tanaid crustaceans: implications for tanaid systematics and biodiversity estimates. Zoological Journal of the Linnean Society 131: 353–79. https://doi.org/10.1111/j.1096-3642.2001.tb02241.x

Lathrop A (1997) Taxonomic review of the megophryid frogs (Anura: Pelobatoidea). Asiatic Herpetological Research 7: 68–79. https://doi.org/10.5962/bhl.part.18857

Li PP, Lu YY, Rao DQ (2008) A new species of Cascade Frog (Amphibia, Ranidae) from Tibet, China. Acta Zootaxonomica Sinica 33: 537–541.

Li PP, Zhao EM, Dong BJ (2010) Amphibians and Reptiles of Tibet. Science Press, Beijing, 103 pp.

Li YL, Jin MJ, Zhao J, Liu ZY, Wang YY, Pang H (2014) Description of two new species of the genus *Megophrys* (Amphibia: Anura: Megophryidae) from Heishiding Nature Reserve, Fengkai, Guangdong, China, based on molecular and morphological data. Zootaxa 3795(4): 449–471. https://doi.org/10.11646/zootaxa.3795.4.5

Li SZ, Xu N, Liu J, Jiang JP, Wei G, Wang B (2018) A new species of the Asian toad genus *Megophrys sensu lato* (Amphibia: Anura: Megophryidae) from Guizhou Province, China. Asian Herpetological Research 9(4): 224–39.

Liu CC (1950) Amphibians of western China. Fieldiana. Zoology Memoires 2: 1–397. https://doi.org/10.5962/bhl.part.4737

Liu CC, Hu SQ, Yang FH (1960) Amphibia of Yunnan collected in 1958. Acta Zoologica Sinica. Beijing 12: 149–174. [In Chinese]

Liu Z, Chen G, Zhu T, Zeng Z, Lyu Z, Wang J, Messenger K, Greenberg AJ, Guo ZX, Yang ZH, Shi SH, Wang YY (2018) Prevalence of cryptic species in morphologically uniform taxa-fast speciation and evolutionary radiation in Asian frogs. Molecular Phylogenetics and Evolution 127: 723–731. https://doi.org/10.1016/j.ympev.2018.06.020

Mahony S (2011) Two new species of *Megophrys* Kuhl and van Hasselt (Amphibia: Megophryidae), from western Thailand and southern Cambodia. Zootaxa 2734: 23–39. https://doi.org/10.11646/zootaxa.2734.1.2

Mahony S, Sengupta S, Kamei RG, Biju SD (2011) A new low altitude species of *Megophrys* Kuhl and van Hasselt (Amphibia: Megophryidae), from Assam, Northeast India. Zootaxa 3059: 36–46. https://doi.org/10.11646/zootaxa.3059.1.2

Mahony S, Teeling EC, Biju SD (2013) Three new species of horned frogs, *Megophrys* (Amphibia: Megophryidae), from northeast India, with a resolution to the identity of *Megophrys boettgeri* populations reported from the region. Zootaxa 3722: 143. https://doi.org/10.11646/zootaxa.3722.2.2

Mahony S, Foley NM, Biju SD, Teeling EC (2017) Evolutionary history of the Asian horned frogs (Megophryinae): integrative approaches to timetree dating in the absence of a fossil record. Molecular Biology and Evolution 34(3): 744–71. https://doi.org/10.1093/molbev/msw267

Mahony S, Kamei RG, Teeling EC, Biju SD (2018) Cryptic diversity within the *Megophrys major* species group (Amphibia: Megophryidae) of the Asian horned frogs: Phylogenetic perspectives and a taxonomic revision of South Asian taxa, with descriptions of four new species. Zootaxa 4523: 1–96. https://doi.org/10.11646/zootaxa.4523.1.1

Malkmus R, Matsui M (1997) *Megophrys kobayashii*, ein neuer pelobatider Frosch vom Mount Kinabalu. Sauria, Berlin 19: 31–37.

Mathew R, Sen N (2007) Description of two new species of *Megophrys* (Amphibia: Anura: Megophryidae) from North-east India. Cobra 1: 18–28.

Mauro DS, Gower DJ, Oommen OV, Wilkinson M, Zardoya R (2004) Phylogeny of caecilian amphibians (*Gymnophiona*) based on complete mitochondrial genomes and nuclear RAG1. Molecular Phylogenetics and Evolution 33: 413–27. https://doi.org/10.1016/j.ympev.2004.05.014

Messenger KR, Dahn HA, Liang YR, Xie P, Wang Y, Lu CH (2019) A new species of the genus *Megophrys* Gunther, 1864 (Amphibia: Anura: Megophryidae) from Mount Wuyi, China. Zootaxa 4554(2): 561–583. https://doi.org/10.11646/zootaxa.4554.2.9

Mo XY, Shen YH, Li HH, Wu MS (2010) A new species of *Megophrys* (Amphibia: Anura: Megophryidae) from the northwestern Hunan Province, China. Current Zoology 56(4): 432–436. https://doi.org/10.1093/czoolo/56.4.432

Munir M, Hamidy A, Farajallah A, Smith EN (2018) A new *Megophrys* Kuhl and Van Hasselt (Amphibia: Megophryidae) from southwestern Sumatra, Indonesia. Zootaxa 4442: 389–412. https://doi.org/10.11646/zootaxa.4442.3.3

Munir M, Hamidy A, Matsui M, Iskandar DT, Sidik I, Shimada T (2019) A new species of *Megophrys* Kuhl & Van Hasselt (Amphibia: Megophryidae) from Borneo allied to *M. nasuta* (Schlegel, 1858). Zootaxa 4679: 1–24. https://doi.org/10.11646/zootaxa.4679.1.1

Oberhummer E, Barten C, Schweizer M, Das I, Haas A, Hertwig ST (2014) Description of the tadpoles of three rare species of megophryid frogs (Amphibia: Anura: Megophryidae) from Gunung Mulu, Sarawak, Malaysia. Zootaxa 3835: 59–79. https://doi.org/10.11646/zootaxa.3835.1.3

Ohler A, Swan SR, Daltry JC (2002) A recent survey of the amphibian fauna of the Cardamom Mountains, Southwest Cambodia with descriptions of three new species. Raffles Bulletin of Zoology, Singapore 50(2): 465–481.

Ohler A (2003) Revision of the genus *Ophryophryne* Boulenger, 1903 (Megophryidae) with description of two new species. Alytes 21(1): 23–44.

Orlov NL, Pyarkov Jr NA, Nguyen TT (2015) Taxonomic notes on *Megophrys* frogs (Megophryidae: Anura) of Vietnam, with description of a new species. Russian Journal of Herpetology 22: 206–218.

Pante E, Schoelinck C, Puillandre N (2014) From integrative taxonomy to species description: one step beyond. Systematic Biology 64: 152–60. https://doi.org/10.1093/sysbio/syu083

Petrusek A, Hobæk A, Nilssen JP, Skage M, ČErný M, Brede N, Schwenk K (2008) A taxonomic reappraisal of the European *Daphnia longispina* complex (Crustacea, Cladocera, Anomopoda). Zoologica Scripta 37: 507–19. https://doi.org/10.1111/j.1463-6409.2008.00336.x

Pope CH (1929) Four new frogs from Fukien Province, China. American Museum Novitates 352: 1–5.

Poyarkov NA, Duong Jr TV, Orlov NL, Gogoleva SI, Vassilieva AB, Nguyen LT, Nguyen VDH, Nguyen SN, Che J, Mahony S (2017) Molecular, morphological and acoustic assessment of the genus *Ophryophryne* (Anura, Megophryidae) from Langbian Plateau, southern Vietnam, with description of a new species. ZooKeys 672: 49–120. https://doi.org/10.3897/zookeys.672.10624

R Development Core Team (2008) R: A Language and Environment for Statistical Computing. Vienna: R Foundation for Statistical Computing. Available at

Rao DQ, Yang DT (1997) The karyotypes of Megophryinae (Pelobatidae) with a discussion on their classification and phylogenetic relationships. Asian Herpetological Research 7: 93–102. https://doi.org/10.5962/bhl.part.18858

Rissler LJ, Apodaca JJ (2007) Adding more ecology into species delimitation: ecological niche models and phylogeography help define cryptic species in the black salamander (Aneides flavipunctatus). Systematic Biology 56: 924–42. https://doi.org/10.1080/10635150701703063

Ronquist F, Teslenko M, Paul VDM, Ayres DL, Darling A, Höhna S, Larget B, Liu L, Suchard MA, Huelsenbeck JP (2012) Mrbayes 3.2: efficient bayesian phylogenetic inference and model choice across a large model space. Systematic Biology 61(3): 539–42. https://doi.org/10.1093/sysbio/sys029

Saikia B, Sinha B (2018) First report of *Megophrys pachyproctus* Huang, 1981 (Anura: Megophyridae) from Talle Valley Wildlife Sanctuary, Arunachal Pradesh, India. Records of the Zoological Survey of India 118: 430–436.

Seifert B (2009) Cryptic species in ants (Hymenoptera: Formicidae) revisited: We need a change in the alpha-taxonomic approach. Myrmecological News 12: 149–66.

Schlegel H (1858) Handleiding tot de Beoefening der Dierkunde (Vol. 2). Koninklijke Militaire Akademie, Breda, 57 pp. https://doi.org/10.5962/bhl.title.11648

Shen YH (1994) A new pelobatid toad of the genus *Megophrys* from China (Anura: Pelobatidae). In: Zoological Society of China (China Zoological Society, Institute of zoology, Chinese academy of sciences, School of life sciences, Peking University, Department of biological science and technology, Tsinghua university) The 60th Anniversary of the Foundation of the Zoological Society of China, Nanking (China), September 1994. China Science and Technology Publishing House, 603–606.

Shen YH, Gu Q, Liao CL (2013) Additional Record of *Megophrys caudoprocta* (Amphibia，Megophryidae). Chinese Journal of Zoology 48(03): 351-356. [In Chinese with English abstract]

Sichuan Institute of Biology Herpetology Department (1977) A survey of amphibians in Xizang (Tibet). Acta Zoologica Sinica/ Dong wu xue bao. 23: 54–63. [In Chinese with English abstract]

Simon C, Frati F, Beckenbach A, Crespi B, Liu H, Flook P (1994) Evolution, weighting and phylogenetic utility of mitochondrial gene sequences and a compilation of conserved polymerase chain reaction primers. Annals of the Entomological Society of America 87(6): 651–701. https://doi.org/10.1093/aesa/87.6.651

Smith MA (1921) New or little-known reptiles and batrachians from southern Annam (Indochina). Proceedings of the Zoological Society of London 1921: 423–440. https://doi.org/10.1111/j.1096-3642.1921.tb03271.x

Stejneger L (1926) Two new tailless amphibians from western China. Proceedings of the Biological Society of Washington 39: 53–54.

Stockman AK, Bond JE (2007) Delimiting cohesion species: extreme population structuring and the role of ecological interchangeability. Molecular Ecology 16: 3374–92. https://doi.org/10.1111/j.1365-294X.2007.03389.x

Stuart BL, Chuaynkern Y, Chan-ard T, Inger RF (2006a) Three new species of frogs and a new tadpole from eastern Thailand. Fieldiana Zoology, New Series 1543: 1–10. https://doi.org/10.3158/0015-0754(2006)187[1:TNSOFA]2.0.CO;2

Stuart BL, Sok K, Neang T (2006b) A collection of amphibians and reptiles from hilly eastern Cambodia. Raffles Bulletin of Zoology. Singapore 54: 129–155.

Sumida M, Ogata M, Nishioka M (2000) Molecular phylogenetic relationships of pond frogs distributed in the palearctic region inferred from DNA sequences of mitochondrial 12s ribosomal RNA and cytochrome b genes. Molecular Phylogenetics and Evolution 16(2): 278–85. https://doi.org/10.1006/mpev.2000.0791

Tamura K, Stecher G, Peterson D, Fiipski A, Kumar S (2013) MEGA6: molecular evolutionary genetics analysis, version 6.0. Molecular Biology and Evolution 30: 2725–2729. https://doi.org/10.1093/molbev/mst197

Tapley B, Cutajar T, Mahony S, Nguyen CT, Dau VQ, Nguyen TT, Luong HV, Rowley JJL (2017) The Vietnamese population of *Megophrys kuatunensis* (Amphibia: Megophryidae) represents a new species of Asian horned frog from Vietnam and southern China. Zootaxa 4344(3): 465–492. https://doi.org/10.11646/zootaxa.4344.3.3

Tapley B, Cutajar TP, Mahony S, Nguyen CT, Dau VQ, Luong AM, Le DT, Nguyen TT, Nguyen TQ, Portway C, Luong HV, Rowley JJL (2018) Two new and potentially highly threatened *Megophrys* Horned frogs (Amphibia: Megophryidae) from Indochina's highest mountains. Zootaxa 4508: 301–333. https://doi.org/10.11646/zootaxa.4508.3.1

Taylor EH (1920) Philippine Amphibia. Philippine Journal of Science 16: 213–359. https://doi.org/10.5962/bhl.part.4751

Thielsch A, Knell A, Mohammadyari A, Petrusek A, Schwenk, K (2017) Divergent clades or cryptic species? mito-nuclear discordance in a daphnia species complex. BMC Evolutionary Biology 17(1): 227. https://doi.org/10.1186/s12862-017-1070-4

Tian WS, Hu QX (1983) Taxonomic study on genus *Megophrys*, with descriptions of two new genera. Acta Herpetologica Sinica New Series 2: 41–8.

Tian YZ, Sun A (1995) A new species of *Megophrys* from China (Amphibia: Pelobatidae). Journal of Liupanshui Teachers College 52(3): 11–15. [In Chinese]

Wang YY, Zhang TD, Zhao J, Sung YH, Yang JH, Pang H, Zhang Z (2012) Description of a new species of the genus *Megophrys* Günther, 1864 (Amphibia: Anura: Megophryidae)

from Mount Jinggang, China, based on molecular and morphological data. Zootaxa 3546: 53–67. https://doi.org/10.11646/zootaxa.3546.1.4

Wang YY, Zhao J, Yang JH, Zhou ZM, Chen GL, Liu Y (2014) Morphology, molecular genetics, and bioacoustics support two new sympatric *Megophrys* (Amphibia: Anura: Megophryidae) species in Southeast China. PLoS ONE 9: e93075. https://doi.org/10.1371/journal.pone.0093075

Wang J, Liu ZY, Lyu ZT, Wang YY (2017a) A new species of the genus *Megophrys* (Amphibia: Anura: Megophryidae) from an offshore island in Guangdong Province, southeastern China. Zootaxa 4324(3): 541–556. https://doi.org/10.11646/zootaxa.4324.3.8

Wang YE, Liu BQ, Jiang K, Jin W, Xu JN, Wu CH (2017b) A new species of the Horn Toad of the genus *Xenophrys* from Zhejiang, China (Amphibia: Megophryidae). Chinese Journal of Zoology 52: 19–29. [In Chinese with English abstract]

Wang L, Deng XJ, Liu Y, Wu QQ, Liu Z (2019a) A new species of the genus *Megophrys* (Amphibia: Anura: Megophryidae) from Hunan, China. Zootaxa 4695(4): 301–330. https://doi.org/10.11646/zootaxa.4695.4.1

Wang J, Lyu ZT, Liu ZY, Liao CK, Zeng ZC, Li YL, Wang YY (2019b) Description of six new species of the subgenus *Panophrys* within the genus *Megophrys* (Anura, Megophryidae) from southeastern China based on molecular and morphological data. ZooKeys 851: 113–164. https://doi.org/10.3897/zookeys.851.29107

Wang B, Wu YQ, Peng JW, Shi SC, Lu NN, Wu J (2020) A new *Megophrys* Kuhl and Van Hasselt (Amphibia: Megophryidae) from southeastern China. ZooKeys 851: 113–164. https://doi.org/10.3897/zookeys.851.29107

Wu YH, Suwannapoom C, Poyarkov Jr NA, Chen JM, Pawangkhanant P, Xu K, Jin JQ, Murphy RW, Che J (2019) A new species of the genus *Xenophrys* (Anura: Megophryidae) from northern Thailand. Zoological Research 40: 564–574. https://doi.org/10.24272/j.issn.2095-8137.2019.032

Wheeler QD, Knapp S, Stevenson DW, Stevenson J, Blum SD, Boom BM, Borisy GG, Buizer JL, de Carvalho MR, Cibrian A (2012) Mapping the biosphere: exploring species to understand the origin, organization and sustainability of biodiversity. Systematics and Biodiversity 10: 1–20. https://doi.org/10.1080/14772000.2012.665095

Yang JH, Wang J, Wang YY (2018) A new species of the genus *Megophrys* (Anura: Megophryidae) from Yunnan Province, China. Zootaxa 4413: 325–338. https://doi.org/10.11646/zootaxa.4413.2.5

Ye CY, Fei L (1992) A new Pelobatid toad of the genus *Megophrys* from Xizang, China. Acta Herpetologica Sinica 1–2: 50–52. [In Chinese]

Ye CY, Fei L (1995) Taxonomic studies on the small type *Megophrys* in China including descriptions of the new species (subspecies) (Pelobatidae: genus *Megophrys*). Herpetologica Sinica 4–5: 72–81. [In Chinese]

Ye CY, Fei L, Xie F (2007) A new species of Megophryidae *Megophrys baolongensis* from China (Amphibia, Anura). Herpetologica Sinica 11: 38–41. [In Chinese]

Yoder AD, Olson LE, Hanley C, Heckman Kl, Rasoloarison R, Russell R, Ranivo J, Soarimalala V, Karanth KP, Raselimanana AP, Goodman SM (2005) A multidimensional approach for detecting species patterns in Malagasy vertebrates. Proceedings of the National Acad-

emy of Sciences of the United States of America 102: 6587–94. https://doi.org/10.1073/pnas.0502092102

Zhang Y, Li G, Xiao N, Li J, Pan T, Wang H, Zhang B, Zhou J (2017) A new species of the genus *Megophrys* (Amphibia: Anura: Megophryicae) from Libo County, Guizhou, China. Asian Herpetological Research 8: 75–85.

Zhao WG, Rao DQ, Lü SQ, Dong BJ (2005) Herpetological surveys of Xizang autonomous region 2. Medog. Sichuan Journal of Zoology 24: 250–253. [In Chinese with English abstract]

Zhao J, Yang JH, Chen GL, Chen CQ, Wang YY (2014) Description of a new species of the genus *Brachytarsophrys* Tian and Hu, 1983 (Amphibia: Anura: Megophryidae) from Southern China based on molecular and morphological data. Asian Herpetological Research 5(3): 150–160. https://doi.org/10.3724/SP.J.1245.2014.00150

Supplementary material 1

Table S1–S5

Authors: Shengchao Shi, Meihua Zhang, Feng Xie, Jianping Jiang, Wulin Liu, Li Ding, Li Luan, Bin Wang

Data type: measurements

Explanation note: **Table S1.** Measurements of the adult specimens of *Megophrys* used in this study. Unit in mm. See abbreviations for the morphological characters in Materials and methods section. **Table S2.** Measurements of the tadpole specimens of *Megophrys* used in this study. Unit in mm. See abbreviations for the morphological characters in Materials and methods section. **Table S3.** Measurements of advertisement call parameters for three *Megophrys* species in Medog. Values are given as mean (ranging). **Table S4.** Mean genetic distance under uncorrected *p*-distance model between *Megophrys* species based on 16S gene. **Table S5.** Morphological comparisons between the *Megophrys* species from the eastern Himalayas. Measurements in mm. See abbreviations for the morphological characters in Materials and methods section.

Link: https://doi.org/10.3897/zookeys.977.55693.suppl1

Supplementary material 2

Figure S1–S5

Authors: Shengchao Shi, Meihua Zhang, Feng Xie, Jianping Jiang, Wulin Liu, Li Ding, Li Luan, Bin Wang

Data type: multimedia

Explanation note: **Figure S1.** *Megophrys medogensis* in life from Medog. **A**, **B** dorsal and ventral views of adult male CIB022017061404DD from Didong village, respectively **C**, **D** dorsal and ventral views of adult male CIB022017061405BB from Beibeng village, respectively **E** unvouchered calling male from Beibeng **F** adult female CIB022017061602 from Beibeng village. **Figure S2.** Photos showing variation of *Megophrys* cf. *pachyproctus* in life **A**, **B** adult male CIB022017061806 **C**, **D** adult male CIB022017061807 **E**, **F** gavid female CIBMT171054. Left: dorsolateral view; and right: ventral view. **Figure S3.** Photos of paratypes of *Megophrys zhoui* sp. nov. in life. **A**, **B** adult female CIBMT171062 **C**, **D** adult female CIBMT171060. Left for dorsolateral view, and right for ventral view. **Figure S4.** Photos of paratypes of *Megophrys yeae* sp. nov. in life **A**, **B** adult female CIB201706MT03 **C**, **D** adult male CIB022017061103 **E** adult male CIBMT171065 **F** adult male CIBMT171066. Left: dorsolateral view, and right: ventral view. **Figure S5.** Typical forests inhabited by *Megophrys* toads in Medog **A** landscape in Didong village at elevations of 600–850 m, harboring the low-middle-elevation *M. medogensis* and *Megophrys yeae* sp. nov. **B** landscape in Bari village and vicinity of Renqingbeng Temple at elevations of ca. 1400–2100 m, the former harboring low-middle-elevation *M. medogensis*, *M.* cf. *pachyproctus*, and *Megophrys yeae* sp. nov., and the latter hosting *M.* cf. *pachyproctus* and *Megophrys zhoui* sp. nov. **C** landscape in Gelin village at elevations of ca. 1500–1800 m, hosting the low-middle-elevation *M. medogensis* and *M. pachyproctus* **D** Gedang village at elevations above 2100 m, harboring the high-elevation *M. medogensis* **E–H** local forests in the four sites, respectively.

Link: https://doi.org/10.3897/zookeys.977.55693.suppl2